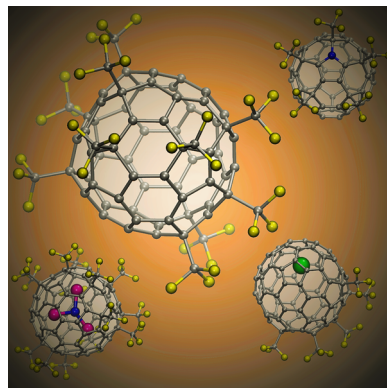


## Perfluoroalkylfullerenes

Olga V. Boltalina,\*<sup>†</sup> Alexey A. Popov,\*<sup>‡</sup> Igor V. Kuvychko,<sup>†</sup> Natalia B. Shustova,<sup>†</sup> and Steven H. Strauss\*,<sup>†</sup>

<sup>†</sup>Department of Chemistry, Colorado State University, Fort Collins, Colorado 80523, United States

<sup>‡</sup>Leibniz Institute for Solid State and Materials Research (IFW) Dresden, D-01171 Dresden, Germany



### CONTENTS

1. Introduction	1052
2. Synthetic Methods	1058
2.1. Liquid-Phase Fullerene Perfluoroalkylation	1058
2.2. PFAF Generation during Fullerene Synthesis	1061
2.3. PFAF Formation during Fullerene Fluorination	1062
2.4. Fullerene Trifluoromethylation with Metal Trifluoroacetates	1062
2.5. Reactions of Solid Fullerenes with Gaseous Perfluoroalkyl Iodides	1064
2.5.1. Reactions with CF <sub>3</sub> I	1064
2.5.2. Reactions with Other R <sub>f</sub> I's	1065
2.6. Formation of New Isomers by Thermal Treatment of PFAFs	1066
2.7. PFAF Preparation via Reactions with Metal R <sub>f</sub> Reagents	1066
2.8. Summary Remarks on Synthetic Methods	1067
3. Physical Properties and Separation Methods of PFAFs	1068
3.1. Separation of PFAFs	1068
4. X-ray Crystallography and <sup>19</sup> F NMR Spectroscopy of PFAFs	1068
4.1. C <sub>60</sub> (R <sub>f</sub> ) <sub>n</sub> Derivatives	1068
4.1.1. Determination of C <sub>60</sub> (R <sub>f</sub> ) <sub>n</sub> Addition Patterns	1071
4.1.2. Single and Double Bonds in C <sub>60</sub> (CF <sub>3</sub> ) <sub>n</sub> Derivatives and Validation of DFT Calculations	1072
4.2. X-ray Crystallographic Studies of C <sub>70</sub> (R <sub>f</sub> ) <sub>n</sub> Derivatives	1073
5. PFAF Addition Patterns	1073
5.1. Additions to C <sub>60</sub>	1073
5.1.1. 1,2 ( <i>ortho</i> ) and 1,4 ( <i>para</i> ) Addition and Double Bonds in Pentagons	1073

5.1.2. Multiple Additions of Bulky Groups to C <sub>60</sub> : General Principles	1073
5.1.3. Addition Patterns of C <sub>60</sub> (CF <sub>3</sub> ) <sub>n</sub> , n = 2–18	1075
5.1.4. Thermodynamic versus Kinetic Aspects of CF <sub>3</sub> Addition	1077
5.1.5. Addition of Bulky R <sub>f</sub> Groups to C <sub>60</sub>	1077
5.2. CF <sub>3</sub> Addition to C <sub>59</sub> N	1078
5.3. R <sub>f</sub> Addition to C <sub>70</sub>	1079
5.3.1. Earlier Studies on Multiple Addition to C <sub>70</sub>	1079
5.3.2. CF <sub>3</sub> Addition to C <sub>70</sub>	1080
5.3.3. Addition of Bulky R <sub>f</sub> Groups to C <sub>70</sub>	1082
5.4. R <sub>f</sub> Addition to Hollow Higher Fullerenes (HHFs)	1083
5.5. R <sub>f</sub> Addition to Endohedral Metallofullerenes	1085
5.5.1. Derivatives of Monometallofullerenes	1085
5.5.2. Derivatives of Sc <sub>3</sub> N@C <sub>80</sub>	1086
6. Optical Excitations of PFAFs	1086
6.1. UV–Vis–NIR Absorption Spectroscopy	1086
6.2. Fluorescence Spectroscopy	1088
7. Electrochemical Properties of PFAFs	1088
7.1. Reduction Potentials of Trifluoromethylfullerenes (TMFs)	1089
7.1.1. C <sub>60</sub> (CF <sub>3</sub> ) <sub>n</sub> Derivatives	1089
7.1.2. C <sub>70</sub> (CF <sub>3</sub> ) <sub>n</sub> Derivatives	1092
7.1.3. Sc <sub>3</sub> N@C <sub>80</sub> (CF <sub>3</sub> ) <sub>n</sub>	1093
7.2. ESR and Vis–NIR Spectroscopic Studies of PFAF Anions	1093
7.2.1. Electron Spin Resonance	1093
7.2.2. Vis–NIR Absorption Spectroscopy	1094
7.3. Reduction Potentials of R <sub>f</sub> Derivatives	1094
7.3.1. Substituent Effect in 1,7-C <sub>60</sub> (R <sub>f</sub> ) <sub>2</sub> Compounds	1094
7.3.2. The Role of Addition Pattern for Bulky R <sub>f</sub> Groups: i-C <sub>3</sub> F <sub>7</sub> Derivatives	1095
7.3.3. CF <sub>2</sub> Derivatives	1096
8. Chemical Properties of PFAFs	1096
9. Conclusions and Outlook	1098
Author Information	1099
Corresponding Authors	1099
Notes	1099
Biographies	1099
Acknowledgments	1100
Glossary	1101
References	1101

Special Issue: 2015 Fluorine Chemistry

Received: May 15, 2014

Published: January 15, 2015

## 1. INTRODUCTION

In an experiment performed nearly 30 years ago that involved laser desorption of graphite a substrate followed by plume cooling in the He carrier gas and mass analysis of the generated ionic clusters, a new form of carbon, a fullerene, was conceived.<sup>1</sup> An equally important discovery of the bulk synthesis of fullerenes, via arc discharge of graphite, was made by Huffman and Krätschmer in 1990.<sup>2</sup> These two discoveries of the nearly spherical  $I_h$ - $C_{60}$  molecule, with a 1 nm diameter, marked the beginning of nanoscience, a vibrant field of multidisciplinary research and cutting-edge modern technology.

The past 25 years of flourishing fullerene research have resulted in many thousands of new chemical materials, true technological breakthroughs, and a lot of promise that is yet to be met in the practical world. What remains constant throughout the relatively short history of fullerene chemistry (cf., 200-year old chemistry of benzene) is the unsurpassed richness and diversity of chemical transformations and continued unprecedented dedication of scores of researchers to the field that is frequently rewarded by newly discovered reaction mechanism or unexpected functions of their molecular designs with fullerenes.

Several excellent books, series of conference proceedings volumes, a specialized journal, dedicated journal issues, and tens of thousands of original articles were published since 1985. More recently, comprehensive general reviews on various aspects of fullerene chemistry have been published in *Chemical Reviews*.<sup>3</sup>

The scope of this Review is the first attempt to provide a general and in-depth overview of the research activity in the field of perfluoroalkylation of fullerenes that occurred in 1993–2014. The authors of this work are a team of very close collaborators from three scientific generations who have continuously worked in this field since 2001, and some of us were involved in fullerene research as early as Fall 1992.

Even though perfluoroalkylfullerenes (PFAFs) may appear at first sight as a too-specialized group of fullerene compounds in the diverse and vast library of fullerenes, we are convinced that such a focused and detailed review is warranted and timely. First, PFAFs represent by far the largest single family of fullerene derivatives with multiple additions that have well-defined molecular structures, systematically measured fundamental physical properties, and theoretically determined relative stabilities, frontier orbital energies, and molecular geometries. This wealth and breadth of data allowed for in-depth analysis of the structure–property relationship for many dozens of compounds that led to the formulations of the general reactivity and structural principles and trends that are valid for other classes of fullerene derivatives. Finally, emerging areas of practical interest to PFAFs, and in particular, in organic electronics and biomedical research, reinforce the necessity to overview the current state of the art in this field.

This Review is structured as follows: it starts with a section describing synthetic methods used to prepare PFAFs (in most cases as mixtures of products) and separation methods used to isolate purified single isomers; it is then followed by a discussion of molecular structures and physicochemical properties; and it ends with an outlook on future developments. The presence of the glossary of abbreviations and several large tables with a compilation of synthetic (Table 1) structural, nomenclature (Tables 2 and 3), and other data is necessary

due to a large variety of the isomeric structures with subtle differences in the addition patterns that are difficult to discern for an untrained eye. The team has developed a convenient way of referencing PFAF compounds that was used in the original research publications, and that our collaborators from various research fields adopted too, so we share these notations with our readers to simplify their browsing through different sections of this Review. One example below may convince those who dislike jargon and acronyms in academic writing and prefer precision in terminology. The PFAF compound for which the first X-ray structure was determined is an isomer of composition  $C_{60}(CF_3)_{10}$ .<sup>4</sup> Its proper IUPAC-recommended name is 1,3,7,10,14,17,23,28,31,40-decakis(trifluoromethyl)-1,3,7,10,14,17,23,28,31,40-decahydro( $C_{60}-I_h$ )[5,6]fullerene (see Figure 1 for  $C_{60}$  and  $C_{70}$  numbering). It is apparent that

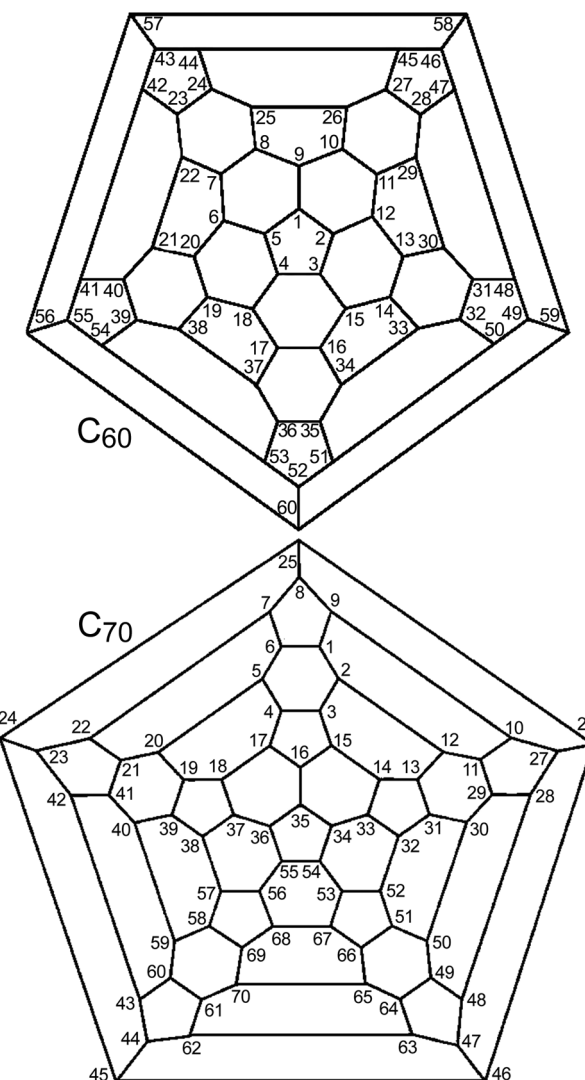


**Figure 1.** Schlegel diagrams of  $C_{60}$  (top) and  $C_{70}$  (bottom) showing IUPAC-approved numbering.

the use of the proper PFAF names is not practical, and even a simplified version, in which only IUPAC numbering is listed before the molecular formula (i.e., 1,3,7,10,14,17,23,28,31,40- $C_{60}(CF_3)_{10}$ ), is also quite cumbersome. In the first publication, it was referred to as  $C_{60}(CF_3)_{10}\text{-}3$ . Number “3” designated the number of the isomer for the  $C_{60}(CF_3)_{10}$  composition; it was

**Table 1. Compilation of Data on Fullerene( $R_F$ )<sub>n</sub> Generation, Synthesis, Isolation, and Characterization, 1991–Present<sup>a</sup>**

entry # [year] <sup>ref</sup>	crude product composition	isolated isomers [purity; yield <sup>b</sup> ]	reagents, rxn. conditions, and separation methods	characterization method(s)
1 [1991] <sup>6</sup>	C <sub>60</sub> (CF <sub>3</sub> )·		C <sub>60</sub> , (CF <sub>3</sub> CO <sub>2</sub> ) <sub>2</sub> , UV, Freon-113	ESR
2 [1993] <sup>7</sup>	C <sub>60</sub> (n-C <sub>6</sub> F <sub>13</sub> ) <sub>9,5</sub> H <sub>2</sub>		C <sub>60</sub> , n-C <sub>6</sub> F <sub>13</sub> I (62 equiv.), TCB, 175 °C, 24 h	ELAN, EC-MS, <sup>c</sup> <sup>1</sup> H/ <sup>13</sup> C/ <sup>19</sup> F NMR, EM, TGA, DSC, contact angle <sup>d,e</sup>
3 [1993] <sup>7</sup>	C <sub>60</sub> (CF <sub>3</sub> ) <sub>1-13</sub> H <sub>1-30</sub> <sup>f</sup>		C <sub>60</sub> , CF <sub>3</sub> I (excess), C <sub>6</sub> H <sub>6</sub> , RT, UV, 30 min	EIAn, EC-MS, NI-FTMS
4 [1993] <sup>7</sup>	C <sub>60</sub> (R <sub>F</sub> ) <sub>3-14</sub>		C <sub>60</sub> , xs R <sub>F</sub> I (R <sub>F</sub> = CF <sub>3</sub> , C <sub>2</sub> F <sub>5</sub> , n-C <sub>3</sub> F <sub>7</sub> , n-C <sub>6</sub> F <sub>13</sub> ), C <sub>6</sub> F <sub>6</sub> , 200 °C, 24 h	EC-MS <sup>g</sup>
5 [1993] <sup>7</sup>	C <sub>60,70</sub> (C <sub>2</sub> F <sub>5</sub> ) <sub>9-16</sub>		C <sub>60,70</sub> , (C <sub>2</sub> F <sub>5</sub> CO <sub>2</sub> ) <sub>2</sub> , Freon-113, 25 °C	EC-MS
6 [1993] <sup>7</sup>	C <sub>60</sub> (n-C <sub>6</sub> F <sub>13</sub> ); C <sub>60</sub> (C <sub>2</sub> F <sub>5</sub> )· and [C <sub>60</sub> (C <sub>2</sub> F <sub>5</sub> ) <sub>2</sub> ]		C <sub>60</sub> , n-C <sub>6</sub> F <sub>13</sub> I, C <sub>2</sub> F <sub>5</sub> I, or (C <sub>2</sub> F <sub>5</sub> CO <sub>2</sub> ) <sub>2</sub> (1–2 equiv.), C <sub>6</sub> H <sub>5</sub> C(CH <sub>3</sub> ) <sub>3</sub> , ca. 130 °C	ESR
7 [1993] <sup>8</sup>	C <sub>60</sub> , C <sub>60</sub> (R <sub>F</sub> )OH, C <sub>60</sub> (O) <sub>2</sub> CR <sub>F</sub> OH, etc.	C <sub>60</sub> (R <sub>F</sub> )OH, C <sub>60</sub> (O) <sub>2</sub> CR <sub>F</sub> OH [n/r; 10–31%]	C <sub>60</sub> , (R <sub>F</sub> CO <sub>2</sub> ) <sub>2</sub> (R <sub>F</sub> = CF <sub>3</sub> , n-C <sub>3</sub> F <sub>7</sub> ), CB, 40 °C, 15 h, GPC	FAB-MS, IR, UV-vis, <sup>13</sup> C/ <sup>19</sup> F NMR
8 [1994] <sup>9</sup>	C <sub>70</sub> (R <sub>F</sub> )·		C <sub>70</sub> , CF <sub>3</sub> Br or (C <sub>2</sub> F <sub>5</sub> CO <sub>2</sub> ) <sub>2</sub> , UV, C <sub>6</sub> H <sub>6</sub>	ESR
9 [1994] <sup>10</sup>		[C <sub>60</sub> R <sub>F</sub> ] <sub>2</sub> [n/r; n/r], C <sub>60</sub> R <sub>F</sub> H [n/r; 41–73% <sup>h</sup> ]	[C <sub>60</sub> R <sub>F</sub> ] <sub>2</sub> or C <sub>60</sub> R <sub>F</sub> OH (R <sub>F</sub> = n-C <sub>3</sub> F <sub>7</sub> , CF <sub>3</sub> , CF <sub>2</sub> Cl), (n-Bu) <sub>3</sub> SnH, C <sub>6</sub> H <sub>6</sub> , 20–80 °C, 15 h; separated using flash chromatography	FAB-MS, <sup>1</sup> H/ <sup>13</sup> C/ <sup>19</sup> F NMR
10 [1994] <sup>11</sup>	C <sub>60</sub> (R <sub>F</sub> )·		C <sub>60</sub> , R <sub>F</sub> I (R <sub>F</sub> = CF <sub>3</sub> , C <sub>2</sub> F <sub>5</sub> , (CF <sub>3</sub> ) <sub>2</sub> CF, (CF <sub>3</sub> ) <sub>3</sub> C), UV, methylcyclohexane or toluene or C <sub>6</sub> H <sub>5</sub> C(CH <sub>3</sub> ) <sub>3</sub>	ESR
11 [1995] <sup>12</sup>	C <sub>60</sub> (CXYZ)·		C <sub>60</sub> , CXYZ-Hal (X, Y, Z = H, F, CH <sub>3</sub> , CF <sub>3</sub> , Hal = Br or I), UV, C <sub>6</sub> H <sub>5</sub> C(CH <sub>3</sub> ) <sub>3</sub>	ESR
12 [1995] <sup>13</sup>	C <sub>60</sub> (CF <sub>3</sub> ) <sub>1-8</sub> H <sub>0-9</sub>		graphite doped with (CF <sub>2</sub> CF <sub>2</sub> ) <sub>n</sub> or NaTFA, electric arc under He (or pure graphite arc-vaporized under He/C <sub>2</sub> F <sub>6</sub> atmosphere)	EI-MS, <sup>19</sup> F NMR
13 [1996] <sup>14</sup>		C <sub>60</sub> (R <sub>F</sub> )H	C <sub>60</sub> , (n-Bu) <sub>3</sub> SnH (5–15 equiv.), R <sub>F</sub> -Hal (6–20 equiv, R <sub>F</sub> = CF <sub>2</sub> COOEt, n-C <sub>6</sub> F <sub>13</sub> , CF <sub>2</sub> Br, n-C <sub>12</sub> F <sub>25</sub> , (CF <sub>2</sub> ) <sub>6</sub> I), C <sub>6</sub> H <sub>6</sub> , reflux, AIBN (0 or 0.1 equiv.)	<sup>1</sup> H/ <sup>13</sup> C/ <sup>19</sup> F NMR, FAB MS
14 [1996] <sup>15</sup>	C <sub>60,70</sub> (R <sub>F</sub> ) <sup>i</sup>		C <sub>60,70</sub> , R <sub>F</sub> Br (1–20 equiv., R <sub>F</sub> = CF <sub>3</sub> or C <sub>2</sub> F <sub>5</sub> ) or (C <sub>2</sub> F <sub>5</sub> CO <sub>2</sub> ) <sub>2</sub> , C <sub>6</sub> H <sub>6</sub> or C <sub>6</sub> H <sub>5</sub> C(CH <sub>3</sub> ) <sub>3</sub> , UV, RT	ESR
15 [1999] <sup>16</sup>	C <sub>60</sub> (CF <sub>3</sub> ) <sub>1-4</sub> H <sub>0-3</sub>		C <sub>60</sub> , Scherer radical, <sup>j</sup> mass spectrometer, in situ	MS
16 [1999] <sup>16</sup>	C <sub>60</sub> (CF <sub>3</sub> ) <sub>18</sub> H <sub>n</sub>		C <sub>60</sub> , Scherer radical, <sup>j</sup> TCB, 200 °C	MS
17 [1999] <sup>17</sup>	[C <sub>60</sub> (R <sub>F</sub> )] <sub>2</sub>	[C <sub>60</sub> (R <sub>F</sub> )] <sub>2</sub> (meso and racemic) [n/r; 37–24%]	C <sub>60</sub> , R <sub>F</sub> I (5 equiv., R <sub>F</sub> = n-C <sub>3</sub> F <sub>7</sub> , n-C <sub>4</sub> F <sub>9</sub> , n-C <sub>6</sub> F <sub>13</sub> ), [R <sub>3</sub> Sn] <sub>2</sub> (5–10 equiv., R = n-Bu, Me), oDCB, UV, RT; GPC separated <sup>k</sup>	<sup>13</sup> C/ <sup>19</sup> F NMR, UV-vis, ESR (thermal homolytic dissociation observed)
18 [1999] <sup>18</sup>	C <sub>60</sub> (C <sub>6</sub> F <sub>13</sub> ) <sub>-5</sub>		C <sub>60</sub> , n-C <sub>6</sub> F <sub>13</sub> I (ca. 60 equiv), TCB, 200 °C, 24 h	EA
19 [2000] <sup>19</sup>	C <sub>60</sub> , C <sub>60</sub> F <sub>18</sub> , etc.	C <sub>s</sub> - and C <sub>1</sub> -C <sub>60</sub> F <sub>17</sub> CF <sub>3</sub> [n/r; 1%] <sup>l</sup>	C <sub>60</sub> , K <sub>2</sub> PtF <sub>6</sub> , 465 °C, ca. 0.1 Torr; sublimed; <sup>m</sup> HPLC separated <sup>n</sup>	HPLC, EI-MS, IR, <sup>19</sup> F/ <sup>19</sup> F- <sup>19</sup> F COSY NMR
20 [2000] <sup>20</sup>	C <sub>60</sub> , C <sub>60</sub> F <sub>18</sub> , etc.	C <sub>s</sub> -C <sub>60</sub> F <sub>17</sub> CF <sub>2</sub> CF <sub>3</sub> [n/r; n/r]; C <sub>s</sub> - and C <sub>1</sub> -C <sub>60</sub> F <sub>17</sub> CF <sub>3</sub> [n/r; n/r]	C <sub>60</sub> , K <sub>2</sub> PtF <sub>6</sub> , 465 °C, ca. 0.1 Torr; <sup>m</sup> HPLC separated <sup>n</sup>	HPLC, EI-MS, IR, <sup>19</sup> F NMR, X-ray
21 [2001] <sup>21</sup>	C <sub>60,70</sub> (CF <sub>3</sub> ) <sub>2-22</sub>		C <sub>60</sub> /C <sub>70</sub> (75/25 mol%), AgTFA (Cu(TFA) <sub>2</sub> , Pd(TFA) <sub>2</sub> , Cr(TFA) <sub>2</sub> ), 300–400 °C, 6 h	EI-MS, <sup>29</sup> LDI-MS
22 [2002] <sup>22</sup>	C <sub>60</sub> , C <sub>60</sub> F <sub>18</sub> , etc. <sup>o</sup>	<b>60-2-1<sup>p</sup></b> [n/r; 1%]	C <sub>60</sub> , K <sub>2</sub> PtF <sub>6</sub> , 470 °C (or AgF at 520 °C), ca. 75 Torr; HPLC <sup>n</sup>	HPLC, EI-MS, <sup>19</sup> F NMR, IR
23 [2002] <sup>23</sup>	C <sub>60</sub> F <sub>m</sub> , C <sub>60</sub> F <sub>7</sub> (CF <sub>3</sub> ) <sup>q</sup> , C <sub>60</sub> F <sub>2</sub> O		C <sub>60</sub> , K <sub>2</sub> PtF <sub>6</sub> , 470 °C, ca. 0.1 Torr; <sup>m</sup> HPLC <sup>n</sup>	HPLC, EI-MS, <sup>19</sup> F/ <sup>19</sup> F- <sup>19</sup> F COSY NMR
24 [2002] <sup>24</sup>		La@C <sub>82</sub> (n-C <sub>8</sub> F <sub>17</sub> ) <sub>2</sub> (7 isomers)	La@C <sub>82</sub> (II), n-C <sub>8</sub> F <sub>17</sub> I (1.8 equiv.), toluene/C <sub>6</sub> F <sub>14</sub> , RT, UV, 15 h; HPLC <sup>r</sup>	HPLC, LDI-MS, ESR, UV-vis
25 [2003] <sup>25</sup>	C <sub>60</sub> (CF <sub>3</sub> ) <sub>n≤20</sub> , C <sub>70</sub> (CF <sub>3</sub> ) <sub>n≤12</sub>	C <sub>60,70</sub> (CF <sub>3</sub> ) <sub>2,4</sub> <sup>s</sup> [n/r; n/r]	C <sub>60,70</sub> , AgTFA (20–23 equiv), 300 °C, ca. 0.04 Torr; HPLC <sup>r</sup>	HPLC, <sup>13</sup> C/ <sup>19</sup> F NMR, EI-MS
26 [2003] <sup>26</sup>	C <sub>60</sub> (CF <sub>3</sub> ) <sub>n≤20</sub> , C <sub>60</sub> (CF <sub>3</sub> ) <sub>n</sub> H <sub>m</sub>	C <sub>60</sub> (CF <sub>3</sub> ) <sub>2,4,6,8,10,12,14</sub> <sup>s</sup> , C <sub>60</sub> (CF <sub>3</sub> ) <sub>5</sub> H [n/r; n/r]	C <sub>60</sub> , AgTFA, 300 °C, ca. 0.04 Torr; C <sub>60</sub> , Scherer radical, <sup>j</sup> TCB, 100 °C, 3 h; HPLC <sup>r</sup>	HPLC, <sup>1</sup> H and <sup>19</sup> F NMR, EI-MS, IR, UV-vis
27 [2003] <sup>27</sup>	C <sub>60</sub> (CF <sub>3</sub> ) <sub>2-10</sub>	<b>60-2-1</b> , <b>60-4-1</b> , <b>60-4-O</b> , <sup>u</sup> <b>60-6-1</b> [80-90%; n/r]	C <sub>60</sub> , AgTFA (4.4 equiv.), 280 °C, 6 h; sublimed; <sup>v</sup> HPLC <sup>r</sup>	HPLC, EI-MS, IR, <sup>19</sup> F/ <sup>19</sup> F- <sup>19</sup> F COSY NMR, AM1 and DFT <sup>36</sup>

Table 1. continued

entry # [year] <sup>ref</sup>	crude product composition	isolated isomers [purity; yield <sup>b</sup> ]	reagents, rxn. conditions, and separation methods	characterization method(s)
28 [2003] <sup>28</sup>	C <sub>60</sub> F <sub>n</sub> (CF <sub>3</sub> ) <sub>m</sub> , C <sub>60</sub> (CF <sub>3</sub> ) <sub>1-18</sub>		C <sub>60</sub> , AgTFA/K <sub>2</sub> PtF <sub>6</sub> or AgTFA, 430 or 300 °C, mass spectrometer effusion cell	MS
29 [2004] <sup>29</sup>	C <sub>70</sub> (CF <sub>3</sub> ) <sub>2-10</sub>	C <sub>70</sub> (CF <sub>3</sub> ) <sub>2,4,6,8,10</sub> <sup>s</sup> [n/r; n/r]	C <sub>70</sub> , AgTFA (12 equiv.), 285–300 °C; HPLC <sup>t</sup>	HPLC, EI-MS, <sup>1</sup> H/ <sup>13</sup> C/ <sup>19</sup> F NMR
30 [2005] <sup>30</sup>		<b>Y-82(9)-1-1</b> , <b>Y-82(9)-3-1</b> , <b>Y-82(9)-5-1</b> , Y <sub>2</sub> @C <sub>80</sub> (CF <sub>3</sub> ) [95+%; <sup>w</sup> n/r]	Y@C <sub>82</sub> , Y <sub>2</sub> @C <sub>80</sub> extract, AgTFA, 400 °C, 10 <sup>-6</sup> Torr, 10 h; HPLC <sup>x</sup>	HPLC, <sup>19</sup> F/ <sup>19</sup> F- <sup>19</sup> F COSY NMR, ATR-IR, MALDI-MS, DFT
31 [2005] <sup>31</sup>	C <sub>60</sub> , C <sub>60</sub> F <sub>18</sub> , C <sub>60</sub> F <sub>n</sub> (CF <sub>3</sub> )	C <sub>s</sub> <sup>r, C<sub>1</sub>-C<sub>60</sub>F<sub>17</sub>(CF<sub>3</sub>), 1,7- and 1,9-C<sub>60</sub>F(CF<sub>3</sub>), C<sub>60</sub>F<sub>3,5,7</sub>(CF<sub>3</sub>), [90–98%; up to 0.4%]</sup>	C <sub>60</sub> , K <sub>2</sub> PtF <sub>6</sub> (6.1 equiv.); 450 °C, vacuum, 6 h; HPLC <sup>x</sup>	HPLC, VT <sup>19</sup> F NMR, MALDI-MS, DFT
32 [2005] <sup>32</sup>	C <sub>60</sub> (CF <sub>3</sub> ) <sub>6-12</sub> , C <sub>70</sub> (CF <sub>3</sub> ) <sub>8-14</sub>	<b>60-4-1</b> , <b>60-6-1</b> , <b>60-10-(1,2,3)</b> [95%; 5%], <b>70-10-1</b> [95%; 27%]	C <sub>60,70</sub> , CF <sub>3</sub> I (760 Torr, flow tube), 420–480 °C, 1–2 h; HPLC <sup>u</sup>	<sup>19</sup> F/ <sup>19</sup> F- <sup>19</sup> F COSY NMR, HPLC, X-ray, EI- and MALDI-MS,
33 [2005] <sup>32</sup>	C <sub>70</sub> (CF <sub>3</sub> ) <sub>8-14</sub>	<b>70-10-1</b> [95%; 27%]	C <sub>70</sub> , CF <sub>3</sub> I (flow tube), 470 °C, 1 h; HPLC <sup>u</sup>	X-ray, AM1 and DFT
34 [2005] <sup>33</sup>		<b>70-8-1</b> [n/r; n/r]	C <sub>70</sub> , AgTFA, 320 °C, 1 h; sublimed; HPLC <sup>u</sup>	X-ray
35 [2005] <sup>34</sup>	C <sub>60</sub> (CF <sub>3</sub> ) <sub>2-10</sub>		C <sub>60</sub> , AgTFA	Knudsen-cell ion-molecule equilibrium MS, HPLC <sup>m</sup>
36 [2006] <sup>35</sup>	C <sub>76,78,84</sub> (CF <sub>3</sub> ) <sub>6-20</sub> , C <sub>59</sub> N(CF <sub>3</sub> ) <sub>6-20</sub> , C <sub>60</sub> F <sub>n</sub> (R <sub>F</sub> ) <sub>m</sub>		C <sub>76,78,84</sub> or C <sub>59</sub> N, AgTFA, 300 °C; C <sub>60</sub> , MnF <sub>3</sub> or K <sub>2</sub> NiF <sub>6</sub> , 510 °C, ca. 0.004 Torr; HPLC <sup>v</sup>	HPLC, MS (ionization method not given)
37 [2006] <sup>36</sup>	C <sub>60</sub> (CF <sub>3</sub> ) <sub>n</sub>	<b>60-12-1</b> [n/r; 84%]	C <sub>60</sub> , CF <sub>3</sub> I (11 equiv., sealed amp.), 440°C, 2 days	X-ray, MALDI-MS, IR
38 [2006] <sup>37</sup>	C <sub>60</sub> (CF <sub>3</sub> ) <sub>n</sub>		C <sub>60</sub> , AgTFA, 320 °C, 1 h; sublimed	EI-MS, EC-MS, TSI-MS, MALDI-MS, ESI-MS
39 [2006] <sup>38</sup>	C <sub>70</sub> (CF <sub>3</sub> ) <sub>n</sub> , C <sub>70</sub> (CF <sub>3</sub> ) <sub>n</sub> H <sub>m</sub> , C <sub>70</sub> (CF <sub>3</sub> ) <sub>n</sub> O <sub>x</sub> , C <sub>70</sub> (CF <sub>3</sub> ) <sub>n</sub> H <sub>m</sub> O <sub>x</sub>	<b>70-2-1</b> , <b>70-4-1</b> , <b>70-6-(1,3)</b> , <b>70-8-(1,2)</b> , <b>70-10-1</b> [ca. 90%; n/r]	C <sub>70</sub> , AgTFA (60, 10, or 5 equiv.), 320–340 °C; sublimed; HPLC <sup>u</sup>	HPLC, MALDI-MS, <sup>19</sup> F/ <sup>19</sup> F- <sup>19</sup> F COSY NMR, Raman, AM1 and DFT
40 [2006] <sup>39</sup>		<b>60-6-2</b> , <b>6-4-O</b> [97+%; n/r]	C <sub>60</sub> , CF <sub>3</sub> I (flow tube), 550 °C; HPLC <sup>u</sup>	HPLC, APCI-MS, UV-vis, Raman, VT <sup>19</sup> F NMR, X-ray, DFT
41 [2006] <sup>39</sup>		<b>6-4-O-C<sub>2</sub>F<sub>5</sub></b> [97+%; n/r]	C <sub>60</sub> , Cu powder, C <sub>2</sub> F <sub>5</sub> I (flow tube), 430 °C; HPLC <sup>u</sup>	HPLC, APCI-MS, UV-vis, Raman, <sup>19</sup> F NMR, X-ray, DFT
42 [2006] <sup>40</sup>		<b>60-6-3-C<sub>2</sub>F<sub>5</sub></b> , <b>60-8-6-C<sub>2</sub>F<sub>5</sub></b> [80–90+%; ca. 1%]	C <sub>60</sub> , Cu powder, C <sub>2</sub> F <sub>5</sub> I (flow tube), 400–430 °C; HPLC <sup>u</sup>	HPLC, VT <sup>19</sup> F NMR, X-ray
43 [2006] <sup>41</sup>		C <sub>60</sub> F <sub>7</sub> (CF <sub>3</sub> ) [n/r; n/r]	C <sub>60</sub> , KMnF <sub>4</sub> (28–30 equiv.), 470 °C; HPLC <sup>x</sup>	HPLC, MALDI-MS, DFT, <sup>19</sup> F NMR, IR, Raman
44 [2006] <sup>42</sup>		<b>70-12-1</b> [n/r; n/r]	C <sub>70</sub> , CF <sub>3</sub> I (flow tube), 420–450 °C; HPLC <sup>u</sup>	X-ray
45 [2006] <sup>43</sup>		<b>60-10-2</b> [n/r; n/r]	C <sub>60</sub> , CF <sub>3</sub> I (flow tube), 460 °C; HPLC <sup>u</sup>	X-ray
46 [2006] <sup>43a</sup>		<b>60-10-4</b> [n/r; n/r]	C <sub>60</sub> , CF <sub>3</sub> I (flow tube), 460 °C; HPLC <sup>u</sup>	X-ray
47 [2006] <sup>44</sup>		<b>60-8-2</b> [n/r; n/r]	C <sub>60</sub> , CF <sub>3</sub> I (flow tube), 460 °C; HPLC <sup>u</sup>	X-ray
48 [2006] <sup>45</sup>		<b>70-12-2</b> [n/r; n/r]	C <sub>70</sub> , CF <sub>3</sub> I (flow tube), 420–450 °C; HPLC <sup>u</sup>	X-ray
49 [2006] <sup>46</sup>	C <sub>70</sub> (CF <sub>3</sub> ) <sub>12-20</sub>	<b>70-14-(2,3,4)</b> [n/r; n/r]	C <sub>70</sub> , CF <sub>3</sub> I (5 bar, sealed amp.), 390 °C, 24 h; HPLC <sup>u</sup>	HPLC, X-ray, MALDI-MS, AM1 and DFT
50 [2006] <sup>47</sup>		<b>70-6-3</b> [n/r; n/r]	C <sub>70</sub> , AgTFA (10 equiv), 320 °C; sublimed; HPLC <sup>u</sup>	X-ray, AM1 and DFT
51 [2006] <sup>48</sup>		<b>70-12-(1,2)</b> [n/r; n/r]	C <sub>70</sub> , CF <sub>3</sub> I (5 bar, sealed amp.), 390 °C, 24 h; HPLC <sup>u</sup>	HPLC, MALDI-MS, X-ray, AM1 and DFT
52 [2006] <sup>49</sup>		<b>70-16-1</b> , <b>70-18-1</b> [n/r; n/r]	C <sub>70</sub> , CF <sub>3</sub> I (5 bar, sealed amp.), 390 °C, 24 h; HPLC <sup>u</sup>	HPLC, MALDI-MS, X-ray, AM1 and DFT
53 [2006] <sup>50</sup>		C <sub>2</sub> -(C <sub>74-D<sub>3</sub>h</sub> )(CF <sub>3</sub> ) <sub>12</sub> , C <sub>s</sub> -(C <sub>76-T<sub>d</sub>(2)</sub> )(CF <sub>3</sub> ) <sub>12</sub> , C <sub>2</sub> -(C <sub>78-D<sub>3</sub>h(5)</sub> )(CF <sub>3</sub> ) <sub>12</sub> , C <sub>s</sub> -(C <sub>80-C<sub>2</sub>v(5)</sub> )(CF <sub>3</sub> ) <sub>12</sub> , C <sub>2</sub> -(C <sub>82-C<sub>2</sub>v(5)</sub> )(CF <sub>3</sub> ) <sub>12</sub> , etc. [50-97%; n/r]	mixture of higher fullerenes, Cu powder, CF <sub>3</sub> I (flow tube), 500 °C, 5 h; HPLC <sup>u</sup>	HPLC, APCI-MS, <sup>19</sup> F/ <sup>19</sup> F- <sup>19</sup> F COSY NMR, X-ray, DFT

Table 1. continued

entry # [year] <sup>ref</sup>	crude product composition	isolated isomers [purity; yield <sup>b</sup> ]	reagents, rxn. conditions, and separation methods	characterization method(s)
54 [2007] <sup>51</sup>		<b>60-16-(1,2,3), 60-18-1</b> [n/r; n/r]	C <sub>60</sub> , CF <sub>3</sub> I (5 bar, sealed amp.), 380–400 °C, 18–48 h; HPLC <sup>n</sup>	HPLC, MALDI-MS, X-ray, AM1 and DFT
55 [2007] <sup>5</sup>		<b>60-2-1, 60-4-1, 60-6-(1,2), 60-8-(1,2,3,4,5), 60-10-(1,2,3,4,5,6), 60-12-(1,2,3)</b> [up to 95%; n/r]	C <sub>60</sub> , CF <sub>3</sub> I (flow tube reactor), 460 °C, 2 h; HPLC <sup>n</sup>	HPLC, CV, ESR, UV-vis, fluorescence spectroscopy, <sup>19</sup> F NMR, X-ray, DFT
56 [2007] <sup>52</sup>		<b>60-12-3, 60-14-(1,2)</b> [n/r; n/r]	C <sub>60</sub> (or 60-12-1), CF <sub>3</sub> I (sealed ampoule), 400–440 °C (or 320–360 °C), 2–4 d (or 7–20 d); HPLC <sup>n</sup>	HPLC, UV-vis, X-ray, MALDI-MS, DFT
57 [2007] <sup>53</sup>		<b>60-8-1</b> [n/r; n/r]	C <sub>60</sub> , CF <sub>3</sub> I (5 bar, sealed amp.), 420 °C, 6 h; HPLC <sup>n</sup>	HPLC, X-ray, DFT
58 [2007] <sup>54</sup>		<b>60-8-(3,6,7,8,9,10)-C<sub>2</sub>F<sub>5</sub>, 60-10-(6,7)-C<sub>2</sub>F<sub>5</sub></b> [n/r; n/r]	C <sub>60</sub> , C <sub>2</sub> F <sub>5</sub> I (sealed amp.), 380–440 °C, 40–70 h; HPLC <sup>n</sup>	HPLC, MALDI-MS, X-ray, DFT
59 [2007] <sup>55</sup>	C <sub>70</sub> (C <sub>2</sub> F <sub>5</sub> ) <sub>8,10,12</sub>	<b>70-10-(1,8,9,10,11,12,13)-C<sub>2</sub>F<sub>5</sub></b> [n/r; n/r]	C <sub>70</sub> , C <sub>2</sub> F <sub>5</sub> I (sealed ampoule), 350 °C, 40–60 h; HPLC <sup>n</sup>	HPLC, MALDI-MS, X-ray
60 [2007] <sup>56</sup>		<b>60-12-2</b> [90%; ]	C <sub>60</sub> , CF <sub>3</sub> I (flow tube), 500 °C; HPLC <sup>n</sup>	HPLC, APCI-MS, <sup>19</sup> F NMR, X-ray
61 [2007] <sup>57</sup>		C <sub>2-p</sub> <sup>11</sup> -(C <sub>74-D<sub>3h</sub></sub> )(CF <sub>3</sub> ) <sub>12</sub> , C <sub>2-p</sub> <sup>11</sup> -(C <sub>78-D<sub>3h</sub></sub> )(CF <sub>3</sub> ) <sub>12</sub> [n/r; n/r]	mixture of higher fullerenes, Cu powder, CF <sub>3</sub> I (flow tube), 500 °C, 5 h; HPLC <sup>n,61</sup>	HPLC, <sup>19</sup> F NMR, X-ray
62 [2007] <sup>58</sup>		<b>60-8-1</b> [n/r; n/r]	C <sub>60</sub> , CF <sub>3</sub> I (flow tube), 460 °C; HPLC <sup>n,63</sup>	X-ray
63 [2007] <sup>59</sup>		<b>70-14-1</b> [n/r; n/r]	C <sub>70</sub> , CF <sub>3</sub> I, high temperature	X-ray
64 [2007] <sup>60</sup>		<b>60-6-5-i-C<sub>3</sub>F<sub>7</sub></b> [n/r; n/r]	C <sub>60</sub> , i-C <sub>3</sub> F <sub>7</sub> I (sealed amp.), 300–400 °C; HPLC <sup>n</sup>	X-ray
65 [2007] <sup>61</sup>	C <sub>60</sub> (CF <sub>2</sub> ) <sub>1-3</sub>	[6,6]-, [5,6]-C <sub>60</sub> (CF <sub>2</sub> ) [98+%; <sup>z</sup> 19%]	C <sub>60</sub> , CF <sub>2</sub> ClCOONa, oDCB, 18-crown-6, 1–25 h reflux; HPLC <sup>n</sup>	HPLC, MALDI-MS, IR, UV-vis, <sup>13</sup> C/ <sup>19</sup> F NMR, DFT
66 [2007] <sup>62</sup>		[6,6]-, [5,6]-C <sub>60</sub> (CF <sub>2</sub> ), C <sub>60</sub> (CF <sub>2</sub> ) <sub>2</sub> [n/r; 45%]	C <sub>60</sub> , CF <sub>2</sub> ClCOONa, oDCB, (n-Bu) <sub>4</sub> NBr or 18-crown-6, 1–25 h reflux; HPLC <sup>n</sup>	HPLC, MALDI-MS, IR, <sup>13</sup> C and <sup>19</sup> F NMR, X-ray, DFT
67 [2007] <sup>63</sup>	C <sub>60</sub> (CF <sub>3</sub> ) <sub>2-10</sub>	<b>60-2-1, 60-4-(1,2), 60-4-O, 60-6-(1,6,7), 60-10-2</b> [n/r; up to 12%]	C <sub>60</sub> , AgTFA (3.4–36 equiv), 300–340 °C, 1–3 h, sublimed; HPLC <sup>n</sup>	HPLC, MALDI-MS, UV-vis, X-ray, DFT
68 [2007] <sup>64</sup>	Sc <sub>3</sub> N@C <sub>80</sub> (CF <sub>3</sub> ) <sub>2-12</sub>	(Sc <sub>3</sub> N@C <sub>80</sub> -I <sub>h</sub> )(CF <sub>3</sub> ) <sub>2</sub> , (Sc <sub>3</sub> N@C <sub>80</sub> -D <sub>3h</sub> )(CF <sub>3</sub> ) <sub>2</sub> [n/r; n/r]	Sc <sub>3</sub> N@C <sub>80</sub> (9/1 mixture of I <sub>h</sub> and D <sub>3h</sub> isomers), CF <sub>3</sub> I (flow tube), 510–530 °C, 4 h; HPLC <sup>n</sup>	HPLC, MALDI-MS, CV; <sup>19</sup> F NMR, UV-vis, DFT
69 [2007] <sup>65</sup>	C <sub>60</sub> (C <sub>2</sub> F <sub>4</sub> ) <sub>1-18</sub> , C <sub>70</sub> (C <sub>2</sub> F <sub>4</sub> ) <sub>1-14</sub>	C <sub>60</sub> (C <sub>4</sub> F <sub>8</sub> ) <sub>2-1,2</sub> , C <sub>60</sub> (C <sub>4</sub> F <sub>8</sub> ) <sub>6</sub> , C <sub>70</sub> (C <sub>2</sub> F <sub>4</sub> ) <sub>2</sub> [n/r; n/r]	C <sub>60</sub> or C <sub>70</sub> , I(CF <sub>2</sub> ) <sub>2</sub> I (sealed amp.), 400–450 °C, 4–24 h; HPLC <sup>n</sup>	HPLC, MALDI-MS, X-ray
70 [2007] <sup>66</sup>		<b>Y-82(9)-1-1, Y-82(9)-3-1, Y-82(9)-5-(1,2), Ce-82(9)-5-1,2,3</b> [n/r; n/r]	Y@C <sub>82</sub> or Ce@C <sub>82</sub> extract, AgTFA, 400 °C, 10 h, 10 <sup>-6</sup> Torr; HPLC <sup>x</sup>	HPLC, MALDI-MS, UV-vis, <sup>19</sup> F NMR
71 [2008] <sup>67</sup>		60-12-4 [n/r; n/r]	C <sub>60</sub> , CF <sub>3</sub> I (flow tube), 500 °C, 2 h; HPLC <sup>n</sup>	X-ray
72 [2008] <sup>68</sup>		<b>70-2-(1,2), 70-4-1, 70-4-O, 70-6-(1,2,3), 70-8-(1,2), 70-10-(1,2,3,4,5), 70-12-(1,2,3,4)</b> [ca. 90%; up to 55% for 70-10-1]	C <sub>70</sub> , CF <sub>3</sub> I (flow tube), 420–550 °C, 4 h; HPLC <sup>n</sup>	HPLC, MALDI-MS, APCI-MS, UV-vis, <sup>19</sup> F NMR, CV, DFT
73 [2008] <sup>69</sup>		<b>84-12-2</b> [98%; n/r]	mixture of HHFs, CF <sub>3</sub> I (flow tube), 520–550 °C; HPLC <sup>n</sup>	HPLC, APCI-MS, <sup>19</sup> F/ <sup>19</sup> F COSY NMR, X-ray, DFT
74 [2008] <sup>70</sup>		<b>76-6-1, 76-8-(1,2), 76-10-(1,2,3,4,5), 76-12-2, 78-8-1, 78-10-(1,2,3), 78-12-2, 78-14-1, 84-10-1, 84-12-(1,3), 84-14-1, 90-12-(1,2)</b> [ca. 90%; n/r]	C <sub>76,78,84,90</sub> , CF <sub>3</sub> I (flow tube), 520–550 °C, 2 h; HPLC <sup>n</sup>	HPLC, APCI-MS, MALDI-MS, <sup>19</sup> F NMR, X-ray, DFT
75 [2008] <sup>71</sup>	C <sub>70</sub> (CF <sub>3</sub> ) <sub>10-14</sub>	<b>70-8-(1,2)</b> [n/r; n/r]	C <sub>70</sub> , C <sub>70</sub> (CF <sub>3</sub> ) <sub>12-18</sub> (sealed amp.), 440–450 °C, 60 h; HPLC <sup>n</sup>	HPLC, MALDI-MS, IR, X-ray
76 [2008] <sup>72</sup>		<b>70-8-(3,4,5,6)-n-C<sub>3</sub>F<sub>7</sub></b> [n/r; n/r]	C <sub>70</sub> , n-C <sub>3</sub> F <sub>7</sub> I (sealed amp.), 300–310 °C, 90 h; HPLC <sup>n</sup>	HPLC, MALDI-MS, X-ray
77 [2008] <sup>73</sup>	C <sub>60</sub> F <sub>12-18</sub> (CF <sub>3</sub> ) <sub>5-13</sub>	C <sub>60</sub> F <sub>18</sub> (CF <sub>3</sub> ) <sub>6</sub> , C <sub>60</sub> F <sub>16</sub> (CF <sub>3</sub> ) <sub>6</sub> [n/r; n/r]	C <sub>60</sub> F <sub>18</sub> , CF <sub>3</sub> I (5 bar, sealed amp.), 380–420 °C, 2–7 d; HPLC <sup>n</sup>	HPLC, MALDI-MS, X-ray
78 [2008] <sup>74</sup>		<b>60-12-(5,6), 60-14-3</b> [n/r; n/r]	C <sub>60</sub> /C <sub>70</sub> mixture, CF <sub>3</sub> I (sealed amp.), 380–440 °C, 40–70 h; HPLC <sup>n</sup>	HPLC, MALDI-MS, <sup>19</sup> F/ <sup>19</sup> F-COSY NMR, X-ray, AM1 and DFT
79 [2008] <sup>75</sup>		Gd@C <sub>82</sub> (CF <sub>3</sub> ) <sub>5-1,2</sub>	Gd@C <sub>82</sub> /Gd@C <sub>80</sub> /Gd <sub>2</sub> @C <sub>82</sub> , AgTFA,	HPLC, MALDI-MS,

Table 1. continued

entry # [year] <sup>ref</sup>	crude product composition	isolated isomers [purity; yield <sup>b</sup> ]	reagents, rxn. conditions, and separation methods	characterization method(s)
		Gd <sub>2</sub> @C <sub>80</sub> (CF <sub>3</sub> ) <sub>1,3</sub> [n/r; n/r]	300–400 °C, 10 <sup>-6</sup> Torr, 6–10 h; HPLC <sup>x</sup>	UV-vis
80 [2008] <sup>76</sup>	C <sub>70</sub> (CF <sub>3</sub> ) <sub>n</sub>	<b>70-10-1</b> [n/r; 32%]	C <sub>70</sub> (CF <sub>3</sub> ) <sub>10-18</sub> (sealed amp.), 400 °C, 40 h; HPLC <sup>n</sup>	HPLC, UV-vis
81 [2009] <sup>77</sup>	C <sub>70</sub> (C <sub>2</sub> F <sub>5</sub> ) <sub>10,12</sub>	<b>70-10-(14,15)-C<sub>2</sub>F<sub>5</sub></b> [n/r; n/r]	C <sub>70</sub> , C <sub>2</sub> F <sub>5</sub> I (sealed ampoule), ca. 360 °C, 60–80 h; HPLC <sup>n</sup>	HPLC, MALDI-MS, X-ray, DFT
82 [2009] <sup>77</sup>	C <sub>70</sub> (C <sub>2</sub> F <sub>5</sub> ) <sub>8</sub>	<b>70-8-(1,3,4,5,6,7,8,9,10)-C<sub>2</sub>F<sub>5</sub></b> [n/r; n/r]	C <sub>70</sub> (C <sub>2</sub> F <sub>5</sub> ) <sub>10,12</sub> , 280–300 °C (annealing), 80–90 h; HPLC <sup>n</sup>	HPLC, MALDI-MS, X-ray, DFT
83 [2009] <sup>78</sup>		C <sub>1-p<sup>5</sup>,p,p-(C<sub>78-C<sub>2</sub>,(2)(C<sub>2</sub>F<sub>5</sub>)<sub>10</sub>,</sub></sub> [n/r; n/r]	C <sub>76-96</sub> , C <sub>2</sub> F <sub>5</sub> I (sealed amp.), 250 °C, 4–5 d; HPLC <sup>n</sup>	HPLC, MALDI-MS, X-ray
84 [2009] <sup>79</sup>		<b>70-2-1, 70-8-4, 70-14-5</b> [n/r; n/r]	C <sub>70</sub> , C <sub>70</sub> (CF <sub>3</sub> ) <sub>14-18</sub> , 440–450 °C (annealing), 100 h; HPLC <sup>n</sup>	HPLC, MALDI-MS, X-ray
85 [2009] <sup>79</sup>		<b>70-14-5</b> [n/r; n/r]	C <sub>70</sub> (CF <sub>3</sub> ) <sub>12-18</sub> , 350–380 °C (annealing), 40 h; HPLC <sup>n</sup>	HPLC, MALDI-MS, X-ray
86 [2009] <sup>80</sup>	C <sub>60</sub> (i-C <sub>3</sub> F <sub>7</sub> ) <sub>2-8</sub> , C <sub>60</sub> (CF <sub>3</sub> ) <sub>n</sub> (i-C <sub>3</sub> F <sub>7</sub> ) <sub>m</sub>	<b>60-4-3-(CF<sub>3</sub>/i-C<sub>3</sub>F<sub>7</sub>)</b> , <sup>aa</sup> <b>60-6-(3,5,8)-i-C<sub>3</sub>F<sub>7</sub></b> , <b>60-8-11-i-C<sub>3</sub>F<sub>7</sub></b> [n/r; n/r]	C <sub>60</sub> , i-C <sub>3</sub> F <sub>7</sub> I, Cu powder (sealed amp.), 260–290 °C, 1–3 d; HPLC <sup>n</sup>	HPLC, MALDI-MS, X-ray, DFT
87 [2009] <sup>81</sup>	C <sub>86</sub> (CF <sub>3</sub> ) <sub>n</sub> <sub>≤20</sub>	<b>86(17)-16-(1,2), 86(17)-18-1</b> [n/r; n/r]	mixture of HHFs, CF <sub>3</sub> I (sealed amp.), 400–420 °C; HPLC <sup>n</sup>	HPLC, MALDI-MS, X-ray
88 [2009] <sup>82</sup>		<b>60-18-2</b> [n/r; n/r]	C <sub>60</sub> , CF <sub>3</sub> I (sealed amp.), 440 °C, 2–3 d; sublimed	HPLC, <sup>m</sup> MALDI-MS, <sup>19</sup> F/ <sup>19</sup> F COSY NMR, X-ray
89 [2009] <sup>83</sup>		<b>84(22)-16-1, 84(4)-12-1</b> [n/r; n/r]	C <sub>76-96</sub> , CF <sub>3</sub> I (sealed amp.), 400–420 °C, 2–3 d; HPLC <sup>n</sup>	HPLC, MALDI-MS, X-ray
90 [2009-2012] <sup>83-84</sup>		<b>84(23)-12-1-C<sub>2</sub>F<sub>5</sub>, 84(22)-12-1-C<sub>2</sub>F<sub>5</sub>,</b> <b>84(18)-12-1-C<sub>2</sub>F<sub>5</sub>, 84(16)-12-1-C<sub>2</sub>F<sub>5</sub>,</b> <b>84(16)-12-2-C<sub>2</sub>F<sub>5</sub>, 84(11)-12-1-C<sub>2</sub>F<sub>5</sub></b> [n/r; n/r],	C <sub>76-96</sub> , C <sub>2</sub> F <sub>5</sub> I (sealed amp.), 250 °C, 4–5 d; HPLC <sup>n</sup>	HPLC, MALDI-MS, X-ray
91 [2009] <sup>84a</sup>		<b>94(61)-20-1</b> [n/r; n/r]	C <sub>76-96</sub> , CF <sub>3</sub> I (6 bar, sealed amp.), 400–420 °C, 3 d; HPLC <sup>n</sup>	HPLC, X-ray
92 [2009] <sup>84a</sup>		<b>96(145)-12-1-C<sub>2</sub>F<sub>5</sub></b> [n/r; n/r]	C <sub>76-96</sub> , C <sub>2</sub> F <sub>5</sub> I (20 bar, sealed amp.), 250 °C, 5 d; HPLC <sup>n</sup>	HPLC, X-ray
93 [2009] <sup>85</sup>	C <sub>60,70</sub> (CF <sub>3</sub> ) <sub>n</sub> H <sub>m</sub>		C <sub>60</sub> (or C <sub>70</sub> ), Hg(TFA) <sub>2</sub> , 300–310 °C, mass spectrometer ionization chamber	EI-MS
94 [2009] <sup>86</sup>		<b>88(33)-18-1, 92(82)-16-1</b> [n/r; n/r]	C <sub>76-96</sub> , CF <sub>3</sub> I (6 bar, sealed amp.), 400–420 °C, 2–3 d; HPLC <sup>n</sup>	HPLC, MALDI-MS, X-ray
95 [2009] <sup>87</sup>		<b>70-12-3, 70-14-(x,y,z), 70-16-x</b> [n/r; n/r]	(a) C <sub>70</sub> (or 70-12-(1,2)) CF <sub>3</sub> I (5 bar, sealed amp.), 350–390 °C; HPLC <sup>n</sup> (b) C <sub>70</sub> (CF <sub>3</sub> ) <sub>12,14</sub> , annealed at 340–380 °C, ca. 4.5 d; HPLC <sup>n</sup>	HPLC, MALDI-MS, X-ray, AM1 and DFT
96 [2009] <sup>88</sup>		<b>Sc<sub>3</sub>N-80(7)-14-1, Sc<sub>3</sub>N-80(7)-16-1</b> [n/r; n/r]	Sc <sub>3</sub> N@C <sub>80-I</sub> , AgTFA (62 equiv), 350 °C, 2.5 h; HPLC <sup>n</sup>	HPLC, APPI-MS, X-ray, DFT
97 [2009] <sup>89</sup>	C <sub>60</sub> (C <sub>2</sub> F <sub>4</sub> ) <sub>1-14</sub>	C <sub>60</sub> (C <sub>4</sub> F <sub>8</sub> ) <sub>2-3</sub> , C <sub>60</sub> (C <sub>4</sub> F <sub>8</sub> ) <sub>3</sub> , C <sub>60</sub> (C <sub>4</sub> F <sub>8</sub> ) <sub>4</sub> , C <sub>60</sub> (C <sub>4</sub> F <sub>8</sub> ) <sub>6-1,2</sub> [n/r; n/r]	C <sub>60</sub> , I(CF <sub>2</sub> ) <sub>2,4</sub> I (sealed amp.), 350 or 450 °C; 16 h or 45 min; HPLC <sup>n</sup>	HPLC, MALDI-MS, X-ray
98 [2010] <sup>90</sup>		<b>76(x)-14-1, 76(x)-16-1, 76(x)-18-(1,2)</b> [n/r; n/r]	C <sub>76-96</sub> , CF <sub>3</sub> I (6 bar, sealed amp.), 380–400 °C, 50–100 h; HPLC <sup>n</sup>	HPLC, MALDI-MS, X-ray, DFT
99 [2010] <sup>91</sup>	C <sub>60</sub> (CF <sub>3</sub> ) <sub>15,17</sub>		C <sub>60</sub> (CF <sub>3</sub> ) <sub>12-18</sub> , CF <sub>3</sub> I (sealed quartz amp.), UV, 24 h; HPLC <sup>n</sup>	HPLC, MALDI-MS, ESR
100 [2010] <sup>92</sup>	(C <sub>60</sub> ) <sub>2</sub> (CF <sub>3</sub> ) <sub>n</sub> (CF <sub>2</sub> ) <sub>m</sub>		Na <sub>1,3,10</sub> C <sub>60</sub> , CF <sub>3</sub> I (sealed amp.), 300–420 °C	MALDI-MS
101 [2010] <sup>92</sup>	(C <sub>60</sub> ) <sub>2</sub> (CF <sub>3</sub> ) <sub>n</sub> (CF <sub>2</sub> ) <sub>m</sub>		C <sub>60</sub> , C <sub>60</sub> (CF <sub>3</sub> ) <sub>12,14,16,18</sub> (sealed amp.), 430–440 °C; HPLC <sup>n</sup>	HPLC, MALDI-MS, <sup>19</sup> F NMR
102 [2010] <sup>93</sup>		<b>Sc<sub>3</sub>N-80(7)-2-1, Sc<sub>3</sub>N-80(7)-4-1,</b> <b>Sc<sub>3</sub>N-80(7)-8-(1,2), Sc<sub>3</sub>N-80(7)-10-1,</b> <b>Sc<sub>3</sub>N-80(7)-12-(1,2), Sc<sub>3</sub>N-80(7)-14-(1,2), Sc<sub>3</sub>N-80(7)-16-(1,2)</b> [n/r; n/r]	(a) C <sub>60</sub> /C <sub>70</sub> /Sc <sub>3</sub> N@C <sub>80</sub> (crude extract), Cu powder, CF <sub>3</sub> I (flow tube), 430–530 °C; HPLC <sup>n</sup> (b) Sc <sub>3</sub> N@C <sub>80-I</sub> , AgTFA, 350 °C, 2.5 h; HPLC <sup>n</sup>	HPLC, CV, APCI-MS, APPI-MS, UV-vis, X-ray, <sup>19</sup> F NMR, AM1 and DFT
103 [2010] <sup>93</sup>	Er <sub>3</sub> N@C <sub>80</sub> (CF <sub>3</sub> ) <sub>12,14</sub>		Er <sub>3</sub> N@C <sub>80-I</sub> (7), CF <sub>3</sub> I (GTGS reactor), 500 °C, 5 h	APPI-MS
104 [2010] <sup>94</sup>	C <sub>60</sub> (i-C <sub>3</sub> F <sub>7</sub> ) <sub>2,4,6</sub> , C <sub>70</sub> (i-C <sub>3</sub> F <sub>7</sub> ) <sub>2,4</sub>	<b>60-4-(4,5)-i-C<sub>3</sub>F<sub>7</sub>,</b> <b>60-6-(3,5,8,9)-i-C<sub>3</sub>F<sub>7</sub>,</b> <b>60-8-11-i-C<sub>3</sub>F<sub>7</sub>, 70-2-(1,2)-i-C<sub>3</sub>F<sub>7</sub>,</b>	(a) C <sub>60,70</sub> , i-C <sub>3</sub> F <sub>7</sub> I, toluene (or C <sub>6</sub> F <sub>6</sub> ), UV, 1–7 d; HPLC <sup>n</sup> (b) C <sub>60,70</sub> , Cu powder, i-C <sub>3</sub> F <sub>7</sub> I/N <sub>2</sub> (flow tube),	HPLC, APCI-MS, CV, <sup>19</sup> F NMR, X-ray, DFT

Table 1. continued

entry # [year] <sup>ref</sup>	crude product composition	isolated isomers [purity; yield <sup>b</sup> ]	reagents, rxn. conditions, and separation methods	characterization method(s)
		<b>70-4-(2,34,5,6)-i-C<sub>3</sub>F<sub>7</sub></b> [n/r; n/r]	320–500 °C, 2–9 h; HPLC <sup>a</sup> (c) C <sub>60</sub> , i-C <sub>3</sub> F <sub>7</sub> I (sealed amp.), 290–416 °C; 1 d; HPLC <sup>a</sup>	
105 [2010] <sup>95</sup>	C <sub>60,70</sub> (R <sub>F</sub> ) <sub>n</sub>	<b>60-10-6-C<sub>2</sub>F<sub>5</sub>,</b> <b>70-10-8-C<sub>2</sub>F<sub>5</sub>,</b> <b>70-12-5-C<sub>2</sub>F<sub>5</sub></b> [n/r; n/r]	(a) C <sub>60</sub> or C <sub>60</sub> (CF <sub>3</sub> ) <sub>8-12</sub> , CF <sub>3</sub> I, C <sub>6</sub> F <sub>6</sub> , ca. 20 °C, 2–7 d, UV; HPLC <sup>a</sup> (b) C <sub>60</sub> , Cu powder, C <sub>2</sub> F <sub>5</sub> I (flow tube), 400–500 °C; HPLC <sup>a</sup> (c) C <sub>60,70</sub> , R <sub>F</sub> I/N <sub>2</sub> (flow tube, R <sub>F</sub> = CF <sub>3</sub> , C <sub>2</sub> F <sub>5</sub> , n-C <sub>3</sub> F <sub>7</sub> , n-C <sub>4</sub> F <sub>9</sub> , n-C <sub>6</sub> F <sub>13</sub> ), 320–500 °C; HPLC <sup>a</sup> (d) C <sub>60,70</sub> , R <sub>F</sub> I (sealed amp., R <sub>F</sub> = CF <sub>3</sub> , C <sub>2</sub> F <sub>5</sub> , n-C <sub>3</sub> F <sub>7</sub> , n-C <sub>4</sub> F <sub>9</sub> , n-C <sub>6</sub> F <sub>13</sub> ), 320–550 °C, 1–2 d; HPLC <sup>a</sup>	HPLC, APCI-MS, APPI-MS, UV-vis, CV, X-ray, DFT
106 [2010] <sup>96</sup>	C <sub>82</sub> (CF <sub>3</sub> ) <sub>12-20</sub>	<b>82(3)-12-1, 82(3)-18-(1,2)</b> [n/r; n/r]	C <sub>76-96</sub> , CF <sub>3</sub> I (sealed amp.), 400–420 °C; HPLC <sup>a</sup>	HPLC, MALDI-MS, X-ray
107 [2010] <sup>97</sup>	C <sub>70</sub> (C <sub>2</sub> F <sub>4</sub> ), C <sub>70</sub> (C <sub>4</sub> F <sub>8</sub> ) <sub>1-6</sub>	C <sub>70</sub> (C <sub>2</sub> F <sub>4</sub> ), C <sub>70</sub> (C <sub>4</sub> F <sub>8</sub> ) <sub>1-2</sub> , C <sub>70</sub> (C <sub>4</sub> F <sub>8</sub> ) <sub>2-1</sub> , C <sub>70</sub> (C <sub>4</sub> F <sub>8</sub> ) <sub>4-1</sub> , C <sub>70</sub> (C <sub>4</sub> F <sub>8</sub> ) <sub>5-1,2</sub> , C <sub>70</sub> (C <sub>4</sub> F <sub>8</sub> ) <sub>6-1,2</sub> [n/r; n/r]	C <sub>70</sub> , I(CF <sub>2</sub> ) <sub>2</sub> I (sealed amp.), 380–420 °C; 6–24 h (or I(CF <sub>2</sub> ) <sub>4</sub> I, 450–500 °C, 40–45 min); HPLC <sup>a</sup>	HPLC, MALDI-MS, X-ray, DFT
108 [2010] <sup>98</sup>	C <sub>70</sub> (C <sub>3</sub> F <sub>7</sub> ) <sub>n</sub>	C <sub>70</sub> (n-C <sub>3</sub> F <sub>7</sub> ) <sub>4-1</sub> , C <sub>70</sub> (i-C <sub>3</sub> F <sub>7</sub> ) <sub>4-1,2,3</sub> , C <sub>70</sub> (n-C <sub>3</sub> F <sub>7</sub> ) <sub>8-3,5</sub> , C <sub>70</sub> (n-C <sub>3</sub> F <sub>7</sub> ) <sub>6</sub> O [n/r; n/r]	C <sub>70</sub> , n-C <sub>3</sub> F <sub>7</sub> I, 300–310 °C, 40–90 h (or i-C <sub>3</sub> F <sub>7</sub> I, 250 °C, 38 h, sealed amp.); HPLC <sup>a</sup>	HPLC, MALDI-MS, X-ray, DFT
109 [2010] <sup>99</sup>		<b>70-10-1</b> [98%; 71–79%]	C <sub>70</sub> , CF <sub>3</sub> I (flow tube), Cu powder, 520–550 °C; HPLC <sup>a</sup>	HPLC, <sup>19</sup> F NMR, UV-vis
110 [2011] <sup>100</sup>	Sc <sub>3</sub> N@C <sub>80</sub> (CF <sub>3</sub> ) <sub>14,16,18</sub>	<b>Sc<sub>3</sub>N-80(7)-14-(1,3,4,5),</b> <b>Sc<sub>3</sub>N-80(7)-16-2,</b> <b>Sc<sub>3</sub>N-80(6)-18-1</b> [n/r; n/r]	Sc <sub>3</sub> N@C <sub>80</sub> -I <sub>b</sub> (7) or Sc <sub>3</sub> N@C <sub>80</sub> -D <sub>5b</sub> (6), CF <sub>3</sub> I (sealed amp.), 400 °C, 2 d; HPLC <sup>a</sup>	HPLC, MALDI-MS, X-ray, DFT
111 [2011] <sup>101</sup>	C <sub>60,70</sub> (CF <sub>3</sub> ) <sub>n</sub>	<b>60-2-1, 60-4-(1,3), 60-6-(1,2),</b> <b>70-2-1</b> [98%; up to 20–25%]	C <sub>60,70</sub> , CF <sub>3</sub> I, 5–410 Torr, GTGS reactor, with and without Cu powder, 410–530 °C; HPLC <sup>a</sup>	HPLC, APCI-MS, UV-vis, <sup>19</sup> F NMR
112 [2011] <sup>102</sup>	Sc <sub>3</sub> N@C <sub>80</sub> (CF <sub>3</sub> ) <sub>14,16,18</sub>	<b>Sc<sub>3</sub>N-80(7)-14-6,</b> <b>Sc<sub>3</sub>N-80(7)-16-3</b> [n/r; n/r]	Sc <sub>3</sub> N@C <sub>80</sub> -I <sub>b</sub> (7), CF <sub>3</sub> I (sealed amp.), 400 °C; HPLC <sup>a</sup>	HPLC, MALDI-MS, X-ray, DFT
113 [2011] <sup>103</sup>	C <sub>60</sub> (C <sub>2</sub> F <sub>5</sub> ) <sub>n</sub> H, C <sub>60</sub> (C <sub>2</sub> F <sub>5</sub> ) <sub>n</sub>	C <sub>60</sub> (C <sub>2</sub> F <sub>5</sub> ) <sub>n</sub> H etc. [95%; 5–10%]	C <sub>60</sub> Cl <sub>6</sub> , C <sub>2</sub> F <sub>5</sub> Li, toluene/Et <sub>2</sub> O, -95 °C; HPLC <sup>a</sup>	HPLC, ESI-MS, <sup>19</sup> F NMR, UV-vis, X-ray, DFT
114 [2011] <sup>104</sup>	C <sub>60</sub> (R <sub>F</sub> ) <sub>n</sub>	<b>60-2-1, 60-2-1-(C<sub>2</sub>F<sub>5</sub>, n-C<sub>3</sub>F<sub>7</sub>, i-C<sub>3</sub>F<sub>7</sub>, n-C<sub>4</sub>F<sub>9</sub>, s-C<sub>4</sub>F<sub>9</sub>, n-C<sub>8</sub>F<sub>17</sub>, CF<sub>2</sub>C<sub>6</sub>F<sub>5</sub>, CF<sub>2</sub>COOEt), 60-2-2-CF<sub>2</sub>C<sub>6</sub>F<sub>5</sub></b> [98%; up to 25%]	(a) C <sub>60</sub> , R <sub>F</sub> I, Cu powder, oDCB, 180 °C; HPLC <sup>a</sup> (b) C <sub>60</sub> , C <sub>2</sub> F <sub>5</sub> I, Cu powder, GTGS reactor, 430 °C; HPLC <sup>a</sup>	HPLC, APCI-MS, <sup>19</sup> F NMR, UV-vis, CV, gas-phase electron affinity, X-ray, DFT
115 [2012] <sup>105</sup>	C <sub>60</sub> (CF <sub>3</sub> ) <sub>n</sub>	<b>60-6-2, 60-4-1, 60-4-O, 60-10-5</b>	C <sub>60</sub> , 60-12-1, 530 °C (pressed pellet in sealed amp.), 20 min, HPLC <sup>a</sup>	HPLC, MALDI-MS, X-ray, DFT
116 [2013] <sup>106</sup>	Y@C <sub>2n</sub> (CF <sub>3</sub> ) <sub>1,3</sub>	Y@C <sub>70</sub> (CF <sub>3</sub> ) <sub>3</sub> , Y@C <sub>72</sub> (CF <sub>3</sub> ) <sub>3</sub> , Y@C <sub>74</sub> (CF <sub>3</sub> ) <sub>3</sub> , Y@C <sub>74</sub> (CF <sub>3</sub> ) <sub>3</sub>	Metal-doped graphite electric arc under He in the presence of (CF <sub>2</sub> CF <sub>2</sub> ) <sub>n</sub>	MALDI-MS, UV-Vis, DFT
117 [2013] <sup>107</sup>	C <sub>82,84</sub> (CF <sub>3</sub> ) <sub>12-20</sub>	C <sub>84</sub> (22)(CF <sub>3</sub> ) <sub>12</sub> , C <sub>84</sub> (22)(CF <sub>3</sub> ) <sub>14</sub> , C <sub>84</sub> (22)(CF <sub>3</sub> ) <sub>16</sub> , C <sub>84</sub> (22)(CF <sub>3</sub> ) <sub>20</sub>	(a) C <sub>76-96</sub> , CF <sub>3</sub> I (sealed amp.), 400–420 °C, 2–3 days; 550–560 °C, 1 hour; HPLC <sup>a</sup> (a) C <sub>82</sub> C <sub>82</sub> , CF <sub>3</sub> I (sealed amp.), 400–420 °C, 2–3 days; 550–560 °C, 1 h; HPLC <sup>a</sup>	HPLC, MALDI-MS, X-ray, DFT
118 [2013] <sup>108</sup>	C <sub>82,84</sub> (CF <sub>3</sub> ) <sub>4-18</sub>	C <sub>84</sub> (23)(CF <sub>3</sub> ) <sub>4</sub> , C <sub>84</sub> (23)(CF <sub>3</sub> ) <sub>8</sub> , C <sub>84</sub> (23)(CF <sub>3</sub> ) <sub>10</sub> , C <sub>84</sub> (23)(CF <sub>3</sub> ) <sub>12</sub> , C <sub>84</sub> (23)(CF <sub>3</sub> ) <sub>14</sub> , C <sub>84</sub> (23)(CF <sub>3</sub> ) <sub>16</sub> , C <sub>84</sub> (23)(CF <sub>3</sub> ) <sub>18</sub>	(a) C <sub>76-96</sub> , CF <sub>3</sub> I (sealed amp.), 550 °C; HPLC <sup>a</sup> (b) C <sub>82</sub> C <sub>82</sub> , CF <sub>3</sub> I (sealed amp.), 550 °C; HPLC <sup>a</sup>	HPLC, MALDI-MS, X-ray, DFT
119 [2013] <sup>109</sup>	C <sub>70</sub> (CF <sub>3</sub> ) <sub>10-20</sub>	<b>70-18-2, 70-20-1, 70-20-2</b>	C <sub>70</sub> , CF <sub>3</sub> I, 390 °C (sealed amp.), 24 h, HPLC <sup>a</sup>	HPLC, MALDI-MS, X-ray, DFT
120 [2013] <sup>110</sup>	C <sub>70</sub> (CF <sub>2</sub> ) <sub>1-3</sub>	[6,6]-closed C <sub>70</sub> (CF <sub>2</sub> ), [6,6]-open C <sub>70</sub> (CF <sub>2</sub> )	C <sub>70</sub> , CF <sub>2</sub> ClCOONa, oDCB, 18-crown-6, 1–25 h reflux; HPLC <sup>a</sup>	HPLC, MALDI-MS, UV-vis, <sup>13</sup> C/ <sup>19</sup> F NMR, CV, ESR, DFT
121 [2014] <sup>111</sup>	C <sub>70</sub> (CF <sub>3</sub> ) <sub>8</sub>	<b>70-8-11, 70-8-12, 70-8-13</b>	C <sub>70</sub> , C <sub>70</sub> (CF <sub>3</sub> ) <sub>12-20</sub> , 450 °C (sealed amp.), 40 h, HPLC <sup>a</sup>	HPLC, MALDI-MS, X-ray, DFT
122 [2014] <sup>112</sup>	Sc <sub>3</sub> N@C <sub>80</sub> (CF <sub>3</sub> ) <sub>14,16,18</sub>	<b>Sc<sub>3</sub>N-80(7)-14-(1,3,4,5), Sc<sub>3</sub>N-80(7)-16-2, Sc<sub>3</sub>N-80(6)-18-1</b> [n/r; n/r]	Sc <sub>3</sub> N@C <sub>80</sub> -I <sub>b</sub> (7) or Sc <sub>3</sub> N@C <sub>80</sub> -D <sub>5b</sub> (6), CF <sub>3</sub> I (sealed amp.), 440 °C, 2 d; HPLC <sup>a</sup>	HPLC, MALDI-MS, X-ray, DFT

<sup>a</sup>Abbreviations: rxn = reaction; n/r = not reported; mix = mixture; equiv = number of equivalents relative to fullerene substrate; ex = excess; amp. = ampoule; EM = electron microscopy; ELAN = elemental analysis; for a complete list of acronyms, see the Glossary at the end of the text. <sup>b</sup>Yields are given in mol % and are based on the amount of the fullerene substrate unless otherwise noted. <sup>c</sup>The most intense MS peaks corresponded to

Table 1. continued

$C_{60}(C_6F_{13})_{10}^-$  (see ref 7). <sup>d</sup>Advancing/receding angles for water =  $124 \pm 3^\circ/64 \pm 3^\circ$ , for hexadecane =  $65 \pm 3^\circ/24 \pm 3^\circ$  (films were deposited by vacuum sublimation onto glass slides, see ref 14). <sup>e</sup>"Highly soluble" in  $C_6F_6$  and Freon-113, insoluble in  $CH_2Cl_2$ ; films inert toward aqueous  $H_2SO_4$  and NaOH; sublimed at  $270\text{--}400^\circ C$  based on the TGA study done under He atmosphere (at  $400^\circ C$  virtually all sample sublimed, residual weight  $\approx 2\%$ ); TGA studies in air and quantitative sublimation under vacuum were also reported (see ref 14). <sup>f</sup>Analogous deuterium-substituted products were also prepared in  $C_6D_6$  (see ref 7). <sup>g</sup>See also ref 121 for additional analysis of analogous  $C_{60}(R_F)_n$  samples by electron-capture mass spectrometry. <sup>h</sup>Relative to  $C_{60}(n-C_3F_7)OH$  or  $[C_{60}(n-C_3F_7)]_2$  starting materials. <sup>i</sup>A single isomer was observed by ESR spectroscopy for  $C_{60}(R_F)\cdot$ , four isomers for  $C_{70}(C_2F_5)\cdot$ , and five isomers for  $C_{70}(CF_3)\cdot$  (ref 15). <sup>j</sup>Scherer radical = perfluorodiisopropylethylmethyl ( $C_9F_{19}\cdot$ ; see ref 16). <sup>k</sup>JAIGEL-1H-40 and 2H-40 gel permeation columns were used. These compounds were originally misinterpreted as  $C_7\cdot$  and  $C_1-C_{60}F_{18}CF_2$ . This was subsequently corrected by the same authors in ref 20. <sup>l</sup>The pressure given in the corresponding papers was 0.1 bar (or 76 Torr); a personal communication with one of the authors of the cited papers revealed that the pressure was 0.1 Torr (the reactions were performed under dynamic vacuum using a rotary-vane vacuum pump). <sup>m</sup>Nacalai Tesque Cosmosil Buckyprep HPLC column was used. <sup>n</sup> $C_{60}(CF_3)_4O$ ,  $C_{60}F_5CF_3$ ,  $C_{60}(CF_3)_4H_2$ ,  $C_{60}(CF_3)_2H_2$ , and  $C_{60}(CF_3)_3H$  were detected in the product mixture (see ref 23). <sup>P</sup>The addition pattern of  $C_{60}(CF_3)_2$  was misidentified as the 1,9-isomer (ref 22). It was later shown by X-ray diffraction to be  $1,7-C_{60}(CF_3)_2$  (ref 63). <sup>q</sup>The addition pattern of  $C_{60}F_7(CF_3)$  was originally misidentified as  $16-CF_3-1,2,3,8,9,12,15-C_{60}F_7$ . It was later corrected to  $18-CF_3-1,2,3,6,8,12,15-C_{60}F_7$  (ref 41). <sup>r</sup>Nacalai Tesque Cosmosil SPYE HPLC column used; see ref 24. <sup>s</sup>Multiple isomers were reported. The addition patterns were misidentified as chains contiguous cage  $C(sp^3)$  atoms each bearing a  $CF_3$  group. See refs 27, 32, and 70 for a detailed discussion. <sup>t</sup>Nacalai Tesque Cosmosil SPYE and Buckyprep HPLC columns were used (ref 25). <sup>u</sup>This compound was originally misidentified as 60-4-2 (ref 39). <sup>v</sup>The crude product was sublimed twice, first at  $380^\circ C$  and then at  $500^\circ C$ ; the high-temperature sublimate contained the target materials (ref 27). <sup>w</sup>Based on the HPLC trace integration, MS data, and  $^{19}F$  NMR spectra (ref 30). <sup>x</sup>Nacalai Tesque Cosmosil Buckyprep and Regis Chemical Co. Regis Buckyclutcher HPLC columns used (refs 30 and 31). <sup>y</sup>Permanent degradation of the HPLC columns (Nacalai Tesque Cosmosil Buckyprep and Cosmosil SPYE) was reported (ref 35). <sup>z</sup>Based on the HPLC, MS, and NMR data given in the corresponding reference. <sup>aa</sup> $1,7-(CF_3)_2-11,24-C_{60}(i-C_3F_7)_2C_{60}$  (refs 80 and 95).

chosen arbitrarily and happened to correspond to the order of retention times in the HPLC separation process (i.e.,  $C_{60}(CF_3)_{10-3}$  has a longer retention time than  $C_{60}(CF_3)_{10-2}$ ). In the later publications, these notations/abbreviations continued to be used for new compounds, until they were simplified even further:  $C_{60}(CF_3)_{10-3}$  has become **60-10-3**.<sup>5</sup> The first number here denotes how many carbon atoms are in the fullerene cage, the second one shows how many  $R_F$  groups are in the derivative, and the third one is the number of the isomer. When other  $R_F$  groups (rather than  $CF_3$ ) were added to a fullerene, it was reflected by adding " $-R_F$ ", for example, as in **60-10-7-C<sub>2</sub>F<sub>5</sub>**; and when higher fullerenes were used instead of  $C_{60}$ , it was reflected by replacing the first number in the formula, for example, as in **78-12-1**. For  $C_{60}\cdot$  and  $C_{70}$ -based PFAFs, we compiled tables that list all compounds with their correct IUPAC numbering and the abbreviations used in the text. Additionally, Schlegel diagrams that depict positions of the  $R_F$  groups on the fullerene cage are supplied for the majority of the compounds discussed in this Review in order to help the reader visualize the addition patterns.

## 2. SYNTHETIC METHODS

### 2.1. Liquid-Phase Fullerene Perfluoroalkylation

Radical addition was one of the first reaction types studied when pure macroscopic samples of fullerenes became available.<sup>6,120</sup> Fullerene solutions or suspensions in various solvents were UV irradiated in the presence of radical precursors like alkyl peroxides or diacyl peroxides;<sup>6,120</sup> relatively persistent  $C_{60,70}R\cdot$  and  $C_{60}R_{3,5}\cdot$  radicals were produced under such conditions and studied *in situ* by ESR spectroscopy (with  $R$  = alkyl, benzyl, alkoxy, alkylthio, fluoroalkyl, and perfluoroalkyl).<sup>6,9,11,12,15,120,121</sup> The first PFAF radical species,  $C_{60}(CF_3)\cdot$ , was generated and studied using this approach in 1991 (see Table 1, entry 1, hereinafter denoted T1#1, etc.)<sup>6</sup> followed by a series of  $C_{60,70}(R_F)\cdot$  radicals carrying a variety of  $R_F$  groups ( $R_F = CF_3$ ,  $C_2F_5$ ,  $i-C_3F_7$ ,  $t-C_4F_9$ , as well as partially fluorinated alkyl groups; see T1#8,10,11,14).<sup>9,11,12,15,120</sup> Perfluoroalkyl iodides or bromides and perfluorinated diacyl peroxides were used as  $R_F$  sources.<sup>122</sup> The reactions were typically performed with a fullerene dissolved in an aromatic

solvent, such as benzene, but sometimes suspensions in solvents such as Freon-113 or methylcyclohexane were used (fullerenes have a very low solubility in fluorous solvents and in alkane hydrocarbons<sup>123</sup>). Despite the fact that no weighable amounts of purified PFAFs were isolated in these studies, they provided information on the regioselectivity of radical additions to  $C_{70}$ <sup>9,15</sup> and on the energy barriers of hindered rotations of  $R_F$  groups attached to a fullerene cage.<sup>11,12</sup>

In 1993 Fagan and co-workers used the approach of liquid-phase fullerene perfluoroalkylation to prepare the first weighable samples of PFAF mixtures.<sup>7</sup> Solutions of  $C_{60}$  in benzene, chlorobenzene (CB), 1,2,4-trichlorobenzene (TCB), or *t*-butylbenzene or suspensions of  $C_{60}$  in Freon-113 or  $C_6F_6$  were treated with  $R_FI$  or  $[R_FCO_2]_2$  ( $R_F = CF_3$ ,  $C_2F_5$ ,  $n-C_3F_7$ , and  $n-C_6F_{13}$ ) either at high temperature ( $175\text{--}200^\circ C$ ) or at room temperature under UV irradiation (T1#2,3,4,5,6).<sup>7</sup> The removal of volatiles under vacuum gave bulk solid samples of PFAFs that were studied by elemental analysis, mass spectrometry,  $^1H$ ,  $^{13}C$ , and  $^{19}F$  NMR spectroscopy, thermogravimetry, differential scanning calorimetry, and electron microscopy. The analytical and spectroscopic data suggested that the samples contained multiple isomers of many PFAF compositions with up to 16  $R_F$  groups (i.e., no isomerically pure PFAFs were isolated). When perfluoroalkylation was performed in benzene or TCB, H atom transfers that resulted in the formation of  $C_{60}(R_F)_nH_m$  compounds were observed. Hydrofullerene( $R_F$ )<sub>n</sub> derivatives were not formed when the solvent was Freon-113 or  $C_6F_6$ . The PFAFs were found to be very soluble in aromatic hydrocarbon and in fluorous solvents. Even though  $C_{60}$  is virtually insoluble in fluorous solvents, suspensions of  $C_{60}$  in Freon-113 and  $C_6F_6$  resulted in good conversions to PFAFs because the products were soluble and did not accumulate on the surface of the  $C_{60}$  particles.

The first PFAFs isolated and studied in pure form were  $(C_{60}R_F)_2$  dimers<sup>10,14</sup> (T1#9,17) and the mixed PFAFs  $C_{60}R_FOH$ <sup>15</sup> (T1#7) and  $C_{60}R_FH$ <sup>10</sup> (T1#9). These compounds were also prepared by liquid-phase  $C_{60}$  perfluoroalkylation using  $R_FI$ ,  $R_FBr$ , and  $[R_FCO_2]_2$  in benzene, CB, and/or oDCB solutions either at elevated temperatures (up to  $80^\circ C$ ) or at room temperature under UV irradiation. It is notable that the

**Table 2.**  $C_{60}(R_F)$  Derivatives and Their Addition-Pattern Abbreviations and IUPAC Locants

addition pattern abbreviation	IUPAC locants	$R_F^{\text{ref}}$
60-2-1	1,7	$CF_3^{27,63} C_2F_5^{104} n-C_3F_7^{104} i-C_3F_7^{94,104} s-C_4F_9^{104} n-C_8F_{17}^{104}$
60-4-1	1,6,11,18	$CF_3^{27,63}$
60-4-2	1,7,16,36	$CF_3^{63} i-C_3F_7^{94}$
60-4-3 <sup>a</sup>	1,7,11,24	$CF_3^{113} (2CF_3+2i-C_3F_7)^{80,95} (CF_3+O)^{39} (C_2F_5+O)^{39}$
60-4-4	1,7,28,31	$i-C_3F_7^{94}$
60-6-1	1,6,11,18,24,27	$CF_3^{27,63}$
60-6-2	1,6,9,12,15,18	$CF_3^{39}$
60-6-3	1,7,16,36,46,49	$C_2F_5^{40} i-C_3F_7^{80}$
60-6-5	1,7,16,30,36,47	$i-C_3F_7^{60}$
60-6-6	1,6,11,18,28,31	$CF_3^{63}$
60-6-7	1,6,11,18,33,51	$CF_3^{63}$
60-6-8	1,7,16,36,45,57	$C_2F_5^{54} i-C_3F_7^{80}$
60-6-9	1,7,16,36,43,46	$i-C_3F_7^{94}$
60-8-1	1,6,11,16,18,24,27,36	$CF_3^{53,58} C_2F_5^{95}$
60-8-2	1,6,11,18,24,27,52,55	$CF_3^{44}$
60-8-3	1,6,11,18,24,27,53,56	$CF_3^5 C_2F_5^{95}$
60-8-4	1,6,11,16,18,28,31,36	$CF_3^5$
60-8-5	1,6,11,18,24,27,33,51	$CF_3^5$
60-8-6	1,6,11,18,24,27,32,35	$C_2F_5^{50}$
60-8-7	1,6,11,18,24,27,36,39	$C_2F_5^{82,95}$
60-8-8	1,6,11,18,24,27,41,57	$C_2F_5^{54}$
60-8-9	1,6,11,18,24,27,51,59	$C_2F_5^{54}$
60-8-10	1,6,11,18,32,35,42,56	$C_2F_5^{54}$
60-8-11	1,7,14,31,36,39,45,57	$i-C_3F_7^{80}$
60-10-1	1,6,11,16,18,24,27,36,41,57	$CF_3^5$
60-10-2	1,6,11,16,18,24,27,36,54,60	$CF_3^{43b,63}$
60-10-3	1,3,7,10,14,17,23,28,31,40	$CF_3^4$
60-10-4	1,6,12,15,18,23,25,41,45,57	$CF_3^{43a}$
60-10-5	1,6,11,16,18,26,36,41,44,57	$CF_3^5$
60-10-6	1,6,11,18,24,27,33,51,54,60	$CF_3^{114} C_2F_5^{54,95}$
60-10-7	1,6,11,16,18,28,31,36,42,56	$C_2F_5^{54}$
60-10-8 <sup>b</sup>	1,6,11,18,24,27,34,36,39,50	$CF_3^{115}$
60-12-1	1,6,11,16,18,26,36,44,46,49,54,60	$CF_3^{36}$
60-12-2	1,3,6,11,13,18,24,27,33,51,54,60	$CF_3^{56}$
60-12-3	1,6,9,12,15,18,43,46,49,52,55,60	$CF_3^{5,52}$
60-12-4	1,3,7,10,14,17,21,28,31,42,52,55	$CF_3^{67}$
60-12-5	1,6,8,11,16,18,23,28,31,36,41,57	$CF_3^{74}$
60-12-6	1,6,8,11,16,18,23,28,31,36,54,60	$CF_3^{74}$
60-14-1	1,3,6,8,11,13,18,23,33,41,46,49,51,57	$CF_3^{52}$
60-14-2	1,3,6,11,13,18,26,33,41,44,46,49,51,57	$CF_3^{52}$
60-14-3	1,3,7,10,11,14,17,24,27,31,36,39,47,59	$CF_3^{74}$
60-16-1	1,3,6,11,13,18,21,28,31,34,36,39,42,45,50,57	$CF_3^{51}$
60-16-2	1,3,6,8,11,13,18,23,28,31,34,35,37,50,54,60	$CF_3^{51}$
60-16-3	1,3,6,11,13,18,22,24,27,33,41,43,46,49,51,59	$CF_3^{51}$
60-18-1	1,3,6,8,11,13,18,23,28,31,34,37,43,46,51,53,56,59	$CF_3^{51}$
60-18-2	1,3,6,11,13,18,22,24,27,32,35,37,41,43,46,49,52,54	$CF_3^{82}$

<sup>a</sup>This addition pattern was originally denoted as 60-4-2 in ref 5 but was later changed to 60-4-3. <sup>b</sup>This compound was erroneously denoted as 60-10-7 in ref 115 but is correctly identified as 60-10-8 in this table.

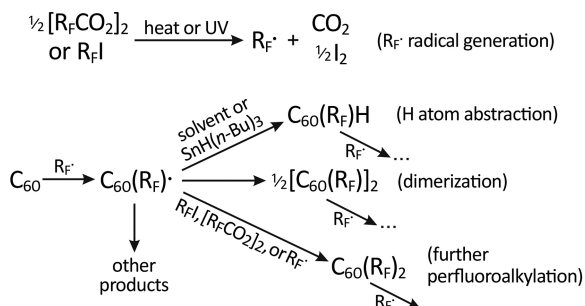
pure PFAFs were isolated using gel-permeation chromatography with 10–37 mol % yields. Mixtures of various TMFs and mixed  $C_{60}(CF_3)_nH_m$ <sup>16,18,25</sup> derivatives were also formed by perfluoroalkylation of  $C_{60}$  in TCB using Scherer's radical (i.e., perfluoro-2,4-dimethyl-3-ethyl-3-pentyl,<sup>124</sup> a persistent radical at room temperature that fragments upon heating to give  $CF_3$  radicals) or  $n$ - $C_6F_{13}I$  at 200 °C (T1#15,16,26). These observations support the general reaction sequence for fullerene perfluoroalkylation under radical conditions shown in Scheme 1.

In 2002 the first perfluoroalkylation of an EMF was reported (T1#24).<sup>24</sup> A 2-mg sample of  $La@C_{82}$  was dissolved in toluene and treated with 1.8 equiv of  $n$ - $C_8F_{17}I$  at room temperature under UV irradiation. It is notable that during the course of the reaction the resulting PFAFs were continuously extracted into a layer of perfluorohexane. Seven isomers of  $La@C_{82}(n-C_8F_{17})_2$  were separated and isolated using HPLC and were characterized by UV-vis and ESR spectroscopy and mass spectrometry. No structural information could be obtained due to very small amounts of the isolated derivatives. UV irradiation was also used to prepare mixtures of  $C_{60,70}(i-C_3F_7)_n$  (up to  $n = 12$ )

Table 3.  $C_{70}(R_F)_n$  Derivatives and Their Addition-Pattern Abbreviations and IUPAC Locants

addition pattern abbreviation	IUPAC locants	$R_F^{\text{ref}}$
70-2-1	7,24	$CF_3^{38,79,116} C_2F_5^{116}$
70-2-2	8,23	$CF_3^{68}$
70-4-1	7,24,44,47	$CF_3^{38}$
70-4-2	7,17,24,36	$i-C_3F_7^{94}$
70-4-3	7,14,24,35	$i-C_3F_7^{94}$
70-4-4	7,24,36,57	$i-C_3F_7^{98}$
70-4-5	7,24,32,54	$i-C_3F_7^{98}$
70-4-6	7,24,54,68	$i-C_3F_7^{94}$
70-4-7	7,24,34,52	$i-C_3F_7^{98}$
70-6-1	1,4,11,19,31,41	$CF_3^{38}$
70-6-2	1,4,11,23,31,44	$CF_3^{38,68}$
70-6-3	1,4,10,19,25,41	$CF_3^{47}$
70-8-1	1,4,11,19,31,41,51,64	$CF_3^{33,38} C_2F_5^{77}$
70-8-2	1,4,11,19,31,41,51,60	$CF_3^{68,38,71}$
70-8-3	7,17,24,36,44,47,53,56	$C_2F_5^{77} n-C_3F_7^{72}$
70-8-4	7,15,24,34,44,47,53,56	$CF_3^{79} C_nF_{2n+1} \quad (n = 1-3)^{72,77}$
70-8-5	1,4,23,28,36,44,46,57	$C_2F_5^{77} n-C_3F_7^{72}$
70-8-6	1,4,23,28,34,44,46,52	$C_2F_5^{77} n-C_3F_7^{72}$
70-8-7	1,4,11,24,43,52,54,68	$C_2F_5^{77}$
70-8-8	1,4,11,33,53,58,61,64	$C_2F_5^{77}$
70-8-9	1,4,23,28,44,46,55,67	$C_2F_5^{77}$
70-8-10	1,4,11,19,31,55,57,67	$C_2F_5^{77}$
70-8-11	1,4,10,19,25,41,60,69	$CF_3^{111}$
70-8-12	1,4,11,19,24,31,51,64	$CF_3^{111}$
70-8-13	1,4,11,19,31,41,46,62	$CF_3^{111}$
70-10-1	1,4,10,19,25,41,49,60,66,69	$CF_3^{32} C_2F_5^{77,117}$
70-10-2	1,4,11,19,31,41,49,60,66,69	$CF_3^{68}$
70-10-3	1,4,11,19,26,31,41,48,60,69	$CF_3^{68}$
70-10-4	1,4,10,19,23,25,44,49,66,69	$CF_3^{68}$
70-10-5	1,4,11,19,24,31,41,51,61,64	$CF_3^{68}$
70-10-6	1,4,10,19,25,41,55,60,67,69	$CF_3^{118}$
70-10-7	1,4,10,19,25,32,41,54,60,67	$CF_3^{119}$
70-10-8	1,4,11,19,31,41,46,55,62,67	$C_2F_5^{117}$
70-10-9	1,4,11,19,23,31,44,55,57,67	$C_2F_5^{117}$
70-10-10	1,4,11,33,38,46,53,55,62,64	$C_2F_5^{117}$
70-10-11	1,4,11,24,33,38,43,48,53,55	$C_2F_5^{117}$
70-10-12	1,4,23,28,33,38,44,46,53,55	$C_2F_5^{117}$
70-10-13	1,4,11,33,38,46,48,53,55,62	$C_2F_5^{117}$
70-10-14	1,4,11,24,33,38,43,53,55,64	$C_2F_5^{77}$
70-10-15	1,11,16,18,33,46,48,54,62,68	$C_2F_5^{77}$
70-12-1	1,4,10,19,25,32,41,49,54,60,66,69	$CF_3^{42,48}$
70-12-2	1,4,10,14,19,25,35,41,49,60,66,69	$CF_3^{45,48}$
70-12-3	1,4,8,11,18,23,31,35,51,58,61,64	$CF_3^{68}$
70-12-4	1,4,8,11,23,31,38,51,55,58,61,64	$CF_3^{68,87}$
70-12-5	1,4,23,25,27,31,38,44,47,51,55,68	$C_2F_5^{95}$
70-14-1	1,4,8,11,19,24,27,31,41,43,51,54,64,68	$CF_3^{46}$
70-14-2	1,4,8,11,19,23,26,31,41,48,55,60,67,69	$CF_3^{46}$
70-14-3	1,4,8,11,19,24,27,31,36,41,43,51,57,64	$CF_3^{46}$
70-14-4	1,4,7,11,18,21,24,31,35,39,51,58,61,64	$CF_3^{46,59}$
70-14-5	1,4,8,11,19,24,27,31,41,43,51,53,56,64	$CF_3^{79}$
70-14-6	1,4,10,14,19,25,28,35,41,46,49,60,66,69	$CF_3^{87}$
70-14-7	1,4,8,11,18,23,31,33,35,51,53,58,61,64	$CF_3^{87}$
70-14-8	1,4,7,11,21,24,31,39,44,47,51,58,61,64	$CF_3^{87}$
70-16-1	1,4,8,11,18,23,24,27,31,35,44,47,51,58,61,64	$CF_3^{49}$
70-16-2	1,4,7,11,18,21,24,31,33,35,39,51,53,58,61,64	$CF_3^{87}$
70-18-1	1,4,8,11,16,19,23,27,31,34,37,41,44,46,47,52,60,69	$CF_3^{49}$
70-18-2	1,4,8,11,16,19,23,26,31,34,37,41,45,48,52,60,63,69	$CF_3^{109}$
70-20-1	1,4,8,11,16,19,23,24,27,31,33,37,44,47,51,53,55,58,61,64	$CF_3^{109}$
70-20-2	1,4,8,11,16,19,23,27,31,34,37,41,44,46,47,52,55,60,67,69	$CF_3^{109}$

**Scheme 1. Radical Perfluoroalkylation of  $C_{60}$ , also Showing Side Reactions That Have Been Observed<sup>a</sup>**



<sup>a</sup>Similar schemes can be drawn for other  $R_F\cdot$  sources and other fullerenes.

(T1#103)) by perfluoroalkylation of the corresponding bare-gage fullerenes suspended in an excess of  $i\text{-}C_3F_7I$  in the presence of copper powder (see below).<sup>94</sup>

In 2007, several single-isomer  $C_{60}(CF_2)_n$  compounds were prepared by vigorous reflux of an oDCB mixture of  $C_{60}$  and solid  $Na(CF_2ClCO_2)$  in the presence of a phase-transfer catalyst (either 18-crown-6 or  $(n\text{-}Bu)_4NBr$ ; T1#65,66).<sup>61,62</sup> The authors hypothesized that upon heating  $Na(CF_2ClCO_2)$  decomposed to give  $:CF_2$ ,  $CO_2$ , and  $NaCl$ . The crude product mixture was filtered and the solvent was removed under vacuum to give a crude product. Subsequent HPLC separations gave pure samples of mono- and bis(difluoromethylene) [60]fullerenes with yields up to 45 mol %. These compounds were characterized by MALDI mass spectrometry, IR, UV-vis,  $^{13}C$  and  $^{19}F$  NMR spectroscopy, and single-crystal X-ray diffraction.

Trifluoromethylation of  $C_{60}$  with  $CF_3I$  in  $C_6F_6$  under UV irradiation was reported in 2010 (T1#104).<sup>95</sup> The resulting product was analyzed using EI mass spectrometry, which showed the presence of TMFs with up to 23  $CF_3$  groups. It is notable that when a mixture of  $C_{60}(CF_3)_{8-12}$  was further trifluoromethylated using the same procedure, it yielded products containing only up to 16  $CF_3$  groups.<sup>95</sup>

Several stable free-radical species  $C_{60}(CF_3)_{15,17}\cdot$  were prepared by UV irradiation of a solution of  $C_{60}(CF_3)_{12-18}$  in liquefied  $CF_3I$  (T1#98).<sup>91</sup> The reaction was carried out in a flame-sealed quartz ampoule at room temperature. The HPLC separation of the crude product gave several purified fractions that contained stable free radical TMFs with an odd number of  $CF_3$  groups (as shown by MALDI mass spectrometry and ESR spectroscopy).

In 2011, a series of the pure single-isomers  $1,7\text{-}C_{60}(R_F)_2$  were prepared by perfluoroalkylation of  $C_{60}$ ,  $R_FI$ , and Cu powder in oDCB at ca. 180–190 °C for 7–72 h depending on the  $R_FI$  reagent ( $R_F = n\text{-}C_3F_7$ ,  $i\text{-}C_3F_7$ ,  $n\text{-}C_4F_9$ ,  $sec\text{-}C_4F_9$ , and  $n\text{-}C_8F_{17}$ ; T1#109).<sup>104</sup> The authors proposed that the presence of Cu powder increased the reaction rate by promoting  $R_FI$  dissociation (as well as scavenging any  $I_2$  byproduct). High selectivity for PFAFs with only two  $R_F$  groups, up to ca. 75 mol %, was achieved at the expense of  $C_{60}$  conversion by limiting the reaction time (an approach similar to that used for the synthesis of  $La@C_{82}(n\text{-}C_8F_{17})_2$ <sup>24</sup> and for the selective preparation of  $C_{60}(CF_3)_2$ <sup>101</sup>). The solvent and other volatile compounds were removed from the product mixtures under vacuum, and the crude products were separated using HPLC to give pure  $C_{60}(R_F)_2$  products with up to 25 mol % yield based

on  $C_{60}$ . The five new  $1,7\text{-}C_{60}(R_F)_2$  compounds,  $1,7\text{-}C_{60}(CF_3)_2$ , and  $1,7\text{-}C_{60}(C_2F_5)_2$  were studied using APCI mass spectrometry,  $^{19}F$  NMR and UV-vis spectroscopy, cyclic voltammetry, low-temperature gas-phase photoelectron spectroscopy (from which the gas-phase electron affinities of all seven compounds were determined), and, for  $1,7\text{-}C_{60}(n\text{-}C_3F_7)_2$ , single-crystal X-ray diffraction. When  $C_6F_5CF_2I$  was used as described in the previous paragraph,  $1,7\text{-}C_{60}(C_6F_5CF_2)_2$  was also formed.<sup>125</sup> However,  $C_6F_5CF_2I$  is more reactive than the other  $R_FI$  reagents, and the reaction was also performed at 130 °C. This yielded two compounds with the composition  $C_{60}(C_6F_5CF_2)_2$ :  $1,7\text{-}C_{60}(C_6F_5CF_2)_2$  and an isomer that may be  $1,9\text{-}C_{60}(C_6F_5CF_2)_2$ . It has been shown that the highest unpaired spin density in  $C_{60}R\cdot$  radicals is on the cage C atoms *ortho*- to the cage C atom bearing the R substituent.<sup>121b</sup> It has also been shown that  $1,9\text{-}C_{60}(X)_2$  (*ortho*) isomers are thermodynamically more stable than the corresponding  $1,7\text{-}C_{60}(X)_2$  (*para*) isomers for small substituents X such as H and F atoms, whereas *para* isomers are more stable for larger substituents such as  $CH_3$  and  $CF_3$ .<sup>126</sup> It is possible that *ortho*- $C_{60}(R_F)_2$  isomers are kinetic products that can only be prepared at a lower temperature and rearrange to more stable *para*- $C_{60}(R_F)_2$  isomers at higher temperatures. Furthermore, while *para*- $C_{60}(R_F)_2$  derivatives were prepared with 99% isomeric purity at 180 °C, HPLC analysis and mass spectra of the crude reaction mixtures were consistent with multiple isomers of the compositions  $C_{60}(R_F)_4$  and  $C_{60}(R_F)_6$ .<sup>104</sup> It is likely that the relatively low 180–190 °C temperatures used for these liquid-phase perfluoroalkylations are not sufficient to anneal multiple kinetic isomers into fewer thermodynamic ones. This is consistent with the observation that fewer isomers of  $C_{60}(R_F)_{4,6}$  were prepared when higher reaction temperatures were used for perfluoroalkylations in sealed glass ampoules in the absence of solvent (T1#103);<sup>94,95</sup> (see also the discussion of fullerene trifluoromethylation with metal trifluoroacetates, below)

## 2.2. PFAF Generation during Fullerene Synthesis

The first report of PFAF generation during arc discharge fullerene synthesis was published in 1995 (T1#12).<sup>13</sup> Graphite rods doped with Teflon or NaTFA were used to generate  $CF_3\cdot$  radicals during the arc discharge; the resulting soot was extracted with  $CS_2$ , and the extract was analyzed by EI mass spectrometry and  $^{19}F$  NMR spectroscopy. Fluorine-19 NMR spectroscopy confirmed the presence of  $CF_3$  groups, while mass spectroscopy showed that positive ions corresponding to  $C_{60}(CF_3)_{1-8}H_{0-9}^+$  species (the hydrogenation was attributed to traces of moisture). The yield of the PFAFs was low (ca. 0.12% of the raw soot), and no isolation was carried out. Although the arc discharge synthesis of PFAFs has not become a practical synthetic technique, it showed that trifluoroacetate salts can be used as sources of  $CF_3$  radicals for fullerene trifluoromethylation (see below). In 2013, a preliminary study of the in situ trifluoromethylation during arc discharge was carried out by Shinohara et al., in which metal-doped graphite rods were burned in the presence of PTFE resulting in a number of mono- and tri-trifluoromethylated  $Y@C_{2x}$  derivatives, where  $2x = 70$ , 72, and 74 (T1#116).<sup>106</sup> As shown previously with small-band gap fullerenes such as  $C_{74}^{50,57}$  or other endometallofullerenes, such as  $Y@C_{82}^{30,66}$  and  $Ce@C_{82}^{127}$  the addition of  $CF_3$  groups improved the air stability and solubility of otherwise reactive and insoluble fullerenes. More optimization work needs to be done to improve yields in

such *in situ* arc discharge trifluoromethylation reactions so that they become attractive for synthetic chemists.

### 2.3. PFAF Formation during Fullerene Fluorination

In 2000, the first isolation of a mixed perfluoroalkylated/fluorinated fullerene was reported (T1#19).<sup>19</sup> The compound was initially misidentified as  $C_{60}F_{18}CF_2$ ,<sup>19</sup> but in the follow-up publication by the same group it was correctly identified as a mixture of  $C_s$ - and  $C_1\text{-}C_{60}F_{17}(CF_3)$  ( $C_s\text{-}C_{60}F_{17}(C_2F_5)$  was also isolated).<sup>20</sup> These compounds were formed as minor products along with the major product  $C_{60}F_{18}$  by  $C_{60}$  fluorination with  $K_2PtF_6$  in the solid state (see also T1#28<sup>28</sup>). Both materials were ground together and heated at 465 °C under reduced pressure; the crude materials were dissolved in toluene and separated by HPLC. A single-crystal X-ray diffraction study showed that both  $C_s$ - and  $C_1\text{-}C_{60}F_{17}(CF_3)$  have two fluorine substituents vicinal to the  $CF_3$  groups (X-ray crystallography showed that the crystal contained 68% of the  $C_s$ -isomer and 32% of the enantiomer pair of  $C_1\text{-}C_{60}F_{17}(CF_3)$ ). No signals corresponding to the  $CF_3$  groups of  $C_s$ - and  $C_1\text{-}C_{60}F_{17}(CF_3)$  were observed in the  $^{19}F$  NMR spectra although other fluorine signals due to F atom substituents were accounted for and were well-resolved. This was explained later shown to be due to relatively slow rotation of the  $CF_3$  groups leading to extremely broad  $CF_3$ <sup>19</sup> signal broadening.<sup>31</sup>

In 2002, a similar solid-phase fluorination of  $C_{60}$  by  $K_2PtF_6$  at 470 °C (or  $AgF$  at 520 °C) under reduced pressure resulted in the HPLC isolation and characterization of the first simple and isomerically pure PFAF  $C_{60}(CF_3)_2$  (T1#22).<sup>22</sup> On the basis of  $^{19}F$  NMR and UV-vis spectra, it was erroneously assigned as the *ortho*- isomer  $1,9\text{-}C_{60}(CF_3)_2$ . Later, this structural assignment was later corrected to  $1,7\text{-}C_{60}(CF_3)_2$  based on the reinterpretation of the  $^{19}F$  NMR and UV-vis spectra<sup>27</sup> and later by single-crystal X-ray diffraction<sup>63</sup>. In a separate report also published in 2002 another mixed fluoro(perfluoroalkyl)-fullerene,  $C_{60}F_7(CF_3)$ , was isolated by HPLC from the crude product of  $C_{60}$  fluorination with  $K_2PtF_6$  at 470 °C. Its tentative structure was proposed on the basis of its  $^{19}F$  NMR and 2D  $^{19}F\text{-}^{19}F$  COSY NMR spectra.

In 2005, a number of mixed fluoro(perfluoroalkyl)fullerene compounds, including 1,7- and 1,9- $C_{60}F(CF_3)$ ,  $C_{60}F_{3,5,7}(CF_3)$ , and  $C_s$ - and  $C_1\text{-}C_{60}F_{17}(CF_3)$  were prepared using the same method.<sup>31</sup> Solid  $C_{60}$  was fluorinated with  $K_2PtF_6$  at 450 °C and the crude product, mostly  $C_{60}F_{18}$  and small amounts of the above-mentioned compounds, was subjected to HPLC separation (T1#31).<sup>31</sup> The hindered rotation of the  $CF_3$  groups in  $1,9\text{-}C_{60}F(CF_3)$  and in  $C_s$ - and  $C_1\text{-}C_{60}F_{17}(CF_3)$ , all of which had at least one cage C atom bearing an F atom adjacent to the  $C_{cage}\text{-}CF_3$  group, resulted in slow-exchange  $^{19}F$  NMR spectra at low temperatures (at the time there were only ca. 30 other compounds of any type for which slow-exchange  $CF_3$   $^{19}F$  NMR spectra had been reported).<sup>31</sup> At -30 °C, the single  $CF_3$  group in  $C_1\text{-}C_{60}F_{17}(CF_3)$  gave rise to three  $^{19}F$  multiplets with a total of 40 individual  $^{19}F$  resonances, from which eight  $^{2,4,5}J_{FF}$  coupling constants ranging from 5 to 126 Hz were determined. DFT calculations predicted the activation barriers for  $CF_3$  rotation in  $1,9\text{-}C_{60}F(CF_3)$  and  $C_s$ - and  $C_1\text{-}C_{60}F_{17}(CF_3)$  to be 46, 44, and 54 kJ·mol<sup>-1</sup>, respectively (the experimental value for  $1,9\text{-}C_{60}F(CF_3)$  was 46.8(7) kJ·mol<sup>-1</sup>). In contrast, the DFT-predicted barrier for  $CF_3$  rotation in the *para* isomer  $1,7\text{-}C_{60}F(CF_3)$  was 20 kJ·mol<sup>-1</sup>.

Various mixed  $C_{60}F_n(R_F)_m$  compounds were also isolated using HPLC from crude mixtures resulting from  $C_{60}$

fluorination with  $MnF_3$  or  $K_2NiF_6$  under vacuum at 510 °C (T1#36).<sup>35</sup> These purified compounds were only characterized by mass spectrometry, so no structural information was obtained. It is notable that compounds carrying multiple  $R_F$  groups,  $C_{60}F_4(CF_3)_4$ ,  $C_{60}F_5(CF_3)_3$ , and  $C_{60}F_4(CF_3)(C_2F_5)$ , were among the compounds reported.

In all of these cases, the formation of PFAFs was rationalized by side-reactions with small amounts of the  $R_F\cdot$  radicals (mostly  $CF_3\cdot$ ) resulting from an advanced fullerene fluorination leading to the breakup of the cage upon high-temperature treatment with high-valency metal fluorides. Indirect evidence in support of this hypothesis was obtained when fluorinated fullerene species with the  $C_{88}$  cage (e.g.,  $C_{88}F$ ) were first detected by our group in 2004,<sup>128</sup> followed by a report in *Science*<sup>129</sup> (see also ref 130 for additional information on the proposed mechanism of such a process). This explanation is consistent with the very small yields of mixed fluoro(perfluoroalkyl) compounds prepared by this method. Analogous effects of chemical degradation of fluorofullerenes to small fluorocarbons under high temperature conditions were earlier observed by Gakh et al.<sup>131</sup>

### 2.4. Fullerene Trifluoromethylation with Metal Trifluoroacetates

Metal carboxylates are known to yield radical species upon heat- or radiation-induced decomposition.<sup>132</sup> In 2001, this property was used for the trifluoromethylation of a mixture of  $C_{60}$  and  $C_{70}$  using various transition metal trifluoroacetates ( $AgTFA$ ,  $Cu(TFA)_2$ ,  $Pd(TFA)_2$ ,  $Cr(TFA)_2$ ; see T1#21).<sup>21</sup> The fullerene mixture was ground with a metal trifluoroacetate salt and heated to 300–400 °C. The crude products were studied by EI and LDI mass spectrometry, showing that multiple  $C_{60,70}(CF_3)_n$  species were formed. A later report also described the successful use of  $Hg(CF_3SO_3)_2$  as a fullerene trifluoromethylation reagent (the reaction was carried out at 300–310 °C in the ionization chamber of mass spectrometer (T1#92)).<sup>85</sup> Despite the successful use of trifluoroacetates of other transition metals for fullerene trifluoromethylation,  $AgTFA$  has been used almost exclusively (see Table 1).

In 2003 and 2004, three papers reported the synthesis of a large number of  $C_{60,70}(CF_3)_n$  compounds using  $AgTFA$  (T1#25,26,29).<sup>25,26,29</sup> An excess of  $AgTFA$  (ca. 12–23 equiv) was intimately ground with either a mixture of  $C_{60}$  and  $C_{70}$ ,<sup>25</sup> pure  $C_{60}$ ,<sup>26</sup> or pure  $C_{70}$ <sup>29</sup> and heated to 300 °C under dynamic vacuum for about 1 h. The resulting TMFs were retained with the solid products of  $AgTFA$  decomposition (they did not sublime during the course of the reaction) and were later extracted using toluene. The HPLC analysis and separation of the toluene extracts showed that extremely complex mixtures of TMFs were produced: ca. 60 TMFs were isolated from the products of  $C_{60}$  trifluoromethylation (T1#26)<sup>26</sup> and 46 from the products of  $C_{70}$  trifluoromethylation (T1#28).<sup>29</sup> Some of the isolated TMFs were analyzed by  $^{13}C$  and  $^{19}F$  NMR, IR, and UV-vis spectroscopy and by mass spectrometry. The authors suggested that the addition patterns of these TMFs were chains of adjacent cage  $C(sp^3)$  atoms bearing the  $CF_3$  groups.<sup>25,26,29</sup> This was later shown to be incorrect in almost every case, TMF addition patterns consist of ribbons of edge-sharing *meta*- and/or *para*- $C_6(CF_3)_2$  hexagons (each shared edge is a cage  $C(sp^3)\text{-}C(sp^2)$  bond; very few TMFs studied to date have  $CF_3$  groups on adjacent cage  $C(sp^3)$  atoms; see refs 27, 39, and 70 for a detailed discussion).

The synthetic procedure used for a fullerene trifluoromethylation with AgTFA in refs 25,26,29 suffered from several problems. First, it was observed that part of the volatile AgTFA sublimed out of the hot reaction zone and was lost unproductively. Two other problems were more serious. A very large number of TMFs were produced, necessitating labor-intensive HPLC separation and leading to low yields. Furthermore, it was found that a crude filtered toluene extract caused irreparable clogging of the very expensive specialized HPLC columns that were used (Cosmosil BuckyPrep; the formation of unstable soluble TMF–silver complexes was thought to be responsible).<sup>25,26,29</sup> Formation of some mixed  $C_{60}(CF_3)_nH_m$  compounds was also observed and attributed to side-reactions with trace amounts of adventitious moisture.<sup>26</sup>

Solutions to these problems were first reported in 2003 (T1#27)<sup>27</sup> and were used for all subsequent AgTFA trifluoromethylations of hollow fullerenes (T1#27,34,38,39,50,67).<sup>27,33,38,47,63</sup> First, an intimately ground mixture of the fullerene and AgTFA was placed inside a glass insert that was sealed inside a metal tube (typically copper) and heated in a tube furnace (see Figure 2A). The use of a sealed reactor prevented the unproductive loss of AgTFA by sublimation and improved the control of the reaction stoichiometry. The glass insert was used to prevent contact between the reaction mixture and the walls of the metal tube. The other problems mentioned above were solved by vacuum sublimation of the TMFs from the crude product mixture at

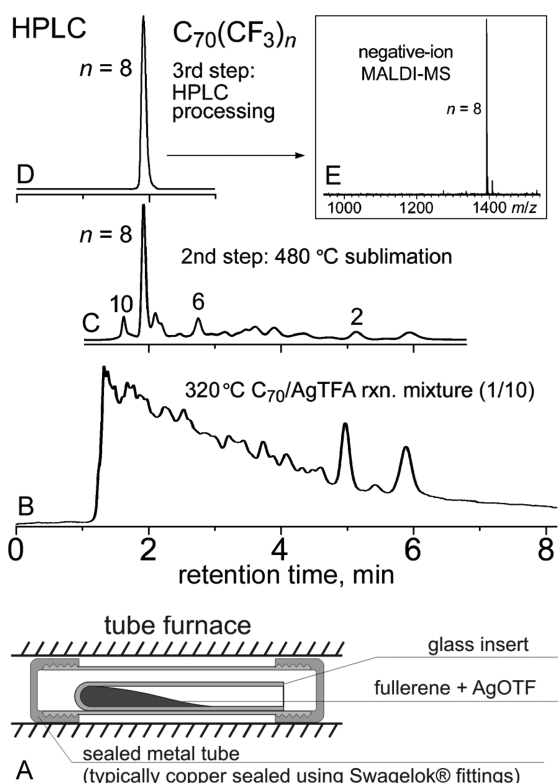
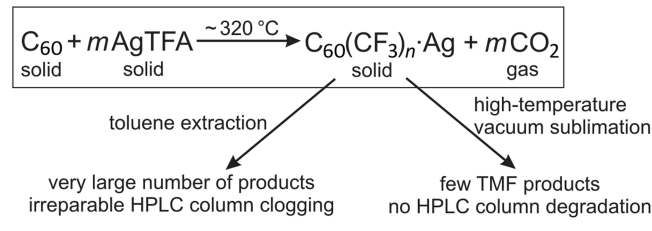


**Figure 2.** (A) Experimental setup typically used for fullerene trifluoromethylation with AgTFA. (B) HPLC trace of the crude product mixture from a reaction of  $C_{70}$  with AgTFA prior to high-temperature sublimation. (C) HPLC trace of the sublimed mixture of products. (D) HPLC trace and (E) MALDI mass spectrum of pure  $C_{70}(CF_3)_8$  resulting from the HPLC separation of the sublimed mixture of products. Parts (B)–(E) of this figure were reproduced, with permission, from ref 38 (Copyright 2006 Wiley).

420–540 °C.<sup>27,38</sup> The sublimed TMFs were dissolved in toluene and separated by HPLC with no column clogging or degradation (which can be attributed to the thermal decomposition of the TMF–silver complexes during sublimation).<sup>27,33,38,47,63</sup> The high-temperature sublimation also simplified the composition of the TMFs (see Figure 2B–E and Scheme 2).<sup>27,38</sup> This can be explained by the thermal

### Scheme 2. Fullerene Trifluoromethylation with AgTFA



rearrangement of multiple kinetic isomers produced at lower temperatures into a few thermodynamically more-stable products during the high-temperature sublimation (see the section on PFAF rearrangement below).

In contrast, the original “sublimation-free” method<sup>21</sup> was used successfully for the trifluoromethylation of EMFs. The lower volatility of EMFs prevented the preliminary sublimation stage from being used; however, no clogging of the HPLC columns was reported (T1#30,70,79,95,101).<sup>30,66,75,88</sup> An extract containing Y@C<sub>82</sub> and Y<sub>2</sub>@C<sub>80</sub> was successfully trifluoromethylated with AgTFA under dynamic vacuum at 300–400 °C to produce Y@C<sub>82</sub>(CF<sub>3</sub>)<sub>1,3,5</sub> (all three compounds were structurally characterized using a combination of 1D <sup>19</sup>F and 2D <sup>19</sup>F–<sup>19</sup>F COSY NMR spectroscopy and DFT calculations) and Y<sub>2</sub>@C<sub>80</sub>(CF<sub>3</sub>) (see T1#30).<sup>30</sup> Extracts containing Gd@C<sub>82</sub>/Gd<sub>2</sub>@C<sub>80</sub> and Ce@C<sub>82</sub> were treated under similar conditions resulting in the isolation and characterization of several corresponding TMF derivatives (T1#70,79).<sup>66,75</sup> Pure samples of Sc<sub>3</sub>N@C<sub>80</sub>I<sub>h</sub> were also successfully trifluoromethylated using AgTFA in sealed copper tubes at 350 °C, resulting in the isolation and single-crystal X-ray characterization of several TMF derivatives (T1#95,101).<sup>88,93</sup> In all of these cases crude products were extracted with organic solvents and purified using HPLC separation, and no clogging of the HPLC columns was reported.<sup>66,75,88,93</sup>

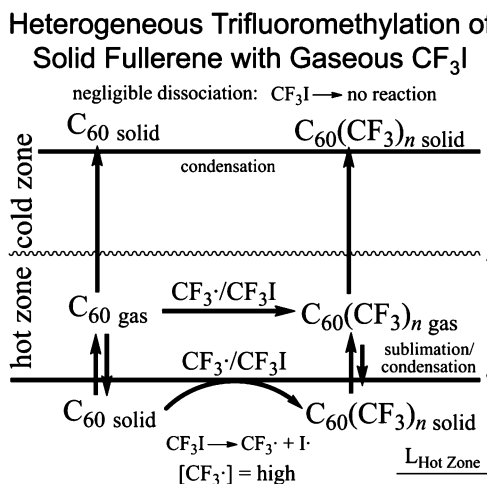
It was reported that some control over the composition of the TMFs resulting from AgTFA trifluoromethylation was possible by a proper choice of the reaction stoichiometry (a higher excess of AgTFA led to higher degrees of trifluoromethylation; AgTFA/fullerene mole ratios between 3.4 and 60 have been reported).<sup>38,63,93</sup> It is notable that the absolute mol % yields of purified TMFs prepared by AgTFA trifluoromethylation were typically not reported, which can be attributed to the small amounts of the purified products that were isolated. A realistic estimate of the mol % yields of isolated isomerically-pure TMFs is unlikely to exceed low single digits, although a yield of 12 mol % was reported for **60-2-1** (T1#67).<sup>63</sup> A comparison of the HPLC traces in ref 63 with those in a paper reporting selective synthesis of **60-2-1**<sup>101</sup> makes the aforementioned 12 mol % yield doubtful.

## 2.5. Reactions of Solid Fullerenes with Gaseous Perfluoroalkyl Iodides

**2.5.1. Reactions with  $\text{CF}_3\text{I}$ .** Trifluoromethyl iodide is a colorless gas with a normal boiling point of  $-21.85^\circ\text{C}$ .<sup>133</sup> It undergoes homolytic dissociation forming  $\text{CF}_3^\cdot$  radicals and I atoms at high temperatures<sup>134</sup> or under UV irradiation.<sup>135</sup> UV irradiation was used in the early studies of liquid-phase fullerene trifluoromethylation with  $\text{CF}_3\text{I}$  and  $\text{CF}_3\text{Br}$  (T1#3,8,10,11);<sup>7,9,11,12</sup> to date no isomerically pure TMFs have been isolated using this approach. On the other hand, thermally induced  $\text{CF}_3\text{I}$  trifluoromethylation of solid fullerene samples has been the method of choice for the synthesis of TMFs, resulting in the isolation and full characterization of dozens of TMFs of hollow higher fullerenes (HHFs) and EMFs (T1#32,33,37,40–49, etc.).<sup>5,32,36,39,50,57,70,79,86,93</sup>

The heterogeneous trifluoromethylation of solid fullerenes with gaseous  $\text{CF}_3\text{I}$  involves several chemical and physical processes that control the resulting selectivity and % conversion, as shown in Scheme 3 (a similar scheme was first

**Scheme 3.** Heterogeneous Trifluoromethylation of Solid  $\text{C}_{60}$  with Gaseous  $\text{CF}_3\text{I}$  at High Temperature<sup>a</sup>



<sup>a</sup>The dimerization of I atoms to form  $\text{I}_2$  is not shown.

used in ref 101). Thermal dissociation of  $\text{CF}_3\text{I}$  takes place within the hot zone of the reactor. The energies of fullerene–I bonds are too low to allow for the isolation of stable fullerene iodides, especially for reactions performed at high temperatures. The only fullerene compound with a chemical bond between the cage and an I atom is  $\text{C}_{60}(\text{OO}-t\text{-Bu})_4(\text{OH})$ <sup>136</sup> (see ref 137 for more details). Therefore, reactions between I atoms and fullerenes at elevated temperatures can be ignored. The I atoms formed during the reaction dimerize to form molecular  $\text{I}_2$  and sublime out of the hot zone.

Trifluoromethyl radicals can react with solid fullerene particles forming a layer of solid TMFs (however, the formation of tight protective layers of TMFs has not been reported and is therefore unlikely). Reaction temperatures of  $380$ – $550^\circ\text{C}$  were used; both bare-cage fullerenes and TMFs can sublime at these temperatures, so the transport of the fullerene species out of the hot zone plays an important role. The volatility (sublimation temperature) of fullerene( $\text{CF}_3$ )<sub>n</sub> species is inversely related to the  $n$  value; for example,  $\text{C}_{60}$  sublimes at ca.  $500^\circ\text{C}$ , while **60-10-3** sublimes at ca.  $250^\circ\text{C}$  under vacuum.<sup>101</sup> Therefore, increasing the reaction temperature has

a counterintuitive effect on the average composition of the TMF products (heavier homologues typically melt, boil, and sublime at higher temperatures relative to lighter homologues).<sup>4,101</sup> Higher reaction temperatures allow the less volatile fullerene( $\text{CF}_3$ )<sub>2,4</sub> products to sublime out of the hot zone more quickly, preventing them from accumulating additional  $\text{CF}_3$  group.<sup>4</sup> Lower reaction temperatures have the opposite effect, since the rapid sublimation of TMF products out of the hot zone does not occur until eight or more  $\text{CF}_3$  groups have been added to the cage.<sup>4</sup> Not surprisingly, the length of the hot zone is also important, since a longer hot zone increases the residence time of the subliming TMF products. It has been shown that, all other things being equal, longer hot zones produce TMFs with higher values of  $n$ ).<sup>101</sup>

Another parameter that was shown to have a strong effect on TMF product composition is the presence or absence of Cu powder. Copper acts as a promoter of  $\text{CF}_3\text{I}$  dissociation (the presence of copper was shown to decrease the decomposition temperature of gaseous  $\text{CF}_3\text{I}$  by ca.  $120^\circ\text{C}$ ).<sup>101</sup> The presence of Cu powder strongly increased the rate of fullerene trifluoromethylation, improved the % conversion of the fullerene to TMFs, lowered the necessary reaction temperature by ca.  $100^\circ\text{C}$ , and increased the average  $n$  values of the resulting TMFs relative to similar trifluoromethylations carried out in the absence of Cu).<sup>101</sup> Promotion with Cu has been used extensively for trifluoromethylation of less reactive HHFs (T1#53,61)<sup>50,57</sup> and  $\text{Sc}_3\text{N}@\text{C}_{80}\text{-I}_h$  (T1#102)<sup>93</sup> and especially for heterogeneous perfluoroalkylation of fullerenes with heavier R<sub>F</sub>I's (see next section for details). See ref 101 for a more detailed discussion of the effects of the experimental parameters on fullerene trifluoromethylation with  $\text{CF}_3\text{I}$ .

Figure 3 shows the three different types of reactors that have been used for fullerene trifluoromethylation with  $\text{CF}_3\text{I}$  gas. The first report on  $\text{CF}_3\text{I}$  trifluoromethylation of solid fullerene at high temperature used a flow-tube reactor like the one shown in Figure 3A (T1#32,<sup>4</sup> see Table 1 for other examples). In a typical procedure, a sample of fullerene was placed inside a fused silica (or glass) tube heated in a tube furnace. A stream of  $\text{CF}_3\text{I}$  gas was slowly passed over the fullerene and vented through an oil bubbler to eliminate a back-diffusion of air (very low flows of  $\text{CF}_3\text{I}$  were used). The resulting TMFs and iodine sublimed on the cold sections of the flow tube reactor. After the reaction was complete, the sublimed TMFs,  $\text{I}_2$ , and unreacted fullerene were dissolved in an aromatic solvent, which was typically toluene. The extract was evaporated to dryness under vacuum to remove  $\text{I}_2$  and redissolved in an organic solvent. This iodine-free solution was filtered and separated using HPLC. This procedure has been commonly used for the workup of crude TMFs and PFAFs prepared using R<sub>F</sub>I reagents (and therefore contaminated with iodine that needs to be removed prior to the HPLC separation). The flow tube reactor has been used to prepare many TMFs and some PFAFs with various numbers of R<sub>F</sub> groups ( $n = 2$ – $12$ ); it was also successfully used for trifluoromethylation of HHFs and EMFs (see Table 1). A typical yield of an isomerically pure TMF prepared in a flow-tube reactor is less than 10 mol % due to the relatively low selectivity of the trifluoromethylation process. Partial tuning of the product composition can be attained by varying reaction temperature, as shown in ref 39. A singular example of a highly selective reaction is the synthesis of **70-10-1**. This compound can be prepared with up to 90% purity (without HPLC separation) and with up to 55 mol % yield.<sup>68,99</sup> Using a gas handling system is used with an oil bubbler serving

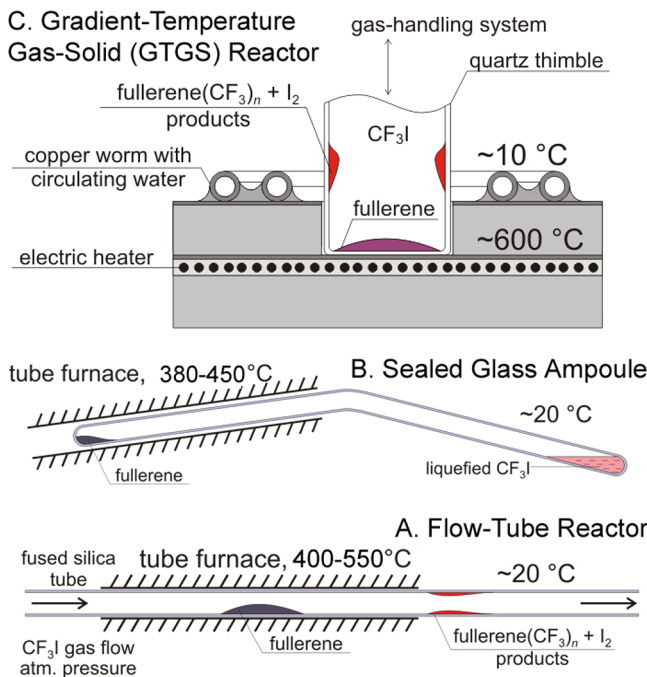


**Figure 3.** Schematic drawings of three reactor types used for the high-temperature heterogeneous trifluoromethylation of solid fullerenes with gaseous CF<sub>3</sub>I.

as a pressure release, and ambient pressure of CF<sub>3</sub>I is maintained during the synthesis (see ref 101 for the only example of a variable-pressure closed-loop flow tube reactor). Very long residence times can be achieved if a long hot zone and a slow CF<sub>3</sub>I flow rate are used. There is evidence that the long residence times of TMF species inside the hot zone lead to crude products with a simpler isomeric composition (see below).<sup>101</sup>

A different type of reactor, shown in Figure 3B, was used by Dimitrov et al. in 2006 to trifluoromethylate C<sub>60</sub><sup>36</sup> (T1#36) and was later applied to the trifluoromethylation of other fullerenes.<sup>51,86,96,100</sup>

In a typical synthesis, a sample of C<sub>60</sub> was loaded into a glass ampoule with two sections. An excess of CF<sub>3</sub>I was condensed into the ampoule at low temperature, and the ampoule was flame-sealed. The section containing the fullerene was placed inside a tube furnace and heated, while the other section, holding liquid CF<sub>3</sub>I at ca. 5 bar, was kept at room temperature.<sup>133</sup> The high pressure of CF<sub>3</sub>I apparently led to high degrees of trifluoromethylation (typically compounds with more than 10 CF<sub>3</sub> groups were formed). It is important to note that even higher pressures can be generated inside the sealed ampoule as the reaction progresses because the byproduct C<sub>2</sub>F<sub>6</sub> has a vapor pressure of ca. 30 bar at 20 °C.<sup>138</sup> For this reason, only properly trained personnel should perform these sealed ampoule trifluoromethylations. The scale-up of such procedures is extremely difficult since, for the same wall thickness, the burst pressure of a sealed glass ampoule is inversely proportional to its diameter. This inverse dependence makes the use of larger-diameter glass ampoules very risky. Metal reactors could potentially be used, but the generation of I<sub>2</sub> is likely to result in severe metal corrosion. The pressure of CF<sub>3</sub>I can be controlled by cooling or heating the end of the ampoule that holds the liquefied gas,<sup>133</sup> but no such experiments have been reported to date. Many TMFs were prepared in sealed

ampoules and isolated in isomerically pure form using HPLC (e.g., **60-8-1** (T1#56),<sup>53</sup> **60-12-1** (T1#36),<sup>36</sup> **60-12-(5,6)**, and **60-14-3** (T1#75);<sup>74</sup> see Table 1 for other examples). This technique was also used to trifluoromethylate HHFs (T1#85, 87, 90, 93, 101)<sup>84,139</sup> and Sc<sub>3</sub>N@C<sub>80</sub> (T1#102,104).<sup>100,102</sup> A sealed-ampoule reactor was also used to trifluoromethylate C<sub>60</sub>F<sub>18</sub>, leading to mixed C<sub>60</sub>F<sub>n</sub>(CF<sub>3</sub>)<sub>m</sub> derivatives (T1#74), and Na<sub>n</sub>·C<sub>60</sub>, leading to complex dimeric species (T1#95).<sup>92</sup> The yields of isolated pure TMFs have typically not been reported, but it is reasonable to expect mol % yields in low single digits. Yields of 84 and 78 mol % were reported for an ampoule synthesis of **60-12-1** (T1#36),<sup>36,140</sup> but these yields could not be reproduced by the authors of ref 95.

Figure 3C shows a specialized gradient-temperature gas-solid (GTGS) reactor that was developed in our lab and used successfully for the trifluoromethylation of C<sub>60</sub> and C<sub>70</sub> (T1#107)<sup>101,113</sup> and Er<sub>3</sub>N@C<sub>80</sub> (T1#102).<sup>93</sup> This reactor allows the CF<sub>3</sub>I partial pressure (as well as the total pressure if a buffer gas is used) to be controlled precisely, from a few Torr up to slightly above ambient pressure; other reaction parameters can also be easily adjusted. It was designed and was used to study the effects of various reaction parameters on the % fullerene conversion and the TMF product composition.<sup>101</sup> A static atmosphere of CF<sub>3</sub>I gas is used, which leads to a more economical use of CF<sub>3</sub>I compared to a flow-tube reactor. The size of the GTGS hot zone can be varied, and very short reaction hot zones can be used. Using a low pressure of CF<sub>3</sub>I (ca. 10 Torr) and a short hot zone, the selective synthesis of **60-2-1** was achieved (with 20–25 mol % yields; it was also shown that the average composition of the TMFs can be controlled over a wide range by changing the CF<sub>3</sub>I pressure and other parameters).<sup>101</sup> It was also shown that the use of a short hot zone led to crude products containing more TMF isomers as compared to reactions performed in a flow-tube reactor with a much longer hot zone.

**2.5.2. Reactions with Other R<sub>F</sub>I's.** Various homologues of CF<sub>3</sub>I have been used successfully for the perfluoroalkylation of hollow fullerenes and EMFs. Two reports published in 2006 described the use of C<sub>2</sub>F<sub>5</sub>I for fullerene perfluoroethylation in a flow-tube reactor at 400–430 °C (T1#41,42; C<sub>2</sub>F<sub>5</sub>I is a gas at room temperature; its normal boiling point is 12.5 °C).<sup>39,40</sup> Heavier R<sub>F</sub>I reagents were also used in flow-tube reactors, but a carrier gas was employed to introduce them into the reaction hot zone (e.g., N<sub>2</sub> was bubbled through the room-temperature liquid R<sub>F</sub>I reagents for R<sub>F</sub> = n-C<sub>3</sub>F<sub>7</sub>, i-C<sub>3</sub>F<sub>7</sub>, n-C<sub>4</sub>F<sub>9</sub>, and n-C<sub>6</sub>F<sub>13</sub>; T1#103,104).<sup>94,95</sup> Copper powder was mixed with the fullerene starting material in all of cases so that lower reaction temperatures could be used (longer-chain R<sub>F</sub><sup>•</sup> radicals are known to fragment at high temperatures, leading to PFAFs with more than one type of R<sub>F</sub> group<sup>95</sup>). In one case, a GTGS reactor was used to prepare **60-2-1**(C<sub>2</sub>F<sub>5</sub>) (T1#109; in this case C<sub>60</sub> was mixed with Cu powder and reacted with 12 Torr of C<sub>2</sub>F<sub>5</sub>I).<sup>104</sup> It is notable that reactions between solid C<sub>60</sub> and gaseous n-C<sub>3</sub>F<sub>7</sub>I and i-C<sub>3</sub>F<sub>7</sub>I failed to give any detectable PFAF products, with or without Cu powder, when carried out in a GTGS reactor with reaction temperatures up to 500 °C). This may be attributed to the low partial pressures of n-C<sub>3</sub>F<sub>7</sub>I and i-C<sub>3</sub>F<sub>7</sub>I that were used (ca. 20 Torr).<sup>104</sup>

Sealed glass ampoules have been used for the majority of reactions with R<sub>F</sub>I reagents other than CF<sub>3</sub>I due to their higher boiling points. Long reaction times have been commonly reported (several days) with reaction temperatures of 380–450

°C (T1#58<sup>54</sup> and other examples in Table 1). Copper powder was only used except in a few cases (T1#85,104).<sup>79,94</sup> In all cases the crude product mixtures were separated using HPLC to give pure single isomers of PFAFs. The yields of the single-isomer PFAFs were typically not reported, but low single-digit mol% yields are likely.

## 2.6. Formation of New Isomers by Thermal Treatment of PFAFs

High-temperature sublimation of crude products prepared using AgTFA was the first synthetic procedure that made use of rearrangement and/or decomposition of kinetic TMF isomers (T1#27).<sup>27</sup> The use of high-temperature sublimation step is typical for the AgTFA synthesis of C<sub>60</sub> and C<sub>70</sub> TMFs; see above. Several later reports have described thermal rearrangement/decomposition of PFAF mixtures prepared using R<sub>F</sub>I reagents (T1#72,78,80,81,82,97).<sup>71,87,111</sup> The first paper describing this approach was published in 2008 (T1#72).<sup>71</sup> A sample of C<sub>70</sub>(CF<sub>3</sub>)<sub>12–18</sub> (prepared by C<sub>70</sub> trifluoromethylation in a sealed glass ampoule) was mixed with C<sub>70</sub> and flame-sealed in a glass ampoule under vacuum. The ampoule was heated to 440–450 °C for a period of 60 h. The HPLC analysis of the product mixture showed that C<sub>70</sub> was completely consumed and a mixture of C<sub>70</sub>(CF<sub>3</sub>)<sub>6–10</sub> was formed (the subsequent HPLC separation of this mixture resulted in the isolation of 70-8-1, 70-8-2, and 70-10-1).<sup>141</sup> This work showed that TMFs can dissociate at high temperature and serve as trifluoromethylating agents themselves (see also T1#80<sup>79,111</sup>). A similar reaction between C<sub>60</sub> and C<sub>60</sub>(CF<sub>3</sub>)<sub>12–18</sub> was reported to give (among simple TMFs) complex dimeric species (C<sub>60</sub>)<sub>2</sub>(CF<sub>3</sub>)<sub>n</sub>(CF<sub>2</sub>)<sub>m</sub> (T1#96).<sup>92</sup>

Thermal treatment of C<sub>70</sub>(CF<sub>3</sub>)<sub>14–18</sub> and C<sub>70</sub>(C<sub>2</sub>F<sub>5</sub>)<sub>10,12</sub> in the absence of the parent fullerene C<sub>70</sub> or other CF<sub>3</sub><sup>·</sup> radical scavengers has been reported (T1#8,<sup>79</sup> T1#91,<sup>87</sup> and T1#78).<sup>77</sup> Temperatures of 340–380 °C (for C<sub>70</sub>(CF<sub>3</sub>)<sub>14–18</sub>)<sup>79,87</sup> and 280–300 °C (for C<sub>70</sub>(C<sub>2</sub>F<sub>5</sub>)<sub>10,12</sub>)<sup>77</sup> were used. In both cases, some loss of CF<sub>3</sub> and C<sub>2</sub>F<sub>5</sub> substituents was observed so that the average composition of the PFAFs shifted toward compounds with fewer R<sub>F</sub> groups. This is likely to proceed via detachment of CF<sub>3</sub><sup>·</sup> or C<sub>2</sub>F<sub>5</sub><sup>·</sup> (and dimerization to C<sub>2</sub>F<sub>6</sub> or C<sub>4</sub>F<sub>10</sub>), which is consistent with theoretical considerations of possible fullerene(R<sub>F</sub>)<sub>n</sub> isomerization mechanisms.<sup>142</sup>

Trifluoromethylation of the pure isomers 70-12-1 and 70-12-2 was also reported (T1#91).<sup>87</sup> These reactions were carried out in sealed glass ampoules in the presence of excess CF<sub>3</sub>I at 350 °C for 48 h. The crude products were found to contain C<sub>70</sub>(CF<sub>3</sub>)<sub>12–20</sub> according to MALDI mass spectrometry. Their further analysis revealed that some amount of 70-12-2 had been transformed into 70-10-1. Trifluoromethylation of 70-12-1 and 70-12-2 also gave C<sub>70</sub>(CF<sub>3</sub>)<sub>14</sub> isomers with addition patterns that were not based on the addition patterns of the starting materials.

More recently, thermal treatments of the mixtures of C<sub>60,70</sub>(CF<sub>3</sub>)<sub>12–20</sub> with the respective bare fullerenes in the sealed ampoules were carried out with the goal of generating new TMF isomers (T1#115,121). This had been achieved more successfully with C<sub>70</sub>(CF<sub>3</sub>)<sub>n</sub> compounds: four new isomers of C<sub>70</sub>(CF<sub>3</sub>)<sub>8</sub> were isolated chromatographically, and structurally characterized. However, when a mixture of 60-12-1 was heated with C<sub>70</sub> at 530 °C, only known isomers of C<sub>70</sub>(CF<sub>3</sub>)<sub>n<12</sub> were found among the products.<sup>111</sup>

These results clearly indicate that PFAFs can undergo detachment/reattachment of R<sub>F</sub> groups at high temperatures,

leading to shifts in composition and/or to isomerization. Whether PFAFs can isomerize by intramolecular migration of R<sub>F</sub> substituents is not known at this time. The detachment/attachment mechanism is believed to be more favorable.<sup>142</sup>

## 2.7. PFAF Preparation via Reactions with Metal R<sub>F</sub> Reagents

The only example of this approach was published in 2011 (T1#110).<sup>103</sup> A mixture of C<sub>60</sub>(C<sub>2</sub>F<sub>5</sub>)<sub>2,4</sub> and C<sub>60</sub>(C<sub>2</sub>F<sub>5</sub>)<sub>1,3,5</sub>H was prepared by the reaction of C<sub>60</sub>Cl<sub>6</sub> with LiC<sub>2</sub>F<sub>5</sub> at ca. –95 °C in toluene solution (note that LiC<sub>2</sub>F<sub>5</sub> is thermally unstable and has to be prepared at low temperature and used immediately). HPLC separation yielded several isomerically pure compounds including C<sub>s</sub>-C<sub>60</sub>(C<sub>2</sub>F<sub>5</sub>)<sub>s</sub>H, which was isolated in ca. 10 mol % yield and characterized by single-crystal X-ray diffraction. Reaction of C<sub>60</sub> with LiC<sub>2</sub>F<sub>5</sub> did not produce any PFAF compound.<sup>103</sup>

## 2.8. Summary Remarks on Synthetic Methods

In the sections above, we reviewed various methods for the preparation of PFAFs. Almost all of these methods rely on radical perfluoroalkylation of fullerenes under a variety of conditions. The only unambiguous exception is the preparation of several C<sub>2</sub>F<sub>5</sub> derivatives of C<sub>60</sub> by nucleophilic substitution (T1#110).<sup>103</sup> The formation of TMFs during the carbon arc discharge synthesis of fullerenes is of historical interest but is not practical because yields are extremely low and because the product mixtures are extremely complex. The formation of mixed fullerene(F)<sub>n</sub>(R<sub>F</sub>)<sub>m</sub> derivatives during fullerene fluorination reactions is also impractical because of extremely low yields. The use of AgTFA as a fullerene trifluoromethylation reagent led to the preparation and isolation of many TMFs, but this method is generally inferior to trifluoromethylation with CF<sub>3</sub>I because it requires additional workup (i.e., sublimation, which also leads to lower yields). Overall the method of choice for PFAF preparation is perfluoroalkylation with R<sub>F</sub>I reagents. This process has been extensively studied under a variety of conditions, including reactions in solution and reactions between solid fullerenes and gaseous R<sub>F</sub>I reagents. Three different reactors were developed and used for the latter process, resulting in the synthesis of many dozens of well-characterized PFAFs. The concentration and mole ratio of R<sub>F</sub>I reagents was shown to have a strong effect on the product distribution and on % fullerene conversion. Other reaction parameters were also investigated and found important; it was shown that the transport of PFAF products out of the hot reaction zone by sublimation plays a very significant role, leading to a relatively narrow ranges of PFAF compositions.<sup>4,32,39,110</sup> Note that, under homogeneous or nearly homogeneous fullerene perfluoroalkylation in solution, the PFAFs produced cannot leave the reaction zone. This has resulted in broad distributions of fullerene(R<sub>F</sub>)<sub>n</sub> products (i.e., a wide range of n values) with different n values when a large excess of the PFAF reagent was used (see ref 104 for a statistical treatment of this phenomenon). Nevertheless, homogeneous solution-phase reactions were found to be ideally suited for the selective synthesis of fullerene(R<sub>F</sub>)<sub>2</sub> compounds.<sup>104</sup> Finally, the preparation of PFAFs with eight or more R<sub>F</sub> groups is best carried out under heterogeneous conditions at high temperatures when the goal is to prepare fewer isomers of a relatively narrow range of PFAF compositions.

### 3. PHYSICAL PROPERTIES AND SEPARATION METHODS OF PFAFs

All perfluoroalkylfullerenes prepared to date are solids. No fullerene( $R_F$ ) $_n$  compound with a melting point below room temperature has been reported. The colors of PFAFs in solution and as single-crystals depend on both the  $R_F$  group and the value of  $n$ . The color palette includes dark brown, red-brown, red, red-orange, orange, yellow-orange, and yellow. This is the order observed as  $n$  increases for TMFs, which is consistent with the color changes expected as the number of cage double bonds decreases (i.e., one fewer double bond for every two additional substituents). In general the compounds are dark-brown or red-brown when  $n = 2$ , red-brown, red or red-orange when  $n = 6$  or 8, red, red-orange, or orange when  $n = 10$ , and orange, yellow-orange, or yellow when  $n \geq 12$ . Typical examples are as follows: **60-2-1** is dark-brown; **60-6-1** is red-brown; **60-6-2**, **60-8-3**, **76-8-2**, and **78-10-1** are red; **60-10-3** is red-orange; **60-10-5**, **76-10-5**, **78-10-1**, and **70-12-1** are orange; and **60-12-1**, **70-12-1**, **78-12-2**, and **84-12-2** are yellow. There are, of course, a few exceptions: **60-4-2** and **70-10-5** are green; and **90-12-1** and **90-12-2** are brown.

However, for reasons that are still not clear, PFAFs with  $C_2F_5$ ,  $n-C_2F_7$ ,  $i-C_3F_7$ , and longer chain  $R_F$  groups have darker colors all the way up to  $n = 10$ . This is a reliable conclusion for  $R_F = C_2F_5$  PFAFs but only a tentative conclusion for longer  $R_F$  groups: in contrast to ca. 40  $R_F = C_2F_5$  PFAFs with  $n \geq 6$ , all of which are either dark-brown or dark-red in color, there are only seven  $R_F = n$ - or  $i-C_3F_7$  PFAFs with  $n \geq 6$  (these are also dark-brown or dark-red) and there are none with longer  $R_F$  groups with  $n \geq 6$  (note there are more than 120  $R_F = CF_3$  PFAFs with  $n \geq 6$ ).

All PFAFs are freely soluble in  $CH_2Cl_2$  and  $CHCl_3$  ( $CDCl_3$  is the solvent most commonly used to prepare solutions for NMR spectroscopy). Many PFAFs have good solubilities in aromatic solvents such as benzene, toluene, CB, oDCB, and TCB, and, to a lesser extent, in aliphatic hydrocarbon solvents such as hexane and heptane. In contrast, PFAFs are virtually insoluble in polar solvents such as water, methanol, acetonitrile, and tetrahydrofuran (as are the parent bare-cage fullerenes from which they are made).<sup>123</sup> PFAFs with  $n \geq 10$   $R_F$  groups and/or with large  $R_F$  groups longer than  $C_2F_5$  are only soluble in fluorous solvents such as Freon-113,  $C_6F_6$ , or perfluoroheptane. The diagram in Figure 4, which is based on qualitative data from the literature, illustrates the solubility behavior of PFAFs. For example, PFAFs with two  $R_F$  groups are soluble in

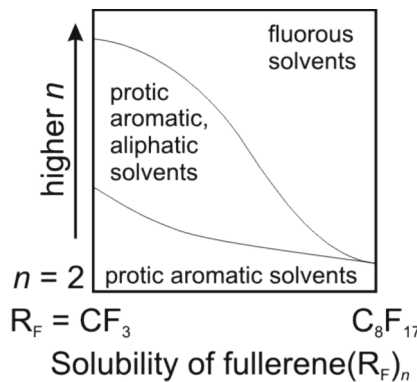


Figure 4. Dependence of PFAF solubility on the type and number of  $R_F$  groups.

aromatic hydrocarbon solvents but not in aliphatic or fluorous ones.<sup>104</sup> PFAFs with  $R_F = CF_3$  or  $C_2F_5$  and with  $n = 6–14$  are readily soluble in both aromatic and aliphatic hydrocarbon solvents but not in fluorous solvents. When  $n$  is greater than 14, PFAF solubilities in both types of hydrocarbon solvents are low but solubilities in fluorous solvents are high. PFAFs with  $R_F = n-C_4F_9$  and  $n = 4$  or 6 are soluble in aromatic and aliphatic hydrocarbon solvents, but not in fluorous solvents. Compounds with the two largest  $R_F$  groups,  $n-C_8F_{17}$  and  $CF_2C_6F_5$ , are soluble in toluene but not in aliphatic hydrocarbons, but compounds with more than two of these groups are only soluble in fluorous solvents.

The only quantitative solubility data published was for a series of  $C_{60}(R_F)_2$  compounds in toluene.<sup>104</sup> It was found that 1,7- $C_{60}(R_F)_2$  (i.e., *para*- $C_{60}(R_F)_2$ ) with  $R_F = CF_3$ ,  $C_2F_5$ ,  $n-C_3F_7$ ,  $i-C_3F_7$ ,  $n-C_4F_9$ ,  $s-C_4F_9$ , and  $n-C_8F_{17}$  have solubilities between 1.5 and 8.5 mg/mL (cf.  $C_{60}$ , with a toluene solubility of 2.4 mg/mL). In contrast, the compound 1,7- $C_{60}(CF_2C_6F_5)_2$  has a toluene solubility of 400 mg/mL, one of the highest solubilities reported for any fullerene derivative. Such a high solubility can be rationalized by strong interactions between the  $C_6F_5$  substituents and toluene molecules (In a related phenomenon, it was reported that the solubility of  $C_{60}$  increased in the presence of 1,7- $C_{60}(CF_2C_6F_5)_2$  (see refs 125 and 143 for further information).

The apparent solubility of some TMFs is related in an interesting way to their relative purities.<sup>95</sup> Before HPLC separation, some reaction mixtures contain higher concentrations of many of the TMFs in the mixture than the saturation concentration of the purified individual components in the same solvent. This is clearly a kinetic phenomenon. For example, **60-12-1** crystallized extremely slowly from a mixture of other TMFs but did not redissolve in the same amount of solvent. In contrast, an HPLC fraction containing only **60-12-1** formed single crystals more quickly even though it was more dilute.

Many TMFs have high thermal stabilities, and melt or sublime without decomposition. For example, a mixture of  $C_{60}(CF_3)_{8–10}$  derivatives melted without decomposition at 400 °C and of a mixture of  $C_{60}(C_2F_5)_{8–10}$  derivatives melted without decomposition at 290 °C.<sup>95</sup> However, the compound **60-12-1** melted at 500 °C with partial decomposition.<sup>140</sup> It is not surprising that the sublimation temperatures of fullerene-( $CF_3$ ) $_n$  species decrease as the  $n$  increases. This is because  $CF_3$  and other  $R_F$  substituents separate the fullerene cages from one another in the solid state, reducing the attractive cage–cage interactions. For example,  $C_{60}$  sublimes at ca. 500 °C under vacuum and **60-10-3** sublimes at ca. 250 °C (under vacuum even though the molar mass of **60-10-3** is nearly twice that of  $C_{60}$ ).<sup>101</sup> Another example is that the enthalpies of sublimation of  $C_{60}$  and **60-12-1** were found to be 175 and 140 kJ·mol<sup>-1</sup>, respectively.<sup>144</sup> The decrease in sublimation temperature or enthalpy of sublimation as  $n$  increases was also observed for fluorinated fullerenes.<sup>145</sup> Finally, it has been observed that PFAFs derived from HHFs or EMFs have higher sublimation temperatures than those derived from  $C_{60}$  and  $C_{70}$ .

Some TMFs are not stable indefinitely at high temperatures, even at the temperature used for their synthesis. Several reports showed that PFAFs with  $R_F = CF_3$  and  $C_2F_5$  lose  $R_F$  groups above 280–350 °C.<sup>71,77,79,92</sup> The thermal stability of PFAFs with  $R_F$  groups larger than  $C_2F_5$  has not been investigated, but is likely to be even lower. It is also notable that heavier  $R_F$  groups themselves undergo cleavage at higher temperatures,

e.g.,  $C_2F_5I$  cleaves to give  $CF_3^\bullet$  radicals (and corresponding mixed  $C_{60}(C_2F_5)_n(CF_3)_m$ ).<sup>95</sup>

### 3.1. Separation of PFAFs

Perfluoroalkylated fullerenes are typically prepared as mixtures of multiple isomers and multiple compositions. In a few cases, higher synthetic selectivity has been realized, but even in these cases a chromatographic separation was necessary to obtain 98% pure PFAFs (for example, see the synthesis of **70-10-1** (T1#39,72)<sup>68,99</sup> and a synthesis of the series of compounds **60-2-1 R<sub>F</sub>** (T1#111,114)<sup>101,104</sup>). Except for a few early reports that used flash chromatography and gel permeation chromatography (T1#7,9,17<sup>10,14,17</sup>), reverse-phase HPLC using specialized columns designed and optimized for fullerene separation has been employed. The most commonly used column is Cosmosil BuckyPrep, although in several publications other HPLC columns were used in conjunction with it to achieve an even better separation (e.g., Cosmosil SPYE and Regis BuckyClutcher). Several aromatic and aliphatic solvents and their mixtures have been used as eluents. It is constructive to compare eluents used for PFAF separation in terms of how “strong” or “weak” they are. In other words, eluents that interact strongly with the stationary phase of the HPLC column (“strong” eluents) will lead to shorter retention times and lower peak resolution. Eluents that interact weakly with the stationary phase will lead to longer retention times and higher peak resolution. Chlorobenzene is a strongest eluent that has been used for PFAF separation, with toluene being somewhat weaker. Aliphatic hydrocarbons (e.g., hexane and heptane) are much weaker solvents compared to aromatics hydrocarbons, and it has been common practice to use mixtures of toluene and hexane (or heptane) to achieve good separation in a reasonable amount of time (solubility issues notwithstanding, the use of 100% hexane or heptane would lead to prohibitively long retention times for many PFAFs). Recently, mixtures of toluene and polar solvents like acetonitrile and 2-propanol (80/20 or 70/30 v/v) were reported to give good results for the separation of some  $C_{60}(R_F)_2$  compounds (see T1#105).

The retention times of PFAFs correlate with the number and size of the  $R_F$  groups. As more  $R_F$  groups are added to a fullerene cage, or as the  $R_F$  groups become larger, retention times become shorter. There are very few exceptions to this rule, T1#65,66<sup>61,62</sup> and T1#109<sup>125</sup>). Therefore, as the number of  $R_F$  groups or their size increases, the separation of PFAFs becomes progressively more difficult.

A typical PFAF HPLC separation is carried out in several stages. The first stage uses a strong eluent typically toluene, and fractions corresponding to mixtures of PFAFs with similar retention times are collected. These fractions are then evaporated to dryness, redissolved in a weaker eluent, then another separation stage. The use of multiple stages allows one to optimize separation times without sacrificing the purity of the isolated PFAFs.

## 4. X-RAY CRYSTALLOGRAPHY AND $^{19}F$ NMR SPECTROSCOPY OF PFAFs

### 4.1. $C_{60}(R_F)_n$ Derivatives

The development of efficient synthetic procedures for  $C_{60}$  PFAFs, and the surprisingly facile formation of suitably sized crystals resulted in the determination of many dozens of  $C_{60}(R_F)_n$  crystal structures ( $n = 2–18$ ). Slow solvent evaporation and solvent diffusion are the most common techniques used for growing  $C_{60}(R_F)_n$  crystals. Synchrotron

radiation sources have often been employed for X-ray data collection because (i) crystals with dimensions in the range of 10–80  $\mu\text{m}$ , and (ii) with the exception of  $EMF(R_F)_n$  derivatives, PFAFs only contain low-Z atoms with small X-ray scattering factors, namely C, F, and occasionally N and O.

Crystallographic studies of PFAFs have been used for three main purposes: (i) determination of their addition patterns, (ii) prediction of the most likely addition sites for further functionalization, and (iii) validation of theoretical calculations.

#### 4.1.1. Determination of $C_{60}(R_F)_n$ Addition Patterns.

Determination of the X-ray structures for various isomers and compositions of  $C_{60}(R_F)_n$  derivatives was very important at the early stages of PFAF research. Early on, there was controversy about addition patterns deduced from the analysis of  $^{19}F$  NMR spectra: on the one hand,  $C_{60}(CF_3)_n$  addition patterns were believed to be chains of contiguous cage  $C(sp^3)$  atoms bearing the  $CF_3$  groups, similar to the types of addition patterns observed for fluorofullerenes.<sup>25,26,35</sup> On the other hand, we proposed that  $CF_3$  groups added to fullerenes at the *para* positions of cage hexagons, and these hexagons were linked so that the intervening hexagons were either *para*- $C_6(CF_3)_2$  or *meta*- $C_6(CF_3)_2$  moieties.<sup>27</sup> This controversy was ultimately resolved in 2005 when we published the first X-ray structure of a PFAF, **60-10-3** (see Table 2 for the IUPAC locants of  $C_{60}(R_F)_n$  isomers).<sup>4</sup> The 10  $CF_3$  groups formed five *p*- $C_6(CF_3)_2$  hexagons, which were linked by three intervening *m*- $C_6(CF_3)_2$  hexagons and one *p*- $C_6(CF_3)_2$  hexagon to form a *para*-*meta*-*para*-*para*-*meta*-*para*-*meta*-*para* ribbon of linked hexagons, which is abbreviated *pmp<sup>3</sup>mpmp*.

Numerous X-ray structures that followed revealed that the most common addition patterns of  $C_{60}(CF_3)_n$  compounds could be described as ribbons or loops of edge-sharing *m*- and/or *p*- $C_6(CF_3)_2$  hexagons (each shared edge is a fullerene  $C(sp^3)-C(sp^2)$  bond); occasionally the addition pattern consisted of a ribbon of  $n - 2$   $CF_3$  groups plus an isolated *para*- $C_6(CF_3)_2$  hexagon. For example, the addition patterns of **60-4-1**, **60-4-2**, and **60-4-3** are abbreviated *pmp*, *p,p* (i.e., two isolated *p*- $C_6(CF_3)_2$  hexagons) and *p<sup>3</sup>* (in some earlier papers the isomer **60-4-3** was referred to as **60-4-2**). There is only one possible *pmp* isomer and one possible *p<sup>3</sup>* isomer for the composition  $C_{60}(CF_3)_4$ ; there are 14 possible ways to arrange two isolated *p*- $C_6(CF_3)_2$  hexagons on  $C_{60}$ , but so far only one such isomer, **60-4-2**, is known. Other examples are **60-6-1** (*p<sup>3</sup>mp*), **60-6-6** (*pmp,p*), **60-6-7** (*pmpmp*), **60-8-1** (*p<sup>3</sup>mpmp*), and **60-10-1** (*p<sup>3</sup>mpmp,p*). For  $n \leq 10$ , only one compound, **60-10-3**, has more than one  $CF_3$  group per pentagon ( $C_{60}$  and all other fullerenes have exactly 12 pentagons), almost certainly for steric reasons ( $CF_3$  groups are sterically more demanding than Br atoms), and only rarely do  $CF_3$  groups occupy adjacent (i.e., *ortho*) cage C atoms. For  $n \leq 12$ , the only examples are **60-6-2** and **60-12-3**. For  $n \geq 14$ , the addition of  $CF_3$  groups to adjacent cage C atoms is more common (e.g., **60-14-3**, **60-16-2**, and **60-16-3**). In contrast, X-ray crystallographic studies of the  $C_{60}$  derivatives with bulkier *i*- $C_3F_7$  groups showed that they form only isolated *p*- $C_6(i-C_3F_7)_2$  hexagons, not ribbons or loops (e.g., **60-6-5-i-C<sub>3</sub>F<sub>7</sub>**, **60-6-8-i-C<sub>3</sub>F<sub>7</sub>**, and **60-8-11-i-C<sub>3</sub>F<sub>7</sub>**). At the same time, less sterically demanding  $C_2F_5$  groups were found to form the same addition patterns observed for both  $C_{60}(CF_3)_n$  and  $C_{60}(i-C_3F_7)_n$  compounds. For example, **60-8-1-C<sub>2</sub>F<sub>5</sub>**, **60-8-3-C<sub>2</sub>F<sub>5</sub>**, and **60-10-6-C<sub>2</sub>F<sub>5</sub>** have the same addition patterns as their  $C_{60}(CF_3)_n$  counterparts. Formation of these isomers as abundant products demonstrates that the steric strain introduced in these structures due to the larger size of

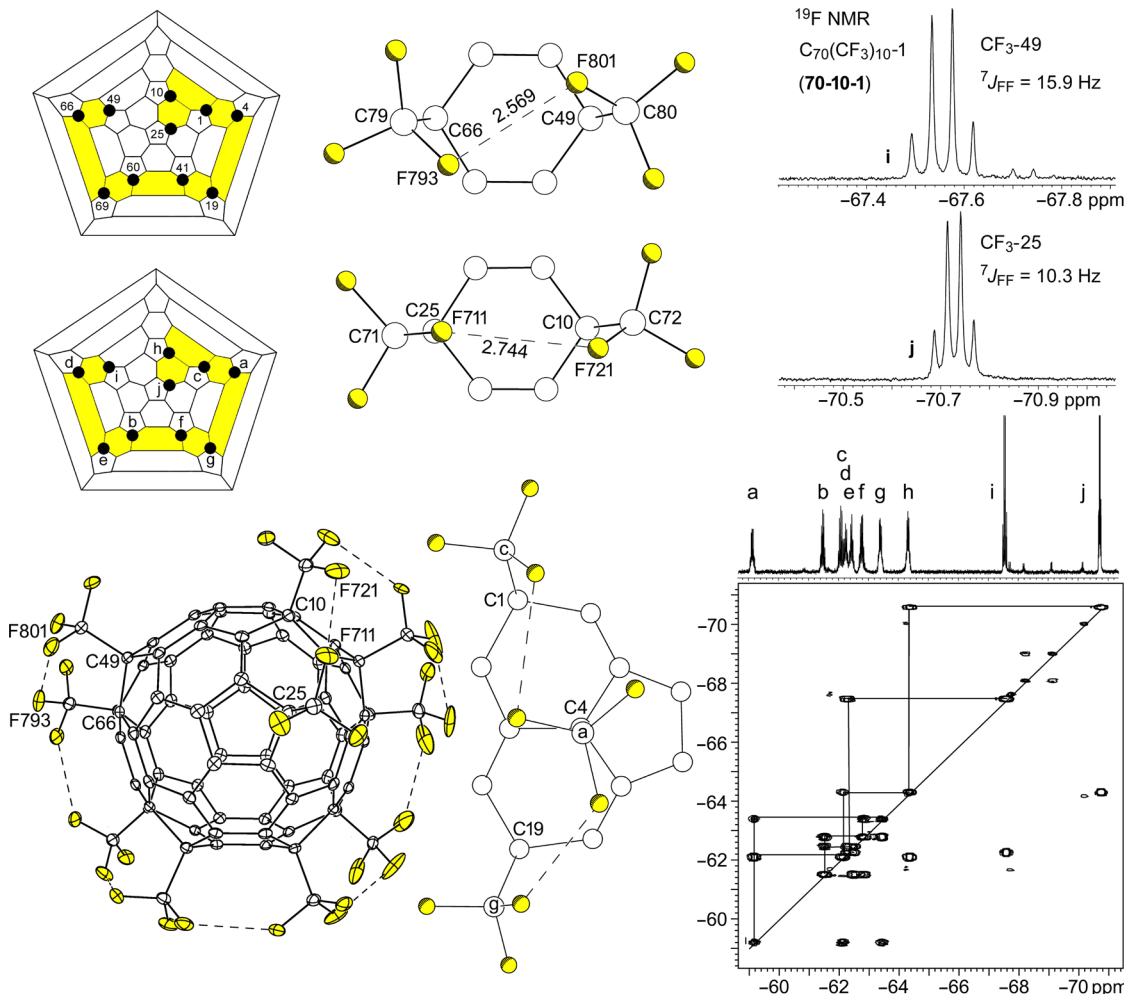


**Figure 5.** X-ray structure of the *pmp*<sup>7</sup> isomer of C<sub>70</sub>(CF<sub>3</sub>)<sub>10</sub> (**70-10-1**, ref 32), its 2D COSY <sup>19</sup>F NMR spectrum (ref 4), fragments of the structure showing four *p*-C<sub>6</sub>(CF<sub>3</sub>)<sub>2</sub> hexagons, and two Schlegel diagrams indicating the placement and IUPAC locants of the ten CF<sub>3</sub> groups and their <sup>19</sup>F NMR multiplet assignments. The CF<sub>3</sub> group attached to C4 on the C<sub>70</sub> cage is nearly eclipsed, and as a consequence its NMR multiplet  $-\delta$  value is less than 60 ppm. The NMR multiplets for the terminal CF<sub>3</sub> groups, attached to C25 and C49, have different <sup>7</sup>J<sub>FF</sub> values as a consequence of different F···F distances and F–C···C–F torsion angles. The shorter F···F distance (2.569(9) Å) and larger F–C···C–F angle (78°) for the CF<sub>3</sub> group on C49 resulted in a larger through-space Fermi-contact  $J_{\text{FF}}$  coupling constant for quartet **i** (15.9 Hz) than for the CF<sub>3</sub> group on C25 (2.744(9) Å, 24°, and 10.3 Hz for quartet **j**).

C<sub>2</sub>F<sub>5</sub> groups than CF<sub>3</sub> does not affect significantly distribution of the most favorable addition patterns; even additions of C<sub>2</sub>F<sub>5</sub> groups in *meta* positions appear in these structures. At the same time, C<sub>2</sub>F<sub>5</sub> groups also demonstrate the tendency known for bulky *i*-C<sub>3</sub>F<sub>7</sub> radicals. For example, the addition pattern of **60-6-8-C<sub>2</sub>F<sub>5</sub>** compound is analogous to that of **60-6-8-i-C<sub>3</sub>F<sub>7</sub>**, in which each pair of R<sub>F</sub> groups attach to the isolated hexagon in *para* position. More details about PFAF addition patterns are discussed in section 5.

The combination of X-ray structures and 1D <sup>19</sup>F and 2D <sup>19</sup>F–<sup>19</sup>F-COSY NMR spectra of C<sub>60</sub>(CF<sub>3</sub>)<sub>n</sub> isomers (and other fullerene(CF<sub>3</sub>)<sub>n</sub> compounds) allowed us to establish a correlation between the conformation of a particular CF<sub>3</sub> group and its <sup>19</sup>F chemical shift. It was found that CF<sub>3</sub> groups that have eclipsed or nearly eclipsed conformations with respect to the three cage C–C bonds that radiate from the C atom to which the CF<sub>3</sub> group is attached have  $-\delta$  values lower than 60 ppm (this was observed in the <sup>19</sup>F NMR spectra of **60-10-3**, **70-10-1**, and **60-12-2**). Figure 5 shows this effect for the CF<sub>3</sub> group attached to C<sub>70</sub> cage atom C4 in the *pmp*<sup>7</sup> ribbon isomer of C<sub>70</sub>(CF<sub>3</sub>)<sub>10</sub> (**70-10-1**).

In TMFs, <sup>6,7</sup>J<sub>FF</sub> spin–spin coupling values are only observed between CF<sub>3</sub> groups sharing the same hexagon or pentagon, because the coupling is almost exclusively mediated by through-space Fermi-contact overlap of F atom lone pairs (see refs 4, 32, 50, and references therein). In all but one case,<sup>39</sup> the rapid rotation of CF<sub>3</sub> groups about their C<sub>cage</sub>–CF<sub>3</sub> bond leads to fast-exchange <sup>19</sup>F NMR spectra, even at low temperature, and time-averaged <sup>6,7</sup>J<sub>FF</sub> values of 8–20 Hz are typically observed. These give rise to quartets for CF<sub>3</sub> groups with only one CF<sub>3</sub> group neighbor on a shared hexagon (i.e., CF<sub>3</sub> groups on isolated *p*-C<sub>6</sub>(CF<sub>3</sub>)<sub>2</sub> hexagons or at the terminus of a ribbon) and quartets-of-quartets (sometimes manifested as apparent septets) for CF<sub>3</sub> groups in the interior of a ribbon. This is also shown for **70-10-1** in Figure 5.

Furthermore, Figure 5 demonstrates that the through-space Fermi-contact  $J_{\text{FF}}$  values depend on the F···F distances and F–C···C–F torsion angles for the F atoms on hexagon-sharing CF<sub>3</sub> groups that face one another across the shared hexagon. These structural parameters can be determined by X-ray crystallography with the caveat that the exact conformations of the CF<sub>3</sub> groups may be different in the solid state and in

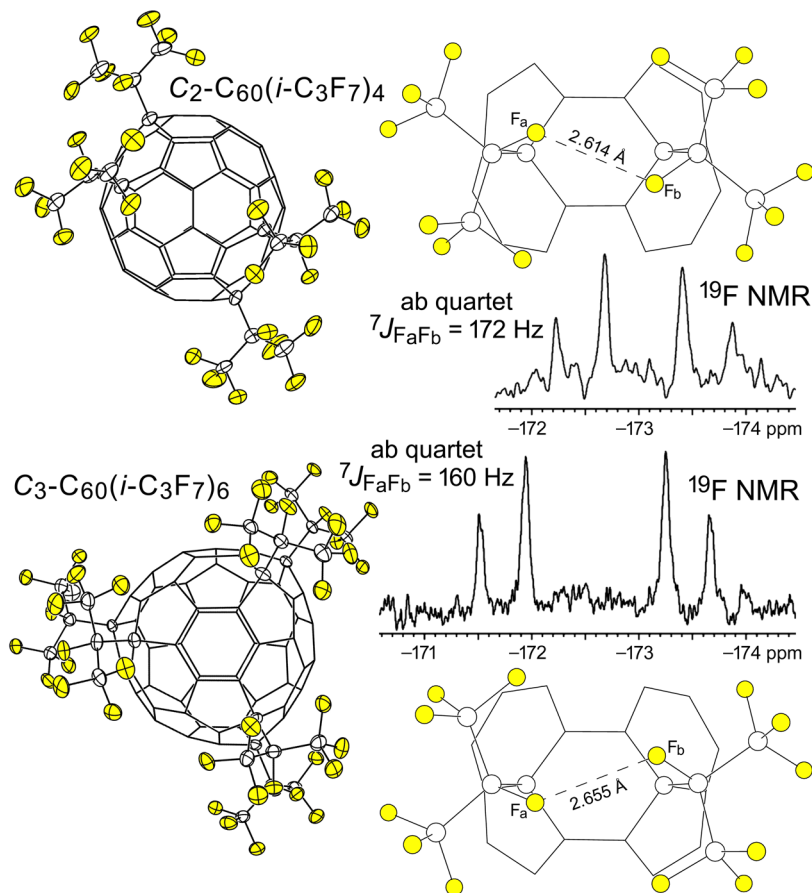


**Figure 6.** X-ray structures of  $C_2\text{-}C_{60}(i\text{-}C_3\text{F}_7)_4$  (**60-4-4-i-C<sub>3</sub>F<sub>7</sub>**; ref 94) and  $C_3\text{-}C_{60}(i\text{-}C_3\text{F}_7)_6$  (**60-6-5-i-C<sub>3</sub>F<sub>7</sub>**; ref 60), fragments of the structures showing  $p\text{-}C_6(i\text{-}C_3\text{F}_7)_2$  hexagons, and portions of their  $^{19}\text{F}$  NMR spectra showing the ab quartets (i.e., the doublets for  $\text{F}_a$  and  $\text{F}_b$ ). The observed  $J_{\text{FF}}$  values of 160 and 172 Hz for proximal fluorine atoms  $\text{F}_a$  and  $\text{F}_b$  in these compounds, which are the largest ever recorded for through-space Fermi-contact spin-spin coupling between F atoms attached to  $\text{C}(\text{sp}^3)$  atoms and separated by five or more bonds, support the hypothesis that the instantaneous  $^{6,7}\text{J}_{\text{FF}}$  values for fullerene( $\text{CF}_3$ )<sub>n</sub> derivatives are nine times the observed, time-averaged  $^{6,7}\text{J}_{\text{FF}}$  values of 8–20 Hz.

solution. Nevertheless, it was observed that shorter distances and/or larger torsion angles invariably lead to larger through-space  $J_{\text{FF}}$  values.<sup>4,31</sup> For example, the  $^7\text{J}_{\text{FF}}$  values for the terminal  $\text{CF}_3$  groups in **70-10-1** are 15.9 and 10.3 Hz, respectively,<sup>4</sup> and the corresponding {F...F distance, F—C...C—F angle} for these  $\text{CF}_3$  groups are {2.569(9) Å, 78°} and {2.744(9), 24°}, respectively.<sup>32</sup>

The hypothesis that the observed  $^{6,7}\text{J}_{\text{FF}}$  values are due almost exclusively to through-space Fermi-contact coupling together with the rapid rotation of TMF  $\text{CF}_3$  groups led to the conclusion that the “instantaneous” coupling constants for a specific pair of F atoms, one on each of the two neighboring  $\text{CF}_3$  groups in question, are *nine times larger* than the 8–20 Hz time-averaged values.<sup>4</sup> Consider the pair of proximal F atoms F793 and F801 in the structure of **70-10-1** shown in Figure 5. Rapid rotation of their respective  $\text{CF}_3$  groups (i.e., rapid on the NMR timescale) would put them 4–5 Å apart 89% of the time (i.e., for eight of the nine possible energy-indistinguishable  $\text{CF}_3$  rotamers). The through-space coupling constant for these eight rotamers would be essentially 0 Hz. Therefore, the instantaneous  $^7\text{J}_{\text{FF}}$  value for F793 and F801 in the pair of rotamers shown in Figure 5 was tentatively predicted to be 143 Hz. This conclusion was experimentally verified for compounds with  $p\text{-}C_6(i\text{-}C_3\text{F}_7)_2$  hexagons, as shown in Figure 6.<sup>60,94</sup> Only one of the nine possible rotamers is populated in solution (the DFT-predicted relative energies of rotamers for **60-2-1-i-C<sub>3</sub>F<sub>7</sub>** with

$\text{F}\cdots\text{F}$ ,  $\text{F}\cdots\text{CF}_3$ , and  $\text{CF}_3\cdots\text{CF}_3$  contacts above the shared hexagon are 0, 22, and 46 kJ·mol<sup>-1</sup>, respectively). The observed  $^7\text{J}(\text{F}_a\text{F}_b)$  values of 172 and 160 Hz for **60-4-4-i-C<sub>3</sub>F<sub>7</sub>** and **60-6-5-i-C<sub>3</sub>F<sub>7</sub>**, respectively, verified the “instantaneous  $^{6,7}\text{J}_{\text{FF}} = 9 \times$  observed  $^{6,7}\text{J}_{\text{FF}}$ ” hypothesis. Note that the coupling between either  $\text{F}_a$  or  $\text{F}_b$  and the  $\text{CF}_3$  moieties on the same  $i\text{-C}_3\text{F}_7$  groups are < 1 Hz, a likely consequence of offsetting negative through-bond and positive through-space  $^3\text{J}_{\text{FF}}$  coupling-constant components.

The analysis of additional X-ray structures and 1D and 2D  $^{19}\text{F}$  NMR spectra for TMFs resulted in the determination of common patterns and correlations. DFT predictions of the ribbon isomers for a given composition up to 20 kJ·mol<sup>-1</sup> higher in relative energy than the most stable isomer (generally a few dozen isomers) almost always included the observed ribbon isomers (in one of the few exceptions, the observed isomer **60-12-2** was predicted to have a relative energy 40 kJ·mol<sup>-1</sup> higher than **60-12-1**, the most stable isomer). These insights were useful for tentatively assigning addition patterns for new fullerene( $\text{CF}_3$ )<sub>n</sub> compounds, in the absence of crystallographic data. In several cases, addition-pattern predictions based on  $^{19}\text{F}$  NMR spectra and DFT calculations were later confirmed by X-ray crystallography. However, there were a few unusual TMF addition patterns that could not be assigned by NMR spectroscopy and DFT calculations and required X-ray crystallography to determine their structures.

The first example we encountered was the ( $p^3m^2$ )<sup>2</sup>-loop isomer of  $C_{60}(CF_3)_{10}$  (**60-10-4**).<sup>43a</sup>

Determining the addition-patterns of PFAFs with  $R_F$  groups other than  $CF_3$  in the absence of an X-ray structure was always problematic because their  $^{19}F$  NMR spectra are much more complicated. For example, the  $CF_2$  moieties in 7,24- $C_{70}(C_2F_5)_2$  (**70-2-1-C<sub>2</sub>F<sub>5</sub>**) exhibit a significantly second-order  $^{19}F$  NMR abcd spin system with more than 40 individual resonances, presumably due to four time-averaged rotamers with DFT relative energies within 4  $\text{kJ}\cdot\text{mol}^{-1}$  of one another.<sup>116</sup> Therefore, the growth of single crystals suitable for X-ray crystallography was necessary to accurately determine their addition patterns, and this required highly-purified compounds. This presented an additional problem, because  $C_{60}(C_2F_5)_n$  product mixtures with  $n \geq 12$  and  $C_{60}(R_F)_n$  product mixtures with  $R_F = n\text{-}C_3F_7$ ,  $n\text{-}C_4F_9$ , or  $n\text{-}C_6F_{13}$  were found to be practically inseparable using HPLC procedures.<sup>95</sup> Finally, even when X-ray diffraction data were collected, solution and refinement of the structures was hampered by rotational disorder of perfluoroalkyl chains and/or the PFAF itself. In several cases, three conformations of  $R_F$  groups generated by rotation of perfluoroalkyl C–C bonds had to be included in the final refined model.

**4.1.2. Single and Double Bonds in  $C_{60}(CF_3)_n$  Derivatives and Validation of DFT Calculations.** The relative stabilities of various fullerene( $R_F$ )<sub>n</sub> isomers are determined by at least four factors: (i) the degree of delocalization/aromatization of the remaining  $\pi$  bonds, (ii) the presence or absence of double bonds in the pentagons, (iii) steric repulsion between the  $R_F$  substituents, and (iv) the rotational conformations of each  $R_F$  group with respect to the three cage C–C bonds that radiate from the cage C atom to which each  $R_F$  group is attached. Thus, to understand the relative stability and chemical reactivity of a PFAF with a particular addition pattern, one has to analyze the cage  $C(sp^2)$ – $C(sp^2)$  bonds with respect to their “single” and “double” bond character, and the most straightforward way to do that is to compare the X-ray diffraction derived C–C distances. In favorable cases, the precision of PFAF X-ray structures (i.e., the standard error for individual cage C–C bonds) allows one to determine statistically significant variations in C–C distances. Furthermore, sufficiently-precise X-ray structures allow a particular computational method to be validated as far as accurately predicting C–C distances in the absence of an X-ray structure (assuming that the addition pattern can be discerned from spectroscopic data) or when an X-ray structure clearly shows the addition pattern but has relatively low precision. For visualization of such validations, it is convenient to plot DFT-calculated cage C–C bond distances vs X-ray derived distances. Figure 7 shows the plot for the  $p^3mpmpmp$  isomer of  $C_{60}(CF_3)_{10}$  (**60-10-2**). This particular isomer is a good example for comparison because it is asymmetric, thereby providing a comparison of the 90 unique cage C–C distances. In this case the standard errors ( $\sigma$ ) for individual C–C distances range from  $\pm 0.0014$  to  $\pm 0.0016$  Å.<sup>43b</sup> The experimental and calculated C–C distances are in excellent agreement with each other; the largest difference is less than  $6\sigma$ , and most of the differences are within  $3\sigma$ , which validated the particular DFT methodology used in that study.<sup>43b</sup>

The addition of  $CF_3$  groups to a fullerene (or any other substituents for that matter) decreases the number of the C–C double bonds on a fullerene cage. For instance, addition of 10  $CF_3$  groups to  $C_{60}$  fullerene decreases the number of double

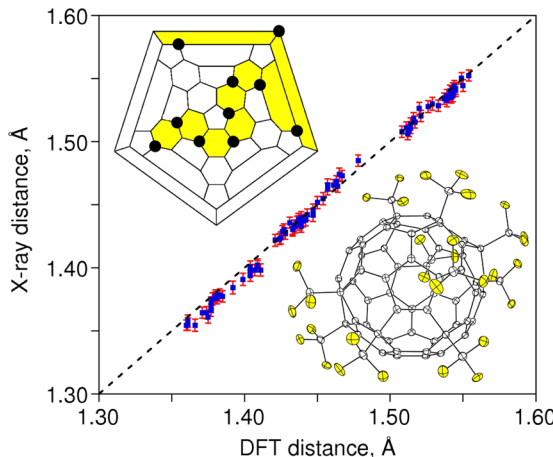


**Figure 7.** Correlation between X-ray determined and DFT-predicted cage C–C distances for **60-10-2**. The uncertainties shown for the X-ray distances are  $\pm 3\sigma$ . A drawing of the X-ray structure with 50% probability ellipsoids and the corresponding Schlegel diagram are also shown.

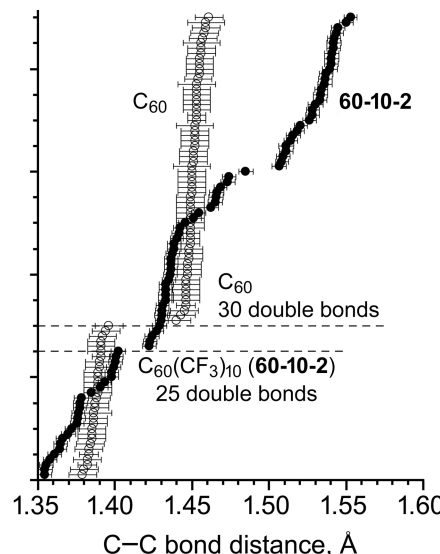


**Figure 8.** X-ray diffraction determined cage C–C bond distances for  $C_{60}$  and the  $p^3mpmpmp$  isomer of  $C_{60}(CF_3)_{10}$  (**60-10-2**) (the uncertainties shown are  $\pm 3\sigma$ ). Note the breaks between sets of  $C(sp^2)$ – $C(sp^2)$  “double bonds” (i.e., those bonds with significant double-bond character),  $C(sp^2)$ – $C(sp^2)$  “single bonds”, and, for **60-10-2**, the 30  $C(sp^2)$ – $C(sp^3)$  single bonds. The  $C_{60}$  distances are from CCDC CIF file 198536 (see also doi 10.1039/B306714A).

bonds from 30 to 25. Figure 8 shows that the 25 short cage C–C distances in **60-10-2** vary from 1.354(2) to 1.402(2) Å. The other C–C distances range from 1.422(2) to 1.552(2) Å. In the X-ray structure of  $C_{60}\cdot Pt(OEP)\cdot 2C_6H_6$ , the 30 “double bonds” and 60 “single bonds” in the underderivatized  $C_{60}$  cage span relatively narrow ranges, 1.379(3)–1.391(3) and 1.440(3)–1.461(3) Å, respectively. Therefore, the  $C(sp^2)$ – $C(sp^2)$  bonds in  $C_{60}(CF_3)_n$  can be assigned as “single bonds” or “double bonds” only as a first approximation. Nevertheless, the shortest ones presumably have the most double-bond character and can be considered the most probable reactive sites for further derivatization. For example, the structure of **60-4-3** revealed the presence of the very short (1.347 Å) double bond in the fulvene-like moiety, as shown in Figure 9. This is the

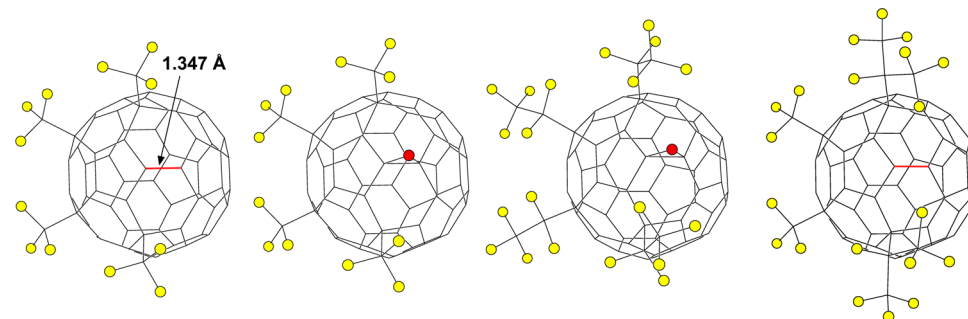


**Figure 9.** X-ray structures of  $p^3\text{-C}_{60}(\text{CF}_3)_4$  (**60-4-3**),  $\text{C}_{60}(\text{CF}_3)_4\text{O}$ ,  $\text{C}_{60}(\text{C}_2\text{F}_5)_4\text{O}$ , and  $\text{C}_{60}(\text{CF}_3)_2(i\text{-C}_3\text{F}_7)_2$  (from left to right). The red bond is the shortest and most reactive double bond in the fulvene-like fragments of the two PFAFs.

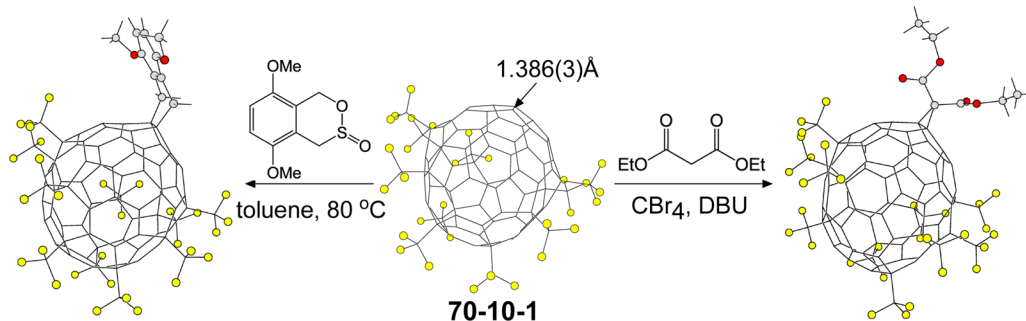


**Figure 10.** X-ray structures of **70-10-1** (middle),  $\text{C}_{70}(\text{CF}_3)_{10}(\text{C}(\text{CO}_2\text{Et})_2)$  (right), and  $\text{C}_{70}(\text{CF}_3)_{10}\text{C}_2\text{H}_4(\text{C}_6\text{H}_2(\text{MeO})_2)$  (left). The reactions that formed the cycloadducts are also shown.

most reactive bond as demonstrated by the rapid epoxidation of **60-4-3** in air to  $\text{C}_{60}(\text{CF}_3)_4\text{O}$ ,<sup>113</sup> the structure of which is also shown in Figure 9. The analogous compound  $\text{C}_{60}(\text{C}_2\text{F}_5)_4\text{O}$  is probably formed by a similar epoxidation of the fulvene-like double bond in the putative intermediate **60-4-3-C<sub>2</sub>F<sub>5</sub>**.<sup>39</sup> Interestingly, an epoxide was not formed by exposure of the isomer of  $\text{C}_{60}(\text{CF}_3)_2(i\text{-C}_3\text{F}_7)_2$  with the **60-4-3** addition pattern (the *i*-C<sub>3</sub>F<sub>7</sub> groups are the terminal R<sub>F</sub> substituents in the *p*<sup>3</sup> ribbon), probably because the bulky *i*-C<sub>3</sub>F<sub>7</sub> groups shield the reactive double bond, as also shown in Figure 9.<sup>95</sup> More recently, an epoxide of  $\text{C}_{60}(\text{CF}_3)_6$  has been isolated and structurally characterized.<sup>105</sup> The O atom in this compound occupies the same position on the cage as in the  $\text{C}_{60}(\text{R}_\text{F})_4\text{O}$  epoxides.

#### 4.2. X-ray Crystallographic Studies of $\text{C}_{70}(\text{R}_\text{F})_n$ Derivatives

There are many dozens of structures in the family of  $\text{C}_{70}(\text{R}_\text{F})_n$  compounds that have been determined by X-ray crystallography. The pool of the known  $\text{C}_{70}(\text{R}_\text{F})_n$  addition patterns is more diverse compared with  $\text{C}_{60}(\text{R}_\text{F})_n$  structures due to the existence of many  $\text{C}_{70}(\text{R}_\text{F})_n$  compounds with *n*-C<sub>3</sub>F<sub>7</sub> groups. HPLC purification of PFAFs of fullerenes with cages larger than C<sub>60</sub> is easier to achieve because larger fullerenes and their derivatives have longer retention times than their C<sub>60</sub> counterparts. This has resulted in a larger number of sufficiently purified and crystallized PFAF isomers for C<sub>70</sub> than for C<sub>60</sub>. Some structural trends observed for  $\text{C}_{60}(\text{R}_\text{F})_n$  compounds are also valid for  $\text{C}_{70}(\text{R}_\text{F})_n$  derivatives. For example, some R<sub>F</sub> groups (R<sub>F</sub> = CF<sub>3</sub>, C<sub>2</sub>F<sub>5</sub>, and *n*-C<sub>3</sub>F<sub>7</sub>) form ribbons and loops on the C<sub>70</sub> cage. Table 3 shows that identical addition patterns have been observed for a number of CF<sub>3</sub> and C<sub>2</sub>F<sub>5</sub> compositions, such as **70-10-1** and **70-10-1-C<sub>2</sub>F<sub>5</sub>** and **70-8-1-C<sub>2</sub>F<sub>5</sub>**. Moreover, four structurally characterized minor isomers of  $\text{C}_{70}(n\text{-C}_3\text{F}_7)_8$  have the same addition patterns as **70-8-3-C<sub>2</sub>F<sub>5</sub>**.

C<sub>2</sub>F<sub>5</sub>, **70-8-4-C<sub>2</sub>F<sub>5</sub>**, **70-8-5-C<sub>2</sub>F<sub>5</sub>**, and **70-8-6-C<sub>2</sub>F<sub>5</sub>**. Remarkably, the **70-8-4** addition pattern is the same for R<sub>F</sub> = CF<sub>3</sub>, C<sub>2</sub>F<sub>5</sub>, and *n*-C<sub>3</sub>F<sub>7</sub>. Thus, the size of the *n*-C<sub>3</sub>F<sub>7</sub> group does not prevent formation of ribbon isomers observed for the smaller CF<sub>3</sub> and C<sub>2</sub>F<sub>5</sub> substituents. However, *i*-C<sub>3</sub>F<sub>7</sub> groups only form isolated *p*-C<sub>6</sub>(*i*-C<sub>3</sub>F<sub>7</sub>)<sub>2</sub> hexagons on both C<sub>60</sub> and C<sub>70</sub> cage. The other important structural principle that was found for  $\text{C}_{70}(\text{R}_\text{F})_n$  derivatives with  $n \leq 20$  and for HHF(R<sub>F</sub>)<sub>n</sub> derivatives in general<sup>57,70</sup> is that the R<sub>F</sub> groups are rarely attached to triple-hexagon junctions because these are the least pyramidalized cage C(sp<sup>2</sup>) atoms. Additions to fullerenes are promoted by the pyramidalization of cage C(sp<sup>2</sup>) atoms when they accept an exohedral substituent and become cage C(sp<sup>3</sup>) atoms, and therefore, other things being equal, the most pyramidalized (i.e., most strained) cage C(sp<sup>2</sup>) atoms in a fullerene or fullerene derivative are the preferred sites for additions. Only a few violations of this principle are known and are discussed in detail in section 5.4.<sup>84a,90</sup>

As discussed earlier, the addition patterns for many  $\text{C}_{70}(\text{CF}_3)_n$  derivatives can be elucidated by a combination of <sup>19</sup>F NMR spectroscopy and DFT calculations.<sup>38,68</sup> However, for R<sub>F</sub> groups other than CF<sub>3</sub>, X-ray crystallography is still the only reliable way to obtain information about R<sub>F</sub> group locations. The relative ease of growing single crystals from solutions of HPLC-purified  $\text{C}_{70}(\text{C}_2\text{F}_5)_n$  isomers enabled the structure determination of several compounds. However, unlike  $\text{C}_{60}(\text{C}_2\text{F}_5)_n$  derivatives in which all major isomers were isolated and structurally characterized,<sup>40,54</sup> the most abundant isomers in  $\text{C}_{70}(\text{C}_2\text{F}_5)_n$  product mixtures have not yet been isolated with high purity.<sup>77,95</sup> Thus, it is premature to generalize trends for the addition patterns and structural features of  $\text{C}_{70}(\text{C}_2\text{F}_5)_n$  derivatives. It is not even known how many isomers of some  $\text{C}_{70}(\text{C}_2\text{F}_5)_n$  compositions are present in some reaction product

mixtures. Further progress in this direction will depend on the new breakthroughs in separation methods.

As in the case of  $C_{60}(R_F)_n$  derivatives, structural information obtained from X-ray crystallography was used to predict the most reactive sites for further functionalization. For example, analysis of the X-ray structure of **70-10-1** (Figure 10) showed that cage C–C distances vary from 1.347(3) to 1.562(3) Å. The C33–C34 bond is the shortest non-terminal double bond in that compound (1.386(3) Å). This bond connects two unoccupied pentagons (the other 10 pentagons each have one  $CF_3$  group), and it was predicted to be the most reactive site for cycloadditions. Structural characterizations of the  $C_{70}(CF_3)_{10}(C(CO_2Et)_2)$  and  $C_{70}(CF_3)_{10}C_2H_4(C_6H_2(MeO))_2$  cycloadducts (see Figure 10) verified the high reactivity of that particular bond.<sup>76,99,146</sup>

## 5. PFAF ADDITION PATTERNS

### 5.1. Additions to $C_{60}$

The  $C_{60}$  molecule has two types of C–C bonds, hexagon/hexagon (hex/hex) edges and pentagon/hexagon (pent/hex) edges, with bond distances of ca. 1.40 and 1.45 Å, respectively, and, as previously discussed, can be thought of as double and single bonds, respectively (see Figure 8). In this section, we will only consider the addition of substituents X that form single bonds to a cage C atom, converting its hybridization from predominantly  $sp^2$  to  $sp^3$ . There are 23 possible isomers of  $C_{60}X_2$ , 4,190 possible isomers of  $C_{60}X_4$ , 418,470 possible isomers of  $C_{60}X_6$ , etc.<sup>147</sup> The numbers of isomers for  $n \geq 10$  is in the millions or, for higher fullerenes, in the billions. It was therefore desirable to find guiding principles that would allow one to limit the number of plausible isomers to consider, and this problem was addressed in a number of computational studies. If a reaction proceeds under thermodynamic control (i.e., if an equilibrium or close-to-equilibrium distribution of isomers of a given composition is expected), the DFT relative energies of the isomers may be used to predict the most abundant products. On the other hand, kinetic factors can be even more important than the isomers' relative thermodynamic stability in some cases, and theoretical predictions of the products may be severely complicated by the fact that the thermodynamic or kinetic control of the reaction is not easily known. As discussed in section 2, perfluoroalkyl additions to fullerenes are usually performed at high temperatures when rearrangements of the  $R_F$  groups on the fullerene surface appear to be possible, and hence the thermodynamic stability of the isomers should determine, in large part, their relative abundance in the product mixture. Therefore, in this section we will analyze the factors affecting thermodynamic stability of fullerene( $R_F$ )<sub>n</sub> isomers and discuss the lowest energy addition pattern trends. However, kinetic factors cannot be fully ignored, and their role will be discussed in section 5.1.4.

**5.1.1. 1,2 (*ortho*) and 1,4 (*para*) Addition and Double Bonds in Pentagons.** Computational studies of  $C_{60}X_2$  isomers ( $X = H, F, Cl, Br, CH_3$ , and  $t\text{-}C_4H_9$ ) performed at semiempirical and DFT levels of theory since the early 1990s showed that only two isomers should be considered for small and medium-size groups.<sup>148</sup> One of these two addition motifs is when the two X groups are added to a hex/hex double bond of  $C_{60}$ , forming two edge-sharing *o*- $C_6X_2$  hexagons (the shared edge is the cage  $C(sp^3)C(sp^3)$  bond), as shown in Figure 11a. In this case, the rest of the fullerene  $\pi$ -system remains unchanged. The other common addition motif for  $C_{60}X_2$

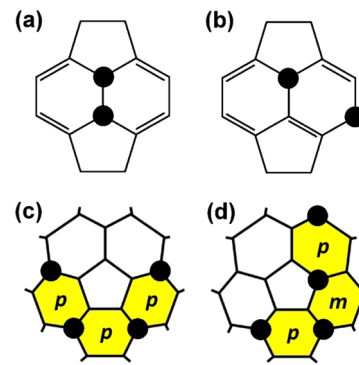


**Figure 11.** (a) A fragment of a 1,9- $C_{60}X_2$  derivative showing the 1,2 or *ortho* addition motif; (b) a fragment of a 1,7- $C_{60}X_2$  derivative showing the 1,4 or *para* addition motif; (c)  $p^3\text{-}C_{60}X_4$ ; (d)  $pmp\text{-}C_{60}X_4$ . In (c) and (d), the *meta*- and/or *para*- $C_6X_2$  hexagons (*p* or *m*, respectively) are highlighted in yellow.

derivatives results in the formation of a *p*- $C_6X_2$  hexagon, and in this case, the remaining  $\pi$ -system is adjusted by relocating one double bond to a pentagon/hexagon edge (i.e., one double bond in a pentagon (DBIP) is formed), as shown in Figure 11b). All other  $C_{60}X_2$  addition patterns require more pronounced changes in the fullerene  $\pi$ -system and result in a larger number of DBIPs.

The number of DBIPs was found to be an important relative-energy predictor: more DBIPs results in a higher relative energy (i.e., a lower thermodynamic stability).<sup>148a</sup> At the semiempirical AM1 and PM3 levels, the penalty for each DBIP in  $C_{60}X_2$  isomers was estimated to be 36–39 kJ·mol<sup>−1</sup> (for  $X = H, F$ , and  $t\text{-}C_4H_9$ ).<sup>148</sup> Accordingly, 1,9- $C_{60}X_2$  isomers should be thermodynamically favored for small substituents such as H and F,<sup>148b,149</sup> in good agreement with the experimental structures 1,9- $C_{60}H_2$ <sup>149</sup> and 1,9- $C_{60}F_2$ .<sup>150</sup> However, the *ortho* position of the X groups in 1,9- $C_{60}X_2$  inevitably leads to an eclipsed conformation and hence a repulsive interaction (i.e., the X–C–C–X torsion angle is 0°). With the increase of the size of the groups, the repulsion is increasing and can balance the destabilizing effect of DBIP. Not surprisingly, computational studies show that for bulky substituents the 1,7- $C_{60}X_2$  isomer is more stable.<sup>27,126,148b</sup> For example, PBE/TZ2P DFT calculations showed that the 1,7- $C_{60}X_2$  isomer is more stable than 1,9- $C_{60}X_2$  by 14 kJ·mol<sup>−1</sup> for  $X = Br$  and by 35 kJ·mol<sup>−1</sup> for  $X = CF_3$ .<sup>151</sup> Note that the different energy differences between the  $X = Br$  and the  $X = CF_3$  isomers is consistent with the fact that  $CF_3$  is sterically larger than a Br atom. In summary, the studies of  $C_{60}X_2$  show that the products of multiple additions of X groups are determined by at least two factors: (i) destabilizing double bonds in pentagons and (ii) destabilizing eclipsing interactions of bulky groups. For bulky groups, such as  $CF_3$ , multiple “1,4”-additions are to be expected.

**5.1.2. Multiple Additions of Bulky Groups to  $C_{60}$ : General Principles.** Important principles of multiple additions of bulky groups to  $C_{60}$  were formulated in the 1990s by Clare and Kepert, who performed extended semiempirical (AM1) computational studies of  $C_{60}X_n$  isomers. In brief, the methodology of the authors included a search of the most stable isomers of  $C_{60}X_n$ , sorting out a majority of the unstable structures, and then a search of the most stable isomers of  $C_{60}X_{n+2}$  based on several most stable isomers of  $C_{60}X_n$ . A gradual increase of  $n$  allowed Clare and Kepert to cover a broad range of compositions, reveal some general principles of the



**Figure 12.** Schlegel diagrams of  $C_{60}(R_F)_x$  derivatives. Color codes: meta- or para- $C_6X_2$  hexagons are highlighted in yellow, “m” denotes meta- $C_6X_2$  hexagons; 1,3,5- $C_6X_3$  hexagons are highlighted in green; pentagon with two  $R_F$  groups are highlighted in blue; positions of attached  $R_F$  groups are denoted as black circles;  $R_F$  groups attached to adjacent carbon atoms are light blue circles with a black border; non-terminal double bonds in pentagons (*nt*-DBIP) are marked red.

multiple addition to  $C_{60}$  and other fullerenes, and predict several addition patterns, which were indeed found later in the

experimental studies. Although the authors did not study  $CF_3$  additions (their work was done before intense studies of

fullerene perfluoroalkylation were started in the early 2000s), their results on the addition of Br atoms to  $C_{60}$  are relevant for  $CF_3$  addition as well and will be briefly discussed here.

Clare and Kepert showed that *para* addition of two Br atoms to  $C_{60}$  is energetically more preferable than *ortho* addition by  $5.1\text{ kJ}\cdot\text{mol}^{-1}$  at the AM1 level. However, the energy difference is not large and the possible formation of  $1,9\text{-}C_{60}\text{Br}_2$  due to kinetic control should not be ruled out. The AM1 study of  $C_{60}\text{Br}_4$  isomers showed that the two lowest energy isomers resulted from consecutive *para* additions while the third most stable isomer was the result of one *ortho* addition and one *para* addition.<sup>152</sup> Regression analysis of the relative energies of  $C_{60}\text{Br}_4$  isomers as a function of the number of  $C_6\text{Br}$ ,  $C_{60}\text{Br}$ ,  $C_6\text{Br}_2$ ,  $C_{60}\text{Br}_3$ , etc. hexagons revealed that the most stable bromofullerene isomers have ribbons of edge-sharing *m*- and/or *p*- $C_6\text{Br}_2$  hexagons rather than isolated *p*- $C_6\text{Br}_2$  hexagons or *o*- $C_6\text{Br}_2$  hexagons (i.e., the addition of pairs of bromine atoms to distant parts of  $C_{60}$ ). For instance, Figure 11 shows that the most stable isomer of  $C_{60}\text{Br}_4$  has the **60-4-3** *p*<sup>3</sup> addition pattern, the second most stable isomer has the **60-4-1** *pmp* addition pattern, and the third most stable isomer has an *omp* addition pattern, which is not observed for any fullerene( $R_F$ )<sub>4</sub> derivative but which is a fragment of the skew-pentagonal pyramid (SPP) addition pattern of **60-6-2** shown as a Schlegel diagram in Figure 12. The SPP addition pattern is a *p*<sup>5</sup> loop of five X groups with the sixth substituent inside the loop, *ortho* to one of the other X groups and *meta* to two others.

Further addition of Br atoms to the *p*<sup>3</sup> or *omp* isomers of  $C_{60}\text{Br}_4$  resulted in the prediction<sup>152</sup> that the SPP addition pattern is the most stable for  $C_{60}\text{Br}_6$ , in harmony with the observed structure of  $C_{60}\text{Br}_6$ <sup>153</sup> and one of the known isomers of  $C_{60}(\text{CF}_3)_6$ .<sup>39</sup> The second most stable isomer of  $C_{60}\text{Br}_6$  predicted in Clare and Kepert's study had the *p*<sup>3</sup>*mp* ribbon exhibited by the most stable isomer of  $C_{60}(\text{CF}_3)_6$ . The next two added Br atoms continue the tendency of the string formation: at the AM1 level, the most stable isomer of  $C_{60}\text{Br}_8$  had a *p*<sup>3</sup>*mpmp* string. For  $C_{60}\text{Br}_{12}$ , the authors predicted that two of the most stable isomers have an addition pattern with two SPP fragments on opposite sides of  $C_{60}$  and a (*pm*)<sup>6</sup>-loop (cf. the structures of **60-12-3** and **60-12-1** in Figure 12, which are known to have these addition patterns).<sup>5,36,52</sup> For further addition of Br atoms, the competition between SPP fragments and ribbons continues up to  $C_{60}\text{Br}_{18}$ , for which the isomer with three SPP fragments is predicted to be the most stable. Finally, Clare and Kepert predicted that the most stable structure for  $C_{60}\text{Br}_{24}$  has  $T_h$  symmetry and no cage  $\text{C}(\text{sp}^3)-\text{C}(\text{sp}^3)$  bonds (24 is the largest number of substituents for which such a restriction is possible).<sup>152,154</sup> This isomer corresponds to the experimentally observed structure of  $C_{60}\text{Br}_{24}$ .<sup>155</sup> In summary, the seminal computational studies of Clare and Kepert revealed important trends for the addition of Br atom to  $C_{60}$ , which later proved to be relevant for the prediction of  $CF_3$  additions to fullerenes. Based on their work, and the similarity in size of a Br atom and a  $CF_3$  group, a significant percentage of the most-stable fullerene( $CF_3$ )<sub>n</sub> isomers were expected to have either one or more ribbons of edge-sharing *m*- and *p*- $C_6(\text{CF}_3)_2$  hexagons (with the occasional isolated *p*- $C_6(\text{CF}_3)_2$  hexagon), SPP fragments (even though they contain *o*- $C_6(\text{CF}_3)_2$  hexagons, or  $CF_3$  groups on adjacent cage C atoms), or both.

**5.1.3. Addition Patterns of  $C_{60}(\text{CF}_3)_n$ ,  $n = 2–18$ .** Clare and Kepert's work, described above, coupled with the large number of well-characterized PFAFs described in this Review, including over 100 TMFs, justified exhaustive independent

theoretical/experimental studies of fullerene( $CF_3$ )<sub>n</sub> compositions/isomers, and these were carried out by Olga Boltalina's former group at Moscow State University (see the papers containing theoretical results co-authored by Alexey Goryunkov and/or Ilya Ioffe, among others) and by Boltalina's current group at Colorado State University and their collaborators (see the papers containing theoretical results co-authored by Alexey Popov at the IFW Dresden; with two exceptions, all of this computational work was performed by Popov at IFW Dresden). Significant progress in computing hardware and software since Clare and Kepert's AM1 studies allowed thousands or tens of thousands of addition patterns to be screened for their relative energies, first at the AM1 level of theory and then, for the ca. 100 most-stable AM1 isomers, by DFT calculations. The isolation of multiple isomers of most  $C_{60}(\text{CF}_3)_n$  compositions for every even  $n$  value from 2 to 18 enabled a more detailed comparison of experimental structures and theoretical predictions (see Table 2 for a list of structurally characterized  $C_{60}(\text{R}_F)_n$  compounds and Figure 12 for their Schlegel diagrams). In this section, we discuss the guidelines of  $CF_3$  addition to  $C_{60}$  revealed in computational studies and then analyze experimentally elucidated  $CF_3$  addition patterns in this context. If not otherwise specified, the relative energies are computed at the PBE/TZ2P level (hereafter designated simply as DFT). The relative energies either are taken from the cited publications or are unpublished results of the authors. In some cases the relative energy of a particular isomer reported by different groups varied by  $1–2\text{ kJ}\cdot\text{mol}^{-1}$  because the optimizations terminated with slightly different sets of  $CF_3$  rotational conformations.

**5.1.3.1.  $C_{60}(\text{CF}_3)_2$ .** Both AM1 and DFT calculations unambiguously showed that  $1,7\text{-}C_{60}(\text{CF}_3)_2$  is considerably more stable than the  $1,9\text{-}C_{60}(\text{CF}_3)_2$ ; the DFT relative energy of the latter was found to be  $34.7\text{ kJ}\cdot\text{mol}^{-1}$ .<sup>151</sup> Therefore, “1,2”-additions of  $CF_3$  groups are not expected to lead to abundant reaction products. Indeed, the sole experimentally characterized isomer of  $C_{60}(\text{CF}_3)_2$  is **p-60-2-1**.<sup>27,63</sup>

**5.1.3.2.  $C_{60}(\text{CF}_3)_4$ .** The DFT-predicted most stable isomers of  $C_{60}(\text{CF}_3)_4$  are *p*<sup>3</sup> ( $0\text{ kJ}\cdot\text{mol}^{-1}$ ) and *pmp* ( $8.2\text{ kJ}\cdot\text{mol}^{-1}$ ), similar to the situation described earlier for  $C_{60}\text{Br}_4$ .<sup>151</sup> The relative energy of the *o,p*- $C_{60}(\text{CF}_3)_4$  isomer is  $36.3\text{ kJ}\cdot\text{mol}^{-1}$  (for comparison, the relative energy of *o,p*- $C_{60}\text{Br}_4$  was found to be only  $9.9\text{ kJ}\cdot\text{mol}^{-1}$ ).<sup>151</sup> Fourteen *p,p*- $C_{60}(\text{CF}_3)_4$  isomers (i.e., structures with two isolated *p*- $C_6(\text{CF}_3)_2$  hexagons span the relative energy range of  $10–34\text{ kJ}\cdot\text{mol}^{-1}$ . These data show that, although the *p*<sup>3</sup> and *pmp* ribbon isomers are more stable than *p,p* addition patterns, the most stable *p,p* isomers are reasonable products to expect in high temperature syntheses. Note that two *p*- $C_6(\text{CF}_3)_2$  hexagons can be combined in such a way that two  $CF_3$  groups share the same pentagon. DFT calculations show that the  $CF_3$  group is sufficiently bulky to induce considerable steric repulsive interactions in  $C_5(\text{CF}_3)_2$  pentagons even when the  $CF_3$  groups are not attached to adjacent cage C atoms. The relative energies of two  $C_{60}(\text{CF}_3)_4$  isomers with a  $1,3\text{-}C_5(\text{CF}_3)_2$  pentagon are  $58$  and  $62\text{ kJ}\cdot\text{mol}^{-1}$ , and the relative energy of the isomer with two  $C_5(\text{CF}_3)_2$  pentagon is  $84\text{ kJ}\cdot\text{mol}^{-1}$ .

Experimental structural studies agree well with these computational results. To date, three isomers of  $C_{60}(\text{CF}_3)_4$  have been structurally characterized. The most abundant isomer has the *pmp* addition pattern (**60-4-1**).<sup>27,63</sup> Another experimentally observed product characterized structure is the most stable *p,p*- $C_{60}(\text{CF}_3)_4$  isomer,  $1,7,16,36\text{-}C_{60}(\text{CF}_3)_4$  (**60-4-**

2).<sup>63</sup> The more stable  $p^3$ -60-4-3 is too reactive and was unambiguously characterized only recently,<sup>113</sup> whereas in earlier studies its epoxide  $C_{60}(CF_3)_4O$  was observed.<sup>27,39</sup> The  $p^3$  addition pattern can be also stabilized by more bulky  $R_F$  groups, which allowed the authors of refs 80 and 95 to characterize  $p^3\text{-}C_{60}(CF_3)_2(i\text{-}C_3F_7)_2$ .

**5.1.3.3.  $C_{60}(CF_3)_6$ .** The addition of six  $CF_3$  groups to  $C_{60}$  follows the guidelines already revealed for  $C_{60}(CF_3)_4$ . The most stable isomer has a  $p^3mp$  ribbon of  $CF_3$  groups. There are two  $pmpmp$  ribbon isomers without a  $1,3\text{-}C_5(CF_3)_2$  pentagon, and their relative energies are 6.5 and  $10.2 \text{ kJ}\cdot\text{mol}^{-1}$ .<sup>63,151</sup> The relative energies of the most stable  $p^3p$  isomers are only 2–3  $\text{kJ}\cdot\text{mol}^{-1}$  above the  $p^3mp$  isomer,<sup>63</sup> whereas the relative energy of the most stable  $pmp,p$  isomer is  $10 \text{ kJ}\cdot\text{mol}^{-1}$  (hereinafter  $p^3p$  and  $pmp,p$  isomers will be designated 4+2 isomers). *Para* additions can also lead to  $p,p,p$  isomers with three isolated  $p\text{-}C_6(CF_3)_2$  hexagons. The most stable isomer of this type is only  $6 \text{ kJ}\cdot\text{mol}^{-1}$  less stable than  $p^3mp$ . Finally, the SPP isomer of  $C_{60}(CF_3)_6$  was predicted to be  $14 \text{ kJ}\cdot\text{mol}^{-1}$  less stable than  $p^3mp$ .<sup>63,151</sup> Interestingly, this value is substantially smaller than the destabilization effect of  $35 \text{ kJ}\cdot\text{mol}^{-1}$  computed for the isomer of  $C_{60}(CF_3)_2$  with two  $CF_3$  groups on adjacent cage C atoms. In summary, many isomers of  $C_{60}(CF_3)_6$  have DFT-predicted relative energies no higher than  $14.4 \text{ kJ}\cdot\text{mol}^{-1}$  and on this basis might be expected to be found in reaction products containing the composition  $C_{60}(CF_3)_6$ .

Known  $C_{60}(CF_3)_6$  isomers include  $p^3mp$  (**60-6-1**) and one of the two possible  $pmpmp$  isomers (**60-6-6**).<sup>27,63</sup> Among the 4+2 isomers, only **60-6-7**, which has a  $pmp,p$  addition pattern with a relative energy of  $16 \text{ kJ}\cdot\text{mol}^{-1}$  has been reported.<sup>63</sup> Isomers of  $C_{60}(CF_3)_6$  with  $p,p,p$  addition patterns are not known, but have been isolated and characterized for  $C_{60}(R_F)_6$  with  $R_F = C_2F_5$  and  $i\text{-}C_3F_7$ , as discussed below.

The only other known isomer of  $C_{60}(CF_3)_6$  is SPP- $C_{60}(CF_3)_6$  (**60-6-2**).<sup>39,105</sup> Its DFT-predicted relative energy is  $14.4 \text{ kJ}\cdot\text{mol}^{-1}$  above **60-6-1** and its relative yield in a 550 C hot-tube synthesis was reported to be ca. 20 times lower than **60-6-1**.<sup>39</sup> If one accounts for the difference in symmetry numbers that favor the  $C_1$  isomer **60-6-1** over the  $C_s$  isomer **60-6-2**, the difference in  $\Delta G_f$  values is  $19.1 \text{ kJ}\cdot\text{mol}^{-1}$ . If the two compounds were in thermal equilibrium at the reaction temperature, then their relative abundances would be 16:1, in reasonable agreement with the observed ca. 20:1 ratio.<sup>39</sup>

**5.1.3.4.  $C_{60}(CF_3)_8$ .** From the aforementioned DFT analysis of the addition of 2–6  $CF_3$  groups to  $C_{60}$ , one would expect that most of the lowest energy isomers of  $C_{60}(CF_3)_n$  would have ribbon and 6+2 addition patterns (i.e., a ribbon of 6  $CF_3$  groups and an isolated  $p\text{-}C_6(CF_3)_2$  hexagon). Indeed, extensive computations showed that the most stable isomer has a  $p^3mp,p$  addition pattern, and the second most stable isomer (3  $\text{kJ}\cdot\text{mol}^{-1}$  less stable) has the one and only  $p^3mpmp$  addition pattern.<sup>5,53</sup> There are only three all-ribbon isomers,  $p^3mpmp$  and two  $pmpmpmp$  addition patterns (both  $pmpmpmp$  isomers have relative energies less than  $20 \text{ kJ}\cdot\text{mol}^{-1}$ ), but many 6+2 isomers. There is also a  $pmp,pmp$  4+4 double-ribbon isomer with  $\Delta E = 11 \text{ kJ}\cdot\text{mol}^{-1}$ , and isomers with SPP, $p$  addition patterns, the most stable of which has  $\Delta E = 17 \text{ kJ}\cdot\text{mol}^{-1}$ . To the extent that experimentally-observed reaction products have reasonably low  $\Delta E$  values, which is almost always the case for high-temperature syntheses, many isomers of  $C_{60}(CF_3)_8$  can be expected: there are four with relative energies below  $10 \text{ kJ}\cdot\text{mol}^{-1}$  and 28 in the range  $10\text{--}20 \text{ kJ}\cdot\text{mol}^{-1}$ .

To date there are two structurally characterized  $C_{60}(CF_3)_8$  isomers with ribbon addition patterns, **60-8-1** and **60-8-4**, and three with  $p^3mp,p$  addition patterns, **60-8-2**, **60-8-3**, and **60-8-5**, all with  $0\text{--}11 \text{ kJ}\cdot\text{mol}^{-1}$   $\Delta E$  values.<sup>5,44,53,58</sup> Several isomers that have not been structurally characterized have also been isolated.

**5.1.3.5.  $C_{60}(CF_3)_{10}$ .** As would be expected, the number of possible isomers increases with the number of added  $CF_3$  groups, and  $C_{60}(CF_3)_{10}$  has the richest family of isomers among all fullerene( $R_F$ )<sub>n</sub> compositions. DFT calculations show that all-ribbon isomers, and many 8+2 and 6+4 isomers have  $\Delta E = 0\text{--}20 \text{ kJ}\cdot\text{mol}^{-1}$  (this includes no fewer than 31 isomers). The four all-ribbon isomers have  $\Delta E \leq 8 \text{ kJ}\cdot\text{mol}^{-1}$ , the two most stable have  $p^3mp,pmp$  and  $p^3mpmpmp$  addition patterns. The large number of DFT-predicted stable isomers is in harmony with the number of isolated isomers with appreciable yields. There are six structurally-characterized isomers with addition patterns described above, **60-10-1**, **60-10-2**, **60-10-3**, **60-10-5**, **60-6-6**, and **60-10-7**.<sup>4,5,43,63</sup> There is also the unusual  $C_2$ -symmetric ( $p^3m^2$ -loop)<sup>2</sup> isomer **60-10-4**, with  $\Delta E = 8 \text{ kJ}\cdot\text{mol}^{-1}$ .<sup>43a</sup>

**5.1.3.6.  $C_{60}(CF_3)_{12}$ .** The situation with 12  $CF_3$  groups on  $C_{60}$  is rather special because one isomer, the  $S_6$ -symmetric ( $pm$ )<sup>6</sup>-loop isomer predicted by Clare and Kepert (but not known experimentally) for  $C_{60}\text{Br}_{12}$ , was found to be at least  $19 \text{ kJ}\cdot\text{mol}^{-1}$  more stable than all others.<sup>56</sup> This turns out to be the only single-ribbon addition pattern that avoids putting more than one  $CF_3$  group in each of the 12 pentagons. The next three most stable isomers have  $\Delta E = 19\text{--}21 \text{ kJ}\cdot\text{mol}^{-1}$  and can be described as “branched” ribbons, with the branching occurring at a  $1,3,5\text{-}C_6(CF_3)_6$  hexagon (interestingly, no stable isomer of  $C_{60}(CF_3)_{10}$  has a  $1,3,5\text{-}C_6(CF_3)_6$  hexagon). All other types of isomers obtained by consecutive 1,4 additions of  $CF_3$  groups have at least one  $1,3\text{-}C_5(CF_3)_2$  pentagon which appears to be quite destabilizing (all have  $\Delta E \geq 31 \text{ kJ}\cdot\text{mol}^{-1}$ ), which is in sharp contrast to the stability of **60-10-3**, which has a  $1,3\text{-}C_5(CF_3)_2$  pentagon and for which  $\Delta E$  is only  $7 \text{ kJ}\cdot\text{mol}^{-1}$ . Another interesting contrast is the relative stability of the SPP addition pattern for **60-6-2** ( $14.1 \text{ kJ}\cdot\text{mol}^{-1}$ ) compared with the  $33\text{--}34 \text{ kJ}\cdot\text{mol}^{-1}$  isomers of  $C_{60}(CF_3)_{12}$  that have two SPP addition-pattern fragments on opposite poles.<sup>56</sup>

The list of six experimentally well-characterized isomers of  $C_{60}(CF_3)_{12}$  includes the most stable  $S_6$ -symmetric ( $pm$ )<sup>6</sup>-loop isomers **60-12-1**,<sup>36</sup> two isomers with branched ribbons but only one  $CF_3$  per pentagon, **60-12-5** ( $C_3$  symmetry) and **60-12-6**,<sup>74</sup> the  $C_{2h}$ -symmetric isomer with two SPP fragments, **60-12-3**,<sup>5,52</sup> and two isomers that have two  $1,3\text{-}C_5(CF_3)_2$  pentagons, **60-12-2** and **60-12-4**.<sup>56,67</sup> The relative energies of **60-12-2** and **60-12-4** are 40 and  $46 \text{ kJ}\cdot\text{mol}^{-1}$ , respectively, so it is quite possible that they are kinetic isomers.

**5.1.3.7.  $C_{60}(CF_3)_{14\text{--}18}$ .** With more than 12  $CF_3$  groups all addition patterns will have at least two “destabilizing”  $1,3\text{-}C_5(CF_3)_2$  pentagons that may compete in overall stability with addition patterns having some  $CF_3$  groups on adjacent cage C atoms. The lowest energy isomer of  $C_{60}(CF_3)_{14}$ , **60-14-1**, is formed by consecutive 1,4 additions, has two  $1,3\text{-}C_5(CF_3)_2$  pentagons, and one  $1,3,5\text{-}C_6(CF_3)_3$  hexagon that forms a branched ribbon.<sup>52</sup> However, the lowest energy isomer with an SPP fragment, **60-14-3**, is only  $0.4 \text{ kJ}\cdot\text{mol}^{-1}$  less stable. The third lowest energy isomer, **60-14-2** ( $\Delta E = 2.2 \text{ kJ}\cdot\text{mol}^{-1}$ ), is based on the  $S_6$ -( $pm$ )<sup>6</sup>-loop addition pattern of **60-12-1** with two additional  $CF_3$  groups forming two  $1,3\text{-}C_5(CF_3)_2$  pentagons. All three are known experimentally.<sup>52,74</sup>

For  $C_{60}(CF_3)_{16}$ , which must have even more  $1,3-C_5(CF_3)_2$  pentagons, SPP and ribbon isomers are equally stable; moreover, it was found that stable addition patterns with  $CF_3$  groups on adjacent carbon atoms can be realized without formation of an SPP moiety.<sup>55</sup> The isomers are densely distributed in the energy scale: seven isomers with relative energies below  $10\text{ kJ}\cdot\text{mol}^{-1}$ , eight isomers in the  $10\text{--}20\text{ kJ}\cdot\text{mol}^{-1}$  range. The three experimentally well-characterized isomers of  $C_{60}(CF_3)_{16}$ , one has  $\sigma\text{-}C_6(CF_3)_2$  hexagon (not as part of an SPP fragment (**60-16-3**,  $\Delta E = 4\text{ kJ}\cdot\text{mol}^{-1}$ )), one has an SPP moiety (**60-16-2**,  $\Delta E = 10\text{ kJ}\cdot\text{mol}^{-1}$ ), and one is based on consecutive 1,4-additions but with no  $CF_3$  groups on adjacent cage C atoms (**60-16-1**,  $\Delta E = 16\text{ kJ}\cdot\text{mol}^{-1}$ ).<sup>54</sup> Many experimentally isolated isomers have not yet been structurally characterized, and the most stable  $C_{60}(CF_3)_{16}$  isomers are not among the three listed above.

For  $C_{60}(CF_3)_{18}$ , theoretical studies have shown that the most stable isomer has  $C_{3v}$ -symmetry, two isolated benzenoid rings, three isolated fulvene fragments, six isolated double bonds, nine  $1,3-C_5(CF_3)_2$  pentagons, and no  $CF_3$  groups on adjacent cage C atoms.<sup>54</sup> The isomer with this addition pattern, **60-18-2**, has been isolated and characterized by single-crystal X-ray diffraction.<sup>82</sup> It is followed by four isomers with SPP moieties ( $\Delta E = 9\text{--}28\text{ kJ}\cdot\text{mol}^{-1}$ ). Note that these isomers span a larger range of relative energies than TMFs with 8, 10, 14, and 16  $CF_3$  groups. Furthermore, it is impossible to distribute 18  $CF_3$  groups on the surface of  $C_{60}$  without significant steric hindrance, and hence the guidelines formulated for stable addition patterns with fewer  $CF_3$  groups are not followed as strictly. In fact, the list of most stable isomers of  $C_{60}(CF_3)_{18}$  includes only a few without  $\sigma\text{-}C_6(CF_3)_2$  hexagons, and the experimentally characterized **60-18-1** is one of them.<sup>55</sup> This isomer is  $33\text{ kJ}\cdot\text{mol}^{-1}$  less stable than **60-18-2**. Up to now, 18 is the largest number of  $CF_3$  groups in structurally characterized  $C_{60}(CF_3)_n$  derivatives.

Calculations show that the energy of  $CF_3$  addition to  $C_{60}(CF_3)_{18}$  is considerably decreased as compared to previous stages of addition, from which one can conclude that  $C_{60}(CF_3)_n$  derivatives with more than 18  $CF_3$  groups are unlikely to be abundant reaction products.<sup>109</sup> For example, the  $T_h$ -symmetric  $C_{60}X_{24}$  structure, known for  $X = \text{Br}$ , is unknown for  $X = CF_3$ .

**5.1.4. Thermodynamic versus Kinetic Aspects of  $CF_3$  Addition.** Analysis of the experimentally available structures of  $C_{60}(CF_3)_n$  derivatives and comparison to the results of exhaustive computational studies show that in many cases the experimentally available isomers are the most stable ones, or at least have low relative energies. Thus, partial thermodynamic control in high-temperature trifluoromethylation of fullerenes can be postulated. Thermodynamic control implies that the isomers with high relative energy can be converted into the products with lower energies, which means that  $CF_3$  groups can rearrange on the fullerene surface (or between two neighboring molecules). The fact that such rearrangements are possible was demonstrated by transalkylation reactions, such as the reaction between  $C_{60}$  and  $C_{60}(CF_3)_{12}$ , which produced products with intermediate numbers of  $CF_3$  groups.<sup>87,105,111</sup> At the same time, there are a number of isolated derivatives with  $n \geq 12$  with high relative DFT-predicted energies. The latter fact indicates that complete thermodynamic equilibrium is not always reached.

It is instructive that at low stages of addition (i.e.,  $n \leq 10$ ), the majority of the most stable isomers of  $C_{60}(CF_3)_{n+2}$  can be conceptually formed by addition of two  $CF_3$  groups to the most stable isomers of  $C_{60}(CF_3)_n$  without rearrangement. The

gradual growth of the thermodynamically most stable ribbon addition patterns from 4 to 10 groups is a clear example:  $p^3 \rightarrow p^3mp \rightarrow p^3mpmp \rightarrow p^3mpmpmp$ , and  $pmp \rightarrow pmpmp \rightarrow pmpmpmp \rightarrow pmpmpmpmp$ . Rearrangement of the precursor  $C_{60}(CF_3)_n$  derivative during the addition of the next two  $CF_3$  groups is not necessary. Therefore, it is possible that thermodynamically stable isomers can be produced even under partial kinetic control.

However, for  $n \geq 12$ , the most stable isomers of  $C_{60}(CF_3)_{n+2}$  are generally not derived from the DFT-predicted most stable  $C_{60}(CF_3)_n$  addition patterns, and their formation would require multiple rearrangements of  $CF_3$  groups on the fullerene surface and/or  $CF_3$  dissociation/reassociation reactions. Hence, it is more difficult to obtain an equilibrium distribution of products for large  $n$  values, and reactions should proceed at higher temperatures, include longer thermal treatments, or both.<sup>156</sup> These requirements were not completely fulfilled in many reported syntheses, which is probably why isomers with high relative energies were isolated. For instance, in a hot tube synthesis with flowing  $CF_3I$ , products with high  $n$  values were removed relatively quickly from the hot reaction zone because of their relatively high volatility. As a result, two  $C_{60}(CF_3)_{12}$  isomers, **60-12-2** and **60-12-4**, with DFT-predicted energies significantly higher than the most stable isomer, were isolated (the latter has the highest energy relative to the most stable isomer,  $46\text{ kJ}\cdot\text{mol}^{-1}$ , of all well-characterized fullerene( $R_F$ )<sub>*n*</sub> derivatives). Similarly, the isomer **60-18-1**, with a high relative energy, was obtained in the first synthesis of  $C_{60}(CF_3)_{18}$  derivatives, and three isolated isomers of  $C_{60}(CF_3)_{16}$  are not the most stable. Thus, for  $n \geq 12$ , kinetic and thermodynamic principles favor different isomers, and hence equilibrium compositions are more difficult to achieve.

DFT calculations show that intra- or intermolecular rearrangements of  $CF_3$  groups have activation barriers higher than  $200\text{ kJ}\cdot\text{mol}^{-1}$ .<sup>142,157</sup> It was proposed that isomer distributions under non-thermodynamic conditions can be rationalized with the Bell–Evans–Polanyi principle,<sup>156</sup> which states that reaction rates correlate with reaction enthalpies for similar reactions. In the case of radical trifluoromethylation, this means then that kinetically preferred  $C_{60}(CF_3)_n$  derivatives should include the most stable  $C_{60}(CF_3)_{n-1}$  radicals as intermediates.<sup>63,87,156</sup>

**5.1.5. Addition of Bulky  $R_F$  Groups to  $C_{60}$ .** It can be expected that the increase of the perfluoroalkyl group from  $CF_3$  to  $C_2F_5$  and beyond should introduce additional sterical hindrances for  $C_{60}(R_F)_n$ . Although this is correct to some extent,  $R_F$  groups cannot be considered as hard spheres, and a careful analysis of their shapes and relative orientations was considered.

**5.1.5.1. Addition of  $C_2F_5$ .** To reiterate some facts presented earlier, (i) each cage C atom in  $C_{60}$  is at the junction of two hexagons and one pentagon, and (ii)  $CF_3$  groups attached to  $C_{60}$  preferably adopt staggered conformation (i.e., the three F atoms are located above the hexagons and pentagon rather than above the C–C bonds). Rotation of a  $CF_3$  group around the  $C(\text{fullerene})-C(R_F)$  bond by  $120^\circ$  leaves a structurally and energetically congruent structure. Clearly the situation is different with  $R_F = C_2F_5$ , as shown in Figure 13 for  $1,7-C_{60}(C_2F_5)_2$ . Staggered conformations are still more stable than eclipsed conformations, but  $120^\circ$  rotations result in three types of steric interactions above the shared hexagon,  $F\cdots F$ ,  $F\cdots CF_3$ , and  $CF_3\cdots CF_3$ . However, if one of the F atoms in the  $CF_3$  group is replaced by another  $CF_3$  group (which yields  $C_2F_5$ ),

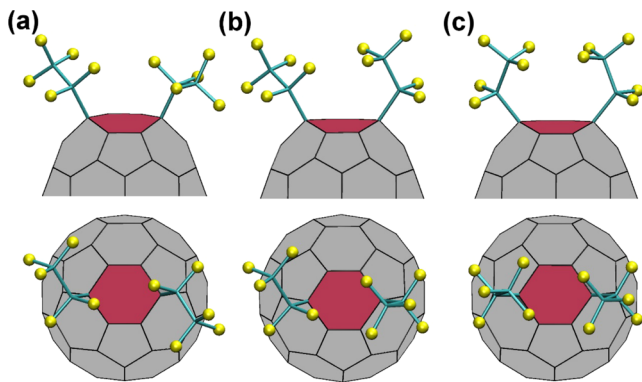


**Figure 13.** Three DFT-optimized conformers of  $1,7\text{-C}_{60}(\text{C}_2\text{F}_5)_2$ : (a) two F atoms above the shared hexagon; (b) one F atom and one  $\text{CF}_3$  group above the shared hexagon; (c) two  $\text{CF}_3$  groups above the shared hexagon (note the eclipsed conformations of the  $\text{C}_2\text{F}_5$  groups). The shared hexagon is highlighted in red. Top and bottom rows show different orientations of the conformers.

the staggered conformation remains preferable, but rotation around the  $\text{C}(\text{fullerene})-\text{C}(\text{R}_\text{F})$  bond yields up to three different conformers. For  $1,7\text{-C}_{60}(\text{C}_2\text{F}_5)_2$ , this conformation variability results in six different conformers, whose energies vary significantly in dependence on the relative orientations of  $\text{C}_2\text{F}_5$  groups. The steric repulsion of two  $\text{C}_2\text{F}_5$  groups in *para* position is dominated by interactions of F atoms and/or  $\text{CF}_3$  fragments located above the hexagon shared by both groups. Hence, there are three possible variants of how  $\text{C}_2\text{F}_5\cdots\text{C}_2\text{F}_5$  interactions can be realized in  $\text{C}_{60}(\text{C}_2\text{F}_5)_2$  (see Figure 13): F...F contacts (two F atoms above the shared hexagon), F... $\text{CF}_3$  (one F atom and one  $\text{CF}_3$  group), and  $\text{CF}_3\cdots\text{CF}_3$  (two  $\text{CF}_3$  groups above the shared hexagon). The former situation is realized in the three most stable conformers ( $\Delta E = 0\text{--}2 \text{ kJ}\cdot\text{mol}^{-1}$ ). Two conformers with F... $\text{CF}_3$  contacts are destabilized by ca.  $10 \text{ kJ}\cdot\text{mol}^{-1}$  ( $\Delta E = 11\text{--}12 \text{ kJ}\cdot\text{mol}^{-1}$ ), and the conformer with two  $\text{CF}_3$  groups over the shared hexagon is the least stable, at the relative energy of  $42 \text{ kJ}\cdot\text{mol}^{-1}$ . It is clear that conformers of  $1,7\text{-C}_{60}(\text{C}_2\text{F}_5)_2$  with F...F contacts above the shared hexagon do not experience significantly increased steric repulsion relative to  $1,7\text{-C}_{60}(\text{CF}_3)_2$ .

For the addition of four or more  $\text{C}_2\text{F}_5$  groups, one should consider either ribbon addition patterns ( $p^3$  or  $pmp$ ) or isomers with isolated  $p\text{-C}_6(\text{C}_2\text{F}_5)_2$  hexagons. Importantly, each  $\text{R}_\text{F}$  group in the middle of the ribbon shares at least two hexagons with other  $\text{R}_\text{F}$  groups. The preference of ribbon isomers for  $\text{C}_{60}(\text{CF}_3)_n$  derivatives means that F...F contacts over shared hexagons do not introduce strong repulsive interactions (note, however, that there are examples of eclipsed conformations for one of the  $\text{CF}_3$  groups in  $1,3\text{-C}_5(\text{CF}_3)_2$  pentagons or  $1,3,5\text{-C}_6(\text{CF}_3)_3$  hexagons, showing that such F...F interactions are not negligible). Ribbon addition patterns are possible for  $\text{C}_2\text{F}_5$  groups because the two  $\alpha$ -F atoms of the non-terminal  $\text{C}_2\text{F}_5$  groups can share both  $p\text{-C}_6(\text{C}_2\text{F}_5)_2$  hexagons in the ribbon (i.e., without any destabilizing F... $\text{CF}_3$  and  $\text{CF}_3\cdots\text{CF}_3$  contacts over the shared hexagons; note that this puts the  $\text{CF}_3$  moieties of the non-terminal  $\text{C}_2\text{F}_5$  groups over pentagons). Indeed, the DFT results listed in Table 4 show that the  $p^3$  isomer of  $\text{C}_{60}(\text{C}_2\text{F}_5)_4$  is more stable than any of the possible  $p,p$  isomers. Nevertheless, the energetic preference for fullerene( $\text{C}_2\text{F}_5)_n$  ribbon isomers is less emphasized than for fullerene( $\text{CF}_3)_n$  ribbon isomers. For example, the  $pmp\text{-C}_{60}(\text{C}_2\text{F}_5)_4$  is a few  $\text{kJ}\cdot\text{mol}^{-1}$  less stable than several  $p,p$  isomers, showing that some

**Table 4. DFT-Predicted Relative Energies of Selected  $\text{C}_{60}(\text{R}_\text{F})_4$  Isomers ( $\text{R}_\text{F} = \text{CF}_3$ ,  $\text{C}_2\text{F}_5$ , and  $i\text{-C}_3\text{F}_7$ )**

IUPAC locants and addition-pattern prefixes	$\text{CF}_3$	$\text{C}_2\text{F}_5$	$i\text{-C}_3\text{F}_7$	exp. obsd examples (see Table 1)
1,7,11,24; $\text{C}_1\text{-}p^3$	0.0	0.0	31.2	<b>60-4-3-<math>\text{CF}_3</math></b>
1,6,11,18; $\text{C}_1\text{-}pmp$	8.1	12.8	71.0	<b>60-4-1-<math>\text{CF}_3</math></b>
1,7,16,36; $\text{C}_1\text{-}p,p$	10.1	8.5	1.5	<b>60-4-2-<math>\text{CF}_3</math></b> , <b>60-40-2-<i>i</i>-<math>\text{C}_3\text{F}_7</math></b>
1,7,28,31; $\text{C}_2\text{-}p,p$	11.2	7.3	0.0	<b>60-4-4-<i>i</i>-<math>\text{C}_3\text{F}_7</math></b>

ribbons with  $m\text{-C}_6(\text{R}_\text{F})_2$  hexagons are relatively less stable than homologous TMF ribbon isomers with  $m\text{-C}_6(\text{CF}_3)_2$  hexagons. Analogous arguments show that ribbon addition patterns may also be expected for  $n\text{-R}_\text{F}$  groups with longer perfluoroalkyl chains.

Many structurally characterized fullerene( $\text{C}_2\text{F}_5)_n$  compounds have the same addition patterns as the corresponding  $\text{CF}_3$  compounds, including SPP- $\text{C}_{60}(\text{R}_\text{F})_4\text{O}$ , **60-8-1**, **60-8-3**, and **60-10-6**. Ribbon addition patterns are also found in four unique isomers of  $\text{C}_{60}(\text{C}_2\text{F}_5)_8$  (i.e., **60-8-6- $\text{C}_2\text{F}_5$**  to **60-8-9- $\text{C}_2\text{F}_5$** , all of which have a  $p^3mp,p$  addition pattern) and in **60-10-7- $\text{C}_2\text{F}_5$**  ( $pmpmpmp,p$ ). In addition, two isomers of  $\text{C}_{60}(\text{C}_2\text{F}_5)_6$ , **60-6-3- $\text{C}_2\text{F}_5$**  and **60-6-8- $\text{C}_2\text{F}_5$** , have  $p,p,p$  addition patterns. Recall that  $\text{C}_2\text{F}_5$  addition is usually performed at lower temperatures than  $\text{CF}_3$  addition because  $\text{C}_2\text{F}_5$  groups can fragment and mixed  $\text{C}_2\text{F}_5/\text{CF}_3$  adducts can be formed, and for this reason it is possible that kinetic factors may play a more important role in determining which isomers are produced in many  $\text{C}_2\text{F}_5$  addition reactions (see section 5.1.4).

**5.1.5.2. Addition of *i*- $\text{C}_3\text{F}_7$ .** A significantly different addition-pattern situation arises for the perfluoroisopropyl group. The relative energies of  $1,7\text{-C}_{60}(i\text{-C}_3\text{F}_7)_2$  conformers with F...F, F... $\text{CF}_3$ , and  $\text{CF}_3\cdots\text{CF}_3$  interactions above the shared hexagon were found to be 0, 22, and  $46 \text{ kJ}\cdot\text{mol}^{-1}$ , respectively. In fact, the conformer with two  $\text{CF}_3$  groups over the shared hexagon was so unstable that its optimization yielded staggered conformations for both  $i\text{-C}_3\text{F}_7$  groups. It was also found that F... $\text{CF}_3$  and  $\text{CF}_3\cdots\text{CF}_3$  repulsions are more destabilizing than in  $\text{C}_2\text{F}_5$  derivatives.

Since the  $i\text{-C}_3\text{F}_7$  group has only one  $\alpha$ -F atom, it is not possible to avoid F... $\text{CF}_3$  contacts over shared hexagons in a hypothetical ribbon of edge-sharing  $m$ - and/or  $p\text{-C}_6(i\text{-C}_3\text{F}_7)_2$  hexagons. The results for  $1,7\text{-C}_{60}(i\text{-C}_3\text{F}_7)_2$  conformers indicate that unavoidable F... $\text{CF}_3$  contacts for each non-terminal  $i\text{-C}_3\text{F}_7$  group in a ribbon destabilize the structure by ca.  $20 \text{ kJ}\cdot\text{mol}^{-1}$ . This estimate agrees well with the DFT calculations listed in Table 4, which show that the  $p^3\text{-C}_{60}(i\text{-C}_3\text{F}_7)_4$  isomer is less stable than the most stable  $p,p\text{-C}_{60}(i\text{-C}_3\text{F}_7)_4$  isomer by  $31 \text{ kJ}\cdot\text{mol}^{-1}$  (i.e., for comparison, recall that  $p^3\text{-C}_{60}(\text{CF}_3)_4$  is more stable than the lowest energy  $p,p$  isomer by  $42 \text{ kJ}\cdot\text{mol}^{-1}$ ). Furthermore, the DFT-predicted relative energy of  $pmp\text{-C}_{60}(i\text{-C}_3\text{F}_7)_4$  is extremely high,  $71 \text{ kJ}\cdot\text{mol}^{-1}$ , which shows that F... $\text{CF}_3$  contacts in  $m\text{-C}_6(i\text{-C}_3\text{F}_7)_2$  hexagons are even more destabilizing than in  $p\text{-C}_6(i\text{-C}_3\text{F}_7)_2$  hexagons. As a result, the addition patterns of all PFAFs with 2, 4, 6, or 8  $i\text{-C}_3\text{F}_7$  groups are composed of isolated  $p\text{-C}_6(i\text{-C}_3\text{F}_7)_2$  hexagons.<sup>60,80,94</sup>

## 5.2. $\text{CF}_3$ Addition to $\text{C}_{59}\text{N}$

The azafullerene monomer  $\text{C}_{59}\text{N}$  is a radical and is stabilized by spontaneous dimerization. Trifluoromethylation of  $(\text{C}_{59}\text{N})_2$  produced a series of  $\text{C}_{59}\text{N}(\text{CF}_3)_n$  derivatives with odd values of  $n$  from 5 to 19 with closed-shell electronic configurations.<sup>158</sup> In the analysis of addition patterns, N can be thought of as a

cage  $C(sp^3)$  atom bearing a small substituent that does not sterically prevent substituents from being attached to the three cage C atoms adjacent to the N atom. DFT calculations showed that the addition of a  $CF_3$  group *ortho* to the N atom is energetically more favorable by  $27\text{ kJ}\cdot\text{mol}^{-1}$  than addition to the *para*-position to the N atom. Further addition of  $CF_3$  groups is governed by the same guidelines as for  $C_{60}$ : multiple 1,4 additions with a preference for forming ribbons of *m*- and/or *p*- $C_6(CF_3)_2$  hexagons. The most stable isomer of  $C_{59}N(CF_3)_5$  has an SPP-like addition pattern with the N atom, which does not have a  $CF_3$  substituent at the apex of the idealized skew-pentagonal pyramid, as shown in Figure 14. It is

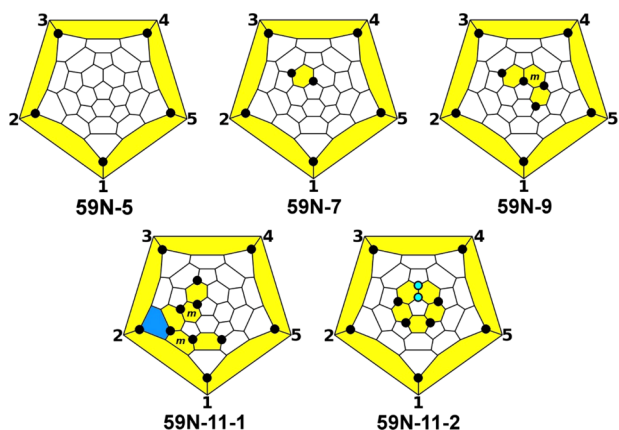


**Figure 14.** Schlegel diagrams of characterized  $C_{59}N(CF_3)_n$  PFAFs. Except for 59N-5, each Schlegel diagram represents multiple isomers by virtue of the fact that the N atom can occupy two or more of the numbered positions 1–5. See Figure 12 for color codes.

predicted to be  $53\text{ kJ}\cdot\text{mol}^{-1}$  more stable than the next most-stable isomer. In harmony with this prediction, SPP- $C_{59}N(CF_3)_5$  (i.e., 6,9,12,15,18- $C_{59}N(CF_3)_5$ ) was the only isomer of this composition isolated experimentally. Interestingly,  $C_{59}N(CF_3)_n$  derivatives with  $n = 1$  or 3 were not observed in trifluoromethylation reactions of  $(C_{59}N)_2$ , presumably because they react with  $CF_3$  radicals too fast until the  $C_{59}N(CF_3)_5$  is formed.

High stability of the SPP-like moiety in  $C_{59}N(CF_3)_5$  results in its presence in addition patterns of  $C_{59}N(CF_3)_n$  derivatives with  $n > 5$ . The most stable isomer of  $C_{59}N(CF_3)_7$  has the SPP-like fragment and an additional *p*- $C_6(CF_3)_2$  hexagon on the opposite side of the cage. This isomer is  $20\text{ kJ}\cdot\text{mol}^{-1}$  more stable than isomers with the *p*- $C_6(CF_3)_2$  hexagon in different positions, which shows that the presence of the SPP-like moiety controls the reactivity of the cage as far as further additions are concerned. Similarly, the lowest energy isomer of  $C_{59}N(CF_3)_9$  has the SPP-like moiety and a *pmp* ribbon on the opposite side of the cage. These addition patterns were assigned to experimentally isolated compounds based on their  $^{19}\text{F}$  NMR spectra.

Two isomers of  $C_{59}N(CF_3)_{11}$  were characterized and assigned to the most stable isomers predicted by DFT. In the first one, the six “additional”  $CF_3$  groups are arranged in a *pmpmp* ribbon that joins the SPP-like moiety by forming a 1,3- $C_5(CF_3)_2$  pentagon, whereas in the second these six  $CF_3$  groups form an SPP moiety on the opposite side of the cage. These two isomers differ in energy by only  $5\text{ kJ}\cdot\text{mol}^{-1}$ . Note that the ribbon of 6 or more  $CF_3$  groups forms at least one sterically hindered  $C_5(CF_3)_2$  pentagon.

### 5.3. $R_F$ Addition to $C_{70}$

**5.3.1. Earlier Studies on Multiple Addition to  $C_{70}$ .** The fullerene  $I_h\text{-}C_{60}$  has only two types of C–C bonds, which can be straightforwardly classified according to their bond distances as “single” and “double” bonds. For  $C_{70}$  and higher fullerenes, the molecular symmetry is much lower, which results in a larger number of different kinds of C–C bonds, the distances of which are more uniformly distributed. It is therefore almost impossible to make an unambiguous classification of the bond types to “single” and “double”, and the relevant chemical properties (such as addition pathways) are much harder to predict.

A detailed analysis of addition patterns for  $C_{70}X_n$  derivatives ( $n = 2–12$ ,  $X = H, F, Br$ , and  $C_6H_5$ ) was performed by Clare and Kepert at the AM1 level of theory.<sup>159</sup> The structure of  $C_{70}$  can be imagined as a combination of two  $C_{60}$ -like hemispheres on the poles separated by a belt of 10 triple-hexagon-junction C atoms (forming five relatively planar benzenoid rings) around the equator. Geometrical parameter of the cage at the pole is similar to that in  $C_{60}$ . In contrast, the cage C–C bonds around the equator are significantly longer as compared to the C–C bonds in  $C_{60}$ . For small substituents, such as H atoms, the “polar” *ortho* isomer 8,25- $C_{70}X_2$  has about the same energy as is the “equatorial” *para* isomer 1,4- $C_{70}X_2$ .

This observation deserves further comment. Neither the addition of two X groups to C1 and C4 of  $C_{70}$ , producing a *p*- $C_6(CF_3)_2$  hexagon on the  $C_{70}$  equator, nor that to C8 and C25, producing a pair of *o*- $C_6(CF_3)_2$  hexagons near one of the  $C_{70}$  poles, produces a destabilizing DBIP, accounting for the comparable stabilities of 1,4- and 8,25- $C_{70}H_2$ . However, *para* additions to any of the other 20 hexagons of  $C_{70}$  that do not straddle the equator would form a DBIP, similar to the *para* addition of two substituents to any of the hexagons of  $C_{60}$ . Furthermore, *ortho* additions of two substituents to the hexagon–hexagon edges of  $C_{70}$  other than the 10 edges symmetry related to the C8–C25 bond, would be less favorable because the C atoms that form the polar pentagons are the most pyramidal, and, in general, conversion of the most pyramidal cage  $C(sp^3)$  atoms to cage  $C(sp^2)$  atoms by the addition of substituents relieves more of the steric strain intrinsic to the curved surfaces of fullerenes.

For  $C_{70}H_4$ , the AM1 calculations showed that formation of a  $p^3$ -ribbon at the equator is energetically preferable than consequent 1,2-addition in the pole region, and the studies of  $C_{70}H_n$  with  $n = 6–10$  further emphasized the preference of consecutive 1,4-additions with formation of a  $p^{n-1}$ -ribbon around the  $C_{70}$  equator. The most stable isomer for  $C_{70}H_{10}$  is obtained by the closure of the  $p^7$  ribbon of  $C_{70}H_8$  by addition of the last two H atoms to a pentagon/hexagon edge forming a  $C_s$ - $p^9$ -*o*-loop addition pattern, which cuts the  $\pi$ -system of  $C_{70}$  into two independent (and nearly equal) parts. Computations for the bulkier groups Br and  $C_6H_5$  have also shown that formation of  $p^{n-1}$  ribbons around the equator is preferred.<sup>159</sup> Results of these calculations agree very well with experimental observations. The majority of experimentally available  $C_{70}X_{10}$  compounds ( $X = H, Cl, Br, Ph, CH_3$ ) have the  $C_s$ - $p^9$ -*o*-loop addition pattern.<sup>160</sup> However, the placement of two bulky  $OO'Bu$  groups (or, as we shall see, bulky  $CF_3$  groups) on adjacent cage C atoms is not observed, and  $C_{70}(t\text{-}BuOO)_{10}$  has the  $C_2$ - $p^9$  addition pattern, for which most of the ribbon wraps around the equator.<sup>161</sup> Thus, both computational and experimental data revealed that the most energetically stable addition motif for  $C_{70}X_n$  derivatives with  $n = 4–10$  include  $p^{n-1}$

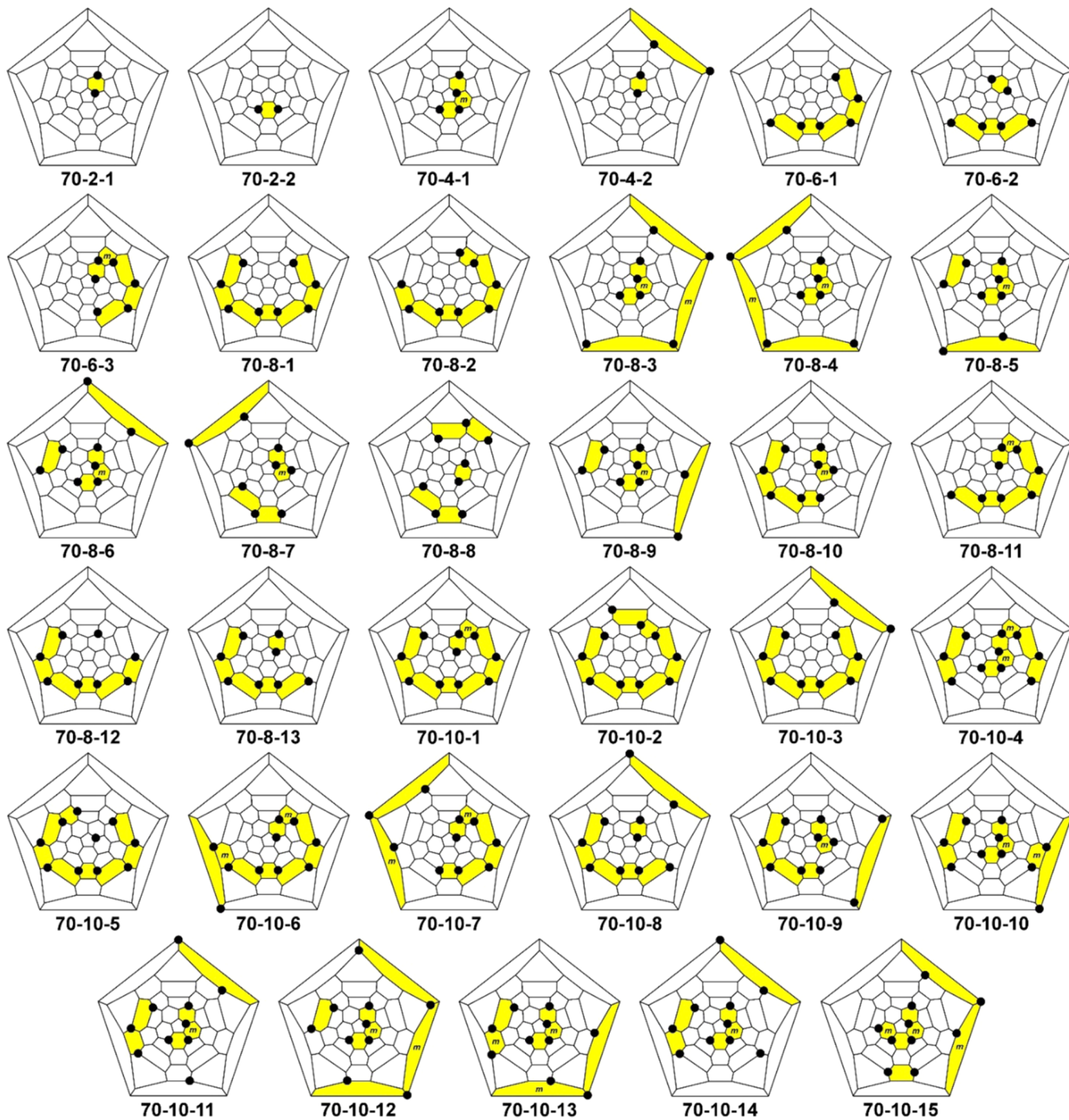


Figure 15. Schlegel diagrams of  $C_{70}(R_F)_n$  derivatives with  $n = 2-10$ .

ribbons around the equator, even for sterically-innocent H atoms.

**5.3.2.  $CF_3$  Addition to  $C_{70}$ .** Extended studies on  $C_{70}$  trifluoromethylation during the past decade produced many well-characterized compounds with compositions ranging from  $C_{70}(CF_3)_2$  to  $C_{70}(CF_3)_{20}$  (and with at least two isomers for each composition).<sup>32,33,38,46-48,68,109,156</sup> The experimental studies were either combined with or were preceded by theoretical analyses at the AM1 and PBE/TZ2P level of theory. Using these extensive results, we will now discuss  $C_{70}(CF_3)_n$  addition patterns and their relative stabilities in a comprehensive way. A complete list of structurally characterized

$C_{70}(R_F)_n$  derivatives is given in Table 3, and their Schlegel diagrams are shown in Figures 15 ( $n = 2-10$ ) and 16 ( $n = 12-20$ ).

**5.3.2.1.  $C_{70}(CF_3)_2$ .** The two lowest energy isomers of  $C_{70}(CF_3)_2$  have *p*- $C_6(CF_3)_2$  hexagon on the pole of the molecule, and these structures are assigned to the experimentally available isomers 70-2-1 ( $\Delta E = 0 \text{ kJ}\cdot\text{mol}^{-1}$ ) and 70-2-2 ( $\Delta E = 5 \text{ kJ}\cdot\text{mol}^{-1}$ ).<sup>38,68,79</sup> The most stable isomer with equatorial addition is 9  $\text{kJ}\cdot\text{mol}^{-1}$  higher in energy at the DFT level of theory; meanwhile, the same method shows that the isomer of  $C_{70}H_2$  with equatorial addition is 8  $\text{kJ}\cdot\text{mol}^{-1}$  more stable than the isomer with a *p*- $C_6H_2$  hexagon on the pole. The

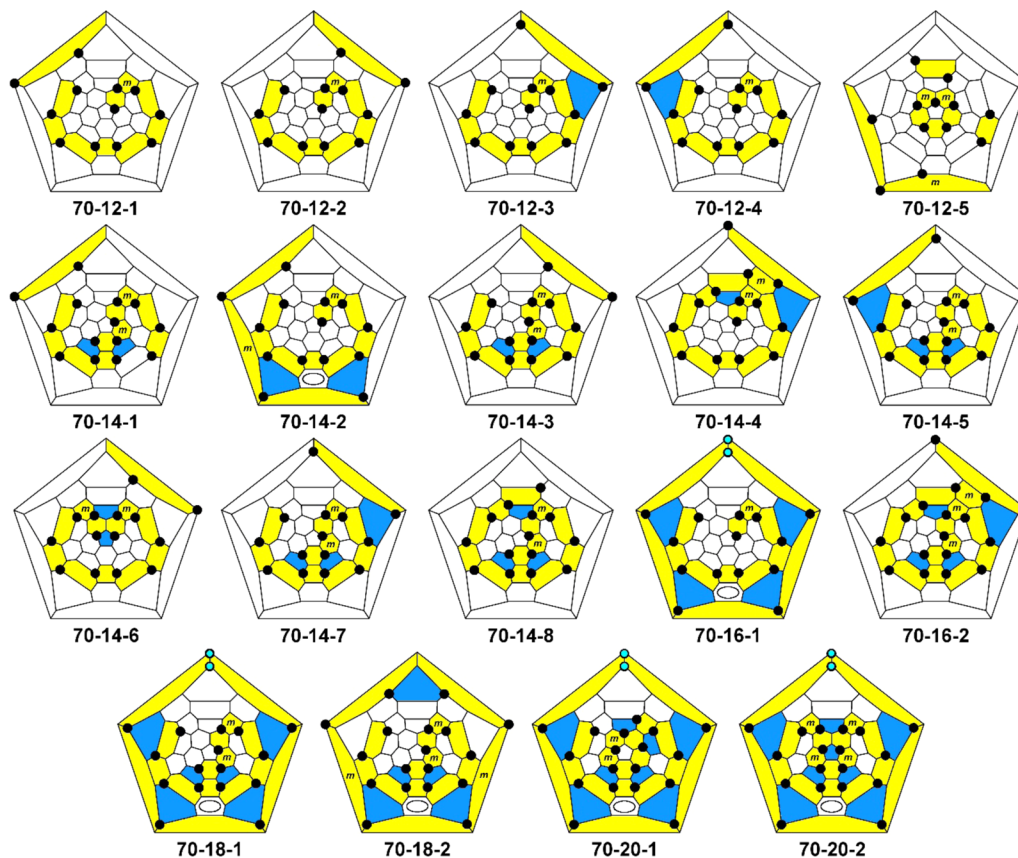


**Figure 16.** Schlegel diagrams of  $C_{70}(R_F)_n$  derivatives ( $n = 12\text{--}20$ ). Color codes:  $m$ - or  $p$ - $C_6(R_F)_2$  hexagons are highlighted in yellow;  $m$ - $C_6(R_F)$  hexagons are also indicated with the letter  $m$ ; pentagons with two  $R_F$  groups are highlighted in blue; the positions of the attached  $R_F$  groups are indicated with black circles;  $R_F$  groups attached to adjacent carbon atoms are light blue circles with black borders.

reason for such a difference is presumably a much higher curvature of  $C_{70}$  cage at the poles as compared to the flattened equatorial region. Therefore, the distance between two  $CF_3$  groups is longer for  $p$ - $C_6(CF_3)_2$  hexagon on the pole than for the hexagon on the equator; hence the repulsion between the groups is weaker on the pole. For  $C_{70}H_2$ , repulsion between the atoms is a less important factor, and the equatorial addition is more preferable.

**5.3.2.2.  $C_{70}(CF_3)_4$ .** Addition on the pole is more preferable for  $C_{70}(CF_3)_4$  as well. Similar to  $C_{60}(CF_3)_4$ , the most stable isomers have  $C_s$ - $p^3$  and  $C_1$ - $pmp$  strings with the energy difference of only 1  $\text{kJ}\cdot\text{mol}^{-1}$  (PBE/TZ2P).<sup>38</sup> Both can be isolated experimentally; however, the  $p^3$  isomer is kinetically unstable, and the isolable form is its epoxide  $C_{70}(CF_3)_4O$ ,<sup>68</sup> similar to its  $C_{60}$  counterpart. DFT calculations have also shown that there are at least 15 other isomers of  $C_{70}(CF_3)_4$  within the range of 20  $\text{kJ}\cdot\text{mol}^{-1}$ , including the isomer with a  $C_s$ - $p^3$  ribbon at the equator ( $\Delta E = 7 \text{ kJ}\cdot\text{mol}^{-1}$ , PBE/TZ2P),<sup>38</sup> but no other structure has been characterized experimentally. Note that the model calculations of  $C_{70}H_4$  and  $C_{70}Br_4$  isomers at the PBE/TZ2P level have also shown that the equatorial addition is more energetically preferable for H and even Br (the relative energies of the pole  $C_s$ - $p^3$  isomers for Br and H are 20 and 34  $\text{kJ}\cdot\text{mol}^{-1}$ , respectively, relative to the equatorial  $C_s$ - $p^3$  isomer).

**5.3.2.3.  $C_{70}(CF_3)_6$ .** Starting from  $C_{70}(CF_3)_6$ , energetically preferable addition pathway switches to the equatorial motif. The lowest energy isomer has a  $C_2$ - $p^5$  ribbon at the equator, and this is indeed the most abundant experimentally characterized isomer (**70-6-1**).<sup>38</sup> Two other characterized

structures are **70-6-2** ( $\Delta E = 9 \text{ kJ}\cdot\text{mol}^{-1}$ ) with a  $p^3$  ribbon at the equator and a separate  $p$ - $C_6(CF_3)_2$  fragment on the pole (resembling **70-2-2**),<sup>68</sup> and **70-6-3** ( $\Delta E = 12 \text{ kJ}\cdot\text{mol}^{-1}$ ) with a  $p^3mp$  ribbon connecting the equator and pole regions of the carbon cage.<sup>47</sup> DFT calculations predict a plethora of stable isomers of  $C_{70}(CF_3)_6$  (10 isomers with  $\Delta E < 10 \text{ kJ}\cdot\text{mol}^{-1}$ , and 23 isomers in the energy range 10–20  $\text{kJ}\cdot\text{mol}^{-1}$ ).<sup>47</sup>

**5.3.2.4.  $C_{70}(CF_3)_8$ .** Unlike  $C_{70}(CF_3)_4$  and  $C_{70}(CF_3)_6$ ,  $C_{70}(CF_3)_8$  has only two isomers in the 0–10  $\text{kJ}\cdot\text{mol}^{-1}$  energy range. These isomers have  $C_s$ - $p^7$  (**70-8-1**,  $\Delta E = 0 \text{ kJ}\cdot\text{mol}^{-1}$ ) and  $C_2$ - $p^7$  (**70-8-2**,  $\Delta E = 6 \text{ kJ}\cdot\text{mol}^{-1}$ ) equatorial ribbons, and both isomers were synthesized, isolated, and characterized by single-crystal X-ray diffraction (**70-8-1** is the most abundant one).<sup>33,71</sup> The third characterized isomer (**70-8-4**,  $\Delta E = 26 \text{ kJ}\cdot\text{mol}^{-1}$ ) has two  $pmp$  ribbons on opposite poles of the cage. Three new isomers were characterized recently, all with  $p^5$  equatorial ribbon as in **70-6-1** and different positions of two additional  $CF_3$  groups.<sup>111</sup> **70-8-11** ( $\Delta E = 23 \text{ kJ}\cdot\text{mol}^{-1}$ ) has  $p^5mp$  ribbon, in which the equatorial  $p^5$  ribbon is continued by an  $mp$  fragment toward the pole (the isomer hence has common motifs with both **70-6-1** and **70-6-3**). **70-8-12** ( $\Delta E = 14 \text{ kJ}\cdot\text{mol}^{-1}$ ) has  $p^6$  equatorial ribbon (i.e., the  $p^5$  ribbon of **70-6-1** is extended by one more  $CF_3$  group) and one “isolated”  $CF_3$  group. Finally, **70-8-13** ( $\Delta E = 21 \text{ kJ}\cdot\text{mol}^{-1}$ ) has  $p^5$  ribbon and an additional  $p$ - $C_6(CF_3)_2$  fragment on the pole (as in **70-2-1**).

**5.3.2.5.  $C_{70}(CF_3)_{10}$ .** As was already discussed in the previous section, the  $C_s$ - $p^7$  equatorial ribbon motif of **70-8-1** is very common for many  $C_{70}X_8$  derivatives, and in  $C_{70}X_{10}$  derivatives the ribbon is “closed” to the  $C_s$ - $p^9$ -loop around equator via

addition of two  $\text{CF}_3$  groups to a pair of adjacent carbon atoms. The large size of  $\text{CF}_3$  groups makes the lowest energy addition pattern different from that for many other addends. Repulsion of  $\text{CF}_3$  groups on adjacent cage C atoms destabilizes the  $C_s\text{-}p^9o$ -loop isomer of  $\text{C}_{70}(\text{CF}_3)_{10}$ , and the more stable isomer is obtained if the  $C_s\text{-}p^7$  equatorial ribbon is continued by an equator-to-pole  $mp$  fragment (also present in **70-6-3** and **70-8-11**), resulting in the formation of the  $C_1\text{-}p^7mp$  ribbon addition pattern of **70-10-1**.<sup>32</sup> This structure appears to be the most stable isomer of  $\text{C}_{70}(\text{CF}_3)_{10}$  (there are ca. 19 billion possible isomers of  $\text{C}_{70}\text{X}_{10}$ , so only a very small fraction can be investigated even at the lowest level of theory), with all other isomers examined at least 10  $\text{kJ}\cdot\text{mol}^{-1}$  higher in energy. In accordance with its DFT-predicted high thermodynamic stability, the  $C_1\text{-}p^7mp$  isomer **70-10-1** is the most abundant isomer of  $\text{C}_{70}(\text{CF}_3)_{10}$ , and it can be obtained with an unprecedented high yield.

The second and the third most stable isomers have the  $C_2\text{-}p^9$  equatorial ribbon and  $C_s\text{-}p^9o$ -loop addition patterns ( $\Delta E = 12 \text{ kJ}\cdot\text{mol}^{-1}$  for both). (For comparison, the  $C_1\text{-}p^7mp$  isomer of  $\text{C}_{70}\text{Br}_{10}$  is 15  $\text{kJ}\cdot\text{mol}^{-1}$  less stable than the  $C_s\text{-}p^9o$ -loop isomer.) The  $C_2\text{-}p^9$  isomer of  $\text{C}_{70}(\text{CF}_3)_{10}$ , **70-10-2**, is known, but the  $C_s\text{-}p^9o$ -loop isomer has never been observed.<sup>68</sup> The list of structurally characterized isomers of  $\text{C}_{70}(\text{CF}_3)_{10}$  also includes the following five compounds:  $p^7,p\text{-}70-10-3$  (21  $\text{kJ}\cdot\text{mol}^{-1}$ , a  $C_s\text{-}p^7$  equatorial ribbon with an additional  $p\text{-C}_6(\text{CF}_3)_2$  hexagon on the pole);  $p^2mpmp,p^3\text{-}70-10-4$  (20  $\text{kJ}\cdot\text{mol}^{-1}$ , 7+3 double ribbon);  $p^8,i\text{-}70-10-5$  (14  $\text{kJ}\cdot\text{mol}^{-1}$ , a rare example of a fullerene( $R_F$ )<sub>n</sub> addition pattern with an isolated  $R_F$  group on one of the  $\text{C}_{70}$  poles);  $C_2\text{-}pmp^5mp\text{-}70-10-6$  (21  $\text{kJ}\cdot\text{mol}^{-1}$ , a pole-to-pole ribbon);  $p^4mp,pm\text{-}70-10-7$  (32  $\text{kJ}\cdot\text{mol}^{-1}$ , another 7+3 double ribbon).<sup>68,118</sup>

**5.3.2.6.  $\text{C}_{70}(\text{CF}_3)_{12-20}$ .** The  $p^7mp$  addition pattern of **70-10-1** is found in all except one experimentally isolated addition patterns of  $\text{C}_{70}(\text{CF}_3)_{12-20}$  (see Figure 16). Four of the five most stable addition patterns ( $\Delta E < 10 \text{ kJ}\cdot\text{mol}^{-1}$ ), and the only structurally characterized isomers of  $\text{C}_{70}(\text{CF}_3)_{12}$  have  $p^7mp,p$  addition patterns with an isolated  $p\text{-C}_6(\text{CF}_3)_2$  hexagon on the other  $\text{C}_{70}$  pole.<sup>42,45,48,68,87</sup>

DFT calculations for  $\text{C}_{70}(\text{CF}_3)_{14}$  revealed a very dense distribution of low-energy isomers: there are 10 with  $\Delta E < 10 \text{ kJ}\cdot\text{mol}^{-1}$ , and six more in the energy range 10–20  $\text{kJ}\cdot\text{mol}^{-1}$ .<sup>46</sup> In all of these isomers, the  $p^7mp$  ribbon of **70-10-1** is either (i) continued on one or both ends to make a longer ribbon, (ii) continued on one pole with an additional  $p\text{-C}_6(\text{CF}_3)_2$  hexagon located on the opposite pole (12+2), or (iii) combined with a  $p^3$  or  $pmp$  ribbon on the opposite pole (10+4). Five of the eight well-characterized isomers have “12+2 addition” patterns, **70-14-1** (0  $\text{kJ}\cdot\text{mol}^{-1}$ ), **70-14-3** (2  $\text{kJ}\cdot\text{mol}^{-1}$ ), **70-14-5** (2  $\text{kJ}\cdot\text{mol}^{-1}$ ), **70-14-6** (18  $\text{kJ}\cdot\text{mol}^{-1}$ ), and **70-14-7** (2  $\text{kJ}\cdot\text{mol}^{-1}$ ). The isomer **70-14-2** (7  $\text{kJ}\cdot\text{mol}^{-1}$ ) has a 10+4 ( $pmp$ ) pattern with one isolated benzenoid ring, and two other isomers have long ribbons,  $C_2\text{-}pmp^9mp\text{-}70-14-4$  (5  $\text{kJ}\cdot\text{mol}^{-1}$ ) and  $C_1\text{-}p^9mpmp\text{-}70-14-8$  (5  $\text{kJ}\cdot\text{mol}^{-1}$ ).<sup>46,59,79,87</sup>

The two DFT-predicted most stable isomers of  $\text{C}_{70}(\text{CF}_3)_{16}$  have been isolated. **70-16-1** has a  $p^7mp$  ribbon, and an SPP moiety on the opposite pole (and has an isolated benzenoid ring).<sup>49</sup> **70-16-2** ( $\Delta E = 1 \text{ kJ}\cdot\text{mol}^{-1}$ ) has the longest single ribbon observed to date,  $pmp^9mpmp$ , and is related to both **70-14-4** and **70-14-8**.<sup>87</sup> Note that among the most stable isomers with  $\Delta E < 10 \text{ kJ}\cdot\text{mol}^{-1}$ , three structures have  $\text{CF}_3$  groups on adjacent cage C atoms.

**70-18-1**, predicted to be the most stable isomer of this composition, has the same arrangement of  $\text{CF}_3$  groups as in **70-16-1** with an additional pair of  $\text{CF}_3$  groups continuing the  $p^7mp$  ribbon.<sup>49</sup> Another characterized isomer, **70-18-2** ( $\Delta E = 11 \text{ kJ}\cdot\text{mol}^{-1}$ , predicted to be the fifth most stable), also has  $p^7mp$  ribbon and a  $p^5$ -loop on the opposite pole.<sup>109</sup>

The highest degree of trifluoromethylation reached so far for  $\text{C}_{70}$  is  $\text{C}_{70}(\text{CF}_3)_{20}$ , and two isomers of this composition were characterized.<sup>136</sup> The most stable isomer, **70-20-1** is the only isomer of  $\text{C}_{70}(\text{CF}_3)_{12-20}$  that does not include the archetypical  $p^7mp$  ribbon of **70-10-1** as part of its addition pattern. Moreover, **70-20-1** cannot be obtained by  $\text{CF}_3$  additions to stable  $\text{C}_{70}(\text{CF}_3)_n$  precursors. The structure has an SPP moiety on one pole, a  $p^8$  equatorial loop, and a  $p^3m^2$  loop (analogous to that in **60-10-4**) on the other pole. Other remarkable features of this addition pattern are two isolated and two semi-isolated benzenoid hexagons and a cyclopentadienoide fragment. **70-20-2** ( $\Delta E = 10 \text{ kJ}\cdot\text{mol}^{-1}$ , the fifth most stable isomer) also has an SPP moiety and includes a  $p^7mp$  ribbon continued by four more  $\text{CF}_3$  groups. It has one isolated and two semi-isolated benzenoid hexagons as well as isolated phenanthrenoide fragments. Unlike **70-20-1**, **70-20-2** can be obtained from **70-18-1** by addition of two  $\text{CF}_3$  groups. At the same time, **70-20-1** and **70-20-2** have 17  $\text{CF}_3$  groups in common positions.  $\text{C}_{70}(\text{CF}_3)_{20}$  is likely to be the largest degree of trifluoromethylation that is possible to achieve for  $\text{C}_{70}$  because further addition of  $\text{CF}_3$  groups is predicted to be substantially less exothermic.

To summarize, the majority of isolated  $\text{C}_{70}(\text{CF}_3)_n$  compounds are DFT-predicted stable isomers with relative energies below 20  $\text{kJ}\cdot\text{mol}^{-1}$ , suggesting and hence partial thermodynamic control of trifluoromethylation. Although 1,4 additions of  $\text{CF}_3$  groups to the  $\text{C}_{70}$  equator are possible without the formation of DBIPs, addition to the pole is energetically preferable at early stages ( $n = 2-4$ ). An equatorial ribbon is found to be the main addition motif for  $n > 6$ . For larger numbers ( $n \geq 16$ ), when the  $\text{C}_{70}$  surface has become extremely crowded, steric strain induced by repulsion of the  $\text{CF}_3$  groups located in one pentagon becomes comparable to the repulsion of the  $\text{CF}_3$  groups in adjacent positions, and hence the SPP fragments appear in the most stable isomers. The interplay between kinetic and thermodynamic factors in  $\text{CF}_3$  addition to  $\text{C}_{70}$  is similar to that described for  $\text{C}_{60}$  in section 5.1.4.<sup>156</sup>

**5.3.3. Addition of Bulky  $R_F$  Groups to  $\text{C}_{70}$ .** In the discussion of  $\text{C}_2\text{F}_5$  addition to  $\text{C}_{60}$  (section 5.1.5), we showed that steric hindrances introduced by perfluoroethyl and other  $n$ -perfluoroalkyl groups are comparable to those of  $\text{CF}_3$ , and hence ribbon addition patterns were still expected, and found, for  $\text{C}_2\text{F}_5$  derivatives of  $\text{C}_{60}$ . However, in long ribbons, the strain often increases to the middle of the ribbon so that some  $R_F$  groups adopt an eclipsed conformation. For such fragments, substitution of  $\text{CF}_3$  by  $\text{C}_2\text{F}_5$  with lower conformational freedom increases the strain, and hence shorter ribbons are expected for longer alkyl chains. These factors are also applicable in the analysis of addition patterns for  $\text{C}_{70}(\text{C}_2\text{F}_5)_n$  derivatives. For example,  $\text{C}_{70}(\text{C}_2\text{F}_5)_2$  has the stable **70-2-1** addition pattern.<sup>116</sup> The compound  $\text{C}_{70}(n\text{-C}_3\text{F}_7)_4$  has a  $p,p$  addition pattern with the two  $p\text{-C}_6(n\text{-C}_3\text{F}_7)_2$  hexagons on opposite poles.

Among the eight characterized isomers of  $\text{C}_{70}(\text{C}_2\text{F}_5)_8$ , two are isostructural with the  $\text{C}_{70}(\text{CF}_3)_8$  compounds **70-8-1** ( $C_s\text{-}p^7$ ) and **70-8-4** ( $pmp,pmp$ ). Six other isomers have unique addition patterns comprising two or three small ribbon fragments (each small ribbon fragment has 2–4 groups): 4+4  $pmp,pmp$  (**70-8-**

3), 4+2+2 *pmp,p,p* (**70-8-5**, **70-8-6**, and **70-8-9**), and 4+3+1 *p<sup>3</sup>pm,p* (**70-8-7**). The **70-8-3**, **70-8-4**, **70-8-5**, and **70-8-6** patterns are also confirmed for  $C_{70}(n\text{-}C_3F_7)_8$  derivatives. Likewise, one isomer of  $C_{70}(C_2F_5)_{10}$  is isostructural with **70-10-1**, and eight others are unique and have several small ribbon fragments: 6+2+2 *p<sup>6</sup>p,p* (**70-10-8**), 6+3+1 *p<sup>4</sup>pm,p* (**70-10-9**), 4+3+3 *pmp,p<sup>2</sup>pm* (**70-10-10**, **70-10-13**), 4+3+2+1 *pmp,p<sup>2</sup>p,i* (**70-10-11**, **70-10-14**), 4+4+2 *pmp,pmp,p* (**70-10-12**), and 5+3+2 *p<sup>2</sup>mp,pm,p* (**70-10-15**). Finally, the only characterized isomer of  $C_{70}(C_2F_5)_{12}$  has a 5+3+2+2 *p<sup>3</sup>m<sup>2</sup>-loop,pm,p,p* addition pattern.

Whereas  $C_2F_5$  and  $n\text{-}C_3F_7$  groups prefer to form small ribbons rather than isolated  $p\text{-}C_6(R_F)_2$  hexagons, the latter is the only addition pathway known for *i-C<sub>3</sub>F<sub>7</sub>* groups. Two isomers of  $C_{70}(i\text{-}C_3F_7)_2$  and six isomers of  $C_{70}(i\text{-}C_3F_7)_4$  have been described. All isomers with four groups have two  $p\text{-}C_6(i\text{-}C_3F_7)_2$  hexagons on opposite poles of  $C_{70}$ .<sup>94,98</sup>

#### 5.4. R<sub>F</sub> Addition to Hollow Higher Fullerenes (HHFs)

As briefly discussed earlier, one of the important factors governing the chemical reactivity of fullerenes is the strain caused by the non-planarity of  $sp^2$ -hybridized cage C atoms. A numerical measure of pyramidalization, the angle  $\theta_p$ , has been proposed using  $\pi$ -orbital vector analysis (POAV):  $\theta_p = \theta_{\sigma\pi} - 90^\circ$ , as shown in Figure 17.<sup>162</sup> The ideal geometrical

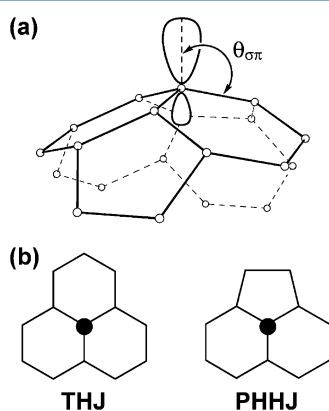


**Figure 17.** (a) Definition of the  $\theta_{\sigma\pi}$  angle as given in terms of  $\pi$ -orbital vector analysis (POAV); (b) The black circles designate a triple hexagon junction (THJ) and a pentagon/hexagonhexagon junction (PHHJ) in hollow higher fullerenes (HHFs).

arrangements for  $C(sp^2)$  and  $C(sp^3)$  atoms have  $\theta_p$  values of  $0.0^\circ$  and  $19.4^\circ$ , respectively. In  $C_{60}$ , all of the cage C atoms have a  $\theta_p$  value of  $11.6^\circ$ . In  $C_{70}$  the values range from  $8.6^\circ$  to  $12.0^\circ$ . Thus, pyramidalization angles in fullerenes have values between those of ideal  $C(sp^2)$  and  $C(sp^3)$  atoms in spite of the formal  $sp^2$  hybridization of the cage C atoms. When an addend is attached, the cage C atom becomes  $sp^3$  hybridized and the steric strain is partially released. Furthermore, cage  $C(sp^2)$  atoms attached to cage  $C(sp^3)$  atoms become more planar, further reducing the strain energy. As a consequence, the most pyramidal cage C atoms are generally the most reactive and the least pyramidal cage C atoms are the least reactive. Hollow fullerenes that obey the isolated pentagon rule have two types of carbon atoms: those at the junction of a pentagon and two hexagons (PHHJ), and those at triple-hexagon junctions (THJ), as also shown in Figure 17. Pyramidalization in fullerenes is caused by pentagons, and therefore the lowest  $\theta_p$  angles are usually found for THJ cage C atoms.

One of the important findings revealed in studies of multiple additions to  $C_{70}$  is the fact that isomers in which substituents are bonded to THJ carbon atoms are very unstable. This rule is fulfilled for all  $C_{70}$  derivatives except for  $C_{70}F_{38}$ <sup>163</sup> and  $C_{70}Cl_{28}$ .<sup>164</sup> Avoidance of additions to THJs also appears to be a useful guideline for  $HHF(R_F)_n$  derivatives in general, at least for  $n \leq 12$ . As an example, Figure 18 shows a correlation

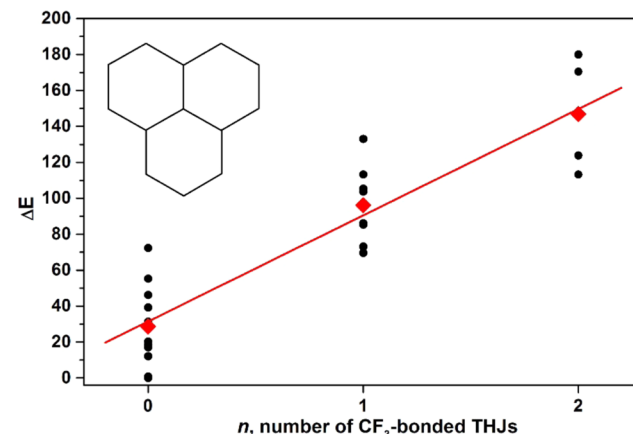


**Figure 18.** Correlation between the relative energies of  $C_{78}(CF_3)_2$  isomers ( $\text{kJ}\cdot\text{mol}^{-1}$ ) and the number,  $n$ , of  $CF_3$  groups attached to THJs. Individual relative energies are shown as black dots; the average relative energy for each value of  $n$  is shown as a red diamond.

of the relative energies of  $C_{78}(CF_3)_2$  isomers and the number of  $sp^3$  THJs.<sup>70</sup> For each number of  $sp^3$  THJs (0, 1, or 2), the relative energy of the isomers spans the range of ca. 70  $\text{kJ}\cdot\text{mol}^{-1}$ . The centers of the distribution are found at 29  $\text{kJ}\cdot\text{mol}^{-1}$  for isomers with no  $sp^3$  THJs, at 96  $\text{kJ}\cdot\text{mol}^{-1}$  for isomers with one  $sp^3$  THJ, and at 147  $\text{kJ}\cdot\text{mol}^{-1}$  for isomers with two  $sp^3$  THJs. On the basis of these data, the penalty for each  $sp^3$  THJ is roughly estimated to be ca. 60  $\text{kJ}\cdot\text{mol}^{-1}$ . Therefore, when considering  $HHF(R_F)_n$  isomers with  $n \leq 12$ , additions to THJs atoms can be safely ignored as possibilities, dramatically reducing the number of isomers to be computationally investigated. Note that for higher degree of addition this rule is not very strict, and an isomer of  $C_{76}(CF_3)_{14}$ , two isomers of  $C_{76}(CF_3)_{16}$ , and one isomer of  $C_{76}(CF_3)_{18}$  and  $C_{94}(CF_3)_{20}$  have been found to have  $CF_3$  on THJs.<sup>84a,90,165</sup>

The first studies of the trifluoromethylation of higher fullerenes either by pyrolysis with silver trifluoroacetate or by flow reaction with  $CF_3I$  gas in hot tubes showed that adducts with 12  $CF_3$  groups are formed predominantly.<sup>50,70</sup> This number is exactly the number of pentagons present in each fullerene and is therefore the largest degree of addition accessible when no more than one  $CF_3$  group is added to one pentagon. 2D connectivity patterns in  $^{19}\text{F}$  NMR spectra proved that ribbon addition patterns are typical for higher fullerenes similar to  $C_{60}$  and  $C_{70}$ , although short ribbons and  $p\text{-}C_6(CF_3)_2$  pairs are also not very uncommon.<sup>50,70</sup> Structure elucidation of higher fullerene derivatives solely by  $^{19}\text{F}$  NMR data is complicated by the presence of at least two cage isomers starting from  $C_{76}$  and by the fact the reactions were usually performed with mixtures of fullerenes. Therefore, it is necessary to consider different carbon cages and different addition patterns for each carbon cage. However, the number of plausible structures can be reduced dramatically when several rules discussed above are applied. The following structural motifs are destabilizing and hence can be excluded: (i) addition

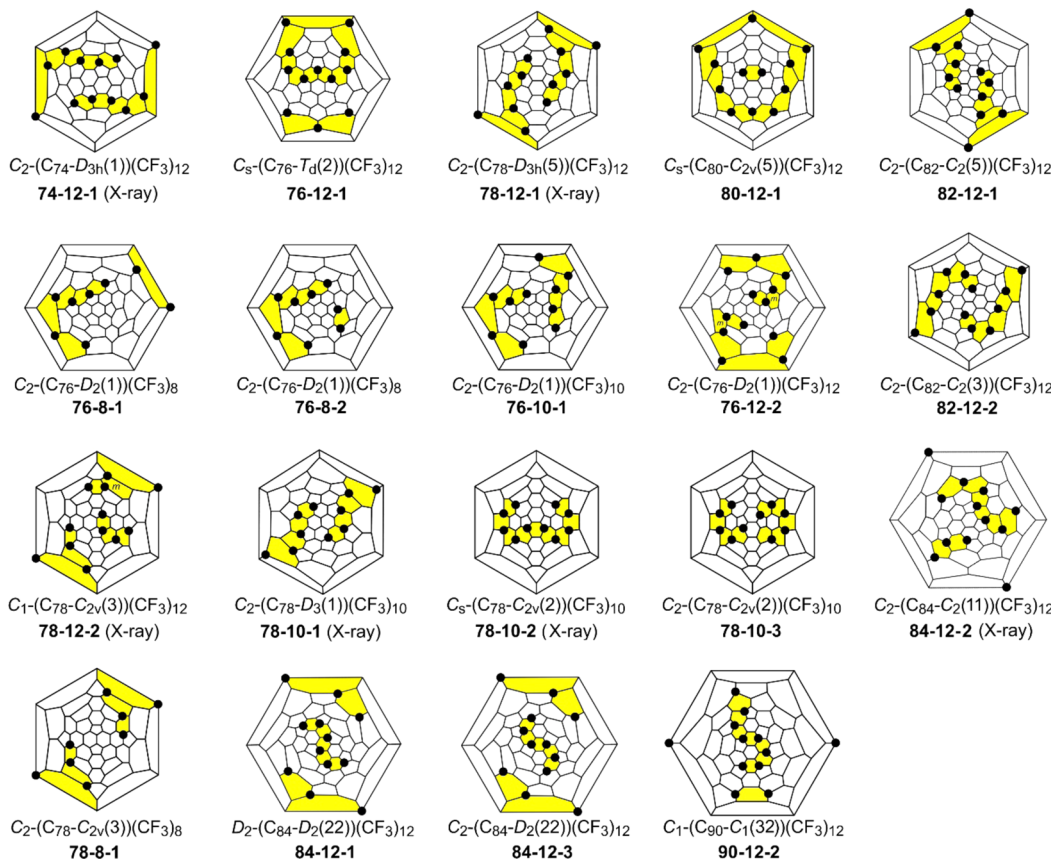


**Figure 19.** Schlegel diagrams of selected higher fullerene PFAFs with  $n \leq 12$ . Reproduced with permission from ref 70. Copyright 2008 American Chemical Society.

to adjacent carbon atoms; (ii) addition to THJ carbon atoms; (iii) addition of more than one  $\text{CF}_3$  group to one pentagon. When these guidelines were applied to  $\text{CF}_3$  derivatives of higher fullerenes, the number of possible isomers reduced from millions to only a few, and realistic addition patterns could be then pinpointed on the basis of NMR data with the help of DFT calculations.

This approach was especially useful in the work described in ref 50, where trifluoromethylation of “insoluble” HHFs was performed. These fullerenes usually remain in the carbon soot after extraction of the soluble fullerenes presumably due to polymerization, and hence their molecular structures and even their existence as discrete cages before polymerization remained unknown. Their trifluoromethylation afforded soluble HHF- $(\text{CF}_3)_n$  derivatives, the cage isomers and addition patterns of which were determined by a combined NMR/DFT study. Trifluoromethylation was thus found to be a convenient method to prove the formation of some fullerenes in the arc discharge synthesis and to determine their molecular structures.

Figure 19 shows Schlegel diagrams of selected PFAFs based on the “insoluble” HHFs described in ref 50 and the soluble HHFs described in ref 70 (see Table 5 for the list of well-characterized HHF( $\text{R}_\text{F}$ ) $_n$  derivatives). Their structures were determined by NMR/DFT analysis and confirmed for some of them by X-ray crystallography.<sup>57,69,96,108</sup>

Analysis of the  $\text{CF}_3$  addition patterns in higher fullerene PFAFs reveals predominant formation of long all-*para* ribbons. Typical patterns include the  $p^{11}$ -ribbon in  $\text{C}_{74}\text{-D}_{3h}(1)(\text{CF}_3)_{12}$ ,  $(\text{C}_{78}\text{-D}_{3h}(5))(\text{CF}_3)_{12}$ , and  $(\text{C}_{82}\text{-C}_2(5))(\text{CF}_3)_{12}$ , the  $p^{10}$ -loop, $p$  addition pattern in  $(\text{C}_{82}\text{-C}_2(5))(\text{CF}_3)_{12}$ , the  $p^9$ -loop, $p^2$  addition

pattern in  $(\text{C}_{76}\text{-T}_d(2))(\text{CF}_3)_{12}$ , the double ribbon  $p^5$ , $p^5$  double ribbon addition pattern in  $(\text{C}_{82}\text{-C}_2(3))(\text{CF}_3)_{12}$  and in two isomers of  $(\text{C}_{84}\text{-D}_2(22))(\text{CF}_3)_{12}$ . Out of two dozen isolated and characterized HHF( $\text{CF}_3$ ) $_n$  compounds, only two had  $m\text{-C}_6(\text{CF}_3)_2$  hexagons:  $p^3\text{mp}, p^3\text{mp}\text{-}(\text{C}_{76}\text{-D}_2(2))(\text{CF}_3)_{12}$  (76-12-2) and  $p^5\text{mp}, p^3\text{-}(\text{C}_{78}\text{-C}_{2v}(3))(\text{CF}_3)_{12}$  (78-12-2). Another  $\text{CF}_3$  addition guideline proposed in ref 69 is the avoidance of additions to cage C atoms that form interpentagonal double bonds. Although such C atoms have high pyramidalization angles and therefore would be expected to be among the most reactive cage C atoms, their inclusion in ribbon addition patterns requires either the formation of DBIPs or additions to THJs.

Starting in 2009, extensive studies of higher fullerene perfluoroalkylation were reported by Troyanov and co-workers.<sup>78,83,84,86,90,96,139,166</sup> A complete list of HHF( $\text{CF}_3$ ) $_n$  ranging from  $\text{C}_{76}(\text{CF}_3)_n$  to  $\text{C}_{96}(\text{CF}_3)_n$  is given in Table 5. In many cases, X-ray structure determination afforded the first crystallographic proof of particular higher fullerene cages. Troyanov and coworkers used relatively harsh reaction conditions (e.g., reactions with ca. 6 bar of  $\text{CF}_3\text{I}$  for 3 days in a sealed ampoule at 400–420 °C), which often resulted in a high degrees of perfluoroalkylation ( $n = 14\text{--}20$ ). With 14 or more added  $\text{CF}_3$  groups, some pentagons must have more than one  $\text{CF}_3$  group, as shown in Figure 20. The rule limiting one  $\text{CF}_3$  group to one pentagon is obviously violated (Figure 20 shows Schlegel diagrams of selected PFAFs with 14–20  $\text{CF}_3$  groups). A common motif for HHF( $\text{CF}_3$ ) $_n$  derivatives with  $n > 12$  is the presence of isolated double bonds connecting two 1,3- $\text{C}_5(\text{CF}_3)_2$  pentagons. Another typical feature is the formation of

Table 5. Perfluoroalkyl Derivatives of Higher Fullerenes

fullerene	characterized PFAFs	structural method	ref
C <sub>74</sub> -D <sub>3h</sub> (1)	C <sub>74</sub> (CF <sub>3</sub> ) <sub>12</sub>	X-ray, <sup>19</sup> F NMR	50,57
C <sub>76</sub> -D <sub>2</sub> (1)	C <sub>76</sub> (CF <sub>3</sub> ) <sub>6</sub>	<sup>19</sup> F NMR	70
	C <sub>76</sub> (CF <sub>3</sub> ) <sub>8</sub> , two isomers	<sup>19</sup> F NMR	70
	C <sub>76</sub> (CF <sub>3</sub> ) <sub>10</sub> , five isomers	<sup>19</sup> F NMR	70
	C <sub>76</sub> (CF <sub>3</sub> ) <sub>12</sub>	<sup>19</sup> F NMR	70
	C <sub>76</sub> (CF <sub>3</sub> ) <sub>14</sub>	X-ray	90
	C <sub>76</sub> (CF <sub>3</sub> ) <sub>16</sub> , three isomers	X-ray	90,165
	C <sub>76</sub> (CF <sub>3</sub> ) <sub>18</sub> , two isomers	X-ray	90
C <sub>76</sub> -T <sub>d</sub> (2)	C <sub>76</sub> (CF <sub>3</sub> ) <sub>12</sub>	<sup>19</sup> F NMR	50
C <sub>78</sub> -D <sub>3</sub> (1)	C <sub>78</sub> (CF <sub>3</sub> ) <sub>10</sub>	X-ray, <sup>19</sup> F NMR	70
C <sub>78</sub> -C <sub>2v</sub> (2)	C <sub>78</sub> (CF <sub>3</sub> ) <sub>10</sub> , two isomers	X-ray, <sup>19</sup> F NMR	70
	C <sub>78</sub> (C <sub>2</sub> F <sub>5</sub> ) <sub>10</sub>	X-ray	78
C <sub>78</sub> -C <sub>2v</sub> (3)	C <sub>78</sub> (CF <sub>3</sub> ) <sub>8</sub>	<sup>19</sup> F NMR	70
	C <sub>78</sub> (CF <sub>3</sub> ) <sub>12</sub>	X-ray, <sup>19</sup> F NMR	70
C <sub>78</sub> -D <sub>3h</sub> (5)	C <sub>78</sub> (CF <sub>3</sub> ) <sub>12</sub>	X-ray, <sup>19</sup> F NMR	50,57
C <sub>80</sub> -D <sub>2</sub> (2)	C <sub>80</sub> (CF <sub>3</sub> ) <sub>12</sub>	X-ray	139c
C <sub>80</sub> -C <sub>2v</sub> (5)	C <sub>80</sub> (CF <sub>3</sub> ) <sub>12</sub>	<sup>19</sup> F NMR	50
C <sub>82</sub> -C <sub>2</sub> (3)	C <sub>82</sub> (CF <sub>3</sub> ) <sub>12</sub>	<sup>19</sup> F NMR, X-ray	50,96
	C <sub>82</sub> (CF <sub>3</sub> ) <sub>16</sub> , two isomers	X-ray	165
	C <sub>82</sub> (CF <sub>3</sub> ) <sub>18</sub> , two isomers	X-ray	96
C <sub>82</sub> -C <sub>2</sub> (5)	C <sub>82</sub> (CF <sub>3</sub> ) <sub>12</sub>	<sup>19</sup> F NMR	50
C <sub>84</sub> -D <sub>2d</sub> (4)	C <sub>84</sub> (CF <sub>3</sub> ) <sub>12</sub>	X-ray	84b
C <sub>84</sub> -D <sub>2</sub> (5)	C <sub>84</sub> (CF <sub>3</sub> ) <sub>16</sub>	X-ray	166a
C <sub>84</sub> -C <sub>2</sub> (11)	C <sub>84</sub> (CF <sub>3</sub> ) <sub>12</sub>	<sup>19</sup> F NMR, X-ray	69
	C <sub>84</sub> (C <sub>2</sub> F <sub>5</sub> ) <sub>12</sub>	X-ray	83
C <sub>84</sub> -C <sub>s</sub> (16)	C <sub>84</sub> (C <sub>2</sub> F <sub>5</sub> ) <sub>12</sub> , two isomers	X-ray	83,84b
C <sub>84</sub> -C <sub>2v</sub> (18)	C <sub>84</sub> (C <sub>2</sub> F <sub>5</sub> ) <sub>12</sub>	X-ray	83
C <sub>84</sub> -D <sub>2</sub> (22)	C <sub>84</sub> (CF <sub>3</sub> ) <sub>6</sub>	X-ray	167
	C <sub>84</sub> (CF <sub>3</sub> ) <sub>12</sub> , two isomers	<sup>19</sup> F NMR, X-ray	70,107
	C <sub>84</sub> (C <sub>2</sub> F <sub>5</sub> ) <sub>12</sub>	X-ray	83
	C <sub>84</sub> (CF <sub>3</sub> ) <sub>14</sub> , two isomers	X-ray	107
	C <sub>84</sub> (CF <sub>3</sub> ) <sub>16</sub> , four isomers	X-ray	83,107
	C <sub>84</sub> (CF <sub>3</sub> ) <sub>20</sub>	X-ray	107
C <sub>84</sub> -D <sub>2d</sub> (23)	C <sub>84</sub> (CF <sub>3</sub> ) <sub>4</sub>	X-ray	108
	C <sub>84</sub> (CF <sub>3</sub> ) <sub>8</sub>	X-ray	108
	C <sub>84</sub> (CF <sub>3</sub> ) <sub>10</sub>	X-ray	108
	C <sub>84</sub> (CF <sub>3</sub> ) <sub>12</sub>	X-ray	108
	C <sub>84</sub> (C <sub>2</sub> F <sub>5</sub> ) <sub>12</sub>	X-ray	83
	C <sub>84</sub> (CF <sub>3</sub> ) <sub>14</sub> , two isomers	X-ray	108
	C <sub>84</sub> (CF <sub>3</sub> ) <sub>16</sub> , two isomers	X-ray	108
	C <sub>84</sub> (CF <sub>3</sub> ) <sub>18</sub>	X-ray	108
C <sub>86</sub> -C <sub>2</sub> (17)	C <sub>86</sub> (CF <sub>3</sub> ) <sub>16</sub> , two isomers	X-ray	81
	C <sub>86</sub> (CF <sub>3</sub> ) <sub>18</sub>	X-ray	81
C <sub>88</sub> -C <sub>2</sub> (33)	C <sub>88</sub> (CF <sub>3</sub> ) <sub>16</sub>	X-ray	139b
	C <sub>88</sub> (CF <sub>3</sub> ) <sub>18</sub>	X-ray	86
	C <sub>88</sub> (CF <sub>3</sub> ) <sub>18</sub>	X-ray	139b
C <sub>90</sub> -C <sub>1</sub> (30)	C <sub>90</sub> (CF <sub>3</sub> ) <sub>18</sub>	X-ray	168
C <sub>90</sub> -C <sub>1</sub> (32)	C <sub>90</sub> (CF <sub>3</sub> ) <sub>12</sub>	<sup>19</sup> F NMR	70
C <sub>90</sub> -C <sub>s</sub> (35)	C <sub>90</sub> (CF <sub>3</sub> ) <sub>14</sub>	X-ray	168
C <sub>92</sub> -D <sub>2</sub> (82)	C <sub>90</sub> (CF <sub>3</sub> ) <sub>16</sub>	X-ray	86
C <sub>94</sub> -C <sub>2</sub> (61)	C <sub>94</sub> (CF <sub>3</sub> ) <sub>20</sub> ; two THJs	X-ray	84a
C <sub>96</sub> -C <sub>1</sub> (145)	C <sub>96</sub> (C <sub>2</sub> F <sub>5</sub> ) <sub>12</sub>	X-ray	84a

isolated or nearly-isolated benzenoid hexagons, which are formed at the expense of additions to THJs. At the same time, the preference for all-*para* additions is preserved (as stated above, only a few derivative have *m*-C<sub>6</sub>(CF<sub>3</sub>)<sub>2</sub> hexagons) and the addition to interpentagon double bonds is avoided (in fact, these double bonds often become isolated from the rest of the π-system).

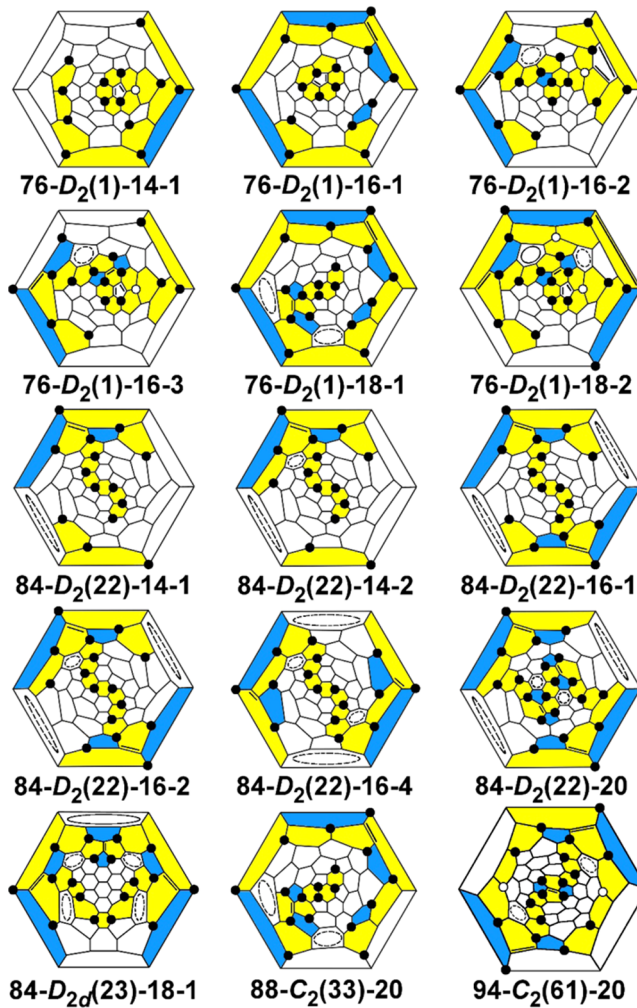
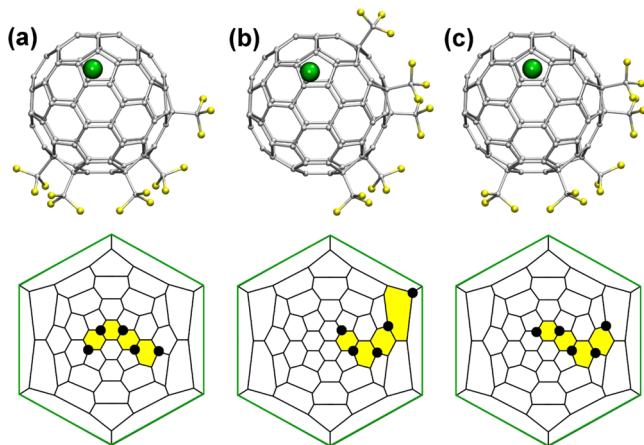


Figure 20. Schlegel diagrams of selected hollow higher-fullerene PFAFs with  $n \geq 14$ . See Figures 12 and 16 for color codes. R<sub>F</sub> groups attached to THJ carbon atoms are shown as empty circles. Semi-isolated and fully isolated benzenoid rings (five or six adjacent fullerene C(sp<sup>3</sup>) atoms, respectively) are shown as dashed and solid ovals; the positions of isolated double bonds (i.e., double bonds with four adjacent fullerene C(sp<sup>2</sup>) atoms) are also shown.

## 5.5. R<sub>F</sub> Addition to Endohedral Metallofullerenes

**5.5.1. Derivatives of Monometallofullerenes.** Perfluoroalkylation of two groups of endohedral metallofullerenes (EMF) has been reported so far. One group includes monometallofullerenes such as M@C<sub>82</sub> (M = Y, Ce, Gd, etc.)<sup>30,66,75</sup> as well as Y@C<sub>2x</sub> EMFs with different cage sizes ( $2x = 60$  to 74).<sup>106</sup> These EMFs are paramagnetic in the pristine state (metal atom transfers three valence electrons to the carbon cage), and their perfluoroalkylation results in diamagnetic EMF(R<sub>F</sub>)<sub>n</sub> derivatives with an odd numbers of R<sub>F</sub> groups (typically  $n = 1$ –5). Structural studies of such derivatives are limited so far to <sup>19</sup>F NMR spectroscopic studies of two isomers of Y@C<sub>82</sub>(CF<sub>3</sub>)<sub>5</sub>.<sup>30</sup> According to 1D <sup>19</sup>F and 2D <sup>19</sup>F–<sup>19</sup>F COSY NMR data, both isomers had non-symmetric ribbon addition patterns. DFT computations of 56 ribbon isomers of Y@C<sub>82</sub>(CF<sub>3</sub>)<sub>5</sub> in which *para*-C<sub>6</sub>(CF<sub>3</sub>)<sub>2</sub> hexagons had various arrangement and locations on the Y@C<sub>82</sub>-C<sub>2v</sub>(9) cage revealed two stable isomers, which were 14 kJ·mol<sup>-1</sup> more stable than the third one and at least 50 kJ·mol<sup>-1</sup> more stable than 53 other isomers (see Figure 21). The molecular

structures of  $\text{Y}@\text{C}_{74}(\text{CF}_3)$ ,  $\text{Y}@\text{C}_{70}(\text{CF}_3)$ , and  $\text{Y}@\text{C}_{70}(\text{CF}_3)_3$  were proposed in ref 106 on the basis of UV-vis–NIR absorption spectra and DFT calculations.



**Figure 21.** DFT-optimized molecular structures of three lowest energy isomers of  $\text{Y}@\text{C}_{82}(\text{CF}_3)_5$  (top row) and their Schlegel diagrams (bottom row) according to ref 30. The Y atoms are shown as green spheres. The hexagons to which the metal atom is coordinated are highlighted with green lines in the Schlegel diagrams.

**5.5.2. Derivatives of  $\text{Sc}_3\text{N}@\text{C}_{80}$ .** Trifluoromethylation of  $\text{Sc}_3\text{N}@\text{C}_{80}$  was a subject of detailed studies in several reports.<sup>64,93,100,102</sup> The first characterized compounds were  $\text{Sc}_3\text{N}@\text{C}_{80}(\text{CF}_3)_2$  (a mixture with the  $\text{C}_{80}\text{-}I_h(7)$  or  $\text{C}_{80}\text{-}D_{5h}(6)$  cage isomers both present), the  $^{19}\text{F}$  NMR spectra of which indicated a symmetric addition pattern. DFT calculations showed that the lowest energy isomers for both carbon cages had *para*- $\text{C}_6(\text{CF}_3)_2$  hexagon with  $\text{CF}_3$  groups avoiding THJ carbon atoms.<sup>64</sup> Whereas the  $\text{Sc}_3\text{N}$  cluster rotates freely inside the  $\text{C}_{80}\text{-}I_h$  cage (barriers do not exceed 10 kJ·mol<sup>-1</sup>; see ref 169), exohedral addition of  $\text{CF}_3$  groups dramatically changes the internal dynamics of the endohedral cluster. The two most stable optimized structures of  $\text{Sc}_3\text{N}@\text{C}_{80}(\text{CF}_3)_2$  each have two of the three Sc atoms bonded to the cage C atom that is *para* to each of the cage  $\text{C}(\text{CF}_3)$  atoms (see Figure 22), whereas conformers with different positions of the  $\text{Sc}_3\text{N}$  cluster have much higher relative energies (from 13 to 65 kJ·mol<sup>-1</sup>).<sup>169,170</sup> The exohedral R<sub>F</sub> groups and endohedral  $\text{Sc}_3\text{N}$  cluster thus determine their mutual positions, and this influence is found in all PFA- $\text{Sc}_3\text{N}@\text{C}_{80}$  derivatives.

A significant step forward in the analysis of  $\text{CF}_3$  addition patterns to  $\text{Sc}_3\text{N}@\text{C}_{80}$  was done in 2009, when the first single-crystal X-ray structures of  $\text{Sc}_3\text{N}@\text{(C}_{80}\text{-}I_h)\text{(CF}_3)_n$  derivatives (**Sc-14-1** and **Sc-16-1**) were reported.<sup>88</sup> This report was followed in 2011 by the structural elucidation of **Sc-14-3** and **Sc-16-2**,<sup>100</sup> and X-ray structures were also published for **Sc-10-1** and **Sc-12-1**,<sup>93</sup> and for three new isomers of  $\text{Sc}_3\text{N}@\text{C}_{80}(\text{CF}_3)_{14}$ .<sup>102</sup> In addition,  $^{19}\text{F}$  spectroscopic characterization combined with an extensive computational study was reported for **Sc-4**, two isomers of **Sc-8**, **Sc-10-1**, two isomers of **Sc-12**, and **Sc-14-2**.<sup>93</sup> In 2014, the structures of two more isomers of  $\text{Sc}_3\text{N}@\text{C}_{80}(\text{CF}_3)_{14}$ , **Sc-14-7** and **Sc-14-8**, were determined by single-crystal X-ray diffraction.<sup>112</sup> The authors of ref 112 pointed out that addition patterns of **Sc-14-2** (determined by  $^{19}\text{F}$  NMR and DFT calculations) and **Sc-14-4** (determined by X-ray) are very similar (see Figure 22) and that the structure of **Sc-14-2** should probably be reassigned. The definitive state-

ment would require the measurement of the  $^{19}\text{F}$  NMR spectrum of **Sc-14-4**, which was not reported. Whereas the majority of PFAFs belong to the  $I_h(7)$  cage isomer of  $\text{Sc}_3\text{N}@\text{C}_{80}$ , two structures with the  $\text{Sc}_3\text{N}@\text{C}_{80}\text{-}D_{5h}(6)$  cage with 16 and 18  $\text{CF}_3$  groups were also determined.<sup>100,112</sup> Schlegel diagrams of structurally characterized  $\text{Sc}_3\text{N}@\text{C}_{80}(\text{CF}_3)_n$  derivatives are shown in Figure 22. Analysis of their addition patterns shows that the presence of the  $\text{Sc}_3\text{N}$  cluster (which formally transfers six electrons to the carbon cage) has a dramatic effect on the distribution of  $\text{CF}_3$  groups on the fullerene surface. Similar to HHF( $\text{CF}_3$ ) derivatives, the  $\text{CF}_3$  groups in  $\text{Sc}_3\text{N}@\text{C}_{80}(\text{CF}_3)_n$  tend to form ribbons. However, some of the other rules governing perfluoroalkylation of HHFs are not valid for  $\text{Sc}_3\text{N}@\text{C}_{80}$ . The general principles of multiple addition of  $\text{CF}_3$  groups to  $\text{Sc}_3\text{N}@\text{C}_{80}$  compared with multiple additions to HHFs were formulated in ref 93 as follows:

(1) In  $\text{Sc}_3\text{N}@\text{C}_{80}(\text{CF}_3)_n$  derivatives with  $n \geq 8$ , the ribbon addition patterns commonly include  $\text{C}_5(\text{CF}_3)_2$  pentagons. This differs from the behavior of hollow fullerene PFAFs where formation of  $\text{C}_5(\text{CF}_3)_2$  pentagons is usually avoided (at least for the fullerene( $\text{CF}_3$ )<sub>n</sub> with  $n \leq 12$ ).

(2) The addition of  $\text{CF}_3$  groups to triple-hexagon junctions (THJs) is known to be energetically unfavorable for hollow fullerenes. As discussed in section 5.4, there are only a few hollow fullerene derivatives with THJ-bonded  $\text{CF}_3$  groups,  $\text{C}_{76}(\text{CF}_3)_{14-18}$  and  $\text{C}_{94}(\text{CF}_3)_{20}$  and all have a high degree of trifluoromethylation.<sup>84,90</sup> In contrast, stable  $\text{Sc}_3\text{N}@\text{C}_{80}(\text{CF}_3)_x$  structures with THJ-bonded  $\text{CF}_3$  groups are formed for  $n \geq 8$ . For instance, **Sc-8-1**, **Sc-8-2**, **Sc-10-1**, and **Sc-12-1** all have one  $\text{CF}_3$  group bonded to a THJ, **Sc-14** isomers have up to four THJ-bonded  $\text{CF}_3$  groups, and **Sc-16-1** has eight functionalized THJs.

(3) “Isolated”  $\text{CF}_3$  groups are very rare for HHF( $\text{CF}_3$ )<sub>n</sub> (the only structures described are minor isomers of  $\text{C}_{70}(\text{R}_F)_{8,10}$ : **70-8-12**, **70-10-5**, **70-10-11**, and **70-10-14**). In contrast, such isolated  $\text{CF}_3$  groups were found to be common for  $\text{Sc}_3\text{N}@\text{C}_{80}(\text{CF}_3)_x$  compounds, for example, for **Sc-8-2**, **Sc-10-1**, **Sc-12-1**, **Sc-14-5**. In all of these compounds, “isolated”  $\text{CF}_3$  groups are attached to THJ carbon atoms. Several other  $\text{Sc}_3\text{N}@\text{C}_{80}(\text{CF}_3)_x$  compounds with the isolated  $\text{CF}_3$  groups (according to  $^{19}\text{F}$  NMR spectroscopy) have also been obtained, but the details of their structures remain unknown.

Other common addition patterns include the formation of isolated or semi-isolated benzenoid hexagons (starting with  $n = 8$ ) and the formation of isolated (**Sc-16-1**) or semi-isolated pentagons (**Sc-12-2**, **Sc-14-1**, **Sc-14-6**) at high degrees of trifluoromethylation. Importantly,  $\text{CF}_3$  addition pattern determines and fixes the position of the  $\text{Sc}_3\text{N}$  cluster inside the fullerene cage because only a few metal-cage bonding sites are preserved.

## 6. OPTICAL EXCITATIONS OF PFAFs

### 6.1. UV–Vis–NIR Absorption Spectroscopy

UV–vis–NIR absorption spectroscopy is a relatively simple and very convenient spectroscopic method for the characterization of fullerenes and their derivatives. It is not therefore surprising that a vast majority of synthesized PFAFs, at least those with  $\text{C}_{60}$  and  $\text{C}_{70}$  cages, are characterized by absorption spectroscopy. Absorption spectra of fullerenes and their derivatives in the visible range are dominated by  $\pi-\pi^*$  excitations and can deliver valuable information on the electronic and sometimes molecular structure of PFAFs. First,

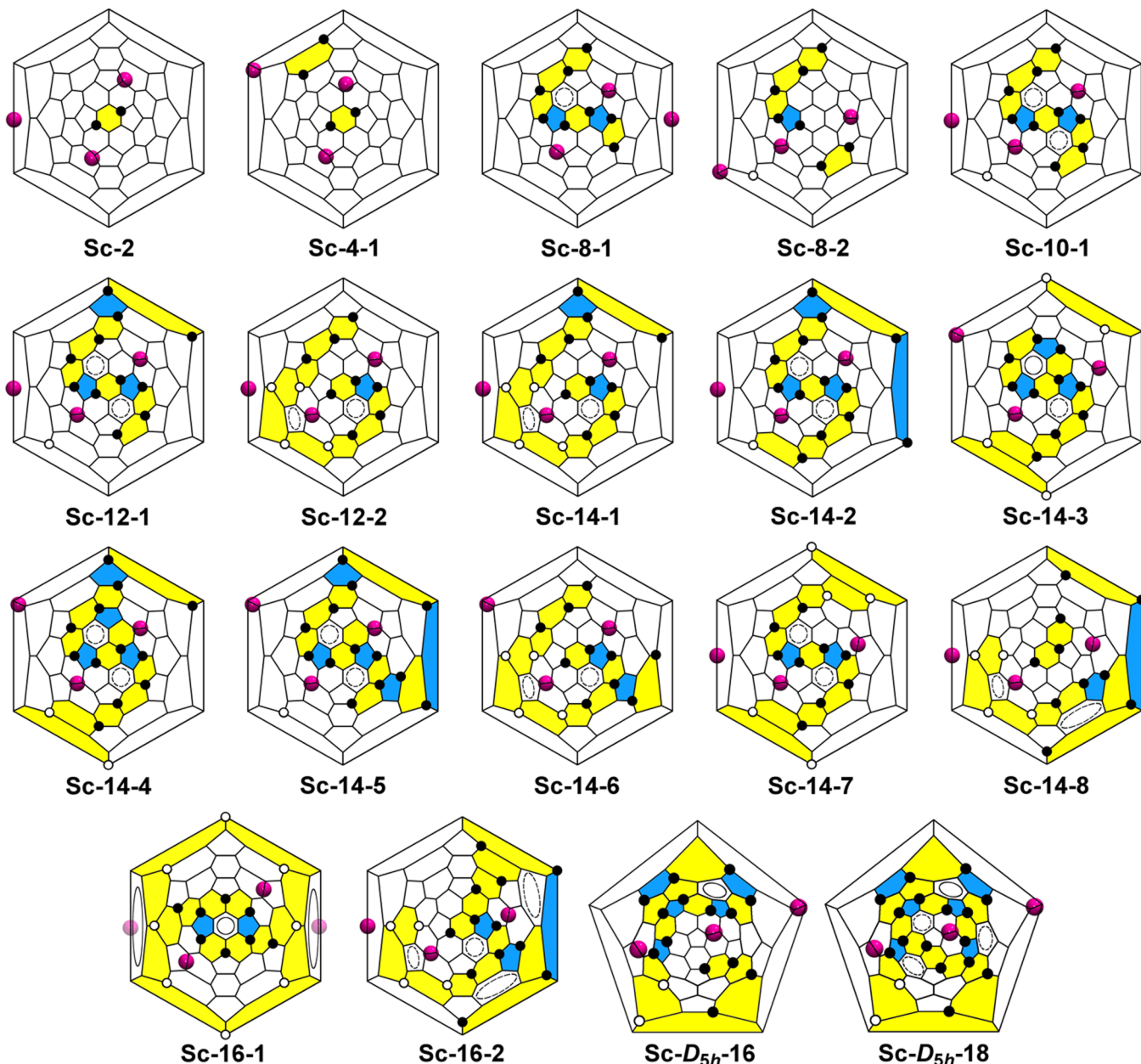


**Figure 22.** Schlegel diagrams of structurally characterized  $\text{Sc}_3\text{N}@C_{80}(\text{CF}_3)_n$  derivatives ( $n = 2\text{--}18$ ).  $\text{R}_f$  groups attached to THJ cage C atoms are shown as empty circles. Semi-isolated and fully isolated benzenoid hexagons (i.e., with five and six fullerene  $\text{C}(\text{sp}^3)$  atoms, respectively) are shown as dashed and solid ovals, respectively. Magenta circles mark the approximate positions of the Sc atoms with respect to the cage C atoms; in **Sc-16-1**, one Sc atom is disordered between two positions shown as half-transparent magenta circles. Unless otherwise noted, these are PFA derivatives of  $\text{Sc}_3\text{N}@C_{80}-I_h(7)$ ; two PFA derivatives of  $\text{Sc}_3\text{N}@C_{80}-D_{5h}(6)$  are designated with " $D_{5h}$ ".

the lowest energy transition detectable in the absorption spectrum usually corresponds to the  $\text{HOMO} \rightarrow \text{LUMO}$  excitation and therefore can be used to estimate the HOMO–LUMO gap (also referred to as “optical bandgap”). When absorption features are not well resolved and hence determination of the lowest peak position is not possible, the spectral onset can be used for a rough estimation. Analysis of the absorption spectra of PFAFs published in many reports on the synthesis of PFAFs shows that their lowest energy excitations usually span the range of 500–800 nm; that is, optical gaps of the majority of PFAFs are found in the range of 1.5–2.5 eV. Thus, PFAFs can be classified as medium-gap molecular semiconductors. The color of the PFAF solutions in organic solvents ranges from pale yellow to deep green.

Another important feature of UV–vis–NIR absorption spectra is their high structural sensitivity. Compounds with the same addition pattern usually exhibit an identical spectral pattern with insignificant variations of the band position and bandwidths irrespective of the substituents (if they are not chromophores themselves). Therefore, absorption spectra may be used for tentative structure elucidation by comparison with the spectra of compound with definitive molecular structure. As an example, Figure 23 shows that the UV–vis absorption spectra of  $C_s\text{-}C_{60}(\text{CF}_3)_4\text{O}$ ,  $C_s\text{-}C_{60}(\text{CF}_3)_6$  (**60-6-2**),  $\text{C}_{60}\text{Cl}_6$ , and  $\text{C}_{59}\text{N}(\text{CF}_3)_5$  exhibit pronounced similarity in the 300–600 nm range. All of these compounds have SPP or SPP-like addition patterns with isolated cyclopentadiene fragments and identical  $\pi$ -system for the non-functionalized part of the fullerene cage.

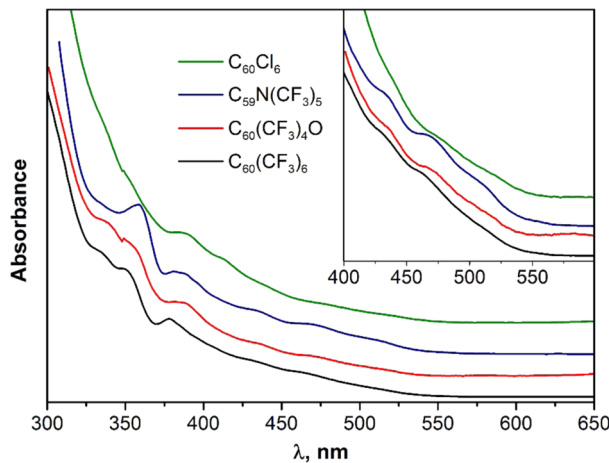


**Figure 23.** Absorption spectra of fullerene derivatives with skew-pentagonal-pyramid addition patterns:  $C_5-C_{60}(CF_3)_6$ ,<sup>39</sup>  $C_{60}(CF_3)_4O$ ,<sup>39</sup>  $C_{59}N(CF_3)_5$ ,<sup>158</sup> and  $C_{60}Cl_6$ .<sup>171</sup>

## 6.2. Fluorescence Spectroscopy

When it comes to a discussion of the luminescent properties of carbonaceous compounds, numerous aromatic fluorophores, carbon nanotubes, and carbon dots are much spoken about, whereas fullerenes usually remain in the shadows because of their very weak fluorescence. Fullerenes  $C_{60}$  and  $C_{70}$  have dipole-forbidden  $S_0 \leftrightarrow S_1$  transitions,<sup>172</sup> which lead to small values of radiative decay constants (e.g.,  $k_F = 2.7 \times 10^5 \text{ s}^{-1}$  for  $C_{60}$  and  $8.8 \times 10^5 \text{ s}^{-1}$  for  $C_{70}$ ), in agreement with the Strickler–Berg rule.<sup>173</sup> Furthermore, both fullerenes show high rates of intersystem crossing with almost quantitative formation of a triplet state. These two factors result in short fluorescence lifetimes (e.g.,  $\tau_F = 1.2 \text{ ns}$  for  $C_{60}$  and  $0.7 \text{ ns}$  for  $C_{70}$ ) and very low fluorescence quantum yields (e.g.,  $\Phi_F = \text{ca. } 0.0003$  for  $C_{60}$  and ca.  $0.0006$  for  $C_{70}$  in toluene).<sup>173,174</sup> Derivatization of the fullerenes reduces the symmetry and changes their  $\pi$ -system. Thus, absorptions of the derivatives are usually optically allowed, and hence higher values of  $k_F$  can be reached. However, the relatively small perturbation of the fullerene  $\pi$ -system at early stages of functionalization preserves the low  $S_0 \rightarrow S_1$  absorption intensities and efficient intersystem crossing and leads to relatively low  $\Phi_F$  values.<sup>175</sup>

The first measurements of the PFAF fluorescence were reported in 2007.<sup>5</sup> Fluorescence spectra were recorded for several isomers of  $C_{60}(CF_3)_{10}$  and helped in estimation of their

optical gaps. However, numerical parameters (such as quantum yields) were not measured at that time.

A photophysical study of pristine and malonate-functionalized **70-10-1** was reported in 2010.<sup>99</sup> The authors derivatized **70-10-1** via Bingel–Hirsch reaction and introduced a malonate group carrying two donor bis- $\pi$ -extended tetraphiafulvalene (exTTF) moieties. **70-10-1** and its bare malonate derivative exhibited fluorescence with quantum yields of  $\sim 0.02$ . In a **70-10-1**/exTTF donor–acceptor dyad, fullerene-based fluorescence was partially quenched, and fluorescence lifetime was decreased from 3–3.5 to only 0.1 ns. Femtosecond transient absorption studies of the dyad proved photoinduced intramolecular electron transfer. The lifetime of the radical-ion pair varied from 289 ps in toluene to 23 ps in benzonitrile.

A dedicated study of the fluorescence of two isomers of  $C_{70}(CF_3)_8$  (**70-8-1** and **70-8-2**) and three isomers of  $C_{70}(CF_3)_{10}$  (**70-10-1**, **70-10-2**, and **70-10-5**) was published in 2013.<sup>176</sup> The authors found that in contrast to the non-luminescent parent  $C_{70}$ ,  $C_{70}(CF_3)_n$  compounds can be strong fluorophores, whose quantum yields strongly depend on the addition pattern (Figure 24). The quantum yield of fluorescence ( $\Phi_F$ ) determined for **70-10-5** in toluene solution is as high as 0.68, which makes this compound the strongest fullerene fluorophore ever studied. For comparison,  $\Phi_F$  values of two other isomers are 0.05 (**70-10-1**) and 0.29 (**70-10-2**). Importantly, addition patterns of **70-10-1** and **70-10-2** are different from that of **70-10-5** only in location of one  $CF_3$  group (Figure 24), which however leads to 14-fold and 2-fold changes in their  $\Phi_F$  values, respectively. Thus, similar to reduction potentials, luminescent properties of PFAFs are to a large extent determined by addition pattern. Time-dependent DFT computations showed that among the five studied PFAFs, the highest quantum yields are found for molecules with (i) the largest oscillator strengths of  $S_0 \rightarrow S_1$  excitation and (ii) the largest energy gap between  $S_1$  and  $T_1$  states.

## 7. ELECTROCHEMICAL PROPERTIES OF PFAFs

Fullerenes are known to be good electron acceptors with high electron affinity values (viz., gas-phase EAs of  $C_{60}$ ,  $C_{70}$ , and  $C_{76}$  are 2.66, 2.68, and 2.88 eV, respectively).<sup>177</sup> In solution at room temperature fullerenes exhibit several reversible single-electron reduction steps;<sup>178</sup> under optimized conditions, up to six such steps can be measured for  $C_{60}$  and  $C_{70}$ .<sup>179</sup> Reduction results in the population of the low-energy unoccupied MOs with  $\pi^*$  character, and hence the redox potentials are to a large extent determined by the topology of the  $\pi$ -system and can vary for

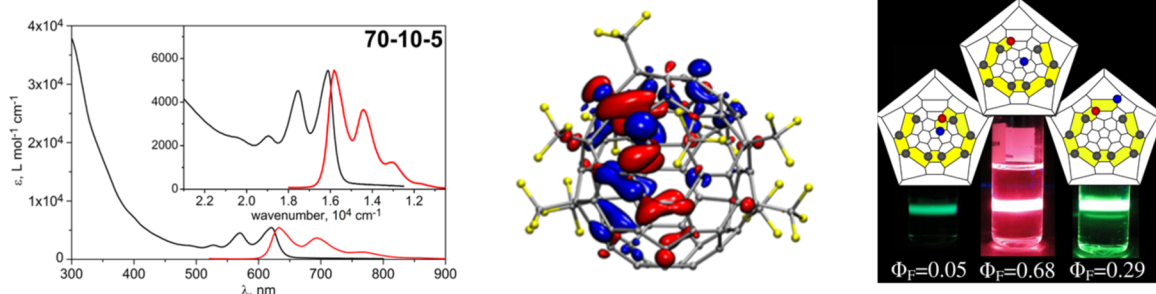


**Figure 24.** Left: Absorption (black) and luminescence (red) spectra of **70-10-5**. Middle: TD-DFT computed difference of the electronic density for the  $S_0 \rightarrow S_1$  excitation of **70-10-5**. Right: Schlegel diagrams and photos of fluorescing solutions of three isomer of  $C_{70}(CF_3)_{10}$  along with the determined fluorescence quantum yields (from left to right: **70-10-1**, **70-10-5**, and **70-10-2**). Red and blue dots in Schlegel diagrams denote  $CF_3$  groups whose positions are different in three isomers. Reproduced with permission from ref 176. Copyright 2013 American Chemical Society.

the cage isomers in the range of 0.36 V as found for six isomers of  $C_{84}^{180}$ .

Derivatization of fullerenes via addition reactions converts the  $sp^2$ -state of some carbon atoms into the  $sp^3$ -state and hence inevitably results in a partial saturation of their  $\pi$ -system. Saturation of the  $\pi$ -system tends to decrease the electron affinity and shift the reduction potentials to more negative values. Besides, the chemical nature of the addends can be also important in determining the direction of the reduction potential shift after derivatization: electron-donating groups obviously shift the first reduction potential into the negative direction (in comparison to the pristine fullerene), whereas a positive shift can be anticipated for electron-withdrawing groups. The interplay of these factors determines the resulting shift of the reduction potential after the fullerene derivatization. For instance, the first reduction potentials of  $C_{60}$  derivatives with two  $C-sp^3$  cage atoms (monocycloadducts and  $C_{60}R_2$  compounds) are usually near  $-0.10$  V vs  $C_{60}^{0/-}$ , but the values can reach  $-0.19$  V for hydrosilylated adduct of  $C_{60}$  (electron-donating substituent)<sup>181</sup> or  $+0.17$  V for strongly electron-withdrawing tetracyanotetrahydrofuran addend.<sup>182</sup>

Considering the effect of the strong electron-withdrawing groups, examples of cyano- and fluorofullerenes are especially illustrative. The first reduction potentials of  $C_{60}(CN)_2$  and  $C_{60}(CN)_4$  are found at  $+0.14$  and  $+0.28$  V vs  $C_{60}^{0/-}$ , respectively.<sup>183</sup> For fluorofullerenes  $C_{60}F_n$  ( $n = 2-48$ ), the positive shift of  $E_{1/2}(0/-)$  values increases gradually with increasing  $n$  and reaches  $+1.38$  V for  $C_{60}F_{48}$ .<sup>184</sup> However,  $C_{cage}-F$  bonds were found to be very unstable in the conditions of electron transfer, and fluorofullerenes tend to lose F atoms rapidly upon reduction. For groups with a medium electron-withdrawing strength, the interplay between the size of the  $\pi$ -system and the number of substituents can be more complex. For a series of  $C_{70}(Ph)_n$  derivatives ( $n = 2-10$ ), Avent et al. reported a positive shift of  $+0.10$  V vs  $C_{70}^{0/-}$  for  $C_{70}(Ph)_2$  and  $C_{70}(Ph)_4$ , but progressively negative shifts for a larger numbers of phenyl groups reaching  $-0.99$  V for  $C_{70}(Ph)_{10}$ .<sup>185</sup> The authors proposed that for  $n = 6-10$ , saturation of the  $\pi$ -system outweighed the weakly electron-withdrawing effect of the phenyl groups.

Addition of two or more single-bonded groups and two or more cycles to  $C_{60}$  can modify the  $\pi$ -system of the fullerene core in a different way depending on the addition pattern. However, before the results of electrochemical properties of PFAFs were published, this factor was not well studied, mainly because of the limited number of the well-characterized isomers of fullerene derivatives suitable for dedicated electrochemical studies. However, the scarce data available before 2007<sup>184b,186</sup> (e.g., isomers of bis-pyrrolidinofullerene adducts<sup>186e</sup> or 1,7- vs 1,9- $C_{60}R_2$  derivatives<sup>186b,d,f,g</sup>) showed that the first reduction potential of isomers with different addition patterns can vary by 0.16 V (this was considered by the authors to be a large difference). Although an explanation of these variations was not given at that time, these examples show that the two-factor paradigm “ $\pi$ -system/nature of the group” cannot provide the correct interpretation of the electrochemical properties of fullerene derivatives with multiple electron-withdrawing groups of medium strength and should be revised.

The unprecedented number of PFAFs provided a unique opportunity to discover the influence of the addition pattern, the number of added groups, and their electron-withdrawing nature on the redox properties of fullerene derivatives.

## 7.1. Reduction Potentials of Trifluoromethylfullerenes (TMFs)

**7.1.1.  $C_{60}(CF_3)_n$  Derivatives.** The first study of the electrochemical properties of  $C_{60}(CF_3)_n$  derivatives in 2005 was published (CVs of **60-2-1**, **60-10-1**, **60-10-2**, and **60-10-3** were reported), and revealed the characteristic redox features of these compounds,<sup>184c</sup> which were then confirmed and solidified in a number of following works. First, in contrast to fluorofullerenes,  $C_{60}(CF_3)_n$  derivatives exhibit several reversible reductions at room temperature in DCM or oDCB in anaerobic conditions, pointing to the high stability of the anion radicals of TMFs (ESR studies showed that some TMF anion radicals were stable for hours or days in fluid solution at room temperature<sup>115</sup>). Second, for a majority of TMFs, reduction potential is shifted positively vs  $C_{60}^{0/-}$ , which agrees with the electron-withdrawing nature of  $CF_3$  groups. Third, the first reduction potential of three isomers of  $C_{60}(CF_3)_{10}$  spanned the unprecedentedly large range of 0.27 V, indicating that the addition pattern plays a crucial role in determination of the redox potentials. These conclusions were then confirmed and developed in a dedicated study of electrochemical properties of 18  $C_{60}(CF_3)_n$  derivatives ( $n = 2-12$ ) published in 2007.<sup>5</sup> The work reported on the redox properties of **60-2-1**, **60-4-1**, two isomers of **60-6**, five isomers of **60-8**, six isomers of **60-10**, and three isomers of **60-12** and revealed that the range of the  $E_{1/2}(0/-)$  values for different isomers can be as high as 0.50 V (see Figure 25 for CV curves of **60-10** isomers and Table 6 for

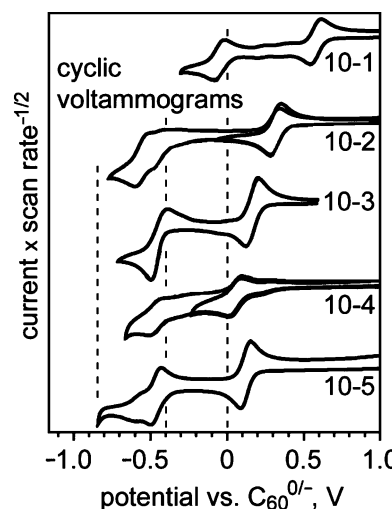


**Figure 25.** Cyclic voltammograms of five isomers of  $C_{60}(CF_3)_{10}$  (DCM solution, TBABF<sub>4</sub> electrolyte, room temperature). Reproduced with permission from ref 5. Copyright 2007 American Chemical Society.

a complete list of all experimentally measured reduction potentials of PFAFs). **60-10-1** exhibited the largest positive shift of the first reduction potential vs  $C_{60}^{0/-}$ ,  $+0.57$  V, but a few compounds (**60-6-2**, **60-12-1**, **60-12-3**) exhibited a negative shift of the first reduction potential (the most negative value was for **60-12-1**). The fact that the range of the  $E_{1/2}(0/-)$  values within a group of isomers is comparable to the range of  $E_{1/2}$  values spanned by the whole set of  $C_{60}(CF_3)_n$  derivatives irrespective of  $n$  (see Figure 26) clearly showed that there is no correlation between the number of  $CF_3$  groups and TMF reduction potentials. Therefore, the addition pattern plays a much more important role than the number of substituents. At

**Table 6. Reduction Potentials of PFAFs<sup>a</sup>**

compound	ref	gap <sup>b</sup>	E(LUMO) <sup>b</sup>	$E_{1/2}(0/-)$	$E_{1/2}(1-/2-)$	$E_{1/2}(2-/3-)$	solvent <sup>c</sup>
$C_{60}$	104	1.639	-4.379	0.00	-0.40	-0.85	DCM
	104			0.00	-0.39	-0.85	oDCB
	104			0.00	-0.41		PhCN
$C_{60}(CF_2)$	187			0.15	-0.19	-0.79	oDCB
$C_{60}(CF_2)_2$	187			0.14	-0.20	-0.80	oDCB
<b>60-2-1</b>	104	1.430	-4.592	0.15	-0.30	-0.80	DCM
	104			0.13	-0.28	-0.81	oDCB
	104			0.13	-0.32		PhCN
<b>60-2-1-C<sub>2</sub>F<sub>5</sub></b>	104	1.431	-4.599	0.17	-0.24	-0.78	DCM
	104			0.13	-0.30	-0.82	oDCB
	104			0.13	-0.31		PhCN
<b>60-2-1-n-C<sub>3</sub>F<sub>7</sub></b>	104	1.427	-4.598	0.13	-0.28	-0.82	DCM
	104			0.13	-0.29	-0.82	oDCB
	104			0.13	-0.30		PhCN
<b>60-2-1-i-C<sub>3</sub>F<sub>7</sub></b>	104	1.435	-4.589	0.14	-0.29	-0.82	DCM
	104			0.13	-0.31	-0.83	oDCB
	104			0.10	-0.36		PhCN
<b>60-2-1-n-C<sub>4</sub>F<sub>9</sub></b>	104	1.425	-4.607	0.11	-0.31	-0.84	DCM
	104			0.13	-0.30	-0.83	oDCB
	104			0.14	-0.30		PhCN
<b>60-2-1-s-C<sub>4</sub>F<sub>9</sub></b>	104	1.434	-4.595	0.14	-0.29	-0.83	DCM
	104			0.11	-0.32	-0.85	oDCB
	104			0.10	-0.36		PhCN
<b>60-2-1-n-C<sub>8</sub>F<sub>17</sub></b>	104	1.425	-4.609	0.15	-0.27	-0.81	DCM
	104			0.12	-0.30	-0.82	oDCB
	104			0.13	-0.34		PhCN
<b>60-4-1</b>	5	1.443	-4.682	0.17	-0.26	-1.01	DCM
<b>60-4-4-i-C<sub>3</sub>F<sub>7</sub></b>	94	1.242	-4.786	0.32	-0.32	-0.80	oDCB
<b>60-4-5-i-C<sub>3</sub>F<sub>7</sub></b>	94	1.444	-4.680	0.20	-0.26	-0.78	oDCB
<b>60-6-1</b>	5	1.445	-4.796	0.26	-0.28	-0.93	DCM
<b>60-6-2</b>	5	1.859	-4.378	-0.07	-0.53	-1.02	DCM
<b>C59N-5</b>	158	1.872	-4.374	-0.05	-0.54		DCM
<b>60-6-3-i-C<sub>3</sub>F<sub>7</sub></b>	94	1.369	-4.830	0.32	-0.32	-0.80	oDCB
<b>60-6-5-i-C<sub>3</sub>F<sub>7</sub></b>	94	1.461	-4.735	0.32	-0.32	-0.80	oDCB
<b>60-6-8-i-C<sub>3</sub>F<sub>7</sub></b>	94	1.187	-4.900	0.32	-0.32	-0.80	oDCB
<b>60-8-1</b>	5	1.498	-4.850	0.33	-0.19	-0.66	DCM
<b>60-8-2</b>	5	1.482	-4.912	0.32	-0.19	-0.79	DCM
<b>60-8-3</b>	5	1.333	-5.017	0.45	-0.03	-0.96	DCM
<b>60-8-4</b>	5	1.701	-4.585	0.06	-0.38	-1.06	DCM
<b>60-8-5</b>	5	1.420	-4.863	0.31			DCM
<b>60-10-1</b>	5	1.139	-5.129	0.57	-0.07		DCM
<b>60-10-2</b>	5	1.550	-4.894	0.32	-0.47		DCM
<b>60-10-3</b>	5	1.662	-4.754	0.17	-0.44		DCM
<b>60-10-4</b>	5	1.636	-4.529	0.07	-0.47		DCM
<b>60-10-5</b>	5	1.748	-4.638	0.12	-0.46		DCM
<b>60-10-6</b>	5	1.445	-4.922	0.33	-0.34		DCM
<b>60-10-8</b>	115	1.429	-4.904	0.28	-0.36	-0.98	oDCB
<b>60-12-1</b>	5	2.245	-4.278	-0.16			DCM
<b>60-12-2</b>	5	1.614	-4.919	0.32	-0.39		DCM
<b>60-12-3</b>	5	2.086	-4.331	-0.13	-0.59		DCM
<b>C<sub>70</sub></b>	68	1.703	-4.315	0.00	-0.40	-0.80	DCM
				0.00	-0.37	-0.78	oDCB
<b>open-C<sub>70</sub>(CF<sub>2</sub>)</b>	110			0.15	-0.18	-0.76	oDCB
<b>closed-C<sub>70</sub>(CF<sub>2</sub>)</b>	110			0.01	-0.28	-0.75	oDCB
<b>70-2-1</b>	68	1.372	-4.697	0.28	-0.14	-0.71	DCM
<b>70-2-1-C<sub>2</sub>F<sub>5</sub></b>	116	1.369	-4.706	0.27	-0.16	-0.73	DCM
<b>70-2-1-i-C<sub>3</sub>F<sub>7</sub></b>	94	1.367	-4.708	0.28	-0.15	-0.79	oDCB
<b>70-2-2</b>	68	1.232	-4.533	0.12	-0.26	-0.74	DCM
<b>70-2-2-i-C<sub>3</sub>F<sub>7</sub></b>	94	1.230	-4.528	0.10	-0.31	-0.83	oDCB
<b>70-4-1</b>	68	1.334	-4.648	0.21	-0.18	-0.77	DCM
<b>70-4-3-i-C<sub>3</sub>F<sub>7</sub></b>	94	1.367	-4.764	0.30	-0.15	-0.64	oDCB

Table 6. continued

compound	ref	gap <sup>b</sup>	E(LUMO) <sup>b</sup>	$E_{1/2}(0/-)$	$E_{1/2}(1-/2-)$	$E_{1/2}(2-/3-)$	solvent <sup>c</sup>
70-4-4-i-C <sub>3</sub> F <sub>7</sub>	94	1.252	-4.896	0.49	0.00	-0.77	oDCB
70-6-1	68	1.333	-4.731	0.30	-0.14	-0.57	DCM
70-6-2	68	1.304	-4.758	0.34	-0.13	-0.48	DCM
70-6-3	68	1.560	-4.639	0.17	-0.27		DCM
70-8-1	68	1.707	-4.555	0.04	-0.41	-1.04	DCM
70-8-2	68	1.263	-4.829	0.31	-0.21	-1.28	DCM
70-10-1	68	2.071	-4.351	-0.11 <sup>d</sup>	-0.66		DCM
70-10-2	68	1.823	-4.536	-0.01	-0.50		DCM
70-10-3	68	1.679	-4.588	0.04	-0.41		DCM
70-10-4	68	1.628	-4.599	0.08	-0.48	-0.86	DCM
70-10-5	68	1.370	-4.813	0.28	-0.21	-1.11	DCM
70-12-1	68	1.700	-4.664	0.09	-0.46	-0.91	DCM
70-12-2	68	1.671	-4.676	0.07	-0.47	-0.98	DCM
70-12-3	68	1.634	-4.777	0.26	-0.37	-0.90	DCM
70-12-4	68	1.687	-4.774	0.25	-0.41	-0.90	DCM
Sc <sub>3</sub> N@C <sub>80</sub>		1.463	-3.907	0.00	-0.36	-1.11	oDCB
Sc-2	188	1.149	-4.184	0.10	-0.39	-0.88	oDCB
Sc-4-1	93	1.103	-4.247	0.20	-0.29	-0.77	oDCB
Sc-10-1	93	1.079	-4.535	0.42	-0.06	-0.85	oDCB
Sc-12-1	93	1.238	-4.423	0.32	-0.12	-0.72	oDCB

<sup>a</sup>The values for PFAF derivatives are given vs the  $E_{1/2}(0/-)$  of the parent non-functionalized fullerene, selected  $E_{1/2}(0/-)$  values vs  $\text{Fe}(\text{Cp})_2^{+0}$  are:  $C_{60}$ , -0.98 V in DCM and -1.06 V in oDCB;  $C_{70}$ , -0.98 V in DCM, -1.06 V in oDCB;  $\text{Sc}_3\text{N}@C_{80}$ , -1.26 V in oDCB. <sup>b</sup>PBE/TZ2P computed value. <sup>c</sup>DCM = dichloromethane; oDCB = *o*-dichlorobenzene; PhCN = benzonitrile. <sup>d</sup>Irreversible.

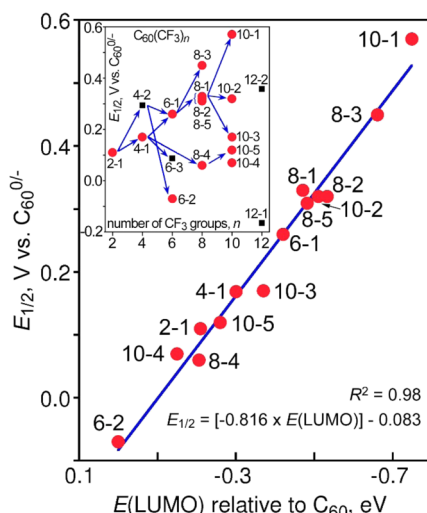


Figure 26. Correlation between the first reduction potentials of  $C_{60}(\text{CF}_3)_n$  derivatives and DFT-computed LUMO energy (all values are relative to  $C_{60}$ ). The inset is a plot of  $E_{1/2}(0/-)$  values vs the number of  $\text{CF}_3$  groups. Reproduced with permission from ref 5. Copyright 2007 American Chemical Society.

the same time, a DFT study revealed a very good linear correlation between the  $E_{1/2}(0/-)$  and the LUMO energy of the neutral TMF ( $R^2 = 0.98$ ; see Figure 26), which allowed the prediction of  $E_{1/2}(0/-)$  values with the precision of 0.02–0.03 V. As a result of these observations, the addition pattern, the topology of the  $\pi$ -system, and their influence on the spatial localization of the LUMO were analyzed to explain the structure–property relationships. Note that first reduction potentials correspond to gas-phase electron affinities corrected for the solvation of the neutral molecule and the anion radical, but in many cases a much more simple quantity, the neutral-molecule LUMO energy, produced a good correlation with  $E_{1/2}(0/-)$  values and was used for the analysis. See section

7.3.1 for a discussion of electron affinities, solvation energies, and reduction potentials.

As discussed in section 5, the *para* additions typical for  $\text{CF}_3$  groups inevitably result in the formation of DBIPs, which can be classified into two groups: *terminal* (*t*-DBIPs) with three adjacent fullerene  $\text{C}(\text{sp}^3)$  atoms (shown in blue in Figure 27; these are usually the shortest bonds in the molecule) and *non-terminal nt*-DBIPs with two adjacent fullerene  $\text{C}(\text{sp}^3)$  atoms (shown in red in Figure 27).

Careful analysis of the spatial localization of LUMO in a large series of  $C_{60}(\text{CF}_3)_n$  derivatives showed that LUMO is always anchored to *nt*-DBIPs, and hence the number and relative position of *nt*-DBIPs determine the energy of the LUMO and

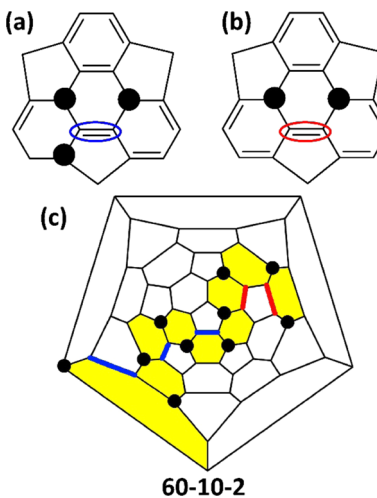
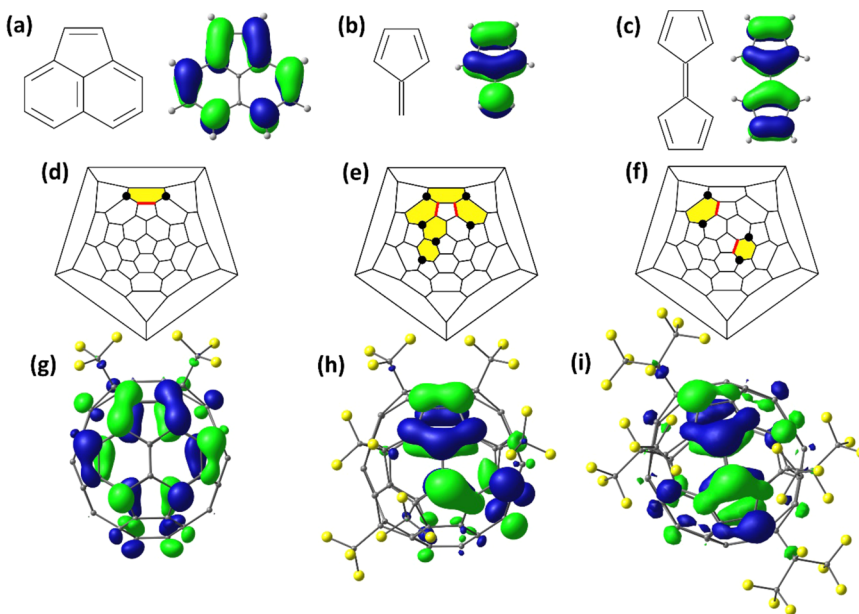


Figure 27. Double bonds in pentagons (DBIPs) formed as the result of *para*  $\text{CF}_3$  additions: (a) a terminal DBIP (*t*-DBIP, highlighted with a blue oval); (b) a non-terminal DBIP (*nt*-DBIP, highlighted with a red oval); (c) the Schlegel diagram for 60-10-2 with *t*-DBIPs and *nt*-DBIPs highlighted as blue and red lines, respectively.



**Figure 28.** Polyaromatic hydrocarbon-like fragments and their LUMOs: (a) acenaphthalene, (b) fulvene, (c) pentafulvalene. Examples of PFAFs with different types of LUMOs and their LUMO isosurfaces: (d,g) **60-2-1** with an acenaphthalene-like LUMO; (e,h) **60-6-1** with a fulvene-like LUMO; and (f,i) **60-4-4-i-C<sub>3</sub>F<sub>7</sub>** with a pentafulvalene-like LUMO motif.

consequently the first reduction potential of the PFAF molecule. When only one *nt*-DBIP is present, the delocalized LUMO pattern resembles that of acenaphthalene (Figure 28), and  $E_{1/2}(0/-)$  potential is shifted positively vs C<sub>60</sub><sup>0/-</sup> by 0.06–0.17 V. Besides **60-2-1**, this situation was found in all PFAFs with *p(mp)<sup>x</sup>* ribbons, including **60-4-1** (*pmp*), **60-8-4** (*pmpmpm*), and **60-10-5** (*pmpmpmpm*).

A large number of PFAFs have addition patterns with *p*<sup>3</sup> fragments. In the *p*<sup>3</sup> moiety, two *nt*-DBIPs are located in one pentagon; that is, they form a cyclopentadiene fragment communicating with the rest of the fullerene  $\pi$ -system through the fifth C-sp<sup>2</sup> atom of the pentagon. When this fragment is present, LUMO of PFAF is largely localized in the vicinity of the cyclopentadiene fragment and resembles the LUMO of fulvene, as shown in Figure 28. The first reduction potentials of C<sub>60</sub>(CF<sub>3</sub>)<sub>*n*</sub> derivatives with such LUMO (e.g., *p*<sup>3</sup>*mp* **60-6-1**, *p*<sup>3</sup>*mpmp* **60-8-1** and **60-8-3**, *p*<sup>3</sup>*mpmpmp* **60-10-2**, *p*<sup>3</sup>*mpmpmpmp* **60-12-2**) are shifted positively vs C<sub>60</sub><sup>0/-</sup> by 0.26–0.33 V. Note that communication of the *p*<sup>3</sup> moiety to the fullerene  $\pi$ -system is crucial for the large positive shift of the reduction potential: in **60-10-3**, the fulvene fragment is isolated from the rest of the  $\pi$ -system, and the  $E_{1/2}(0/-)$  potential of **60-10-3** is only 0.17 V vs C<sub>60</sub><sup>0/-</sup>. Moreover, when a cyclopentadiene fragment is isolated from the fullerene  $\pi$ -system (and hence *p*<sup>3</sup> moiety is formed by *terminal* DBIPs as in **60-6-2**, **60-10-4**, **60-12-3**), LUMO is localized on other parts of the molecule.

An interesting situation appears when the addition pattern includes both a *p*<sup>3</sup> moiety and single *nt*-DBIP (e.g., a *p*<sup>3</sup> ribbon with an isolated *p* or *pmp* fragment such as found in *p*<sup>3</sup>*mp,p* **60-8-2** and **60-8-5**, *p*<sup>3</sup>*mpmp,p* **60-10-1**, *p*<sup>3</sup>*mp,pmp* **60-10-6**, etc.). In this case, the shape of the LUMO and the reduction potential depend on the relative position of these fragments. When they are far from each other, the LUMO has a fulvene-like motif and the reduction potential is similar to those of compounds with a *p*<sup>3</sup> moiety described in the previous paragraph (the LUMO+1 orbital in this case has an acenaphthalene-like shape and is

anchored to the single *nt*-DBIP). However, when the *p*<sup>3</sup> moiety and the single *nt*-DBIP are close to one another, the LUMO is strongly stabilized by delocalization between these fragments resulting in an enhancement of the positive  $E_{1/2}(0/-)$  shift. This situation is found in **60-8-3** (+0.45 V vs C<sub>60</sub><sup>0/-</sup>) and **60-10-1** (+0.57 V vs C<sub>60</sub><sup>0/-</sup>), the latter exhibiting the most positive reduction potential among all PFAFs, comparable to the values reported for C<sub>60</sub>F<sub>36</sub> isomers.<sup>184b</sup> DFT calculations predicted that a hypothetical isomer of C<sub>60</sub>(CF<sub>3</sub>)<sub>8</sub>, with two *p*<sup>3</sup> moieties in conjugation, could have a reduction potential of 0.73 V, but this compound has not yet been isolated.

In summary, reduction potentials of C<sub>60</sub>-based PFAFs can be very well understood taking into account their addition patterns, and in particular the number and relative position of *nt*-DBIPs. The only PFAFs not considered so far are those that have no *nt*-DBIPs. Analysis of the redox potentials of three such C<sub>60</sub>(CF<sub>3</sub>)<sub>*n*</sub> compounds, **60-6-2**, **60-12-1**, and **60-12-3**, shows that in this case  $E_{1/2}(0/-)$  values are shifted negatively vs C<sub>60</sub><sup>0/-</sup>.

**7.1.2. C<sub>70</sub>(CF<sub>3</sub>)<sub>*n*</sub> Derivatives.** The redox properties of C<sub>70</sub>(CF<sub>3</sub>)<sub>*n*</sub> derivatives are similar to those of C<sub>60</sub>(CF<sub>3</sub>)<sub>*n*</sub> in that they also show several reversible reductions and a positive shift of  $E_{1/2}(0/-)$  potentials vs C<sub>70</sub><sup>0/-</sup>.<sup>68,116</sup> The only compound that does not follow these guidelines is **70-10-1**, whose first reduction of which is irreversible and cathodically shifted by 0.11 V vs C<sub>70</sub><sup>0/-</sup>. Similar to C<sub>60</sub>(CF<sub>3</sub>)<sub>*n*</sub> derivatives, the range of  $E_{1/2}$  values for isomers of C<sub>70</sub>(CF<sub>3</sub>)<sub>*n*</sub> can be as high as 0.35 V for the first reduction and 0.45 V for the second reduction (the highest ranges are found for **70-10** isomers).

The interpretation of C<sub>70</sub>(CF<sub>3</sub>)<sub>*n*</sub>  $E_{1/2}$  values in terms of their addition patterns and LUMO localization is not as straightforward as it is for C<sub>60</sub>(CF<sub>3</sub>)<sub>*n*</sub>  $E_{1/2}$  values because C<sub>70</sub>(CF<sub>3</sub>)<sub>*n*</sub> addition patterns are much more diverse. In particular, for C<sub>70</sub> 1,4-additions do not necessarily form DBIPs. Yet, when *nt*-DBIPs are formed in C<sub>70</sub>(CF<sub>3</sub>)<sub>*n*</sub> derivatives, their crucial role in determining reduction potentials becomes apparent. An illustrative example is the pair of C<sub>70</sub>(CF<sub>3</sub>)<sub>8</sub> isomers **70-8-1**

and **70-8-2**. The former has one *nt*-DBIP, and its LUMO resembles that of the acenaphthalene-like fragments in  $C_{60}(CF_3)_n$  derivatives with one *nt*-DBIP (Figure 29).

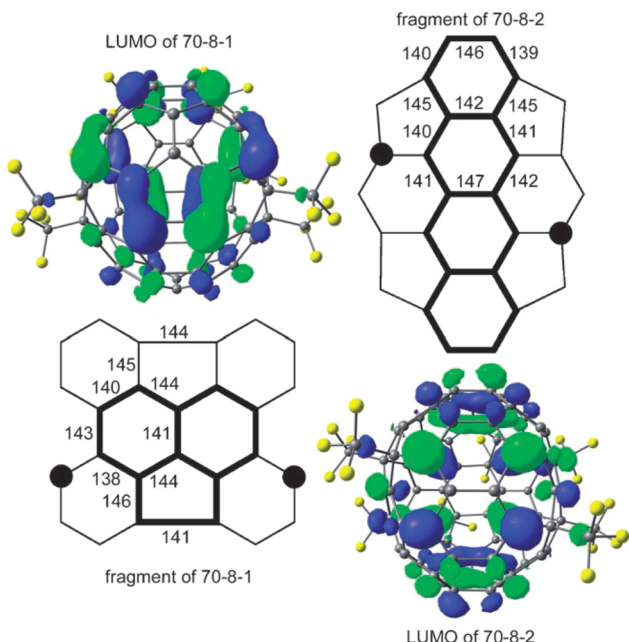


**Figure 29.** Fragments of the DFT-predicted structures and the DFT-predicted LUMOs for **70-8-1** and **70-8-2**. The numbers in the structure fragments are cage C–C distances in pm (the black circles indicate the cage C atoms to which the  $CF_3$  groups are attached). Reproduced with permission from ref 68. Copyright 2008 Wiley-VCH Verlag GmbH & Co. KGaA, Weinheim.

contrast, **70-8-2** has several DBIPs near the  $C_{70}$  equator, and its LUMO is more delocalized and resembles the LUMO of the linear acene tetracene. As a result, the LUMO of **70-8-2** is 0.27 eV lower in energy, and its  $E_{1/2}(0/-)$  value is 0.27 V more positive than for **70-8-1**. Similar to  $C_{60}(CF_3)_n$  derivatives, the most negative first reduction potentials for the entire  $C_{70}(CF_3)_n$  family are found for two compounds with no *nt*-DBIPs, **70-10-1** ( $E_{1/2}(0/-)$  = ca. -0.11 V) and **70-10-2** ( $E_{1/2}(0/-)$  = -0.01 V).

**7.1.3.  $Sc_3N@C_{80}(CF_3)_n$ .** Electrochemical studies are reported so far for four  $Sc_3N@C_{80}(CF_3)_n$  derivatives (**Sc-80-x**) with  $n$  ranging from 2 to 14.<sup>64,93,188</sup> All derivatives exhibited one to three reversible reductions. The first oxidation steps of

$Sc_3N@C_{80}(CF_3)_n$  were also accessible in oDCB solution at room temperature (unlike oxidations of empty fullerene PFAFs, which have not been achieved so far), and the second reversible oxidation step was also observed for **Sc-80-2**. Trifluoromethylation of  $Sc_3N@C_{80}$  induced a positive shifts of first reduction potentials, from +0.10 V in **Sc-8-2** to +0.42 in **Sc-10-1** (note that the  $E_{1/2}(0/-)$  value of **Sc-12-1**, +0.31 V, is less positive than for **Sc-10-1**). At the same time, the first oxidation potentials of **Sc-2-1** and **Sc-4-1** are shifted negatively with respect to the  $E_{1/2}(+/0)$  value of  $Sc_3N@C_{80}$  by -0.16 and -0.04 V, respectively, whereas the first oxidation potentials of **Sc-10-1** and **Sc-12-2** are more positive than for  $Sc_3N@C_{80}$  by 0.27 and 0.36 V, respectively.

## 7.2. ESR and Vis–NIR Spectroscopic Studies of PFAF Anions

**7.2.1. Electron Spin Resonance.** The first electrochemical study in 2005<sup>184c</sup> showed that anions of PFAFs can be sufficiently stable to allow their spectroscopic studies by electron spin resonance (ESR) spectroscopy and absorption spectroscopy in the visible and near-infrared (vis–NIR) range. In the ESR spectra, anion radicals of non-derivatized fullerenes exhibit single-line signals whose line width may be rather large due to the Jahn–Teller effect when degenerate LUMO is partially filled (e.g., ESR line width of  $C_{60}^-$  at room temperature is ca. 40 G<sup>189</sup>). The  $^{13}C$  hyperfine structure in the ESR spectra of the charged radicals of fullerenes is usually not sufficiently informative for a detailed analysis of the spin density distribution because of the low natural abundance of  $^{13}C$  isotope. The situation can be changed when fullerene is exohedrally functionalized with substituents carrying magnetic nuclei such as  $^{19}F$ .<sup>68,110,115,116,184c,187</sup>

The first ESR spectrum of the anion radical of PFAF with well-resolved  $^{19}F$ -hyperfine structure was reported in 2005 in the *in situ* ESR spectroelectrochemical study of **60-10-3**.<sup>184c</sup> Although spin density in PFAF anions is mainly localized on the carbon cage, the apparent  $^{19}F$  hyperfine constant  $a(^{19}F)$  in **60-10-3<sup>-</sup>** was ca. 0.5 G. Eventually ESR spectra were reported for 14 anion radicals of empty PFAFs prepared either electrochemically or chemically by a reaction with cobaltocene. Some of them showed complex hyperfine structure attributed to  $CF_3$  groups (see Figure 30a for the ESR spectrum of the anion radical **60-10-3<sup>-</sup>**). The rich hyperfine structure contains information on the spin density distribution in the radical anions, which can be related to the spatial distribution of LUMO in the neutral compounds. However, interpretation of

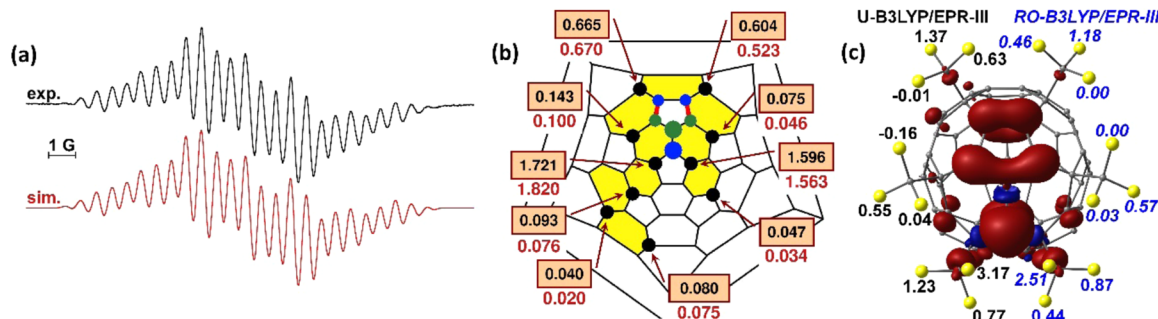


**Figure 30.** (a) Experimental and simulated ESR spectra of **60-10-3<sup>-</sup>**; (b) Schlegel diagram of **60-10-3** with DFT-computed (black) and experimental (red)  $a(^{19}F)$  values for each  $CF_3$  group. Blue and green circles show major LUMO lobes. (c) Spin density in **60-10-3<sup>-</sup>** and  $a(^{19}F)$  values of individual fluorine atoms computed at the U-B3LYP (black) and RO-B3LYP levels. Reproduced with permission from ref 115. Copyright 2010 American Chemical Society.

such rich ESR spectra is not straightforward. Although fast rotation of  $\text{CF}_3$  groups at the ESR time scale averages the value in each group and hence simplifies the situation, unravelling the hyperfine structure of non-symmetric anion radicals with 10  $\text{CF}_3$  groups (such as shown in Figure 30b) still requires finding 10 independent  $a(^{19}\text{F})$  values. Obtaining these parameters as a result of the fitting (i.e., solving inverse problem) can quickly become meaningless for such number of parameters. To solve this problem, in ref 115 the authors first computed  $a(^{19}\text{F})$  values at the B3LYP level of theory with specially tailored basis sets and then used computed values as an initial approximation in the fitting procedure. This approach allowed obtaining physically meaningful sets of  $a(^{19}\text{F})$  values for anion radicals with well-resolved hyperfine structure (Figure 30b). Computational study also allowed analysis of the nature of hyperfine couplings in these compounds. Comparison of unrestricted formalism (U-B3LYP; different spins have different orbitals) and restricted-orbital formalism (RO-B3LYP; spin-up and spin-down orbitals are identical except for a SOMO) showed that the polarization contribution is significant and can reach up to 30–40% of the values for individual fluorine atoms (Figure 30c).

Well-resolved ESR spectra were reported in ref 116 for the anion radicals of  $\text{C}_{70}(\text{CF}_3)_2$  and  $\text{C}_{70}(\text{C}_2\text{F}_5)_2$ . The ESR spectrum of the former exhibited a quartet with an  $a(^{19}\text{F})$  value of 0.32 G and a 1:3:3:1 intensity ratio, which indicated that only one  $\text{CF}_3$  group is significantly coupled to the unpaired electron. The radical  $\text{C}_{70}(\text{CF}_3)_2^-$  is also a rare example of a PFAF anion radical that exhibits a plethora of well-resolved  $^{13}\text{C}$  satellites lines in its ESR spectrum (Figure 31). DFT-calculated  $^{13}\text{C}$  coupling constants allowed interpretation of the data and showed that the largest  $a(^{13}\text{C})$  values are found for carbon atoms in the  $\text{CF}_3$  groups (6.40 and 4.46 G), followed by several carbon atoms near the  $\text{C}_{70}$  equator (Figure 31).

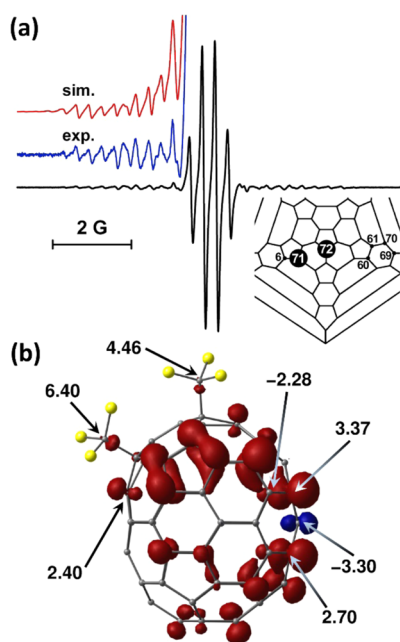


**Figure 31.** (a) ESR spectrum of  $\text{C}_{70}(\text{CF}_3)_2^-$  with enhanced  $^{13}\text{C}$  satellite structure (red and blue lines), the inset shows a fragment of the Schlegel diagram with the numbers of C atoms with the largest  $a(^{13}\text{C})$  values; (b) spin density in  $\text{C}_{70}(\text{CF}_3)_2^-$  and  $a(^{13}\text{C})$  values of selected carbon atoms. Based on results reported in ref 116.

ESR studies were also reported for anion radicals of  $\text{Sc}_3\text{N}@\text{C}_{80}(\text{CF}_3)_n$  ( $n = 2, 10, 12$ ) and for the trianion radical of  $\text{Sc}_3\text{N}@\text{C}_{80}(\text{CF}_3)_2$ .<sup>93,188</sup> ESR spectra of these species had rich hyperfine structure due to  $^{45}\text{Sc}$  nuclei ( $I = 7/2$ ) of the endohedral cluster, and weaker  $^{19}\text{F}$ -based splitting could not be seen. Comparison of the  $a(^{45}\text{Sc})$  values to that of the  $\text{Sc}_3\text{N}@\text{C}_{80}^-$  anion radical showed that with the increase of the number of  $\text{CF}_3$  groups the spin density in the anion radicals of  $\text{Sc}_3\text{N}@\text{C}_{80}(\text{CF}_3)_n$  shifted systematically from the endohedral cluster to the carbon cage.

**7.2.2. Vis-NIR Absorption Spectroscopy.** The anionic states of fullerenes exhibit characteristic absorptions in the near-IR range originating from  $\text{LUMO} \rightarrow \text{LUMO+1}$  excitations (here LUMO is the lowest-unoccupied molecular orbital of the pristine fullerene, which is populated upon reduction).<sup>190</sup> Such excitations are absent in the pristine fullerene, which makes absorption spectroscopy an especially convenient tool for spectroelectrochemical studies. Since derivatization changes the  $\pi$ -system of a fullerene via saturation of some  $\text{C}(\text{sp}^2)$  atoms, hence the NIR absorption features of the anion can also be substantially affected. Vis-NIR absorption spectra in the anionic states were reported for a series of  $\text{C}_{60}(\text{CF}_3)_n$  derivatives ( $n = 2-12$ )<sup>115,191</sup> and for  $\text{C}_{70}(\text{CF}_3)_2$ .<sup>116</sup>

All known PFAF anion radicals exhibited new absorption features in the NIR range, but the spectral patterns were different than those of anionic  $\text{C}_{60}$  and  $\text{C}_{60}$  cycloadducts. While the latter are known to exhibit one NIR band at 1080/950 nm ( $\text{C}_{60}^-/\text{C}_{60}^{2-}$ )<sup>190</sup> or at ca. 1010 nm (monoanions of cycloadducts),<sup>175b</sup> two NIR bands are observed in the spectra **60-2-1** and **60-4-1** in the reduced states.<sup>115</sup> The monoanion of **60-2-1** has two major NIR bands at 942/1550 nm, which are shifted to 880/1336 nm in the dianion. Likewise, **60-4-1** absorbs light at 790/1530 nm in the monoanionic state and at 737/1255 nm in the dianionic state. Time-dependent DFT calculations showed that the intense NIR band of  $\text{C}_{60}^-/\text{C}_{60}^{2-}$  corresponds to the 2-fold degenerate transition from the single-occupied MO to the LUMO+1-derived orbital. Lowering of the symmetry by addition of several groups, while retaining to a large extent an electronic structure of the fullerene, results in the splitting of the NIR band of  $\text{C}_{60}^-/\text{C}_{60}^{2-}$ . This was indeed found for the anions of the  $\text{C}_{60}(\text{CF}_3)_2$ <sup>4</sup> derivatives. Derivatives with a larger number of  $\text{CF}_3$  groups (6–10) exhibited one intense NIR band with position depending on the number groups and isomeric structure.<sup>115</sup> The anion and dianion of **60-6-1** have NIR absorptions at 1850 and 1355 nm, respectively, whereas absorptions of  $\text{C}_{60}(\text{CF}_3)_8^-$  and  $\text{C}_{60}(\text{CF}_3)_{10}^-$  isomers are usually limited to 1000 nm. Absorption spectra of  $\text{S}_6\text{-C}_{60}(\text{CF}_3)_{12}^-$  and  $\text{S}_6\text{-C}_{60}(\text{CF}_3)_{12}^{2-}$  reported recently by Konarev et al. exhibited broad absorption features at 750 and 648 nm, respectively.<sup>191</sup>

### 7.3. Reduction Potentials of $\text{R}_\text{F}$ Derivatives

#### 7.3.1. Substituent Effect in 1,7- $\text{C}_{60}(\text{R}_\text{F})_2$ Compounds.

Variation of the perfluoroalkyl groups in PFAFs can influence redox properties in at least two ways. First, as discussed in section 5, the size of the  $\text{R}_\text{F}$  groups affects addition patterns and hence electrochemical properties. Second, electron-withdrawing strength of perfluoroalkyl groups can depend on the chain lengths. Obviously, the role of the second factor can be revealed by analyzing redox potentials of the isostructural compounds. However, until recently, the synthesis of PFAFs with large perfluoroalkyl groups was not well developed because of the complex processes/partial decomposition in high temperature conditions. So far, comparison of redox potentials of isostructural PFAFs with different  $\text{R}_\text{F}$  groups can be done

only for bis-adducts. The first comparison between  $\text{CF}_3$  and  $\text{C}_2\text{F}_5$  study was reported in 2008 and showed that reduction potentials of isostructural **70-2-1** and **70-2-1-C<sub>2</sub>F<sub>5</sub>** are virtually identical.<sup>116</sup> The study of  $1,7\text{-C}_{60}(\text{i-C}_3\text{F}_7)_2$  also did not show a noticeable deviation of its reduction potential in comparison to  $\text{C}_{60}(\text{CF}_3)_2$ .<sup>94</sup>

The development of the new method of PFAF synthesis based on reaction of  $\text{R}_\text{F}\text{I}$  with fullerene in the presence of a copper-powder promoter in degassed refluxing oDCB in a sealed tube at 190 °C afforded isolation of the series of  $1,7\text{-C}_{60}(\text{R}_\text{F})_2$  compounds with long-chain  $\text{R}_\text{F}$  groups (up to  $n\text{-C}_8\text{F}_{17}$ ), and hence a systematic study of their redox properties became possible (Figure 32).<sup>104</sup> The electrochemical study was

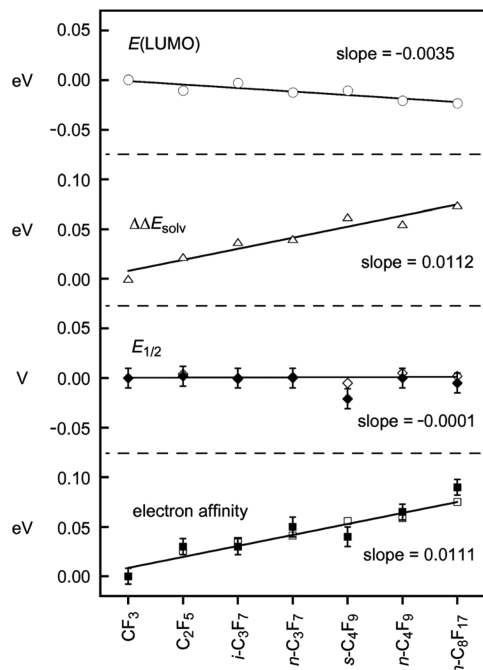


**Figure 32.** LUMO energies, solvation energies ( $\Delta\Delta E_{\text{solv}}$ ), reduction potentials ( $E_{1/2}$ ), and electron affinities of  $1,7\text{-C}_{60}(\text{R}_\text{F})_2$  compounds; all values are relative to  $\text{C}_{60}(\text{CF}_3)_2$ . The solid data points are experimental values (uncertainties are shown as error bars); the hollow data points are DFT-predicted values. The lines are linear least-squares fits to DFT-predicted results. Note that each plot has a y-axis interval of 0.10 eV or V, either from 0.00 to 0.10 or from 0.05 to 0.05. The slopes were derived by assigning each  $\text{R}_\text{F}$  group an x-axis value of successive integers as follows:  $\text{CF}_3 = 1$ ,  $\text{C}_2\text{F}_5 = 2$ , etc. Reproduced with permission from ref 104. Copyright 2012 The Royal Society of Chemistry.

also augmented by the measurements of their gas-phase electron affinities (EA), thus allowing one to address a question of the role of solvent in the redox potentials of PFAFs.

High precision of the EA measurements (the experimental uncertainty was less than 0.01 eV) showed that EAs of  $\text{C}_{60}(\text{R}_\text{F})_2$  derivatives monotonically increase with the perfluoroalkyl chain length from 2.920(8) eV for  $\text{R}_\text{F} = \text{CF}_3$  to 3.010(8) eV for  $\text{R}_\text{F} = n\text{-C}_8\text{F}_{17}$ . It was also found that EAs of  $\text{C}_{60}(\text{R}_\text{F})_2$  derivatives with  $n$ -perfluoroalkyl groups are higher than those with branched groups ( $\text{i-C}_3\text{F}_7$  and  $s\text{-C}_4\text{F}_9$ ). DFT calculations of EA values reproduced these trends. Surprisingly, reduction potentials measured by cyclic voltammetry did not correlate with the results of EA measurements and showed that all  $\text{C}_{60}(\text{R}_\text{F})_2$  derivatives exhibited almost identical  $E_{1/2}(0/-)$  values (within

0.03 V). The lack of correlation was explained by the role of solvation energy. DFT computations of solvation energies in the framework of polarizable continuum model showed that solvation energy of PFAF anions is decreasing with the increase of the  $\text{R}_\text{F}$  chain length. The decrease of solvation energy compensates for an increase of the EA along the series, and hence reduction potentials remain virtually constant.

**7.3.2. The Role of Addition Pattern for Bulky  $\text{R}_\text{F}$  Groups:  $i\text{-C}_3\text{F}_7$  Derivatives.** As discussed in detail in section 5,  $\text{CF}_3$  groups tend to add to fullerenes forming ribbons of edge-sharing *meta*- and/or *para*- $\text{C}_6(\text{CF}_3)_2$  hexagons. A consequence relevant to the electron-accepting properties of PFAFs is the reduced number of *nt*-DBIPs formed in such ribbon-like addition patterns. Although each pair of  $\text{R}_\text{F}$  groups added to  $\text{C}_{60}$  produces one DBIP, in ribbon addition patterns some of these DBIPs become *t*-DBIPs and do not influence the localization of LUMO. As a result,  $\text{C}_{60}(\text{CF}_3)_n$  derivatives usually have only one or two *nt*-DBIPs. At the same time, rare examples of compounds with three *nt*-DBIPs show that for some addition patterns strong stabilization of the LUMO and enhancement of electron-accepting property of the compounds can take place (the examples are **60-8-3** and **60-10-1**). Therefore, it would be desirable, whenever possible to produce the strongest PFAF acceptors by favoring addition patterns having as many *nt*-DBIPs as possible. A conceivable route to such addition patterns is the use of sufficiently bulky  $\text{R}_\text{F}$  groups to prevent formation of  $\text{C}_6(\text{R}_\text{F})_2$  ribbons. On the other hand, the size of the group should not prevent 1,4-addition to fullerene hexagons. Perfluoroisopropyl group,  $\text{i-C}_3\text{F}_7$ , ideally suits these demands: its size still allows formation of *p*- $\text{C}_6(\text{i-C}_3\text{F}_7)_2$  hexagons, but such hexagons cannot form edge-sharing ribbons because of the steric hindrance.<sup>80,94,98,104</sup> In other words, each pair of  $\text{i-C}_3\text{F}_7$  groups added to  $\text{C}_{60}$  necessarily forms one *nt*-DBIP, and hence PFAFs with a larger number of *nt*-DBIP than in  $\text{CF}_3$  derivatives can be obtained.

Electrochemical studies were performed for perfluoroisopropyl derivatives of  $\text{C}_{60}$  and  $\text{C}_{70}$  with 2–6 and 2–4 added groups, respectively.<sup>94</sup> In comparison to trifluoromethyl derivatives with the same number of perfluoroalkyl groups, the isomers of  $\text{C}_{60}(\text{i-C}_3\text{F}_7)_n$  and  $\text{C}_{70}(\text{i-C}_3\text{F}_7)_n$  exhibited a broader range of reduction potentials. For instance, the most positive reduction potentials among the isomers of  $\text{C}_{60}(\text{i-C}_3\text{F}_7)_4$  and  $\text{C}_{60}(\text{i-C}_3\text{F}_7)_6$ , +0.32 and +0.43 V, respectively (see Table 6), can be compared to +0.17 V reported for **60-4-1**, +0.29 V predicted for **60-4-2**, and +0.26 V reported for **60-6-1**. Likewise,  $E_{1/2}$  potential of **70-4-4-i-C<sub>3</sub>F<sub>7</sub>** is as high as +0.49 V, which is more than 2 times higher than in **70-4-1** (+0.21 V). In fact, the reduction potential of **70-4-4-i-C<sub>3</sub>F<sub>7</sub>** is the second most positive value reported for any PFAF (the first one is **60-10-1** with  $E_{1/2} = 0.57$  V).

The lowest LUMO energy among perfluoroisopropyl derivatives of  $\text{C}_{60}$  and  $\text{C}_{70}$  with experimentally characterized addition patterns is predicted by DFT calculations for the isomer **60-6-11-i-C<sub>3</sub>F<sub>7</sub>** (electrochemical measurements of this compound are not reported yet). At the PBE/TZ2P level, its LUMO is stabilized by 0.87 eV relative to  $\text{C}_{60}$ , which means that its  $E_{1/2}$  value may exceed 0.65 V vs  $\text{C}_{60}$ .<sup>94</sup> Thus, both experimental and computational data show that perfluoroisopropyl fullerenes are stronger electron acceptors than  $\text{CF}_3$  derivatives, and that the reason for the enhanced electron-accepting properties lies in the addition patterns with a larger number of *nt*-DBIPs and the variability of their relative positions. Analysis of the LUMO shapes showed that  $\text{i-C}_3\text{F}_7$

PFAFs with the highest reduction potentials (lowest LUMO energies) all have a common LUMO motif resembling the LUMO of pentafulvalene (see Figure 28). Such LUMO motif is realized in PFAF molecules when both pentagons of the pentafulvalene fragments have one *nt*-DBIP as shown in Figure 28 for **60-4-4**. The LUMO of **60-6-11-i-C<sub>3</sub>F<sub>7</sub>** has additionally an acenaphthalene-like fragment anchored to the third *nt*-DBIPs, and such enhanced delocalization between pentafulvalene and acenaphthalene moieties results in the strong stabilization of the LUMO energy.

**7.3.3. CF<sub>2</sub> Derivatives.** Addition of CF<sub>2</sub> groups to fullerenes predominantly occurs across double bonds on hexagon/hexagon edges of the carbon cage ([6,6] hereafter).<sup>61,62</sup> A unique feature of C<sub>60</sub>(CF<sub>2</sub>) is that the C–C bond of the fullerene cage is cleaved (i.e., [6,6]-open, unlike all other C<sub>60</sub>(CR<sub>2</sub>) derivatives, which have [6,6]-closed structure). Cyclic voltammetry study showed that both C<sub>60</sub>(CF<sub>2</sub>) and bisadduct C<sub>60</sub>(CF<sub>2</sub>)<sub>2</sub> exhibit three reversible reductions on oDCB.<sup>187</sup> Both compounds are easier to reduce than C<sub>60</sub> by 0.15 V. Two isomers of C<sub>70</sub>(CF<sub>2</sub>) were isolated, one with [6,6]-open, and one with [6,6]-closed structures.<sup>110</sup> The isomers showed significantly different reduction potentials: reduction potential of the [6,6]-closed isomer is only 0.01 V more positive than that of C<sub>70</sub>, whereas [6,6]-open is easier to reduce than C<sub>70</sub> by 0.15 V, similar to C<sub>60</sub>(CF<sub>2</sub>).

In situ ESR spectroelectrochemical studies of fullerene(CF<sub>2</sub>) derivatives were reported in refs 187 and 110. All monoadducts exhibited resolved hyperfine structure with the *a*(<sup>19</sup>F) values in the range of 1.0–1.7 G. Somewhat smaller values, 0.6 and 0.2 G, were reported for the bisadduct C<sub>60</sub>(CF<sub>2</sub>)<sub>2</sub><sup>−</sup>. Computational studies showed that the energy profile along the distance between bridgeheaded atoms in CF<sub>2</sub> derivatives of fullerenes is very flat in a long range of C···C distances. Furthermore, reduction shifts the energy minimum to longer distances and can even stabilize the open form for the closed isomer as found for the [6,6]-closed isomer of C<sub>70</sub>(CF<sub>2</sub>). This prediction was corroborated by in situ ESR spectroscopic studies of its anion radical: <sup>19</sup>F hyperfine coupling constants in the ESR spectrum of [6,6]-closed C<sub>70</sub>(CF<sub>2</sub>)<sup>−</sup> match predicted values for the open structure much better than for the closed configuration. Thus, spectroelectrochemical study showed that the [6,6]-closed isomer of C<sub>70</sub>(CF<sub>2</sub>) becomes open in the anionic state.

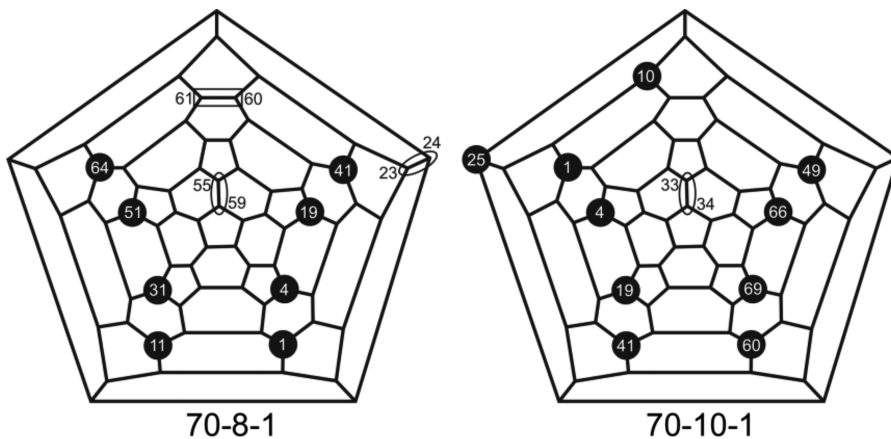
## 8. CHEMICAL PROPERTIES OF PFAFs

The possibility of chemically modifying PFAFs is an attractive and desirable way to tune physical properties such as solubility in different media, to incorporate them into polymers, or to chemically bond them to the material surface of a substrate. Because of the strong C–F bonds on the R<sub>F</sub> moieties, direct replacement of F atoms by other functional groups is challenging; the most common ways of C–F bond activation require strong reducing conditions.<sup>192</sup> Therefore, addition of heterofunctional groups to the cage C atoms of PFAFs appears to be a viable solution.

In some of the earlier synthetic works involving fullerene trifluoromethylation in organic protic solvent<sup>7</sup> or in the solid-phase reactions with AgTFA,<sup>25,27,38</sup> it was observed that hydrogen atom(s) was added to the cage besides CF<sub>3</sub> radicals. Either H abstraction from the solvent or the presence of trace amounts of moisture in the reagents were hypothesized to be responsible for such side reactions. No pure hydrogenated trifluoromethylfullerene isomers were isolated from such reaction products, and the synthesis conditions were further

adjusted to eliminate undesired hydrogenation process. In the high-temperature reactions with R<sub>F</sub>I reagents, another type of hetero-PFAF derivatives was detected, that is, monoepoxides, C<sub>60</sub>(R<sub>F</sub>)<sub>4</sub>O, R<sub>F</sub> = CF<sub>3</sub>, C<sub>2</sub>F<sub>5</sub>, where four R<sub>F</sub> groups have a **60-4-3** addition pattern.<sup>39</sup> It was originally suggested that trace amounts of water in the reaction medium could be the source of oxygen in this case. However, more recently, a detailed study of oxidation of **60-4-3** with different oxidants, including molecular oxygen, ozone, and *m*-chloroperbenzoic acid in the absence or presence of moisture or ambient light, has clearly demonstrated that addition of oxygen to **60-4-3** occurs not during trifluoromethylation of the fullerene, but during subsequent HPLC processing. Interestingly, the oxidation by molecular oxygen only occurred in polar solvents and required the presence of light, indicating that the process involved photoinduced energy transfer, and hence singlet oxygen was the reactive species,<sup>113</sup> in contrast to the reported earlier epoxidations of fullerene derivatives via single electron transfer that may occur in the dark.<sup>193</sup> When three other TMFs (**60-2-1**, **60-4-1**, and **60-10-3**) were subjected to oxidation conditions similar to those of **60-4-3**, no formation of epoxides was observed after 24 h. It was concluded that higher reactivity of **60-4-3** was due to a fulvene moiety on the cage with a very short double bond receptive to the epoxide formation. Noteworthy, **60-10-3** also has a motif of **60-4-3** in its addition pattern, but the short reactive double bonds on fulvene moiety are sterically shielded, which makes epoxidation a much slower process for this TMF. In fact, it was found that gradual and regiospecific diepoxydation occurred after **60-10-3** solutions were exposed to light and air for many weeks.<sup>194</sup> Attempts to intentionally convert **60-10-3** into mono- or bis-epoxide using stronger oxidants resulted in non-selective oxidation. While most of the PFAFs exhibit very high stability as solids and can be kept in ambient conditions for years without chemical changes, the notable differences in the reactivity of PFAFs of different compositions and addition patterns toward oxidation reported in refs 113,194 have brought up awareness that one cannot assume chemical inertness for the entire class of the compounds, unless it is examined case-by-case.

Intentional additions of functional groups to PFAFs have included chlorination,<sup>141</sup> cyanation,<sup>195</sup> methylation,<sup>195</sup> and cycloadditions.<sup>76,99,146,196</sup> Two examples of chlorination of PFAFs were reported; in the first one, the S<sub>6</sub>-symmetric **60-12-1** that could be prepared relatively efficiently was used as a starting material.<sup>141a</sup> This compound was chlorinated by SbCl<sub>5</sub> in a sealed glass ampoule at 270–280 °C for 24 h. The excess of SbCl<sub>5</sub> and a small amount of SbCl<sub>3</sub> were removed from the fullerene products by sublimation. The resulting residue contained some crystalline material, which was studied by single-crystal X-ray diffraction and IR spectroscopy, which showed it to contain a S<sub>6</sub>-symmetric C<sub>60</sub>(CF<sub>3</sub>)<sub>12</sub>Cl<sub>12</sub> product (90% yield was reported, but the purity of the product is hard to ascertain).<sup>141a</sup> It is notable that the addition pattern of the initial **60-12-1** was left unchanged, which highlights the high robustness of PFAF cores under harsh conditions (highly oxidative media at high temperature). The 12 chlorine atoms were added to the cage in such a way as to avoid sterically unfavorable *ortho*-contacts with the CF<sub>3</sub> groups. The high degree of chlorination achieved in this work is undoubtedly due to the harsh conditions used. A chlorination of a different PFAF, **70-8-1**, by a large excess of iodine monochloride at room temperature in oDCB solution led to a selective addition of two chlorine atoms to the equatorial C<sub>60</sub>–C<sub>61</sub> cage bond

Scheme 4. Reactive Sites of 70-8-1 and 70-10-1<sup>a</sup>

<sup>a</sup>Left: reactive site for the chlorination and dimerization is highlighted with a square frame; reactive sites for Bingel reaction are highlighted with ovals. Right: reactive site for Bingel and Diels–Alder reactions is highlighted with an oval. The reactive sites are designated using IUPAC numbering of the original structures.

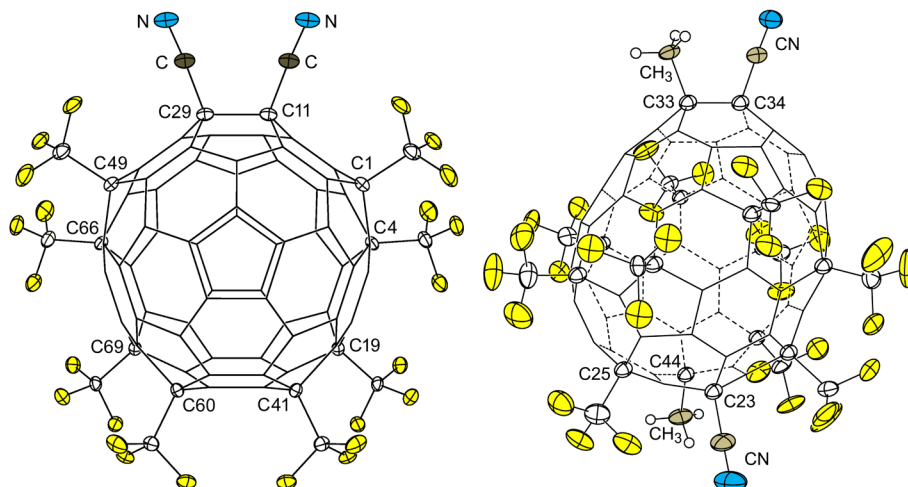


Figure 33. Structure of C<sub>5</sub>-C<sub>70</sub>(CF<sub>3</sub>)<sub>8</sub>(CN)<sub>2</sub> (left) and C<sub>1</sub>-C<sub>70</sub>(CF<sub>3</sub>)<sub>10</sub>(CH<sub>3</sub>)<sub>2</sub>(CN)<sub>2</sub> (right; 50% probability ellipsoids for substituents and the cage carbon atoms to which they are attached for both structures; H atoms shown as spheres of arbitrary size).

(see Scheme 4; the reactive site is highlighted with a square frame; the original numbering of 70-8-1 is used). The resulting single-isomer C<sub>5</sub>-C<sub>70</sub>(CF<sub>3</sub>)<sub>8</sub>Cl<sub>2</sub> product was formed with an ca. 90% yield, and it was characterized by single-crystal X-ray diffraction and by <sup>19</sup>F NMR spectroscopy.<sup>141b</sup> The addition pattern of the C<sub>5</sub>-C<sub>70</sub>(CF<sub>3</sub>)<sub>8</sub>Cl<sub>2</sub> compound was found to be identical to the addition patterns of several other C<sub>5</sub>-C<sub>70</sub>R<sub>10</sub> derivatives (R = H, Cl, and Br; see ref 141b and references therein) with the 10 substituents forming an equatorial belt around the C<sub>70</sub> cage. The theoretical calculations showed both a thermodynamic and a kinetic preference of the C<sub>60</sub>–C<sub>61</sub> bond of 70-8-1 for the addition of smaller-size substituents.<sup>141b</sup> A Bingel–Hirsch addition of diethyl malonate (in the presence of CBr<sub>4</sub> and DBU) to 70-8-1 gave mono- and bis-adducts C<sub>70</sub>(CF<sub>3</sub>)<sub>8</sub>[C(CO<sub>2</sub>Et)<sub>2</sub>]<sub>n</sub> (two isomers with n = 1 and a single isomer with n = 2) with malonate moieties attached to the poles of the 70-8-1 molecule (reactive sites C<sub>23</sub>–C<sub>24</sub> and C<sub>55</sub>–C<sub>59</sub>, see Scheme 4). However, the underderivatized 70-8-1 and C<sub>70</sub>(CF<sub>3</sub>)<sub>8</sub>[C(CO<sub>2</sub>Et)<sub>2</sub>]<sub>n</sub> (n = 1 and 2) compounds were found to dimerize via a [2+2] cyclization of the same C<sub>60</sub>–C<sub>61</sub> bonds (the dimerization was confirmed by single-crystal X-ray studies).<sup>196</sup>

Several studies were also dedicated to the derivatization of 70-10-1, which is probably the most easily available PFAF due to its very efficient synthesis.<sup>32,99</sup> A Bingel–Hirsch reaction of pure 70-10-1 with diethyl malonate and carbon tetrabromide in the presence of DBU base led to a selective [2+1] addition to the C<sub>33</sub>–C<sub>34</sub> bond of the cage (see Scheme 4; the original numbering of 70-10-1 is used).<sup>76</sup> The adduct C<sub>70</sub>(CF<sub>3</sub>)<sub>10</sub>[C(CO<sub>2</sub>Et)<sub>2</sub>] was isolated in 62% yield and characterized by single-crystal X-ray diffraction study, mass spectrometry, and HPLC analysis. The energies of different isomers of C<sub>70</sub>(CF<sub>3</sub>)<sub>10</sub>[C(CO<sub>2</sub>Et)<sub>2</sub>] were also calculated by DFT and AM1 methods.<sup>76</sup> Later, an analogous reaction was used to prepare a dyad consisting of 70-10-1 core tethered to two exTTF molecules (the photophysical behavior of the dyad was also studied).<sup>99</sup> A Bingel–Hirsch reaction of 70-10-1 with a malonate carrying two exTTF molecules led to a [2+1] addition to the same C<sub>33</sub>–C<sub>34</sub> bond and showed a very good selectivity (the yield of the adduct based on the consumed 70-10-1 was 80%).<sup>99</sup> The C<sub>33</sub>–C<sub>34</sub> bond of 70-10-1 was also found to be especially susceptible to [4+2] Diels–Alder addition.<sup>146</sup> A reaction of 70-10-1 with dimethoxy *o*-quinodimethane (3,6-DMQDM, generated in situ by thermolysis of the

corresponding sultine) gave a single-isomer Diels–Alder adduct with 73% yield (based on the consumed **70-10-1**).<sup>146</sup> The single-crystal X-ray diffraction study showed unambiguously that the addition took place across the C33–C34 bond.

These results show that addition of R<sub>F</sub> groups to a fullerene cage can activate some of the cage double bonds and make them significantly more susceptible to further chemical derivatization, with different sites being strongly preferred for different types of reactions (and different steric parameters of the addends).<sup>141b,196</sup> Both steric and electronic factors are likely to play a role in this modification of the cage reactivity. The high reactivity of some sites of PFAF molecules can be used for their selective derivatization with various groups leading to various functional molecules like the first PFAF-based dyad (comprised of **70-10-1** acceptor core and two exTTF donor moieties).<sup>99</sup>

In 2012, several PFAFs were used for one-pot reactions of sequential additions of simple anionic nucleophiles and cationic electrophiles that aimed at probing the reactivity of individual carbon atoms.<sup>195b</sup> When **70-8-1** was used as a substrate dissolved in C<sub>6</sub>D<sub>6</sub>, addition of NEt<sub>4</sub>CN acetonitrile solution at room temperature resulted in an immediate color change to greyish-blue, indicating formation of anionic species C<sub>70</sub>(CF<sub>3</sub>)<sub>8</sub>(CN)<sup>-</sup>. Subsequent reaction with p-TsCN yielded a brown solution that contained two products: the predominant product with 90% selectivity was a symmetric C<sub>5</sub>-C<sub>70</sub>(CF<sub>3</sub>)<sub>8</sub>(CN)<sub>2</sub> (see Figure 33) with the same addition pattern as C<sub>70</sub>Br<sub>10</sub><sup>160e</sup> and C<sub>70</sub>(CF<sub>3</sub>)<sub>8</sub>Cl<sub>2</sub><sup>141b</sup> and one minor product, C<sub>1</sub>-C<sub>70</sub>(CF<sub>3</sub>)<sub>8</sub>(CN)<sub>2</sub>. Even higher regioselectivity of 95 mol % was achieved in consecutive additions of CN<sup>-</sup> and CH<sub>3</sub><sup>+</sup> to **70-10-1**. From the analysis of spectroscopic data and DFT results, it was concluded that in the C<sub>70</sub>(CF<sub>3</sub>)<sub>10</sub>(CN)(CH<sub>3</sub>) product, CN group added to C34, while CH<sub>3</sub> was added to C33 (see Scheme 4, right, for C34 and C33 locations). In another experiment, CH<sub>3</sub><sup>-</sup> was added first to **70-10-1**, followed by the reaction with electrophilic CN<sup>+</sup>. Unexpectedly, this yielded two isomers of C<sub>70</sub>(CF<sub>3</sub>)<sub>10</sub>(CH<sub>3</sub>)<sub>2</sub>(CN)<sub>2</sub>, and the structure of the minor isomer was determined by X-ray crystallography (see Figure 33). A similar synthetic approach, that is, sequential nucleophile/electrophile additions, was later applied to selectively derivatize **60-4-3**, yielding molecules with the skew-pentagonal pyramid addition pattern of **60-6-2**: C<sub>60</sub>(CF<sub>3</sub>)<sub>4</sub>(CN)H.<sup>195a</sup>

These initial studies of PFAF chemical reactivity demonstrate that versatile approaches can be used to purposefully tune structures and properties of selected PFAFs to enable the design of materials and composites for specific applications. Importantly, X-ray crystallography of PFAFs combined with the DFT studies can be used to predict the most likely addition sites and the kinetic and thermodynamic products.

## 9. CONCLUSIONS AND OUTLOOK

Two decades of active research in the perfluoroalkylation of fullerenes have passed, resulting in the creation of diverse libraries of new chemical derivatives that possess the greatest variety of addition patterns than any other class of fullerene derivatives.

These compounds represent an important addition to the existing classes of perfluorocarbons, that is, compounds that are composed only of the two types of atoms, carbon and fluorine. These include aromatic and aliphatic perfluorocarbons such as perfluorodecalin, perfluorononane, hexafluorobenzene, etc., which are important as fluorous solvents used in medicine

and organic synthesis. Perfluorinated polycyclic aromatic hydrocarbons, such as perfluoronaphthalene and perfluoropentacene, have been intensely studied for applications in organic electronics. Fluorofullerenes are derivatives in which a fluorine atom is attached directly to a cage carbon atom and represent an interesting group of compounds with exceptionally high electron affinities, and thus have been used as p-dopants in optoelectronic devices.

What awaits PFAFs in the following decades, from the perspective of both fundamental research and practical use in modern technology and materials? As we have shown in this Review, there are practically unlimited opportunities for discovering new molecules and determining their structures and fundamental properties. The propensity of PFAFs to readily crystallize from organic solutions upon slow evaporation in open air (as long as sufficient purity is achieved) provided a straightforward access to their molecular structures via X-ray crystallography. Noteworthy, in many cases, access to a synchrotron source facilitates such studies significantly, as carbon and fluorine have low X-ray scattering factors, and smaller crystals (that frequently result from solution crystal growth) can be studied. Another crucial aspect that ensures future success in the characterization of numerous PFAFs of higher fullerenes and endohedral metallofullerenes is the possibility to apply HPLC methodologies to the separation of product mixtures. Although labor-intensive, time-consuming, and expensive (even small analytical columns required for this work cost more than \$5000), HPLC allows researchers to achieve high purity of their reaction products. The authors predict that many more exotic PFAFs will be reported in the near future, in particular for fullerene cages that have a small-band gap, or for non-IPR fullerenes, or even for fullerenes with cage sizes smaller than C<sub>60</sub>.

Further use of PFAFs by researchers from nanoscience, material science, and biomedical science, and particularly their practical applications, will depend on the availability of the PFAF samples in larger quantities and with sufficient purity. The methods used to synthesize PFAFs (flow reactor, ampoule synthesis) are usually aimed at ca. 50 mg amounts, and larger-scale syntheses are in the early stages of development. Gram-scale syntheses have been reported for **60-2-1** when the GTGS reactor was used under the conditions for selective synthesis. However, a single-stage HPLC separation was still needed to isolate **60-2-1** from unreacted C<sub>60</sub>. Multihundred milligram amounts of **70-10-1** per batch were produced in flow-tube reactors, the only C<sub>70</sub> PFAF for which a scalable, highly selective, high-yield synthetic procedure that does not require chromatographic separation was developed. Non-chromatographic separation of **60-12-1** based on the low solubility of its crystalline phase was reported, but it remains to be seen if the compound can be synthesized not using a sealed-ampoule approach, which is limited to ca. 120 mg per batch. Access to larger quantities of various isomers of TMFs of C<sub>60</sub> and C<sub>70</sub> produced in flow-tube or GTGS reactors can be readily achieved if appropriate investments are made in preparative HPLC equipment, which still remains a bottleneck.

PFAFs, especially those of C<sub>60</sub> and C<sub>70</sub>, are unique fullerene derivatives in terms of the number of structurally characterized derivatives with different number of R<sub>F</sub> groups and different addition patterns. The availability of such family enabled deeper understanding of relationships between addition patterns and electronic properties of fullerene derivatives. The first reduction potentials of PFAFs vary in the range of 0.6 V, and it is now

well-understood that electron-accepting properties of PFAFs are strongly linked to double bonds in pentagons formed after R<sub>F</sub> addition. Recent studies showed that luminescent properties of PFAFs are also strongly dependent on their addition patterns, and proper functionalization (addition pattern) affords compounds with high quantum yields. More work is necessary to fully understand the photophysical properties of PFAFs, and future studies promise that new bright fluorocarbon fluorophores will become available for a variety of applications.

It is conceivable that some significant developments will occur in the near future in the area of practical applications of PFAFs as powerful and tunable acceptors in the field of organic electronics. In particular, the possibility of energy level engineering of active layers appears attractive. One such example, the use of a PFAF molecule, **60-2-1**, in organic photovoltaic active layers has been recently demonstrated by NREL researchers.<sup>197</sup> Some of the new promising ethynylene-linked donor polymers have low-lying LUMOs, and hence when mixed with a conventional, high-LUMO fullerene acceptor, PCBM, result in low yields of free carrier generation. However, when **60-2-1**, which has a lower LUMO than PCBM, was used instead, a 4-fold increase in free carrier generation was measured by the TRMC method.<sup>197</sup> In another study, the series of TMFs **60-2-1**, **60-4-1**, **60-6-1**, **60-6-2**, **60-8-1**, and **60-10-2**, selected deliberately to cover the widest possible range of reduction potentials, was used to address fundamental questions on the relations between the energetic driving force and yield of free charge generation in OPV active layers. It provided the first experimental evidence for a Marcus theory description of photoinduced electron transfer in the solid state.<sup>198</sup>

A broader impact of the synthetic methodologies developed in the course of PFAF research is that they lead to innovative perfluoroalkylations of other organic or inorganic substrates. For example, new methods for the perfluoroalkylation of polycyclic aromatic hydrocarbons that were directly influenced by the work on PFAFs were recently reported.<sup>199</sup> It was discovered that synthetic methods for the introduction of R<sub>F</sub> groups into robust fullerenes can be adopted for reactions with a wide range of PAHs, including corannulene, acenes, pyrene, coronene, and even azulene and naphthalene.<sup>199</sup> Such an outside-the box approach to organic perfluoroalkylation yielded unprecedented compositions and structures of highly perfluoroalkylated compounds. Some of the perfluoroalkyl PAHs were even found to have electron affinities comparable to, or even higher than, those of C<sub>60</sub> and many PFAFs.<sup>200</sup> There is no doubt that further exploration of high-temperature gas-phase perfluoroalkylations of organic or organometallic substrates is a worthwhile endeavor and will lead to advances in both fundamental and applied research.

## AUTHOR INFORMATION

### Corresponding Authors

\*E-mail: olga.boltalina@colostate.edu

\*E-mail: a.popov@ifw-dresden.de

\*E-mail: steven.strauss@colostate.edu

### Notes

The authors declare no competing financial interest.

## Biographies



Olga Boltalina received her M.S. (1982) and Ph.D. (1990) degrees in Physical Chemistry from Moscow State University (MSU), Russia, working with Lev Sidorov. She earned her D.Sci. degree (i.e., Doctor Nauk (aka Habilitation)) from MSU in 1998. She retired as Professor of Physical Chemistry from MSU in 2005 after having supervised 11 Ph.D. and 10 M.S. students. She is now a Senior Research Scientist at Colorado State University, where she and her husband, Steven Strauss, share contracts, grants, and laboratories and co-advise their graduate and undergraduate research students. She has received the MSU Lomonosov Prize, an Alexander von Humboldt (AvH) Freidrich Bessel Award, two additional AvH Research Fellowships, a Japan Society for the Promotion of Science Fellowship, and a Royal Society of Chemistry Research Award. Her current research interests include the rational design of fluorinated and perfluoroalkylated fullerenes and related carbon materials for specific optoelectronic, energy conversion, energy storage, and biomedical applications.



Alexey Popov received his M.S. (1999) and Ph.D. (2003) degrees in Physical Chemistry from Moscow State University (MSU), Russia, working with Mikhail Korobov and Vladimir Senyavin. He was a Senior Researcher at MSU until 2008, when he received an Alexander von Humboldt Fellowship to study endohedral metallofullerenes (EMFs) with Prof. Dr. Lothar Dunsch at the Leibniz Institute for Solid State and Materials Research Dresden, Germany, where he now heads the Fullerene Group. He has co-authored more than 50 peer-reviewed publications with Olga Boltalina and/or Steven Strauss. His current research interests include experimental and quantum-chemical computational studies of hollow fullerenes and EMFs, including their synthesis, derivatization, spectroelectrochemistry, optical spectroscopy, and magnetic properties.



Igor Kuvychko received his M.S. degree in 2004 from the Higher Chemical College of the Russian Academy of Science in Moscow, Russia, and his Ph.D. in Inorganic Chemistry in 2009 from Colorado State University (CSU), studying chlorofullerenes, perfluoroalkylfullerenes, and related compounds with Olga Boltalina and Steven Strauss. He then initiated a major study on the synthesis and electronic properties of perfluoroalkylated polycyclic aromatic hydrocarbons as a postdoc in the Boltalina/Strauss lab at CSU. He is a co-author or co-inventor with Boltalina and Strauss on no fewer than 40 peer-reviewed publications and 6 patents or patent applications, respectively. In 2013 he joined Intel Corporation in Portland, OR, as a Semiconductor Process Engineer.



Natalia Shustova received her M.S. degree in Materials Science in 2004 from Moscow State University (MSU), Russia, and two Ph.D. degrees, the first in Physical Chemistry in 2005 from MSU, working with Lev Sidorov, and the second in Inorganic Chemistry in 2010 from Colorado State University, studying perfluoroalkylfullerenes and related compounds with Olga Boltalina and Steven Strauss (and co-authoring more than 30 peer-reviewed publications with them). She then did postdoctoral research with Mircea Dincă at the Massachusetts Institute of Technology. In 2013 she joined the faculty at the University of South Carolina as an Assistant Professor of Chemistry. She is the recipient of an MIT Infinite Kilometer Postdoctoral Award, an MIT/Bruker Symposium Award, a German Academic Exchange (DAAD) Graduate Research Scholarship, an Electrochemical Society Herbert H. Uhlig Summer Fellowship, and a Humboldt University (Berlin) L. Euler Student Fellowship. Her current research interests are graphitic hybrid materials for sustainable energy conversion, sensors, switches, and artificial biomimetic systems.



Steven Strauss is Professor of Chemistry at Colorado State University (CSU). He received his B.A. in Chemistry in 1973 from Franklin & Marshall College, his Ph.D. degree in Inorganic Chemistry in 1978 from Northwestern University, working with Duward Shriner, and had an NIH Postdoctoral Fellowship working with Richard Holm at Stanford and Harvard Universities from 1978 to 1981. Since joining the chemistry faculty at CSU in 1981, he has received an Alfred P. Sloan Research Fellowship and four awards for excellence in teaching. He was the 2002 CSU Research Foundation Researcher of the Year and the 2012 CSU College of Natural Sciences Professor Laureate. In 2001 he chaired the ACS Division of Fluorine Chemistry and the Gordon Research Conference on Inorganic Chemistry. As conjoint principal investigators, he and his wife Olga Boltalina have co-authored more than 80 peer-reviewed publications on perfluoroalkylfullerenes, perfluoroalkylated polycyclic aromatic hydrocarbons, and related fluoroorganic compounds and materials. He also studies the synthesis of highly-fluorinated superweak anions and uses them to isolate unusual reactive metal and nonmetal cations.

## ACKNOWLEDGMENTS

We warmly thank our Ph.D. and undergraduate students who over the past decade have been as passionate about and as dedicated to studying PFAFs as we have been. We are grateful for the knowledge and assistance provided by colleagues and technical staff members at our home institutions, Prof. Oren Anderson and Susie Miller (X-ray crystallography), Don Dick, Don Heyse, and Chris Rithner (mass spectrometry and NMR spectroscopy), and U Nitzsche (computational resources). Special thanks are extended to our collaborators-cum-professional friends who generously gave their time and expertise providing exotic fullerene starting materials, investigating our PFAF products, hosting our students in their labs, and spending many hours with us discussing new results and preparing manuscripts for publication: Prof. T. Akasaka (University of Tsukuba); Dr. Robert Bolksar (TDA Research, Wheat Ridge, CO); Dr. Yu-Sheng Chen (University of Chicago Advanced Photon Source); the late Prof. Dr. Lothar Dunsch (IFW Dresden); Prof. J. Paige Phillips (University of Southern Mississippi); Prof. Dr. Dirk Guldi and Prof. Dr. Andreas Hirsch (Friedrich-Alexander-Universität, Erlangen-Nürnberg); Dr. Nikos Kopidakis and Dr. Garry Rumbles (National Renewable Energy Laboratory, Golden, CO); Prof. Dr. Nazario Martín (Universidad Complutense, Madrid); Prof. Jeffrey Rack (Ohio University); Prof. Dr. Konrad Seppelt (Freie Universität Berlin); Prof. Steven Stevenson (Indiana-Purdue University, Fort Wayne); and Dr. Xue-Bin Wang (Pacific Northwest National Laboratory, Richland, WA). Last, but not least, we thank the National Science Foundation (grants CHE-0707223,

CHE-1012468, and CHE-1362302), the National Institutes of Health (grant R21CA140080), the Alexander von Humboldt Foundation, the German Academic Exchange Service (DAAD), the German Research Foundation (projects PO 1602/1-1 and 1602/1-2) (Germany), and the Colorado State University Foundation for financial support and the Supercomputing Center of Moscow State University for providing computational resources that were used for our PFAF DFT studies.

## GLOSSARY

PFAF	perfluoroalkylated fullerene
TMF	trifluoromethylated fullerene
RT	room temperature
TCB	1,2,4-trichlorobenzene
oDCB	1,2-dichlorobenzene
Freon-113	CCl <sub>2</sub> CCl <sub>2</sub> F
CB	chlorobenzene
TFA	OOCCF <sub>3</sub> (trifluoroacetate)
EMF	endohedral metallofullerene
min	minutes
h	hours
d	days
C <sub>60,70</sub>	C <sub>60</sub> or C <sub>70</sub>
AIBN	azobis(isobutyronitrile)
HHF	hollow higher fullerene
ElAn	elemental analysis
EA	electron affinity
IR	IR spectroscopy
ATR-IR	attenuated total reflectance infrared spectroscopy
Raman	Raman spectroscopy
UV-vis	UV-vis spectroscopy
UV	UV irradiation
NI	negative ion
MS	mass spectrometry
PI	positive ion
EC-MS	electron capture mass spectrometry
FTMS	Fourier-transform mass spectrometry
EI-MS	electron impact ionization mass spectrometry
LDI-MS	laser desorption/ionization mass spectrometry
MALDI-MS	matrix-assisted laser desorption/ionization mass spectrometry
FAB-MS	fast atom bombardment mass spectrometry
EC-MS	electron-capture mass spectrometry
TSI-MS	thermal surface ionization mass spectrometry
ESI-MS	electrospray ionization mass spectrometry
APCI-MS	atmospheric pressure chemical ionization mass spectrometry
APPI-MS	atmospheric pressure photoionization mass spectrometry
NMR	nuclear magnetic resonance spectroscopy
COSY NMR	2D correlation nuclear magnetic resonance spectroscopy
VT	variable temperature
ESR	electron spin resonance spectroscopy
TGA	thermogravimetric analysis
HPLC	high performance liquid chromatography
GPC	gel permeation chromatography
X-ray	single-crystal X-ray diffraction study
CV	cyclic voltammetry
GTGS reactor	gradient-temperature gas-solid reactor
DBIP	double bond in pentagon
nt-DBIP	non-terminal double bond in pentagon

SPP	skew-pentagonal-pyramid
THJ	triple hexagon junction
PHHJ	pentagon/hexagon/hexagon junction
PFA-EMF	perfluoroalkylated endohedral metallofullerene

## REFERENCES

- (1) Kroto, H. W.; Heath, J. R.; O'Brien, S. C.; Curl, R. F.; Smalley, R. E. *Nature* **1985**, *318*, 162.
- (2) Kratschmer, W.; Lamb, L. D.; Fostiropoulos, K.; Huffman, D. R. *Nature* **1990**, *347*, 354.
- (3) (a) Thilgen, C.; Diederich, F. *Chem. Rev.* **2006**, *106*, 5049.  
 (b) Dang, M. T.; Hirsch, L.; Wantz, G.; Wuest, J. D. *Chem. Rev.* **2013**, *113*, 3734.  
 (c) Giacalone, F.; Martin, N. *Chem. Rev.* **2006**, *106*, 5136.  
 (d) Matsuo, Y.; Nakamura, E. *Chem. Rev.* **2008**, *108*, 3016.  
 (e) McHedlov-Petrosyan, N. O. *Chem. Rev.* **2013**, *113*, 5149.  
 (f) Popov, A. A.; Yang, S. F.; Dunsch, L. *Chem. Rev.* **2013**, *113*, 5989.  
 (g) Tzirakis, M. D.; Orfanopoulos, M. *Chem. Rev.* **2013**, *113*, 5262.  
 (h) Vostrowsky, O.; Hirsch, A. *Chem. Rev.* **2006**, *106*, 5191.
- (i) Yamada, M.; Akasaka, T.; Nagase, S. *Chem. Rev.* **2013**, *113*, 7209.
- (4) Kareev, I. E.; Kuvychko, I. V.; Lebedkin, S. F.; Miller, S. M.; Anderson, O. P.; Seppelt, K.; Strauss, S. H.; Boltalina, O. V. *J. Am. Chem. Soc.* **2005**, *127*, 8362.
- (5) Popov, A. A.; Kareev, I. E.; Shustova, N. B.; Stukalin, E. B.; Lebedkin, S. F.; Seppelt, K.; Strauss, S. H.; Boltalina, O. V.; Dunsch, L. *J. Am. Chem. Soc.* **2007**, *129*, 11551.
- (6) Krusic, P. J.; Wasserman, E.; Parkinson, B. A.; Malone, B.; Holler, E. R. *J. Am. Chem. Soc.* **1991**, *113*, 6274.
- (7) Fagan, P. J.; Krusic, P. J.; McEwen, C. N.; Lazar, J.; Parker, D. H.; Herron, N.; Wasserman, E. *Science* **1993**, *262*, 404.
- (8) Yoshida, M.; Morinaga, Y.; Iyoda, M.; Kikuchi, K.; Ikemoto, I.; Achiba, Y. *Tetrahedron Lett.* **1993**, *34*, 7629.
- (9) Borghi, R.; Lunazzi, L.; Placucci, G.; Krusic, P. J.; Dixon, D. A.; Knight, J. L. B. *J. Phys. Chem.* **1994**, *98*, 5395.
- (10) Yoshida, M.; Morishima, A.; Morinaga, Y.; Iyoda, M. *Tetrahedron Lett.* **1994**, *35*, 9045.
- (11) Morton, J. R.; Preston, K. F. *J. Phys. Chem.* **1994**, *98*, 4993.
- (12) Morton, J. R.; Negri, F.; Preston, K. F.; Ruel, G. *J. Phys. Chem.* **1995**, *99*, 10114.
- (13) Fritz, H. P.; Hiemeyer, R. *Carbon* **1995**, *33*, 1601.
- (14) Yoshida, M.; Suzuki, D.; Iyoda, M. *Chem. Lett.* **1996**, 1097.
- (15) Borghi, R.; Lunazzi, L.; Placucci, G.; Krusic, P. J.; Dixon, D. A.; Matsuzawa, N.; Ata, M. *J. Am. Chem. Soc.* **1996**, *118*, 7608.
- (16) Lyakhovetsky, Y. I.; Shilova, E. A.; Tumanskii, B. L.; Usatov, A. V.; Avetisyan, E. A.; Sterlin, S. R.; Pleshkova, A. P.; Novikov, Y. N.; Nekrasov, Y. S.; Taylor, R. *Fullerene Sci. Technol.* **1999**, *7*, 263.
- (17) Yoshida, M.; Sultana, F.; Uchiyama, N.; Yamada, Y.; Iyoda, M. *Tetrahedron Lett.* **1999**, *40*, 735.
- (18) Chen, W.; McCarthy, T. J. *Macromolecules* **1999**, *32*, 2342.
- (19) Avent, A. G.; Boltalina, O. V.; Lukonin, A. Y.; Street, J. M.; Taylor, R. *J. Chem. Soc., Perkin Trans. 2* **2000**, 1.
- (20) Boltalina, O. V.; Hitchcock, P. B.; Troshin, P. A.; Street, J. M.; Taylor, R. *J. Chem. Soc., Perkin Trans. 2* **2000**, 2410.
- (21) Uzkikh, I. S.; Dorozhkin, E. I.; Boltalina, O. V.; Boltalin, A. I. *Dokl. Akad. Nauk* **2001**, *379*, 344.
- (22) Avent, A. G.; Boltalina, O. V.; Goryunkov, A. V.; Darwish, A. D.; Markov, V. Y.; Taylor, R. *Fullerenes, Nanotubes, Carbon Nanostruct.* **2002**, *10*, 235.
- (23) Boltalina, O. V.; Darwish, A. D.; Street, J. M.; Taylor, R.; Wei, X.-W. *J. Chem. Soc., Perkin Trans. 2* **2002**, 251.
- (24) Tagmatarchis, N.; Taninaka, A.; Shinohara, H. *Chem. Phys. Lett.* **2002**, *355*, 226.
- (25) Darwish, A. D.; Avent, A. G.; Abdul-Sada, A. K.; Taylor, R. *Chem. Commun.* **2003**, 1374.
- (26) Darwish, A. D.; Abdul-Sada, A. K.; Avent, A. G.; Lyakhovetsky, V. I.; Shilova, E. A.; Taylor, R. *Org. Biomol. Chem.* **2003**, *1*, 3102.
- (27) Goryunkov, A. A.; Kuvychko, I. V.; Ioffe, I. N.; Dick, D. L.; Sidorov, L. N.; Strauss, S. H.; Boltalina, O. V. *J. Fluorine Chem.* **2003**, *124*, 61.

- (28) Boltalina, O. V.; Goryunkov, A. A.; Markov, V. Y.; Ioffe, I. N.; Sidorov, L. N. *Int. J. Mass Spectrom.* **2003**, *228*, 807.
- (29) Darwish, A. D.; Abdul-Sada, A. K.; Avent, A. G.; Martsinovich, N.; Street, J. M.; Taylor, R. *J. Fluorine Chem.* **2004**, *125*, 1383.
- (30) Kareev, I. E.; Lebedkin, S. F.; Bubnov, V. P.; Yagubskii, E. B.; Ioffe, I. N.; Khavrel, P. A.; Kuvychko, I. V.; Strauss, S. H.; Boltalina, O. V. *Angew. Chem., Int. Ed.* **2005**, *44*, 1846.
- (31) Kareev, I. E.; Santiso-Quinones, G.; Kuvychko, I. V.; Ioffe, I. N.; Goldt, I. V.; Lebedkin, S. F.; Seppelt, K.; Strauss, S. H.; Boltalina, O. V. *J. Am. Chem. Soc.* **2005**, *127*, 11497.
- (32) Kareev, I. E.; Kuvychko, I. V.; Popov, A. A.; Lebedkin, S. F.; Miller, S. M.; Anderson, O. P.; Strauss, S. H.; Boltalina, O. V. *Angew. Chem., Int. Ed.* **2005**, *44*, 7984.
- (33) Goryunkov, A. A.; Dorozhkin, E. I.; Ignat'eva, D. V.; Sidorov, L. N.; Kemnitz, E.; Sheldrick, G.; Troyanov, S. I. *Mendeleev Commun.* **2005**, *225*.
- (34) Borschhevskii, A. Y.; Aleshina, V. E.; Markov, V. Y.; Dorozhkin, E. I.; Sidorov, L. N. *Inorg. Mater.* **2005**, *41*, 1318.
- (35) Darwish, A. D.; Abdul-Sada, A. K.; Taylor, R. *Fullerenes, Nanotubes, Carbon Nanostruct.* **2006**, *14*, 111.
- (36) Troyanov, S. I.; Dimitrov, A.; Kemnitz, E. *Angew. Chem., Int. Ed.* **2006**, *45*, 1971.
- (37) Markov, V. Y.; Aleshina, V. E.; Borschhevskii, A. Y.; Khatymov, R. V.; Tuktarov, R. F.; Pogulay, A. V.; Maximov, A. L.; Kardashev, S. V.; Ioffe, I. N.; Avdoshenko, S. M.; Dorozhkin, E. I.; Goryunkov, A. A.; Ignat'eva, D. V.; Gruzinskaya, N. I.; Sidorov, L. N. *Int. J. Mass Spectrom.* **2006**, *251*, 16.
- (38) Dorozhkin, E. I.; Ignat'eva, D. V.; Tamm, N. B.; Goryunkov, A. A.; Khavrel, P. A.; Ioffe, I. N.; Popov, A. A.; Kuvychko, I. V.; Strelets'kiy, A. V.; Markov, V. Y.; Spandl, J.; Strauss, S. H.; Boltalina, O. V. *Chem.—Eur. J.* **2006**, *12*, 3876.
- (39) Kareev, I. E.; Shustova, N. B.; Kuvychko, I. V.; Lebedkin, S. F.; Miller, S. M.; Anderson, O. P.; Popov, A. A.; Strauss, S. H.; Boltalina, O. V. *J. Am. Chem. Soc.* **2006**, *128*, 12268.
- (40) Kareev, I. E.; Kuvychko, I. V.; Lebedkin, S. F.; Miller, S. M.; Anderson, O. P.; Strauss, S. H.; Boltalina, O. V. *Chem. Commun.* **2006**, *308*.
- (41) Goryunkov, A. A.; Kareev, I. E.; Ioffe, I. N.; Popov, A. A.; Kuvychko, I. V.; Markov, V. Y.; Goldt, I. V.; Pimenova, A. S.; Serov, M. G.; Avdoshenko, S. M.; Khavrel, P. A.; Sidorov, L. N.; Lebedkin, S. F.; Mazej, Z.; Zemva, B.; Strauss, S. H.; Boltalina, O. V. *J. Fluorine Chem.* **2006**, *127*, 1423.
- (42) Kareev, I. E.; Miller, S. M.; Anderson, O. P.; Strauss, S. H.; Boltalina, O. V. *Acta Crystallogr.* **2006**, *E62*, o617.
- (43) (a) Kareev, I. E.; Lebedkin, S. F.; Popov, A. A.; Miller, S. M.; Anderson, O. P.; Strauss, S. H.; Boltalina, O. V. *Acta Crystallogr.* **2006**, *E62*, o1501. (b) Kareev, I. E.; Lebedkin, S. F.; Miller, S. M.; Anderson, O. P.; Strauss, S. H.; Boltalina, O. V. *Acta Crystallogr.* **2006**, *E62*, o1498.
- (44) Kareev, I. E.; Shustova, N. B.; Newell, B. S.; Miller, S. M.; Anderson, O. P.; Strauss, S. H.; Boltalina, O. V. *Acta Crystallogr.* **2006**, *E62*, o3154.
- (45) Kareev, I. E.; Lebedkin, S. F.; Miller, S. M.; Anderson, O. P.; Strauss, S. H.; Boltalina, O. V. *Acta Crystallogr.* **2006**, *E62*, o620.
- (46) Goryunkov, A. A.; Ignat'eva, D. V.; Tamm, N. B.; Moiseeva, N. N.; Ioffe, I. N.; Avdoshenko, S. M.; Markov, V. Y.; Sidorov, L. N.; Kemnitz, E.; Troyanov, S. I. *Eur. J. Org. Chem.* **2006**, *2508*.
- (47) Dorozhkin, E. I.; Ignat'eva, D. V.; Tamm, N. B.; Vasilyuk, N. V.; Goryunkov, A. A.; Avdoshenko, S. M.; Ioffe, I. N.; Sidorov, L. N.; Pattison, P.; Kemnitz, E.; Troyanov, S. I. *J. Fluorine Chem.* **2006**, *127*, 1344.
- (48) Ignat'eva, D. V.; Goryunkov, A. A.; Tamm, N. B.; Ioffe, I. N.; Avdoshenko, S. M.; Sidorov, L. N.; Dimitrov, A.; Kemnitz, E.; Troyanov, S. I. *Chem. Commun.* **2006**, *1778*.
- (49) Avdoshenko, S. M.; Goryunkov, A. A.; Ioffe, I. N.; Ignat'eva, D. V.; Sidorov, L. N.; Pattison, P.; Kemnitz, E.; Troyanov, S. I. *Chem. Commun.* **2006**, *2463*.
- (50) Shustova, N. B.; Kuvychko, I. V.; Bolskar, R. D.; Seppelt, K.; Strauss, S. H.; Popov, A. A.; Boltalina, O. V. *J. Am. Chem. Soc.* **2006**, *128*, 15793.
- (51) Troyanov, S. I.; Goryunkov, A. A.; Dorozhkin, E. I.; Ignat'eva, D. V.; Tamm, N. B.; Avdoshenko, S. M.; Ioffe, I. N.; Markov, V. Y.; Sidorov, L. N.; Scheural, K.; Kemnitz, E. *J. Fluorine Chem.* **2007**, *128*, 545.
- (52) Omelyanyuk, N. A.; Goryunkov, A. A.; Tamm, N. B.; Avdoshenko, S. M.; Ioffe, I. N.; Sidorov, L. N.; Kemnitz, E.; Troyanov, S. I. *Chem. Commun.* **2007**, *4794*.
- (53) Goryunkov, A. A.; Dorozhkin, E. I.; Tamm, N. B.; Ignat'eva, D. V.; Avdoshenko, S. M.; Sidorov, L. N.; Troyanov, S. I. *Mendeleev Commun.* **2007**, *17*, 110.
- (54) Tamm, N. B.; Avdoshenko, S. M.; Kemnitz, E.; Troyanov, S. I. *Russ. Chem. Bull. Int. Ed.* **2007**, *56*, 915.
- (55) Troyanov, S. I.; Goryunkov, A. A.; Dorozhkin, E. I.; Ignat'eva, D. V.; Tamm, N. B.; Avdoshenko, S. M.; Ioffe, I. N.; Markov, V. Y.; Sidorov, L. N.; Scheurel, K.; Kemnitz, E. *J. Fluorine Chem.* **2007**, *128*, 545.
- (56) Kareev, I. E.; Shustova, N. B.; Peryshkov, D. V.; Lebedkin, S. F.; Miller, S. M.; Anderson, O. P.; Popov, A. A.; Boltalina, O. V.; Strauss, S. H. *Chem. Commun.* **2007**, *1650*.
- (57) Shustova, N. B.; Newell, B. S.; Miller, S. M.; Anderson, O. P.; Bolskar, R. D.; Seppelt, K.; Popov, A. A.; Boltalina, O. V.; Strauss, S. H. *Angew. Chem., Int. Ed.* **2007**, *46*, 4111.
- (58) Shustova, N. B.; Peryshkov, D. V.; Kareev, I. E.; Boltalina, O. V.; Strauss, S. H. *Acta Crystallogr.* **2007**, *E63*, o3398.
- (59) Shustova, N. B.; Peryshkov, D. V.; Kareev, I. E.; Boltalina, O. V.; Strauss, S. H. *Acta Crystallogr.* **2007**, *E63*, o3928.
- (60) Shustova, N. B.; Kuvychko, I. V.; Boltalina, O. V.; Strauss, S. H. *Acta Crystallogr.* **2007**, *E63*, o4575.
- (61) Pimenova, A. S.; Kozlov, A. A.; Goryunkov, A. A.; Markov, V. Y.; Khavrel, P. A.; Avdoshenko, S. M.; Ioffe, I. N.; Sakharov, S. G.; Troyanov, S. I.; Sidorov, L. N. *Chem. Commun.* **2007**, *374*.
- (62) Pimenova, A. S.; Kozlov, A. A.; Goryunkov, A. A.; Markov, V. Y.; Khavrel, P. A.; Avdoshenko, S. M.; Vorobiev, V. A.; Ioffe, I. N.; Sakharov, S. G.; Troyanov, S. I.; Sidorov, L. N. *Dalton Trans.* **2007**, *5322*.
- (63) Dorozhkin, E. I.; Goryunkov, A. A.; Ioffe, I. N.; Avdoshenko, S. M.; Markov, V. Y.; Tamm, N. B.; Ignat'eva, D. V.; Sidorov, L. N.; Troyanov, S. I. *Eur. J. Org. Chem.* **2007**, *5082*.
- (64) Shustova, N. B.; Popov, A. A.; Mackey, M. A.; Coumbe, C. E.; Phillips, J. P.; Stevenson, S.; Strauss, S. H.; Boltalina, O. V. *J. Am. Chem. Soc.* **2007**, *129*, 11676.
- (65) Pimenova, A. S.; Sidorov, L. N.; Kemnitz, E.; Troyanov, S. I. *Eur. J. Org. Chem.* **2007**, *4999*.
- (66) Kareev, I. E.; Bubnov, V. P.; Fedutin, D. N.; Yagubskii, E. B.; Lebedkin, S. F.; Laukhina, E. E.; Kuvychko, I. V.; Strauss, S. H.; Boltalina, O. V. In *Hydrogen Materials Science and Chemistry of Carbon Nanomaterials*; T. N. V., Ed.; Springer: New York, 2007.
- (67) Shustova, N. B.; Anderson, O. P.; Boltalina, O. V.; Strauss, S. H.; Kareev, I. E. *Acta Crystallogr.* **2008**, *E64*, o159.
- (68) Popov, A. A.; Kareev, I. E.; Shustova, N. B.; Lebedkin, S. F.; Strauss, S. H.; Boltalina, O. V.; Dunsch, L. *Chem.—Eur. J.* **2008**, *14*, 107.
- (69) Kareev, I. E.; Kuvychko, I. V.; Shustova, N. B.; Lebedkin, S. F.; Bubnov, V. P.; Anderson, O. P.; Popov, A. A.; Boltalina, O. V.; Strauss, S. H. *Angew. Chem., Int. Ed.* **2008**, *47*, 6204.
- (70) Kareev, I. E.; Popov, A. A.; Kuvychko, I. V.; Shustova, N. B.; Lebedkin, S. F.; Bubnov, V. P.; Anderson, O. P.; Seppelt, K.; Strauss, S. H.; Boltalina, O. V. *J. Am. Chem. Soc.* **2008**, *130*, 13471.
- (71) Mutig, T.; Ioffe, I. N.; Kemnitz, E.; Troyanov, S. I. *Mendeleev Commun.* **2008**, *18*, 73.
- (72) Mutig, T.; Kemnitz, E.; Troyanov, S. I. *Eur. J. Org. Chem.* **2008**, *3256*.
- (73) Troyanov, S. I.; Goryunkov, A. A.; Tamm, N. B.; Markov, V. Y.; Ioffe, I. N.; Sidorov, L. N. *Dalton Trans.* **2008**, *2627*.

- (74) Samokhvalova, N. A.; Khavrel', P. A.; Goryunkov, A. A.; Ioffe, I. N.; Karnatsevich, V. L.; Sidorov, L. N.; Kemnitz, E.; Troyanov, S. I. *Russ. Chem. Bull.* **2008**, *57*, 2526.
- (75) Kareev, I. E.; Bubnov, V. P.; Yagubskii, E. B. *Russ. Chem. Bull.* **2008**, *57*, 1486.
- (76) Ovchinnikova, N. S.; Ignat'eva, D. V.; Tamm, N. B.; Avdoshenko, S. M.; Goryunkov, A. A.; Loffe, I. N.; Markov, V. Y.; Troyanov, S. I.; Sidorov, L. N.; Yurovskaya, M. A.; Kemnitz, E. *New J. Chem.* **2008**, *32*, 89.
- (77) Tamm, N. B.; Ioffe, I. N.; Kemnitz, E.; Troyanov, S. I. *Dalton Trans.* **2009**, 2740.
- (78) Tamm, N. B.; Troyanov, S. I. *Mendeleev Commun.* **2009**, *19*, 198.
- (79) Mutig, T.; Kemnitz, E.; Troyanov, S. I. *Mendeleev Commun.* **2009**, *19*, 30.
- (80) Mutig, T.; Avdoshenko, S. M.; Kemnitz, E.; Troyanov, S. I. *Fluorine Chem.* **2009**, *130*, 241.
- (81) Troyanov, S. I.; Tamm, N. B. *Crystallogr. Rep.* **2009**, *54*, 598.
- (82) Samokhvalova, N. A.; Khavrel, P. A.; Markov, V. Y.; Samokhvalov, P. S.; Goryunkov, A. A.; Kemnitz, E.; Sidorov, L. N.; Troyanov, S. I. *Eur. J. Org. Chem.* **2009**, 2935.
- (83) Tamm, N. B.; Sidorov, L. N.; Kemnitz, E.; Troyanov, S. I. *Chem.—Eur. J.* **2009**, *15*, 10486.
- (84) (a) Tamm, N. B.; Sidorov, L. N.; Kemnitz, E.; Troyanov, S. I. *Angew. Chem.-Int. Ed.* **2009**, *48*, 9102. (b) Lanskikh, M. A.; Tamm, N. B.; Sidorov, L. N.; Troyanov, S. I. *Inorg. Chem.* **2012**, *51*, 2719.
- (85) Lyakhovetsky, V. I.; Bashilov, V. V.; Efanova, T. V.; Shilova, E. A.; Sokolov, V. I.; Nekrasov, Y. S.; Taylor, T. R. *Fullerenes, Nanotubes, Carbon Nanostruct.* **2009**, *17*, 85.
- (86) Troyanov, S. I.; Tamm, N. B. *Chem. Commun.* **2009**, 6035.
- (87) Ignat'eva, D. V.; Mutig, T.; Goryunkov, A. A.; Tamm, N. B.; Kemnitz, E.; Troyanov, S. I.; Sidorov, L. N. *Russ. Chem. Bull.* **2009**, *58*, 1146.
- (88) Shustova, N. B.; Chen, Y. S.; Mackey, M. A.; Coumbe, C. E.; Phillips, J. P.; Stevenson, S.; Popov, A. A.; Boltalina, O. V.; Strauss, S. H. *J. Am. Chem. Soc.* **2009**, *131*, 17630.
- (89) Gruzinskaya, N. I.; Pimenova, A. S.; Khavrel, P. A.; Sidorov, L. N.; Kemnitz, E.; Troyanov, S. I. *Russ. Chem. Bull.* **2009**, *58*, 2276.
- (90) Tamm, N. B.; Troyanov, S. I. *Mendeleev Commun.* **2010**, *20*, 229.
- (91) Vorobiev, A. K.; Markov, V. Y.; Samokhvalova, N. A.; Samokhvalov, P. S.; Troyanov, S. I.; Sidorov, L. N. *Mendeleev Commun.* **2010**, *20*, 7.
- (92) Markov, V. Y.; Samokhvalova, N. A.; Samokhvalov, P. S.; Ioutsi, V. A.; Khavrel, P. A.; Ovchinnikova, N. S.; Sidorov, L. N. *J. Anal. Chem.* **2010**, *65*, 1495.
- (93) Shustova, N. B.; Peryshkov, D. V.; Kuvychko, I. V.; Chen, Y.-S.; Mackey, M. A.; Coumbe, C. E.; Heaps, D. T.; Confaite, B. S.; Heine, T.; Phillips, J. P.; Stevenson, S.; Dunsch, L.; Popov, A. A.; Strauss, S. H.; Boltalina, O. V. *J. Am. Chem. Soc.* **2011**, *133*, 2672.
- (94) Shustova, N. B.; Kuvychko, I. V.; Peryshkov, D. V.; Whitaker, J. B.; Larson, B. W.; Chen, Y. S.; Dunsch, L.; Seppelt, K.; Popov, A. A.; Strauss, S. H.; Boltalina, O. V. *Chem. Commun.* **2011**, *47*, 875.
- (95) Shustova, N. B.; Kareev, I. E.; Kuvychko, I. V.; Whitaker, J. B.; Lebedkin, S. F.; Popov, A. A.; Chen, Y. S.; Seppelt, K.; Strauss, S. H.; Boltalina, O. V. *J. Fluorine Chem.* **2010**, *131*, 1198.
- (96) Troyanov, S. I.; Tamm, N. B. *Crystallogr. Rep.* **2010**, *55*, 432.
- (97) Gruzinskaya, N. I.; Silin, A. I.; Pimenova, A. S.; Khavrel, P. A.; Markov, V. Y.; Sidorov, L. N.; Kemnitz, E.; Troyanov, S. I. *New J. Chem.* **2010**, *34*, 243.
- (98) Mutig, T.; Kemnitz, E.; Troyanov, S. I. *J. Fluorine Chem.* **2010**, *131*, 861.
- (99) Takano, Y.; Herranz, M. Á.; Martín, N.; Rojas, G. M.; Guldi, D. M.; Kareev, I. E.; Strauss, S. H.; Boltalina, O. V.; Tsuchiya, T.; Akasaka, T. *Chem.—Eur. J.* **2010**, *16*, 5343.
- (100) Yang, S.; Chen, C.; Jiao, M.; Tamm, N. B.; Lanskikh, M. A.; Kemnitz, E.; Troyanov, S. I. *Inorg. Chem.* **2011**, *50*, 3766.
- (101) Kuvychko, I. V.; Whitaker, J. B.; Larson, B. W.; Raguindin, R. S.; Suhr, K. J.; Strauss, S. H.; Boltalina, O. V. *J. Fluorine Chem.* **2011**, *132*, 679.
- (102) Yang, S.; Chen, C.; Lanskikh, M. A.; Tamm, N. B.; Kemnitz, E.; Troyanov, S. I. *Chem.—Asian J.* **2011**, *6*, 505.
- (103) Kuvychko, I. V.; Shustova, N. B.; Avdoshenko, S. M.; Popov, A. A.; Strauss, S. H.; Boltalina, O. V. *Chem.—Eur. J.* **2011**, *17*, 8799.
- (104) Kuvychko, I. V.; Whitaker, J. B.; Larson, B. W.; Folsom, T. C.; Shustova, N. B.; Avdoshenko, S. M.; Chen, Y.-S.; Wen, H.; Wang, X.; Dunsch, L.; Popov, A. A.; Boltalina, O. V.; Strauss, S. H. *Chem. Sci.* **2012**, *3*, 1399.
- (105) Romanova, N. A.; Tamm, N. B.; Markov, V. Y.; Goryunkov, A. A.; Sidorov, L. N.; Troyanov, S. I. *Mendeleev Commun.* **2012**, *22*, 297.
- (106) Wang, Z.; Nakanishi, Y.; Noda, S.; Niwa, H.; Zhang, J.; Kitaura, R.; Shinohara, H. *Angew. Chem., Int. Ed.* **2013**, *52*, 11770.
- (107) Chang, K.; Fritz, M. A.; Tamm, N. B.; Goryunkov, A. A.; Sidorov, L. N.; Chen, C.; Yang, S.; Kemnitz, E.; Troyanov, S. I. *Chem.—Eur. J.* **2013**, *19*, 578.
- (108) Romanova, N. A.; Fritz, M. A.; Chang, K.; Tamm, N. B.; Goryunkov, A. A.; Sidorov, L. N.; Chen, C.; Yang, S.; Kemnitz, E.; Troyanov, S. I. *Chem.—Eur. J.* **2013**, *19*, 11707.
- (109) Ignat'eva, D. V.; Goryunkov, A. A.; Tamm, N. B.; Ioffe, I. N.; Sidorov, L. N.; Troyanov, S. I. *New J. Chem.* **2013**, *37*, 299.
- (110) Samoylova, N. A.; Belov, N. M.; Brotsman, V. A.; Ioffe, I. N.; Lukonina, N. S.; Markov, V. Y.; Ruff, A.; Rybalchenko, A. V.; Schuler, P.; Semivrazhskaya, O. O.; Speiser, B.; Troyanov, S. I.; Magdesieva, T. V.; Goryunkov, A. A. *Chem.—Eur. J.* **2013**, *19*, 17969.
- (111) Belov, N. M.; Apenova, M. G.; Rybalchenko, A. V.; Borkovskaya, E. V.; Lukonina, N. S.; Goryunkov, A. A.; Ioffe, I. N.; Troyanov, S. I.; Sidorov, L. N. *Chem.—Eur. J.* **2014**, *20*, 1126.
- (112) Wei, T.; Tamm, N. B.; Yang, S.; Troyanov, S. I. *Chem.—Asian J.* **2014**, *9*, 2449.
- (113) Whitaker, J. B.; Kuvychko, I. V.; Shustova, N. B.; Chen, Y.-S.; Strauss, S. H.; Boltalina, O. V. *Chem. Commun.* **2014**, *50*, 1205.
- (114) Shustova, N. B.; Peryshkov, D. V.; Popov, A. A.; Boltalina, O. V.; Strauss, S. H. *Acta Crystallogr., Sect. E* **2007**, *63*, O3129.
- (115) Popov, A. A.; Kareev, I. E.; Shustova, N. B.; Strauss, S. H.; Boltalina, O. V.; Dunsch, L. *J. Am. Chem. Soc.* **2010**, *132*, 11709.
- (116) Popov, A. A.; Shustova, N. B.; Boltalina, O. V.; Strauss, S. H.; Dunsch, L. *ChemPhysChem* **2008**, *9*, 431.
- (117) Tamm, N. B.; Troyanov, S. I. *Mendeleev Commun.* **2007**, *17*, 172.
- (118) Shustova, N. B.; Kareev, I. E.; Popov, A. A.; Boltalina, O. V.; Strauss, S. H. *Acta Crystallogr.* **2007**, *E62*, 4073.
- (119) Kareev, I. E.; Boltalina, O. V.; Strauss, S. H.; Popov, A. A. unpublished, predicted on the basis of <sup>19</sup>F NMR data and DFT calculations, 2010.
- (120) Krusic, P. J.; Wasserman, E.; Keizer, P. N.; Morton, J. R.; Preston, K. F. *Science* **1991**, *254*, 1183.
- (121) (a) Cremonini, M. A.; Lunazzi, L.; Placucci, G.; Krusic, P. J. *J. Org. Chem.* **1993**, *58*, 4735. (b) Morton, J. R.; Negri, F.; Preston, K. F. *Acc. Chem. Res.* **1998**, *31*, 63.
- (122) Dolbier, J. W. R. *Chem. Rev.* **1996**, *96*, 1557.
- (123) Ruoff, R. S.; Tse, D. S.; Malhotra, R.; Lorents, D. C. *J. Phys. Chem.* **1993**, *97*, 3379.
- (124) Scherer, K. V.; Ono, T.; Yamanouchi, K.; Fernandez, R.; Henderson, P. *J. Am. Chem. Soc.* **1985**, *107*, 718.
- (125) Kuvychko, I. V.; Strauss, S. H.; Boltalina, O. V. In *Efficient Preparation of Fluorine Compounds*; Roesky, H., Ed.; Wiley: New York, 2012.
- (126) Clare, B. W.; Kepert, D. L. *J. Mol. Struct. (THEOCHEM)* **2003**, *621*, 211.
- (127) Kareev, I. E.; Bubnov, V. P.; Fedutin, D. N.; Yagubskii, E. B.; Lebedkin, S. F.; Laukhina, E. E.; Kuvychko, I. V.; Strauss, S. H.; Boltalina, O. V. Proc. NATO Adv. Res. Workshop on Hydrogen Materials Science and Chemistry of Carbon Nanomaterials, 2007; p 235.
- (128) Goldt, I. V. Ph.D. Dissertation, Moscow State University, 2004.
- (129) Troshin, P. A.; Avent, A. G.; Darwish, A. D.; Martsinovich, N.; Abdul-Sada, A. a. K.; Street, J. M.; Taylor, R. *Science* **2005**, *309*, 278.
- (130) Chambers, R. D. *Fluorine in Organic Chemistry*; Blackwell Publishing Ltd.: Cambridge, MA, 2004.

- (131) Gakh, A. A.; Tuinman, A. A. *J. Phys. Chem. A* **2000**, *104*, 5888.
- (132) Fields, E. K.; Meyerson, S. *J. Org. Chem.* **1971**, *41*, 916.
- (133) Duan, Y. Y.; Shi, L.; Sun, L. Q.; Zhu, M. S.; Han, L. Z. *Int. J. Thermophys.* **2000**, *21*, 393.
- (134) Kumaran, S.; Su, M. C.; Lim, K. P.; Michael, J. V. *Chem. Phys. Lett.* **1995**, *243*, 59.
- (135) Charles, S. W.; Fischer, P. H. H.; McDowell, C. A. *Chem. Phys. Lett.* **1967**, *1*, 451.
- (136) Huang, S.; Yang, X.; Zhang, X.; Hu, X.; Gan, L.; Zhang, S. *Synlett* **2006**, *8*, 1266.
- (137) (a) Kuvychko, I. V.; Streletskaia, A. A.; Shustova, N. B.; Seppelt, K.; Drewello, T.; Popov, A. A.; Strauss, S. H.; Boltalina, O. V. *J. Am. Chem. Soc.* **2010**, *132*, 6443. (b) Hirsch, A.; Brettreich, M. *Fullerenes – Chemistry and Reactions*; Wiley-VCH: Weinheim, 2005. (c) Zenner, T.; Zabel, H. *J. Phys. Chem.* **1993**, *97*, 8690.
- (138) Kao, C. P. C.; Miller, R. *J. Chem. Eng. Data* **2000**, *45*, 295.
- (139) (a) Troyanov, S. I.; Tamm, N. B. *Crystallogr. Rep.* **2010**, *55*, 432. (b) Lanskikh, M. A.; Chang, K.; Tamm, N. B.; Kemnitz, E.; Troyanov, S. I. *Mendeleev Commun.* **2012**, *22*, 136. (c) Yang, S.; Wei, T.; Tamm, N. B.; Kemnitz, E.; Troyanov, S. I. *Inorg. Chem.* **2013**, *52*, 4768.
- (140) Romanova, N. A.; Papina, T. y. S.; Luk'yanova, V. A.; Buyanova, A. G.; Varuschenko, R. M.; Druzhinina, A. I.; Goryunkov, A. A.; Markov, V. Y.; Panin, R. A.; Sidorov, L. N. *J. Chem. Thermodyn.* **2013**, *66*, 59.
- (141) (a) Troyanov, S. I.; Kemnitz, E. *Mendeleev Commun.* **2008**, *18*, 27. (b) Goryunkov, A. A.; Samokhvalova, N. A.; Khavrel, P. A.; Belov, N. M.; Markov, V. Y.; Sidorov, L. N.; Troyanov, S. I. *New J. Chem.* **2011**, *35*, 32.
- (142) Avdoshenko, S. M.; Ioffe, I. N.; Sidorov, L. N. *J. Phys. Chem. A* **2009**, *113*, 10833.
- (143) Li, C.-Z.; Matsuo, Y.; Niinomi, T.; Sato, Y.; Nakamura, E. *Chem. Commun.* **2010**, *46*, 8582.
- (144) Gruzinskaya, N. I.; Aleshina, V. E.; Borchshevskii, A. Y.; Troyanov, S. I.; Sidorov, L. N. *Russ. J. Phys. Chem. A* **2007**, *81*.
- (145) Gigli, G.; Balducci, G.; Markov, V. Y.; Boltalina, O. V.; Goryunkov, A. A.; Sidorov, L. N.; Taylor, R. *J. Chem. Thermodyn.* **2002**, *34*, 57.
- (146) Takano, Y.; Herranz, M. A.; Kareev, I. E.; Strauss, S. H.; Boltalina, O. V.; Akasaka, T.; Martin, N. *J. Org. Chem.* **2009**, *74*, 6902.
- (147) Balasubramanian, K. *Chem. Phys. Lett.* **1991**, *182*, 257.
- (148) (a) Matsuzawa, N.; Dixon, D. A.; Fukunaga, T. *J. Phys. Chem.* **1992**, *96*, 7594. (b) Dixon, D. A.; Matsuzawa, N.; Fukunaga, T.; Tebbe, F. N. *J. Phys. Chem.* **1992**, *96*, 6107.
- (149) Henderson, C. C.; Cahill, P. A. *Science* **1993**, *259*, 1885.
- (150) Boltalina, O. V.; Lukonin, A. Y.; Street, J. M.; Taylor, R. *Chem. Commun.* **2000**, 1601.
- (151) Goryunkov, A. A.; Ioffe, I. N.; Kuvychko, I. V.; Yankova, T. S.; Markov, V. Y.; Streletskaia, A. A.; Dick, D. L.; Sidorov, L. N.; Boltalina, O. V.; Strauss, S. H. *Fullerenes, Nanotubes, Carbon Nanostruct.* **2004**, *12*, 181.
- (152) Clare, B. W.; Kepert, D. L. *J. Mol. Struct. (THEOCHEM)* **1995**, *358*, 79.
- (153) Birkett, P. R.; Hitchcock, P. B.; Kroto, H. W.; Taylor, R.; Walton, D. R. M. *Nature* **1992**, *357*, 479.
- (154) Fowler, P. W.; Rogers, K. M.; Somers, K. R.; Troisi, A. *J. Chem. Soc., Perkin Trans. 2* **1999**, 2023.
- (155) Tebbe, F. N.; Harlow, R. L.; Chase, D. B.; Thorn, D. L.; Campbell, G. C.; Calabrese, J. C.; Herron, N.; Young, R. J.; Wasserman, E. *Science* **1992**, *256*, 822.
- (156) Ignat'eva, D. V.; Goryunkov, A. A.; Ioffe, I. N.; Sidorov, L. N. *J. Phys. Chem. A* **2013**, *117*, 13009.
- (157) Ignat'eva, D. V.; Ioffe, I. N.; Troyanov, S. I.; Sidorov, L. N. *Russ. Chem. Rev.* **2011**, *80*, 631.
- (158) Shustova, N. B.; Kuvychko, I. V.; Popov, A. A.; von Delius, M.; Dunsch, L.; Anderson, O. P.; Hirsch, A.; Strauss, S. H.; Boltalina, O. V. *Angew. Chem., Int. Ed.* **2011**, *50*, 5537.
- (159) Clare, B. W.; Kepert, D. L. *J. Mol. Struct. (THEOCHEM)* **1999**, *491*, 249.
- (160) (a) Birkett, P. R.; Avent, A. G.; Darwish, A. D.; Kroto, H. W.; Taylor, R.; Walton, D. R. M. *J. Chem. Soc., Chem. Commun.* **1995**, 683. (b) Avent, A. G.; Benito, A. M.; Birkett, P. R.; Darwish, A. D.; Hitchcock, P. B.; Kroto, H. W.; Locke, I. W.; Meidine, M. F.; O'Donovan, B. F.; Prassides, K.; Taylor, R.; Walton, D. R. M.; van Wijnkoop, M. *J. Mol. Struct. (THEOCHEM)* **1997**, *437*, 1. (c) Spielmann, H. P.; Weedon, B. R.; Meier, M. S. *J. Org. Chem.* **2000**, *65*, 2755. (d) Al-Matar, H.; Sada, A. K. A.; Avent, A. G.; Taylor, R.; Wei, X. *W. J. Chem. Soc., Perkin Trans. 2* **2002**, 1251. (e) Troyanov, S. I.; Popov, A. A.; Denisenko, N. I.; Boltalina, O. V.; Sidorov, L. N.; Kemnitz, E. *Angew. Chem., Int. Ed.* **2003**, *42*, 2395.
- (161) Xiao, Z.; Wang, F. D.; Huang, S. H.; Gan, L. B.; Zhou, J.; Yuan, G.; Lu, M. J.; Pan, J. Q. *J. Org. Chem.* **2005**, *70*, 2060.
- (162) Haddon, R. C. *Science* **1993**, *261*, 1545.
- (163) Hitchcock, P. B.; Avent, A. G.; Martsinovich, N.; Troshin, P. A.; Taylor, R. *Chem. Commun.* **2005**, 75.
- (164) Troyanov, S. I.; Shustova, N. B.; Ioffe, I. N.; Turnbull, A. P.; Kemnitz, E. *Chem. Commun.* **2005**, 72.
- (165) Lanskikh, M.; Belova, Y.; Tamm, N.; Chang, K.; Kemnitz, E.; Troyanov, S. *Crystallogr. Rep.* **2011**, *56*, 1047.
- (166) (a) Yang, S.; Chen, C.; Wei, T.; Tamm, N. B.; Kemnitz, E.; Troyanov, S. I. *Chem.—Eur. J.* **2012**, *18*, 2217. (b) Tamm, N. B.; Sidorov, L. N.; Troyanov, S. I. *Moscow Univ. Chem. Bull.* **2009**, *64*, 327.
- (167) Romanova, N. A.; Fritz, M. A.; Tamm, N. B.; Troyanov, S. I. *Mendeleev Commun.* **2014**, *24*, 78.
- (168) Tamm, N.; Troyanov, S. *Nanosyst.: Phys., Chem., Math.* **2014**, *5*, 39.
- (169) Popov, A. A.; Dunsch, L. *J. Am. Chem. Soc.* **2008**, *130*, 17726.
- (170) Popov, A. A.; Dunsch, L. *Phys. Chem. Chem. Phys.* **2011**, *13*, 8977.
- (171) Kuvychko, I. V.; Streletskaia, A. V.; Popov, A. A.; Kotsiris, S. G.; Drewello, T.; Strauss, S. H.; Boltalina, O. V. *Chem.—Eur. J.* **2005**, *11*, 5426.
- (172) Orlandi, G.; Negri, F. *Photochem. Photobiol. Sci.* **2002**, *1*, 289.
- (173) Ma, B.; Sun, Y. P. *J. Chem. Soc., Perkin Trans. 2* **1996**, 2157.
- (174) (a) Arbogast, J. W.; Darmanyan, A. P.; Foote, C. S.; Rubin, Y.; Diederich, F. N.; Alvarez, M. M.; Anz, S. J.; Whetten, R. L. *J. Phys. Chem.* **1991**, *95*, 11. (b) Arbogast, J. W.; Foote, C. S. *J. Am. Chem. Soc.* **1991**, *113*, 8886. (c) Kim, D. H.; Lee, M. Y.; Suh, Y. D.; Kim, S. K. *J. Am. Chem. Soc.* **1992**, *114*, 4429. (d) Catalan, J.; Elguero, J. *J. Am. Chem. Soc.* **1993**, *115*, 9249.
- (175) (a) Ma, B.; Bunker, C. E.; Guduru, R.; Zhang, X. F.; Sun, Y. P. *J. Phys. Chem. A* **1997**, *101*, 5626. (b) Sun, Y. P.; Drovetskaya, T.; Bolksar, R. D.; Bau, R.; Boyd, P. D. W.; Reed, C. A. *J. Org. Chem.* **1997**, *62*, 3642. (c) Nakamura, Y.; Taki, M.; Tobita, S.; Shizuka, H.; Yokoi, H.; Ishiguro, K.; Sawaki, Y.; Nishimura, J. *J. Chem. Soc., Perkin Trans. 2* **1999**, 127.
- (176) Castro, K. P.; Jin, Y.; Rack, J. J.; Strauss, S. H.; Boltalina, O. V.; Popov, A. A. *J. Phys. Chem. Lett.* **2013**, *4*, 2500.
- (177) (a) Boltalina, O. V.; Sidorov, L. N.; Borshchevsky, A. Y.; Sukhanova, E. V.; Skokan, E. V. *Rapid Commun. Mass Spectrom.* **1993**, *7*, 1009. (b) Brink, C.; Andersen, L. H.; Hvelplund, P.; Mathur, D.; Voldstad, J. D. *Chem. Phys. Lett.* **1995**, *233*, 52. (c) Wang, X. B.; Ding, C. F.; Wang, L. S. *J. Chem. Phys.* **1999**, *110*, 8217.
- (178) Yang, Y. F.; Arias, F.; Echegoyen, L.; Chibante, L. P. F.; Flanagan, S.; Robertson, A.; Wilson, L. J. *J. Am. Chem. Soc.* **1995**, *117*, 7801.
- (179) Xie, Q. S.; Perezcordero, E.; Echegoyen, L. *J. Am. Chem. Soc.* **1992**, *114*, 3978.
- (180) Azamar-Barrios, J. A.; Dennis, T. J. S.; Sadhukan, S.; Shinohara, H.; Scuseria, G. E.; Penicaud, A. *J. Phys. Chem. A* **2001**, *105*, 4627.
- (181) Nagatsuka, J.; Sugitani, S.; Kako, M.; Nakahodo, T.; Mizorogi, N.; Ishitsuka, M. O.; Maeda, Y.; Tsuchiya, T.; Akasaka, T.; Gao, X.; Nagase, S. *J. Am. Chem. Soc.* **2010**, *132*, 12106.
- (182) Fan, L. Z.; Li, Y. F.; Li, F. Y.; Li, Y. L.; Zhu, D. B. *Chem. Phys. Lett.* **1998**, *294*, 443.
- (183) (a) Keshavarz-K, M.; Knight, B.; Srđanov, G.; Wudl, F. *J. Am. Chem. Soc.* **1995**, *117*, 11371. (b) Jousselle, B.; Sonmez, G.; Wudl, F. *J. Mater. Chem.* **2006**, *16*, 3478.

- (184) (a) Zhou, F. M.; Vanberkel, G. J.; Donovan, B. T. *J. Am. Chem. Soc.* **1994**, *116*, 5485. (b) Paolucci, D.; Paolucci, F.; Marcaccio, M.; Carano, M.; Taylor, R. *Chem. Phys. Lett.* **2004**, *400*, 389. (c) Popov, A. A.; Tarabek, J.; Kareev, I. E.; Lebedkin, S. F.; Strauss, S. H.; Boltalina, O. V.; Dunsch, L. *J. Phys. Chem. A* **2005**, *109*, 9709.
- (185) Avent, A. G.; Birkett, P. R.; Carano, M.; Darwish, A. D.; Kroto, H. W.; Lopez, J. O.; Paolucci, F.; Roffia, S.; Taylor, R.; Wachter, N.; Walton, D. R. M.; Zerbetto, F. *J. Chem. Soc., Perkin Trans. 2* **2001**, 140.
- (186) (a) Boulas, P.; Dsouza, F.; Henderson, C. C.; Cahill, P. A.; Jones, M. T.; Kadish, K. M. *J. Phys. Chem.* **1993**, *97*, 13435. (b) Paolucci, F.; Marcaccio, M.; Roffia, S.; Orlandi, G.; Zerbetto, F.; Prato, M.; Maggini, M.; Scorrano, G. *J. Am. Chem. Soc.* **1995**, *117*, 6572. (c) Echegoyen, L. E.; Djojo, F. D.; Hirsch, A.; Echegoyen, L. J. *Org. Chem.* **2000**, *65*, 4994. (d) Kadish, K. M.; Gao, X.; Van Caemelbecke, E.; Suenobu, T.; Fukuzumi, S. *J. Phys. Chem. A* **2000**, *104*, 3878. (e) Carano, M.; Da Ros, T.; Fanti, M.; Kordatos, K.; Marcaccio, M.; Paolucci, F.; Prato, M.; Roffia, S.; Zerbetto, F. *J. Am. Chem. Soc.* **2003**, *125*, 7139. (f) Hall, M. H.; Shevlin, P.; Lu, H.; Gichuhi, A.; Shannon, C. *J. Org. Chem.* **2006**, *71*, 3357. (g) Zheng, M.; Li, F. F.; Shi, Z. J.; Gao, X.; Kadish, K. M. *J. Org. Chem.* **2007**, *72*, 2538.
- (187) Goryunkov, A. A.; Kornienko, E. S.; Magdesieva, T. V.; A. K. A.; Vorobiev, V. A.; Avdoshenko, S. M.; Ioffe, I. N.; Nikitin, O. M.; Markov, V. Y.; Khavrel, P. A.; Vorobiev, A. K.; Sidorov, L. N. *Dalton Trans.* **2008**, 6886.
- (188) Popov, A. A.; Shustova, N. B.; Svitova, A. L.; Mackey, M. A.; Coumbe, C. E.; Phillips, J. P.; Stevenson, S.; Strauss, S. H.; Boltalina, O. V.; Dunsch, L. *Chem.—Eur. J.* **2010**, *16*, 4721.
- (189) Eaton, S. S.; Eaton, G. R. *Appl. Magn. Reson.* **1996**, *11*, 155.
- (190) Reed, C. A.; Bolksar, R. D. *Chem. Rev.* **2000**, *100*, 1075.
- (191) Konarev, D. V.; Romanova, N. A.; Panin, R. A.; Goryunkov, A. A.; Troyanov, S. I.; Lyubovskaya, R. N. *Chem.—Eur. J.* **2014**, *20*, 5380.
- (192) Hughes, R. P. *Eur. J. Inorg. Chem.* **2009**, 4591.
- (193) (a) Isobe, H.; Tomita, N.; Nakamura, E. *Org. Lett.* **2000**, *2*, 3663. (b) Clavaguera, S.; Khan, S. I.; Rubin, Y. *Org. Lett.* **2009**, *11*, 1389.
- (194) Whitaker, J. B.; Shustova, N. B.; Strauss, S. H.; Boltalina, O. V. *Acta Chim. Slov.* **2013**, *60*, 577.
- (195) (a) Clikeman, T. T.; Deng, S. H. M.; Avdoshenko, S.; Wang, X. B.; Popov, A. A.; Strauss, S. H.; Boltalina, O. V. *Chem.—Eur. J.* **2013**, *19*, 15404. (b) Clikeman, T. T.; Kuvychko, I. V.; Shustova, N. B.; Chen, Y. S.; Popov, A. A.; Boltalina, O. V.; Strauss, S. H. *Chem.—Eur. J.* **2013**, *19*, 5070.
- (196) Ovchinnikova, N.; Goryunkov, A. A.; Khavrel, P. A.; Belov, N. M.; Apenova, M. G.; Ioffe, I. N.; Yurovskaya, M. A.; Troyanov, S. I.; Sidorov, L. N.; Kemnitz, E. *Dalton Trans.* **2011**, *40*, 959.
- (197) Braunecker, W. A.; Oosterhout, S. D.; Owczarczyk, Z. R.; Larsen, R. E.; Larson, B. W.; Ginley, D. S.; Boltalina, O. V.; Strauss, S. H.; Kopidakis, N.; Olson, D. C. *Macromolecules* **2013**, *46*, 3367.
- (198) Coffey, D. C.; Larson, B. W.; Hains, A. W.; Whitaker, J. B.; Kopidakis, N.; Boltalina, O. V.; Strauss, S. H.; Rumbles, G. *J. Phys. Chem. C* **2012**, *116*, 8916.
- (199) Kuvychko, I. V.; Castro, K. P.; Deng, S. H. M.; Wang, X. B.; Strauss, S. H.; Boltalina, O. V. *Angew. Chem., Int. Ed.* **2013**, *52*, 4871.
- (200) Kuvychko, I. V.; Dubceac, C.; Deng, S. H. M.; Wang, X. B.; Granovsky, A. A.; Popov, A. A.; Petrukhina, M. A.; Strauss, S. H.; Boltalina, O. V. *Angew. Chem., Int. Ed.* **2013**, *52*, 7505.